University of New Hampshire
University of New Hampshire Scholars' Repository

Master's Theses and Capstones | Student Scholarship

Winter 2008

Evaluation of the Bailey Method as a tool for improving the rutting resistance of mix designs using New Hampshire aggregate

Felix Alexander Rivera
University of New Hampshire, Durham

Follow this and additional works at: https://scholars.unh.edu/thesis

Recommended Citation
Rivera, Felix Alexander, "Evaluation of the Bailey Method as a tool for improving the rutting resistance of mix designs using New Hampshire aggregate" (2008). *Master's Theses and Capstones*. 430.
https://scholars.unh.edu/thesis/430

This Thesis is brought to you for free and open access by the Student Scholarship at University of New Hampshire Scholars' Repository. It has been accepted for inclusion in Master's Theses and Capstones by an authorized administrator of University of New Hampshire Scholars' Repository. For more information, please contact nicole.hentz@unh.edu.

EVALUATION OF THE BAILEY METHOD AS A TOOL FOR IMPROVING THE RUTTING RESISTANCE OF MIX DESIGNS USING NEW HAMPSHIRE AGGREGATE

BY

FELIX ALEXANDER RIVERA
Civil Engineering (BS), Massachusetts Institute of Technology, 2003

THESIS

Submitted to the University of New Hampshire
in Partial Fulfillment of
the Requirements for the Degree of

Master of Science
in
Civil Engineering

December 2008

UMI Number: 1463234

INFORMATION TO USERS

The quality of this reproduction is dependent upon the quality of the copy submitted. Broken or indistinct print, colored or poor quality illustrations and photographs, print bleed-through, substandard margins, and improper alignment can adversely affect reproduction.

In the unlikely event that the author did not send a complete manuscript and there are missing pages, these will be noted. Also, if unauthorized copyright material had to be removed, a note will indicate the deletion.

UMI®

UMI Microform 1463234

Copyright 2009 by ProQuest LLC.

All rights reserved. This microform edition is protected against unauthorized copying under Title 17, United States Code.

ProQuest LLC
789 E. Eisenhower Parkway
PO Box 1346
Ann Arbor, MI 48106-1346

This thesis has been examined and approved.

Thesis Director, Dr. Jo Sias Daniel
Associate Professor of Civil Engineering
University of New Hampshire

Dr. Erin Santini Bell
Assistant Professor of Civil Engineering
University of New Hampshire

Dr. David L. Gress
Professor of Civil Engineering
University of New Hampshire

Date

Crusher and sieve, loud churning mixers
Sing to the Lord a new song
Asphalt and stone, loud paving workers
Sing to the Lord a new song
He has done marvelous things
I too will praise Him with a new song!

(Tune: Earth and All Stars, David Johnson 1922)

ACKNOWLEDGEMENTS

First I give thanks to the Lord for bringing me through all the lessons I've learned during my time in New Hampshire. Without Him, I would be lost and without meaning. Thank you God for saving me and for helping me in more ways than I must realize.

Secondly, I would like to thank Dr. Daniel for seemingly infinite patience with me and for all of her insight on all the little parts of this project. Thank you for providing support and encouragement to help me finish this.

I would also like to thank my parents, Felix and Elsie, for all of their love and support. Thank you for encouraging me and for all the help on various parts of this project, like suggestions on fixing the MMLS3 and proof reading. I also thank my brother, Sam, for helping me stay sane on those nights I worked with no sleep. Thanks also to my friends Nathan and Jamal for their moral support through the years.

I would like to extend a big thanks to all of the students who have helped me in the lab at various points in this project. Particularly I want to thank Sudip Bhattacharjee, Aravind Krishna Swamy, Jessica Cristallo, Alex Vadney, Jon Lamontagne, Heather Newton, Angela O'Donnell, Luke Mitchell, Steve Hall, Bill Meagher, Heather Bolton, Julie Muldoon, James Browne, Kayla Hampe, Siva Prasad, Abhijeet Singh, Aaron LaChance, and Miles Stetson. Additionally I'd like to thank Patrick Jardin for his help with the statistical comparisons.

I would also like to thank my defense committee, Dr. Erin Bell and Dr. David Gress. I appreciate you taking the time to review my thesis and help me move towards graduating. I want to extend a particular thanks to Pete Merrow who helped immensely with the MMLS3 and general technical issues. I'd also like to thank Claire Euloth for helping me to find my way around the department and the school. Thanks to Kelly Hinton for all her help with financial matters. Thanks to Rob Cinq-Mars who helped keep the laboratory equipment working well. Special thanks to Dr. Tom Attard for being a great professor and a great encouragement. Additionally, all these people often found time to lift my spirits with smile and a nice chat.

I'd like to thank Johan Muller who was a very big help with the MMLS3. He was prompt in his responses and often led us to the right solution in getting that machine to work for us again. Additionally, I'd like to thank Fred Hugo who provided much insight on how to run tests with the MMLS3 and what to consider for analyses. Thanks also the NHDOT for funding this project. I also thank the workers at the Pike facilities in Ossipee, Farmington, and Hooksett and at the Continental facility in Londonderry.

Finally, I'd like to thank the crew of Rocky's Ace for providing suggestions on how to get my lab machines to work, giving me rides, making (thankfully inaccurate) predictions on my completion date, and threatening to park a bunch of bikers on my lawn. Thank you Donna, Roy, Steve, Mike, Bruce, Kim, Glenn, Terry, Mike, Laura, and Andrew.

TABLE OF CONTENTS

DEDICATION	iii
ACKNOWLEDGEMENTS	iv
LIST OF TABLES	vii
LIST OF FIGURES	xi
ABSTRACT	xvi
CHAPTER	PAGE
1. INTRODUCTION	1
Background	1
Problem Statement	3
Objectives	4
Literature Review	5
Bailey Method	5
MMLS3	8
2. BAILEY METHOD	10
Basic Theory	10
Designing Aggregate Blends with the Bailey Method	18
Limitations of the Bailey Method	21
3. THIRD SCALE MOBILE MODEL LOAD SIMULATOR	23
Overview	23
Accelerated Pavement Testing	24
Physical Structure and Capabilities	25
Advantages and Disadvantages	36
4. MATERIALS AND METHODS	38
Overview	38
Materials	39
Methods	40
Overview	40
Fabrication	41
Field Core Sample Preparation	45
Volumetric Measurement	46
MMLS3 Testing	48
Bailey Method Design and Evaluation	54
5. RESULTS AND DISCUSSION	57
Results	57
Overview	57
Original Mix Designs	58
Volumetrics	60
MMLS3 Test Results	62

TABLE OF CONTENTS (continued)

Rut Performance Comparisons 74
Comparisons Based on NMSA 76
Comparisons Based on Aggregate Type 80
Comparisons Based on Rap Content 84
MMLS3 Test on Field Cores 87
Mixtures Redesigned According to the Bailey Method 92
Volumetrics and Bailey Parameters 94
MMLS3 Test Results 99
Discussion 104

6. SUMMARY AND CONCLUSIONS 109
Summary of Final Results 109
Conclusions from the Results 112
Suggested Areas of Further Research 113
Final Remarks 114

LIST OF REFERENCES 116

APPENDIX 1: BAILEY METHOD CALCULATIONS 118
APPENDIX 2: SUPERPAVE ASPHALT CONTENT DESIGN RESULTS 140
APPENDIX 3: AGGREGATE DATA AND MIX DESIGNS 144
APPENDIX 4: VOLUMETRIC MEASURMENTS 151
APPENDIX 5: COMPACTION GRAPHS 154
APPENDIX 6: MMLS3 TEST RESULTS 159
APPENDIX 7: STATISTICAL COMPARISONS 236

LIST OF TABLES

CHAPTER 2: BAILEY METHOD
2.1: Control Sieves for Various NMSAs 13
2.2: The Four Bailey Parameters 14
2.3: Predicted Effect of Bailey Parameters on VMA 15

CHAPTER 4: MATERIALS AND METHODS
4.1: Summary of Original Mix Designs 39
4.2: MMLS3 Test Parameters 53

CHAPTER 5: RESULTS AND DISCUSSION
5.1: Summary of Mix Designs 58
5.2: Volumetrics for Oss 12.5 60
5.3: Volumetrics for Oss 19 61
5.4: Volumetrics for Cont 12.5 61
5.5: Volumetrics for Cont 19 61
5.6: Volumetrics for Farm 62
5.7: Volumetrics for Hook 62
5.8: Comparison of Rut Depths of Oss 12.5 and Oss 19 76
5.9: Comparison of Rut Depths of Cont 12.5 and Cont 19 79
5.10: Comparison of Rut Depths of Oss 12.5 and Cont 12.5 80
5.11: Comparison of Rut Depths of Oss 19 and Cont 19 81
5.12: Comparison of Rut Depths of Farm and Hook 83
5.13: Comparison of Rut Depths of Oss 12.5 and Farm 84
5.14: Comparison of Rut Depths of Cont 12.5 and Hook 86
5.15: Summary of Statistical Comparisons 87
5.16: Volumetrics for Field Core Surface Layer 88
5.17: Volumetrics for Field Core Base Layer 88
5.18: Total Rut Depth Developed between 1,000 and 30,000 Loading Cycles 92
5.19: Bailey Parameters for Redesigned Mixtures 95
5.20: Volumetrics for Oss 12.5-Bailey 95
5.21: Volumetrics for Cont 19-Bailey 96
5.22: Expected Change in VMA from Oss 12.5-Original 97
5.23: Expected Change in VMA from Cont 19-Original 97
5.24: Expected Change in VMA from Farm-Original 97
5.25: Measured VMAs 98
5.26: Comparison of Rut Depths of Oss 12.5-Original and Oss 12.5-Bailey 102
5.27: Comparison of Rut Depths of Cont 19-Original and Cont 19-Bailey 103

APPENDIX 1: BAILEY METHOD CALCULATIONS
A1.1: Aggregate Data 119
A1.2: Input Values 119
A1.3: Output Values 121
A1.4: Oss 12.5 Original Gradation 123
A1.5: Input Values for Oss 12.5 Original Evaluation 123

A1.6: Output Values for Oss 12.5 Original Evaluation 123
A1.7: Oss 12.5 Bailey Gradation 124
A1.8: Input Values for Oss 12.5 Bailey Design 124
A1.9: Output Values for Oss 12.5 Bailey Design 124
A1.10: Cont 19 Original Gradation 125
A1.11: Input Values for Cont 19 Original Evaluation 125
A1.12: Output Values for Cont 19 Original Evaluation 125
A1.13: Cont 19 Bailey Gradation 126
A1.14: Input Values for Cont 19 Bailey Design 126
A1.15: Output Values for Cont 19 Bailey Design 126
A1.16: Farm Original Gradation 127
A1.17: Input Values for Farm Original Evaluation 127
A1.18: Output Values for Farm Original Evaluation 127
A1.19: Farm Bailey Gradation 128
A1.20: Input Values for Farm Bailey Design 128
A1.21: Output Values for Farm Bailey Design 128

APPENDIX 2: SUPERPAVE ASPHALT CONTENT DESIGN RESULTS
A2.1: Oss 12.5-Bailey Aggregate Data 140
A2.2: Oss 12.5-Bailey Calculation Results for Pbi and Pb,est 140
A2.3: Oss 12.5-Bailey Volumetrics of Design Specimens 140
A2.4: Oss 12.5-Bailey Final Volumetrics 141
A2.5: Cont 19-Bailey Aggregate Data 141
A2.6: Cont 19-Bailey Calculation Results for Pbi and Pb,est 141
A2.7: Cont 19-Bailey Volumetrics of Design Specimens 142
A2.8: Cont 19-Bailey Final Volumetrics 142
A2.9: Farm-Bailey Aggregate Data 142
A2.10: Farm-Bailey Calculation Results for Pbi and Pb,est 143
A2.11: Farm-Bailey Volumetrics of Design Specimens 143
A2.12: Farm-Bailey Final Volumetrics 143

APPENDIX 3: AGGREGATE DATA AND MIX DESIGNS
A3.1: Ossipee Aggregates 144
A3.2: Continental Aggregates 145
A3.3: Farmington Aggregates 145
A3.4: Hooksett Aggregates 146
A3.5: Oss 12.5 Blend 146
A3.6: Oss 12.5 Batching Recipes 146
A3.7: Oss 19 Blend 147
A3.8: Oss 19 Batching Recipes 147
A3.9: Cont 12.5 Blend 147
A3.10: Cont 12.5 Batching Recipes 147
A3.11: Cont 19 Blend 148
A3.12: Cont 19 Batching Recipes 148
A3.13: Farm Blend 148
A3.14: Farm Batching Recipes 148

A3.14: Hook Blend 149
A3.15: Hook Batching Recipes 149
A3.15: Oss 12.5-Bailey Blend 149
A3.16: Oss 12.5-Bailey Batching Recipes 149
A3.17: Cont 19-Bailey Blend 150
A3.18: Cont 19-Bailey Batching Recipes 150
A3.19: Farm-Bailey Blend 150
A3.20: Farm-Bailey Batching Recipes 150

APPENDIX 4: VOLUMETRIC MEASURMENTS
A4.1: Gmm Measurements Using Pycnometer 151
A4.2: Gmm Measurements Using CoreLok 151
A4.3 Oss 12.5 Volumetrics 152
A4.4 Oss 19 Volumetrics 152
A4.5 Cont 12.5 Volumetrics 152
A4.6 Cont 19 Volumetrics 152
A4.7 Farm Volumetrics 153
A4.8 Hook Volumetrics 153
A4.9 Oss 12.5-Bailey Volumetrics 153
A4.10 Cont 19-Bailey Volumetrics 153

APPENDIX 6: MMLS3 TEST RESULTS
A6.1: Oss 12.5 Avg Rut Depth from Base Line 163
A6.2: Oss 12.5 Max Rut Depth from Base Line 163
A6.3: Oss 12.5 Max Rut Depth from Max Heave 163
A6.4: Oss 19 Avg Rut Depth from Base Line 169
A6.5: Oss 19 Max Rut Depth from Base Line 169
A6.6: Oss 19 Max Rut Depth from Max Heave 169
A6.7: Cont 12.5 Avg Rut Depth from Base Line 175
A6.8: Cont 12.5 Max Rut Depth from Base Line 175
A6.9: Cont 12.5 Max Rut Depth from Max Heave 175
A6.10: Cont 19 Avg Rut Depth from Base Line 181
A6.11: Cont 19 Max Rut Depth from Base Line 181
A6.12: Cont 19 Max Rut Depth from Max Heave 181
A6.13: Farm Avg Rut Depth from Base Line 187
A6.14: Farm Max Rut Depth from Base Line 187
A6.15: Farm Max Rut Depth from Max Heave 187
A6.16: Hook Avg Rut Depth from Base Line 193
A6.17: Hook Max Rut Depth from Base Line 193
A6.18: Hook Max Rut Depth from Max Heave 193
A6.19: Oss 12.5 Bailey Avg Rut Depth from Base Line 199
A6.20: Oss 12.5 Bailey Max Rut Depth from Base Line 199
A6.21: Oss 12.5 Bailey Max Rut Depth from Max Heave 199
A6.22: Cont 19 Bailey Avg Rut Depth from Base Line 205
A6.23: Cont 19 Bailey Max Rut Depth from Base Line 205
A6.24: Cont 19 Bailey Max Rut Depth from Max Heave 205

A6.25: Oss 12.5 Field Cores Avg Rut Depth from Base Line 211
A6.26: Oss 12.5 Field Cores Max Rut Depth from Base Line 212
A6.27: Oss 12.5 Field Cores Max Rut Depth from Max Heave 212
A6.28: Oss 19 Field Cores Avg Rut Depth from Base Line 218
A6.29: Oss 19 Field Cores Max Rut Depth from Base Line 218
A6.30: Oss 19 Field Cores Max Rut Depth from Max Heave 218
A6.31: Oss 12.5 MMLS3 Test Log 221
A6.32: Oss 19 MMLS3 Test Log 222
A6.33: Cont 12.5 MMLS3 Test Log 225
A6.34: Cont 19 MMLS3 Test Log 226
A6.35: Farm MMLS3 Test Log 228
A6.36: Hook MMLS3 Test Log 229
A6.37: Oss 12.5 Bailey MMLS3 Test Log 230
A6.38: Cont 19 Bailey MMLS3 Test Log 232
A6.39: Oss 12.5 Field Core MMLS3 Test Log 233
A6.40: Oss 19 Field Core MMLS3 Test Log 234

APPENDIX 7: STATISTICAL COMPARISONS
A7.1: Oss 12.5-Original Avg Rut Depth 236
A7.2: Oss 12.5-Bailey Avg Rut Depth 236
A7.3: Combined Rut Values at 4,000 Loading Cycles 237
A7.4: Sum of Ranks 237
A7.5: Oss 12.5 verses Oss 19 238
A7.6: Oss 12.5 verses Cont 12.5 238
A7.7: Oss 12.5 verses Farm 239
A7.8: Oss 19 verses Cont 19 239
A7.9: Cont 12.5 verses Cont 19 239
A7.10: Cont 12.5 verses Hook 240
A7.11: Farm verses Hook 240
A7.12: Oss 12.5 Original verses Oss 12.5 Bailey 240
A7.13: Cont 19 Original verses Cont 19 Bailey 241

LIST OF FIGURES

CHAPTER 2: BAILEY METHOD
2.1: Maximum Density Configuration of Uniformly Sized, Circular Particles 11
2.2: A Fine Particle Filling the Gap Between Coarse Particles 11
2.3: Particles Inside Gaps with Varying Number of Flat Faces 12
2.4: Separation of Aggregate Blend into Find and Coarse Parts 14

CHAPTER 3: THIRD SCALE MOBILE MODEL LOAD SIMULATOR
3.1: The MMLS3 24
3.2: Basic Structure of MMLS3 26
3.3: Close Up of Bogie with Tire 26
3.4: Schematic of Bogie with Tire and Suspension 27
3.5: Load Calibration Unit 28
3.6: Control Unit for the MMLS3 29
3.7: Dry Air Heating/ Cooling Unit 30
3.8: Wet Heating Unit 31
3.9: The Environmental Chamber 32
3.10: Sample Brick 33
3.11: The Test Bed 33
3.12: The Profilometer 35
3.13: A Profile Being Measured 35

CHAPTER 4: MATERIALS AND METHODS
4.1: A Compacted Sample, a Brick, and the Cutting Template 48
4.2: Test Bed Configuration 51

CHAPTER 5: RESULTS AND DISCUSSION
5.1: Gradations for Mixtures with Gravel Stone 59
5.2: Gradations for Mixtures with Fractured Rock 59
5.3: Surface Profile Measurements for O12.5M-8B 63
5.4: Three Methods of Condensing Rut Data from Profile 65
5.5: Modified Range for Average Rut Depth 66
5.6: Longitudinal Profile of Oss 12.5 Bricks, Max Rut Depth 67
5.7: Rut Depth vs. Loading Cycles for Oss 12.5 69
5.8: Rut Depth vs. Loading Cycles for Oss 19 69
5.9: Rut Depth vs. Loading Cycles for Cont 12.5 70
5.10: Rut Depth vs. Loading Cycles for Cont 19 70
5.11: Rut Depth vs. Loading Cycles for Farm 71
5.12: Rut Depth vs. Loading Cycles for Hook 71
5.13: Temperature over the Course of the Cont 19 MMLS3 Test 73
5.14: Performance of Cont 19 Adjusted to a Constant Temperature of 50°C 74
5.15: Comparison Graph of Oss 12.5 and Oss 19 76
5.16: Oss 12.5 and Oss 19 Normalized to the Rut Depth at 1000 Cycles 78
5.17: Comparison Graph of Cont 12.5 and Cont 19 78
5.18: Comparison Graph of Oss 12.5 and Cont 12.5 80

5.19: Comparison Graph of Oss 19 and Cont 19 81
5.20: Oss 19 and Cont 19 Normalized to the Rut Depth at 1000 Cycles 82
5.21: Comparison Graph of Farm and Hook 83
5.22: Comparison Graph of Oss 12.5 and Farm 84
5.23: Comparison Graph of Cont 12.5 and Hook 85
5.24: Rut Depth vs. Loading Cycles for Oss 12.5 Field Cores 89
5.25: Rut Depth vs. Loading Cycles for Oss 19 Field Cores 89
5.26: Comparison Graph of Oss 12.5 Lab Samples and Field Cores 90
5.27: Comparison Graph of Oss 19 Lab Samples and Field Cores 91
5.28: Oss 12.5-Original and Oss 12.5-Bailey Mix Design Gradations 93
5.29: Cont 19-Original and Cont 19-Bailey Mix Design Gradations 93
5.30: Farm-Original and Farm-Bailey Mix Design Gradations 94
5.31: Comparison of Change in VMA, Predicted Verses Measured 99
5.32: Temperature over the Course of the Cont 19-Bailey MMLS3 Test 100
5.33: Rut Depth vs. Loading Cycles for Oss 12.5-Bailey 101
5.34: Rut Depth vs. Loading Cycles for Cont 19-Bailey 101
5.35: Comparison Graph of Oss 12.5-Original and Oss 12.5-Bailey 102
5.36: Comparison Graph of Cont 19-Original and Cont 19-Bailey 103
5.37: Compaction of Cont 19 Mixes 106
5.38: Density over Course of Compaction of Cont 19 Mixes 107
5.39: Density over Course of Compaction of Oss 12.5 Mixes 108

APPENDIX 5: COMPACTION GRAPHS
A5.1: Oss 12.5 Compaction Graphs 154
A5.2: Oss 19 Compaction Graphs 155
A5.3: Cont 12.5 Compaction Graphs 155
A5.4: Cont 19 Compaction Graphs 156
A5.5: Farm Compaction Graphs 156
A5.6: Hook Compaction Graphs 157
A5.7: Oss 12.5 Bailey Compaction Graphs 157
A5.8: Cont 19 Bailey Compaction Graphs 158

APPENDIX 6: MMLS3 TEST RESULTS
A6.1: Oss 12.5 Brick 1 Transverse Profiles 159
A6.2: Oss 12.5 Brick 2 Transverse Profiles 160
A6.3: Oss 12.5 Brick 3 Transverse Profiles 160
A6.4: Oss 12.5 Brick 4 Transverse Profiles 161
A6.5: Oss 12.5 Brick 5 Transverse Profiles 161
A6.6: Oss 12.5 Brick 6 Transverse Profiles 162
A6.7: Oss 12.5 Brick 7 Transverse Profiles 162
A6.8: Oss 12.5 Avg Rut from Base Line Longitudinal Profiles 164
A6.9: Oss 12.5 Max Rut from Base Line Longitudinal Profiles 164
A6.10: Oss 12.5 Max Rut from Max Heave Longitudinal Profiles 165
A6.11: Oss 19 Brick 1 Transverse Profiles 165
A6.12: Oss 19 Brick 2 Transverse Profiles 166
A6.13: Oss 19 Brick 3 Transverse Profiles 166

A6.14: Oss 19 Brick 4 Transverse Profiles 167
A6.15: Oss 19 Brick 5 Transverse Profiles 167
A6.16: Oss 19 Brick 6 Transverse Profiles 168
A6.17: Oss 19 Brick 7 Transverse Profiles 168
A6.18: Oss 19 Avg Rut from Base Line Longitudinal Profiles 170
A6.19: Oss 19 Max Rut from Base Line Longitudinal Profiles 170
A6.20: Oss 19 Max Rut from Max Heave Longitudinal Profiles 171
A6.21: Cont 12.5 Brick 1 Transverse Profiles 171
A6.22: Cont 12.5 Brick 2 Transverse Profiles 172
A6.23: Cont 12.5 Brick 3 Transverse Profiles 172
A6.24: Cont 12.5 Brick 4 Transverse Profiles 173
A6.25: Cont 12.5 Brick 5 Transverse Profiles 173
A6.26: Cont 12.5 Brick 6 Transverse Profiles 174
A6.27: Cont 12.5 Brick 7 Transverse Profiles 174
A6.28: Cont 12.5 Avg Rut from Base Line Longitudinal Profiles 176
A6.29: Cont 12.5 Max Rut from Base Line Longitudinal Profiles 176
A6.30: Cont 12.5 Max Rut from Max Heave Longitudinal Profiles 177
A6.31: Cont 19 Brick 1 Transverse Profiles 177
A6.32: Cont 19 Brick 2 Transverse Profiles 178
A6.33: Cont 19 Brick 3 Transverse Profiles 178
A6.34: Cont 19 Brick 4 Transverse Profiles 179
A6.35: Cont 19 Brick 5 Transverse Profiles 179
A6.36: Cont 19 Brick 6 Transverse Profiles 180
A6.37: Cont 19 Brick 7 Transverse Profiles 180
A6.38: Cont 19 Avg Rut from Base Line Longitudinal Profiles 182
A6.39: Cont 19 Max Rut from Base Line Longitudinal Profiles 182
A6.40: Cont 19 Max Rut from Max Heave Longitudinal Profiles 183
A6.41: Farm Brick 1 Transverse Profiles 183
A6.42: Farm Brick 2 Transverse Profiles 184
A6.43: Farm Brick 3 Transverse Profiles 184
A6.44: Farm Brick 4 Transverse Profiles 185
A6.45: Farm Brick 5 Transverse Profiles 185
A6.46: Farm Brick 6 Transverse Profiles 186
A6.47: Farm Brick 7 Transverse Profiles 186
A6.48: Farm Avg Rut from Base Line Longitudinal Profiles 188
A6.49: Farm Max Rut from Base Line Longitudinal Profiles 188
A6.50: Farm Max Rut from Max Heave Longitudinal Profiles 189
A6.51: Hook Brick 1 Transverse Profiles 189
A6.52: Hook Brick 2 Transverse Profiles 190
A6.53: Hook Brick 3 Transverse Profiles 190
A6.54: Hook Brick 4 Transverse Profiles 191
A6.55: Hook Brick 5 Transverse Profiles 191
A6.56: Hook Brick 6 Transverse Profiles 192
A6.57: Hook Brick 7 Transverse Profiles 192
A6.58: Hook Avg Rut from Base Line Longitudinal Profiles 194
A6.59: Hook Max Rut from Base Line Longitudinal Profiles 194

A6.60: Hook Max Rut from Max Heave Longitudinal Profiles 195
A6.61: Oss 12.5 Bailey Brick 1 Transverse Profiles 195
A6.62: Oss 12.5 Bailey Brick 2 Transverse Profiles 196
A6.63: Oss 12.5 Bailey Brick 3 Transverse Profiles 196
A6.64: Oss 12.5 Bailey Brick 4 Transverse Profiles 197
A6.65: Oss 12.5 Bailey Brick 5 Transverse Profiles 197
A6.66: Oss 12.5 Bailey Brick 6 Transverse Profiles 198
A6.67: Oss 12.5 Bailey Brick 7 Transverse Profiles 198
A6.68: Oss 12.5 Bailey Avg Rut from Base Line Longitudinal Profiles 200
A6.69: Oss 12.5 Bailey Max Rut from Base Line Longitudinal Profiles 200
A6.70: Oss 12.5 Bailey Max Rut from Max Heave Longitudinal Profiles 201
A6.71: Cont 19 Bailey Brick 1 Transverse Profiles 201
A6.72: Cont 19 Bailey Brick 2 Transverse Profiles 202
A6.73: Cont 19 Bailey Brick 3 Transverse Profiles 202
A6.74: Cont 19 Bailey Brick 4 Transverse Profiles 203
A6.75: Cont 19 Bailey Brick 5 Transverse Profiles 203
A6.76: Cont 19 Bailey Brick 6 Transverse Profiles 204
A6.77: Cont 19 Bailey Brick 7 Transverse Profiles 204
A6.78: Cont 19 Bailey Avg Rut from Base Line Longitudinal Profiles 206
A6.79: Cont 19 Bailey Max Rut from Base Line Longitudinal Profiles 206
A6.80: Cont 19 Bailey Max Rut from Max Heave Longitudinal Profiles 207
A6.81: Oss 12.5 Field Cores Brick 1 Transverse Profiles 207
A6.82: Oss 12.5 Field Cores Brick 2 Transverse Profiles 208
A6.83: Oss 12.5 Field Cores Brick 3 Transverse Profiles 208
A6.84: Oss 12.5 Field Cores Brick 4 Transverse Profiles 209
A6.85: Oss 12.5 Field Cores Brick 5 Transverse Profiles 209
A6.86: Oss 12.5 Field Cores Brick 6 Transverse Profiles 210
A6.87: Oss 12.5 Field Cores Brick 7 Transverse Profiles 210
A6.88: Oss 12.5 Field Cores Brick 8 Transverse Profiles 211
A6.89: Oss 12.5 Field Cores Avg Rut from Base Line Longitudinal Profiles 212
A6.90: Oss 12.5 Field Cores Max Rut from Base Line Longitudinal Profiles 213
A6.91: Oss 12.5 Field Cores Max Rut from Max Heave Longitudinal Profiles 213
A6.92: Oss 19 Field Cores Brick 1 Transverse Profiles 214
A6.93: Oss 19 Field Cores Brick 2 Transverse Profiles 214
A6.94: Oss 19 Field Cores Brick 3 Transverse Profiles 215
A6.95: Oss 19 Field Cores Brick 4 Transverse Profiles 215
A6.96: Oss 19 Field Cores Brick 5 Transverse Profiles 216
A6.97: Oss 19 Field Cores Brick 6 Transverse Profiles 216
A6.98: Oss 19 Field Cores Brick 7 Transverse Profiles 217
A6.99: Oss 19 Field Cores Brick 8 Transverse Profiles 217
A6.100: Oss 19 Field Cores Avg Rut from Base Line Longitudinal Profiles 219
A6.101: Oss 19 Field Cores Max Rut from Base Line Longitudinal Profiles 219
A6.102: Oss 19 Field Cores Max Rut from Max Heave Longitudinal Profiles 220
A6.103: Oss 12.5 Temperature Readings 222
A6.104: Oss 19 Temperature Readings, Part 1 224
A6.105: Oss 19 Temperature Readings, Part 2 224

A6.106: Cont 12.5 Temperature Readings 226
A6.107: Cont 19 Temperature Readings 227
A6.108: Farm Temperature Readings 229
A6.109: Hook Temperature Readings 230
A6.110: Oss 12.5 Bailey Temperature Readings, Part 1 231
A6.111: Oss 12.5 Bailey Temperature Readings, Part 2 232
A6.112: Cont 19 Bailey Temperature Readings 233
A6.113: Oss 12.5 Field Core Temperature Readings 234
A6.114: Oss 19 Field Core Temperature Readings 235

ABSTRACT

EVALUATION OF THE BAILEY METHOD

AS A TOOL FOR IMPROVING THE RUTTING RESISTANCE OF MIX DESIGNS

USING NEW HAMPSHIRE AGGREGATE

By

Felix Alexander Rivera

University of New Hampshire, December 2008

Currently the NHDOT uses the Superpave method to design and evaluate its asphalt pavements; however, this method lacks guidelines to adjust an aggregate blend that yields unacceptable mixtures. The objective of this project was to determine if the Bailey Method of aggregate blending would help improve the rutting resistance of mix designs that use NH aggregates. The rutting performances of six typical NH mix designs and two Bailey designs were measured using the Third Scale Mobile Model Load Simulator (MMLS3), an accelerated pavement testing (APT) device, in hot, dry conditions. Out of the two mixtures redesigned according to the Bailey Method, one showed improvement in rutting resistance while the other showed no change. Additionally, the Bailey Method failed to predict the voids in the mineral aggregate (VMA) in the redesigned mixes.

CHAPTER 1

INTRODUCTION

Background

Currently, the New Hampshire Department of Transportation (NHDOT) uses the Superpave Method to design and evaluate the paving mixtures used in the state (meeting with NHDOT, 2004). While Superpave has a detailed procedure to determine the asphalt content of a mix, there is very little instruction given on how to design the aggregate blend. What Superpave does have is a list of criteria for the aggregate blend in the form of control points (upper and lower limits of percent passing for certain standard sieve sizes), and a restricted zone (a range of values of percent passing to avoid for several fine sieve sizes). In addition to the aggregate blend criteria, Superpave lists requirements for the final asphalt mix, which include the air voids (AV), the voids in the mineral aggregate (VMA), and other volumetric measurements. However, Superpave does not give any direction on how to alter the aggregate gradation of a mix if the criteria are not met. The text only tells the engineer to go through the process of trial and error, as stated below:

What could be done at this point if none of the blends were acceptable? Additional combinations of the current aggregates could be tested, or additional materials from different sources could be obtained and included in the trial blend analysis.

(Superpave, SP-2, 2001, p. 82)

Traditionally, engineers have relied on experience, either from themselves or from others, to design the aggregate blend of a mix. However, an additional analytical tool designed for dealing with aggregate blends can be useful, especially when combined with experiential knowledge. The Bailey Method is a tool that offers a simplified explanation of the mechanics of aggregate structure, a procedure for aggregate blend evaluation, and a procedure for aggregate blend design. It was initially developed by Mr. Robert Bailey, now retired, who worked with the Illinois Department of Transportation (Vavrik, et al. 2002). The Bailey Method presents a model of an aggregate matrix based on particle compaction as influenced by particle size distribution. The procedures it describes are simple and straight forward and require no fabrication of samples because it requires only aggregate data and gradings. The evaluation portion of the method makes general predictions about the relative VMA and compactability. However, since the Bailey Method only looks at particle size and includes very little about other aggregate properties that significantly affect the behavior of a blend, such as texture and shape, exact results cannot be expected. Although the Bailey Method doesn't require it, the designer would probably benefit from fabricating samples for verification tests. Still, the Bailey Method along with experience can guide the direction of the mix designs, helping to quickly reach a final design that performs well under actual road conditions.

Among the range of tests that can be done to evaluate a mix design, accelerated pavement testing (APT) is a very useful kind of test that applies scaled traffic loading to directly evaluate the performance of the asphalt mix. One such APT device is the Third Scale Mobile Model Load Simulator (MMLS3) that simulates truck traffic at one third the actual size. It is versatile with the ability to test asphalt bricks or slabs in a laboratory and road pavement in the field. It has several pieces of accompanying equipment that allow it to modify and maintain the testing environment to emphasize a desired pavement failure, such as rutting, stripping, or fatigue cracking. Due to its larger scale, it is closer to simulating actual truck traffic than some other APT devices like the Asphalt Pavement Analyzer and the Hamburg Wheel Tester. However, it can also be used simply as a comparative tool to quickly distinguish between good and bad performing mixtures.

Problem Statement

The Bailey Method was developed to help engineers design better performing mixtures. However, it has not been as useful as expected in some states, because the predictions it makes regarding VMA do not always coincide with the verification tests. The goal of this project is to see if the Bailey Method can help design mixtures with improved performance using New Hampshire aggregate. The mode of improvement given attention in this project is resistance to rutting under loading by the MMLS3 in hot, dry conditions.

Objective

The objective of this research project was to evaluate the applicability of the Bailey Method to New Hampshire materials. The steps taken to meet this objective are as follows:

- Obtain a number of mix designs currently used by the NHDOT that represent a broad spectrum of mixture types employed in road pavement.
- Evaluate the New Hampshire mix designs according to Bailey Method procedures.
- Test the New Hampshire mix designs using the MMLS3 and compare their rutting resistances.
- Redesign the aggregate blends of three mixtures according to the Bailey Method design procedures. The Bailey design calculations and fabricated samples will use the same aggregates as the corresponding original mix designs.
- Design the asphalt content according to the Superpave Method.
- Use Superpave criteria and Bailey Method procedures to evaluate the new mix designs.
- Test the new mixes using the MMLS3 and compare their rutting resistance to those of the corresponding original mixes.
- Make recommendations, if possible, regarding the usefulness of the Bailey Method in designing better performing asphalt mixes.

Literature Review

The Bailey Method

Transportation Research E-Circular, No. E-C044, Bailey Method for Gradation selection in HMA Mixture Design (Vavrik, et al. 2002), is the main document used for this project. This was a joint effort by W.R. Vavrik and Mr. Bailey along with several others. As stated above, the Bailey Method looks at particle packing based on particle size. The goal is to design a blend that uses the aggregate particles efficiently, meaning that there is a balance of coarse particles and fine particles. Such a balance allows the coarse aggregate to interlock, meaning each (relatively) large stone is transferring its load to as many other large stones as possible, and allows the fine aggregate to fully support the coarse aggregate by filling the void spaces fully without over filling them, which would push the coarse particles apart. A balanced blend should be strong against rutting and still be easy to compact (Vavrik, et al. 2002).

The procedures in the Bailey Method make use of four parameters. These include the chosen unit weight (CUW) of the coarse aggregate, the coarse aggregate weight ratio (CA), the coarse part of the fine aggregate weight ratio (FAc), and the fine part of the fine aggregate weight ratio (FAf). The Bailey Method predicts certain changes in the VMA and compactability of a mix based on changes in these parameters. However, in a study in Oklahoma, the predictions made by the Bailey Method about the VMA were very different from the actual changes that took place when test samples were fabricated and

measured (Gierhart 2007). The reason for this discrepancy might have been the influence of other aggregate properties. If the aggregate is weak, then it will break into smaller pieces, effectively making a blend finer. If the aggregate is particularly rough, then the VMAs of the test samples may be larger than expected because the particles resisted compaction more than usual. Conversely, if there are a number of rounded or smooth particles, more compaction may happen.

A study in Oregon (Thompson 2006) noted that the Bailey Method only uses certain sieves to calculate the weight ratios from which its predictions are made. However, the other sieves that are ignored may have a stronger influence on changes in the VMAs of the fabricated specimens. The Bailey Method's model of particle compaction starts with aggregate particles approximated as circles, then spheres. Coarse particles are defined as those that carry the bulk of the load and have spaces between them. Fine particles are those that perfectly fill the voids between the coarse ones and the ratio of diameters, large to small, can be calculated (Vavrik, et al. 2002). Since real aggregate is not spherical, an average diameter ratio is used. With some aggregate, such as the Oregon aggregate, the average value does not work very well, at least with the initial separation of coarse and fine particles. This is where further testing and experience guide the results of the Bailey Method so that an acceptable blend is found using a combination of all these tools.

The type of mix designed can also make a difference in the reliability of the Bailey Method. Its general procedure deals with coarse graded blends, but there are

additional guidelines that adapt both the evaluation and design for fine, dense graded blends, and for stone matrix asphalt (SMA) blends. One study found the Bailey Method to be very good at predicting VMA results based on the CA ratio in SMA mix designs (Qiu 2006). This study did not look at the FAc or the FAf ratios because fine aggregate generally does not influence an SMA mix significantly. On the other hand, the mixes that were studied in Oklahoma were fine graded as defined by the Bailey Method because they had a CUW well below 90% (Gierhart 2007). Although the fine aggregate played a dominant role in influencing VMA in those mix designs, other factors like the coarse aggregate or ignored sieves could have been affecting the VMA enough to throw off the results. One study ignored the predictions made by the Bailey Method and simply calculated a mathematical model of the influence of the weight ratios on VMA based on measurements from a number of samples (Khosla 2005). This model showed that the FAc and FAf ratios had the greatest influence on VMA, which is the same prediction the Bailey Method makes.

Although the Bailey Method only discusses the changes in VMA and expected problems with compaction, other attributes of the asphalt pavement can be predicted based on changes in the parameters. The Oregon study looked at the correlation of changes in the weight ratios to rutting performance under testing by their APT device (Thompson 2006). This study found that the same weight ratios from the unused sieve sizes that most strongly influenced the voids were also the main influence on rut resistance. This shows that the Bailey Method, or a slightly modified version of it, can be used to predict the performance of an aggregate blend. Data from another study showed

a correlation between permeability and the CA ratio (Khosla 2005). This can be related to the VMA and gives some indication about the durability against weathering of the asphalt mix.

MMLS3

The MMLS3 is a very useful tool in assessing the performance of asphalt pavement. However, because it is only a simulation, there are several aspects that differ from true traffic loading. These differences are part of the nature of the test and must be accounted for through transformation coefficients and mathematical modeling. One difference is the fact that the tires are pulled over the surface of the pavement as opposed to driven, which means that the horizontal force will be in the same direction as wheel travel instead of the opposite direction as with actual truck loads (personal communication with Fred Hugo, 2006). Another difference is the fact that the MMLS3 is only one third scale and cannot develop very large stresses in layers deep below the surface, which makes it difficult to predict the behavior of multi layered asphalt pavements (Smit, et al 1999).

There have been various studies done at places like Jacksboro (Smit, et al 1999), WesTrack (Epps, et al 2001), and the National Center for Asphalt Technology (NCAT) test track (Smit, et al 2003). In these studies, the results from loading by the MMLS3 are compared to results from the Texas Model Load Simulator (TxMLS) and to actual truck loading. The goal in these projects was to develop a model to predict the performance of

a pavement based on preliminary test results. This would allow engineers to try out various mix designs at a fraction of the cost of actually paving stretches of highway with them.

There are established procedures for using the MMLS3 and in reporting the results. A consistency in results publications can help researchers across the country and across the world compare one pavement to another (Kruger 2004). The studies in which the MMLS3 has been run for 1,000,000 loading cycles or more show that rut development after the first 100,000 cycles is comparatively very slow (Smit, et al 1999). Therefore this project followed most of the conventions for MMLS3 testing including maximum number of cycles run, target test temperature, and frequency of profile measurements (Kruger 2004).

CHAPTER 2

THE BAILEY METHOD

Basic Theory

The Bailey Method was initially developed by Robert Bailey, now retired, who worked with the Illinois Department of Transportation. The goal was to design a tool to help engineers better understand the mechanics of aggregate packing and its contribution to the compressive strength of asphalt pavement. The basic principle of the Bailey Method is that maximum compressive strength of an asphalt mix is best achieved when there is stone to stone contact of as many aggregate particles as possible. This allows a spreading of the load from the vehicle tire to the sub layers beneath the pavement through as many particles as possible, leaving no particle under utilized or unsupported. The proper stone to stone contact is achieved when the aggregate blend has a balance of coarse and fine particles. This means that the coarse particles are all touching with the voids between them neither under nor over filled with fine particles (Vavrik, et al. 2002).

The theory of maximum particle compaction in the Bailey Method starts by looking at a two dimensional space in which all the particles are the same size and perfectly circular. It can be mathematically proven that the configuration for maximum density is achieved when all particles are touching six other particles at 60° intervals, as shown in

Figure 2.1. The spaces between these particles can be filled with circular particles with diameters 0.15 times the diameter of the large particles. Figure 2.2 illustrates this.

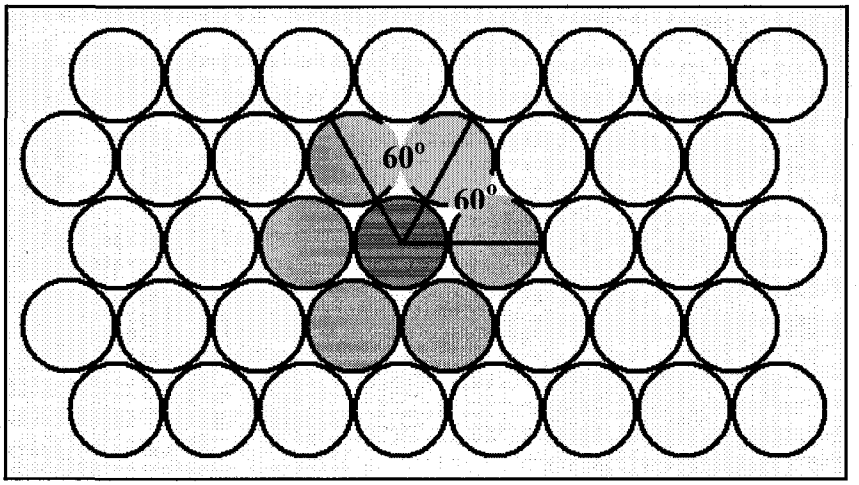

Figure 2.1: Maximum Density Configuration of Uniformly Sized, Circular Particles

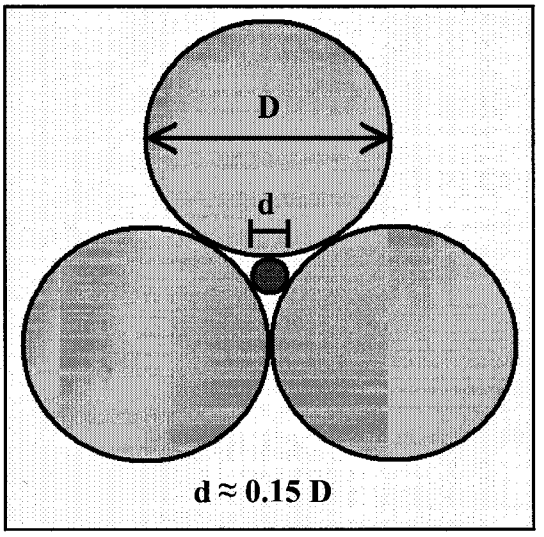

Figure 2.2: A Fine Particle Filling the Gap Between Coarse Particles

The Bailey Method accounts for the irregularity in particle shape by assuming that some of the faces touching the smaller particle are flat. As more of the large particles have flat faces, the gap between them grows, allowing a larger small particle inside it.

Figure 2.3 illustrates the increasing size of the small particle with an increasing number of flat faces along with the corresponding ratio of diameters of small to large particles.

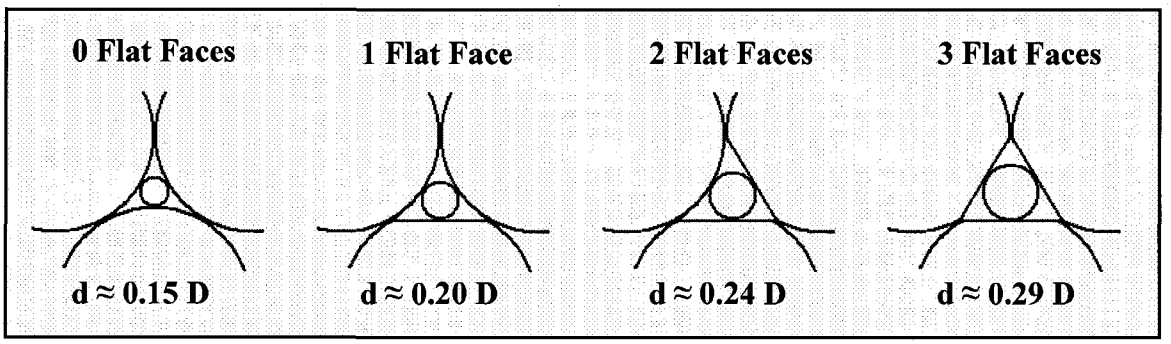

Figure 2.3: Particles Inside Gaps with Varying Number of Flat Faces

Since the gap between any random three large particles contains an unknown number of round and flat faces, the Bailey Method uses an average of the four ratios: 0.22. Although real aggregate is three dimensional, the method assumes that a particle diameter ratio of 0.22 is appropriate for normal aggregate particles, for the purposes of practicality.

The Bailey Method uses this ratio of small to large particles to establish three sieves that separate the aggregate blend into coarse and fine sections. The Nominal Maximum Size Aggregate (NMSA) is the sieve size that is one higher than the first sieve to retain more than 10% of the aggregate blend. The Primary Control Sieve (PCS) is defined as the sieve closest to 0.22 times the NMSA. The Secondary Control Sieve (SCS) is defined as the sieve closest to 0.22 times the PCS, and the Tertiary Control Sieve (TCS) is defined as the sieve closest to 0.22 times the SCS. The Half Sieve is defined as the sieve closest to 0.5 times the NMSA. The Half Sieve is used for calculating aggregate weight ratios, which will be discussed later. Table 2.1 shows the

breakdown of control sieves for various NMSA sizes with all values in millimeters. For an NMSA of 12.5 mm, the Bailey Method allows using a calculated value for a fictitious Half Sieve of 6.25 mm instead of the closest normally used sieve, which is the #4 (4.75 mm) sieve. The percent passing the 6.25 mm sieve is calculated by linear interpolation.

Table 2.1: Control Sieves for Various NMSAs

NMSA	25.0		19.0		12.5		9.5	
	Calc.	Chosen	Calc.	Chosen	Calc.	Chosen	Calc.	Chosen
Half	12.5	12.5 (1/2")	9.5	9.5 (3/8")	6.25	6.25	4.75	4.75 (#4)
PCS	5.50	4.75 (#4)	4.18	4.75 (#4)	2.75	2.36 (#8)	2.09	2.36 (#8)
SCS	1.05	1.18 (#16)	1.05	1.18 (#16)	0.52	0.60 (#30)	0.52	0.60 (#30)
TCS	0.26	0.30 (#50)	0.26	0.30 (#50)	0.13	0.15 (#100)	0.13	0.15 (#100)

These control sieves first separate the aggregate into coarse and fine parts, and then separates the fine portions further. Everything larger than the PCS in the blend is considered "coarse", and everything smaller is considered "fine". Within the fine portion, aggregate larger than the SCS is considered the coarse part of the fine aggregate, and smaller aggregate is the fine part of the fine aggregate. The TCS separates the fine part of the fine aggregate similarly. The aggregate smaller than the Half Sieve and larger than the PCS is the fine part of the coarse aggregate. The Bailey Method refers to these particles as "interceptors". Figure 2.4 is a graphical representation of this separation.

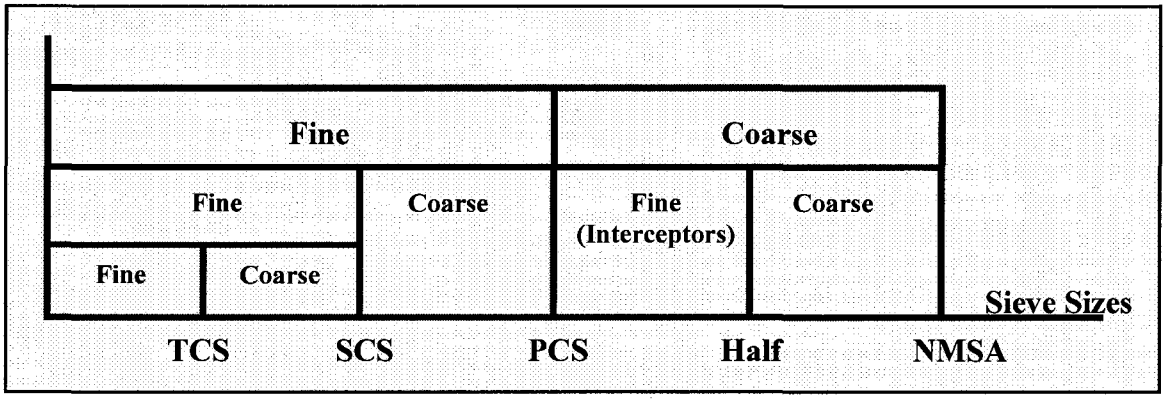

Figure 2.4: Separation of Aggregate Blend into Find and Coarse Parts

To achieve a balanced blend in a practical way, with enough coarse aggregate to form a complete skeleton and enough fine aggregate to fill in the gaps without over filling, it is necessary to know the density of the coarse aggregate. The Chosen Unit Weight (CUW) is a percentage of the measured Loose Unit Weight of the coarse aggregate. It indicates how much void space must be filled by the fine aggregate, which influences the distribution of the amount of aggregate in each section between the control sieves. The Bailey Method uses these weights to calculate three weight ratios that help the engineer better understand and predict how the aggregate blend will behave. These are the Coarse Aggregate (CA) Ratio, the Fine Aggregate - Coarse (FAc) Ratio, and the Fine Aggregate - Fine (FAf) Ratio. Table 2.2 shows the four Bailey parameters including the chosen unit weight, the three ratios, their equations, and their recommended limits.

Table 2.2: The Four Bailey Parameters

Parameter	Calculation*	Recomended Limits
CUW	None	95% - 105% (for coarse graded mix)
CA Ratio	=(Half - PCS)/(100 - Half)	0.50 - 0.65 (for NMSA of 12.5mm) 0.60 - 0.75 (for NMSA of 19mm)
FAc Ratio	=(SCS)/(PCS)	0.35 - 0.50
FAf Ratio	=(TCS)/(SCS)	0.35 - 0.50

* Each calculation uses the percent passing the control sieves

The CUW can affect the properties of the final asphalt mix by affecting the whole aggregate blend. Since the Loose Unit Weight represents the coarse aggregate under no compactive force, there are lots of spaces for fine aggregate to exist, meaning there will be more aggregate passing the PCS than in a denser configuration. Generally, a higher CUW means greater stone on stone contact for the coarse aggregate because it has been compacted to some degree. This means the blend will be stronger in compression and better at resisting ruts. However, it also means that the asphalt mix will be more difficult to compact. These effects combine to produce, in general, larger voids in the mineral aggregate (VMA). A lower CUW has the opposite effect: greater void space for fine aggregate, greater compactability, less compressive strength, and generally lower VMA. However, the final VMA of a mix will be determined by a combination of all the parameters. The influence of each can be numerically added together for a total predicted influence on VMA. Table 2.3 summarizes the influence of each of the parameters.

Table 2.3: Predicted Effect of Bailey Parameters on VMA

Parameter	Change in parameter	Predicted effect on VMA
CUW	+ 0.5%	+ 0.5% to + 1.0%
CA	+ 0.2	+ 0.5% to + 1.0%
FAc	+ 0.05	− 0.5% to − 1.0%
FAf	+ 0.05	− 0.5% to − 1.0%

In the Bailey Method the coarse aggregate has a strong influence over the strength and workability of the final blend; therefore, it is important to understand the role of the interceptors. A configuration of coarse particles with maximum stone on stone contact would look like a three dimensional version of Figure 2.1. However the actual aggregate particles are neither perfectly spherical nor uniform in size, which leaves irregularly sized

gaps throughout. Additionally, there are often not enough particles in the coarse portion of the coarse aggregate to make up a complete skeleton for the whole volume of the pavement. The interceptors can fill in the larger gaps and fill out the rest of the coarse aggregate skeleton. The CA Ratio compares these interceptors, the fine part of the coarse aggregate, to the coarse part of the coarse aggregate to indicate the behavior of the final asphalt mix. Generally, as the CA Ratio increases, the VMA also increases. However, problems can occur if the CA Ratio is too high or too low.

If there are not enough interceptors, the CA Ratio drops below the prescribed limits and the Bailey Method predicts that the compacted asphalt mix may segregate. The Method does not give any mathematical support for this prediction, so it is assumed that it is made on empirical evidence. A pavement that has segregated has patches that are predominantly fine or coarse aggregate (Roberts, et al. 1996). Sections of mainly fine aggregate will have a higher tendency to rut, while the sections of coarse aggregate may be too porous or start to ravel and wear away. The interceptors are needed to fill in any large gaps to complete the coarse aggregate framework, keeping the density generally uniform throughout the pavement so there are no segregated sections.

Another problem may arise when there are too many interceptors. If the CA Ratio is above the limits, then the interceptors push apart the large stones. The large particles from the coarse part of the coarse aggregate still contribute to the strength of the pavement, but their effectiveness is reduced because they are not touching each other. While the interceptors are still coarse aggregate, they are generally only half the size of

the very coarse particles. The extreme case is where the interceptors become the new "coarse aggregate" with voids that are too small for the particles passing the PCS. In this scenario, the fine aggregate pushes apart the interceptor frame, thus reducing the strength and promoting rutting. The very coarse particles are not very useful because they have relatively little support.

The FAc Ratio compares the fine part of the fine aggregate to the coarse part of the fine aggregate, and the FAf Ratio in turn compares the coarse and fine portions of the fine part of the fine aggregate. As the fine aggregate fills in the gaps of the larger aggregate, it adds to the strength of the mix by providing support to the coarse aggregate and it brings down the Air Void (AV) ratio to an acceptable level. In addition, the finer portions of the fine aggregate act as a dry lubricant to the larger particles allowing easier compaction. These combined effects mean that as the FAc and FAf Ratios increase, the VMA of the final mix tends to decrease. The problems that can occur when either of these ratios is too high or too low are similar.

If either the FAc or the FAf ratio is allowed to get too high, above 0.5, then the fine particles push their way between the larger ones, overfilling the gaps in the coarse aggregate. The result is a mix that can be too tender and easily deformable as the large particles slide around on their coating of tiny particles. Additionally, the AV and VMA may decrease to below their own limits. When the FAc or FAf ratios drop too low, then the small gaps are under filled. This causes the VMA to rise, but also deprives the mix of the lubricating effect of the fine particles, which may make it difficult to compact the mix

to the proper level. Improperly compacted pavement can have too many voids for water and air to invade, which can cause the asphalt binder to be stripped from the aggregate or allow excessive frost heaves in the winter.

Designing Aggregate Blends with the Bailey Method

The calculations given in the Bailey Method determine the volume of the voids in the coarse aggregate and put in just enough fine aggregate to fill those voids. Then the contributions of the coarse and fine aggregate are adjusted to account for any fine or coarse parts in each respective aggregate. Finally mineral filler is added as needed and final adjustments are made. Several pieces of information about the aggregate stockpiles are required: the Bulk Specific Gravity (Gsb), the Loose Unit Weight, the Rodded Unit Weight, and the grading. For any mineral filler in the mix, such as Bag House Fines, only the grading is required. The full calculations can be found in the Appendix 1.

There are several input values that the engineer must chose and include in the calculations. These include the CUW, the contributions of each stockpile, and the desired dust content. For a coarse graded mix, the designer should select a CUW between 95% and 105%. This produces a blend in which the coarse aggregate dominates, yet is still loose enough for reasonable workability. A CUW less than 90% leads to a mix where the coarse aggregate is separated, leaving the fine aggregate to dominate. Altered limits are given for the weight ratios if the designer wants a fine graded mix in this way. According to the Bailey Method, a CUW between 95% and 90% produces a mix where coarse

aggregate is not dense enough to adequately dominate, yet doesn't provide enough space for the fine aggregate to adequately dominate. A CUW greater than 110% leads to a very dense configuration of coarse aggregate most commonly associated with a Stone Matrix Asphalt (SMA). Just as with a fine graded mix, alternate limits on the weight ratios are given for designers who want an SMA mix.

Next, the designer chooses the initial contributions of the coarse and fine aggregate stockpiles. Since the amount of fine aggregate needed is not known until the approximate volume of the voids in the coarse aggregate is known, the initial contributions of all the stockpiles are not given as percentages of the whole blend. The contributions of the coarse stockpiles are inputted as percentages of the whole coarse aggregate and the fine stockpiles are inputted as percentages of the whole fine aggregate. Therefore all the coarse contributions add up to 100%, as do all of the fine aggregate contributions. The designer can expect the final blend contributions to closely match the input values.

The final choice for the designer is the amount of dust material that is desired, as defined by particles smaller than 0.075 mm. This is limited to 3.5% to 6% for the entire blend. If the amount of dust provided by the coarse and fine aggregate stockpiles does not satisfy the requirement, then a mineral filler stockpile is added. The final contributions of the fine aggregate are adjusted to account for the added mineral filler. Filler is too fine to affect the final calculations for the coarse aggregate.

Once the calculations have been run, the engineer is left with a final aggregate blend that can be tested against the control points as prescribed by Superpave. The Bailey aggregate ratios can also be directly calculated and compared to the recommended limits. These calculations do not require the fabrication of any samples and can be iterated by a computer as many times as needed to find an acceptable blend. Additionally, when redesigning a blend, the Bailey weight ratios and CUWs of the old and new blends can be compared to have an idea of the expected change in VMA and behavior of the new mix design.

To evaluate an existing mix design using the Bailey Method, the engineer must first ascertain the aggregate stockpile data including grading, bulk specific gravity, and loose and rodded unit weights. The calculations described above are performed with these data. The engineer varies the input parameters until the calculated aggregate blend matches the original mix design. The purpose is to find the chosen unit weight for this mix. If the chosen unit weight falls between 95% and 105%, then the mix is considered a coarse graded mix. If the chosen unit weight is found to be less than 95% then the mix is considered fine graded, and if it is more than 105% then it is considered an SMA mix.

The next part of the evaluation is to look at the three weight ratios, CA, FAc, and FAf, for the original mix design. The weight ratios are calculated directly from the original mix grading, not the calculated mix grading, and are compared to recommended limits. If the mix is coarse graded, then the calculations and limits stated in Table 2.2 can be used. If the CUW is low enough to put the mix in the fine graded range, there are

different calculations for the Bailey weight ratios. Basically, the grading above the coarse graded PCS, which is 0.22 times the NMSA, is ignored and the coarse PCS is considered the new NMSA. The control sieves are recalculated based on this fine NMSA and the weight ratios are calculated from the fine control sieves. The limits on the FAc and FAf ratios are the same; however, the limit for the CA ratio is changed to 0.6 to 1.0 regardless of the original NMSA.

Limitations of the Bailey Method

The Bailey Method is mainly suited to design well graded asphalt mixes based on particle size distribution. It includes modifications to the ratio limits to accommodate fine graded mixes and SMA mix designs as well. However, the Bailey Method has a couple of limitations. These include accounting for aggregate properties other than size and how to include Recycled Asphalt Pavement (RAP).

The Bailey Method mentions several different aggregate properties that affect performance including size, angularity, texture, and material strength. The calculations and procedures mainly use particle size to design the mix. There are various points where it cautions the engineer not to forget the other properties because they can affect the VMA despite the predictions of the Bailey Method. However, there are no calculations or procedures that describe how to account for these properties. The only time aggregate properties other than size play a practical role in the Bailey Method is by using the loose and rodded unit weights. This is because the configuration of the

aggregate particles by rodding or pouring is easily affected by shape and texture. Engineers that use the Bailey Method should compare the results of the calculations to their own experience and make a proper judgement call.

Finally, the Bailey Method does not give very detailed provisions for working with RAP. The main reason RAP cannot be included as simply another aggregate stockpile is because there is often no bulk specific gravity or loose or rodded unit weight data for it. Although bulk specific gravity could be measured, it often isn't and might vary widely throughout the stockpile. Taking measurements on the rodded unit weight might be difficult since there is binder present in the aggregate. Additionally, the RAP may or may not fully blend with the virgin aggregate and binder making the grading approximate at best. Because of this, the Bailey Method states that the engineer should use only virgin aggregates in the calculations. The method directs the designer to add in the RAP at the end, using the RAP grading measured after binder extraction. The engineer should then adjust the virgin contributions so that the total combined grading has the same, or as close to the same, percent passing the PCS as calculated with the virgin aggregate alone. However, there is no mention as to how the virgin contributions should be changed and the preservation of the fine weight ratios is ignored. Additionally, when evaluating an existing mix designed with RAP, the calculations should be done on the virgin aggregate only and then adjusted to account for the RAP. Again, the method of adjustment is left to the engineer.

CHAPTER 3

THIRD SCALE MOBILE MODEL LOAD SIMULATOR

Overview

The Mobile Model Load Simulator (MMLS3) simulates truck tires, at one third scale, driving over asphalt pavement. Unlike uniaxial testing, including dynamic modulus, strength, and fatigue tests, this kind of machine tests the performance of the asphalt mix directly with all the complex forces and factors acting at once. Additionally, this machine can simulate years of traffic loading in only a few hours. This kind of testing is more commonly known as accelerated pavement testing (APT). The MMLS3, with its accompanying accessories, is able to simulate various conditions, both in the laboratory and in the field. There are various advantages the MMLS3 has over other kinds of APT devices and several limitations as well. Figure 3.1 shows a picture of the MMLS3 on its test bed in the laboratory at UNH.

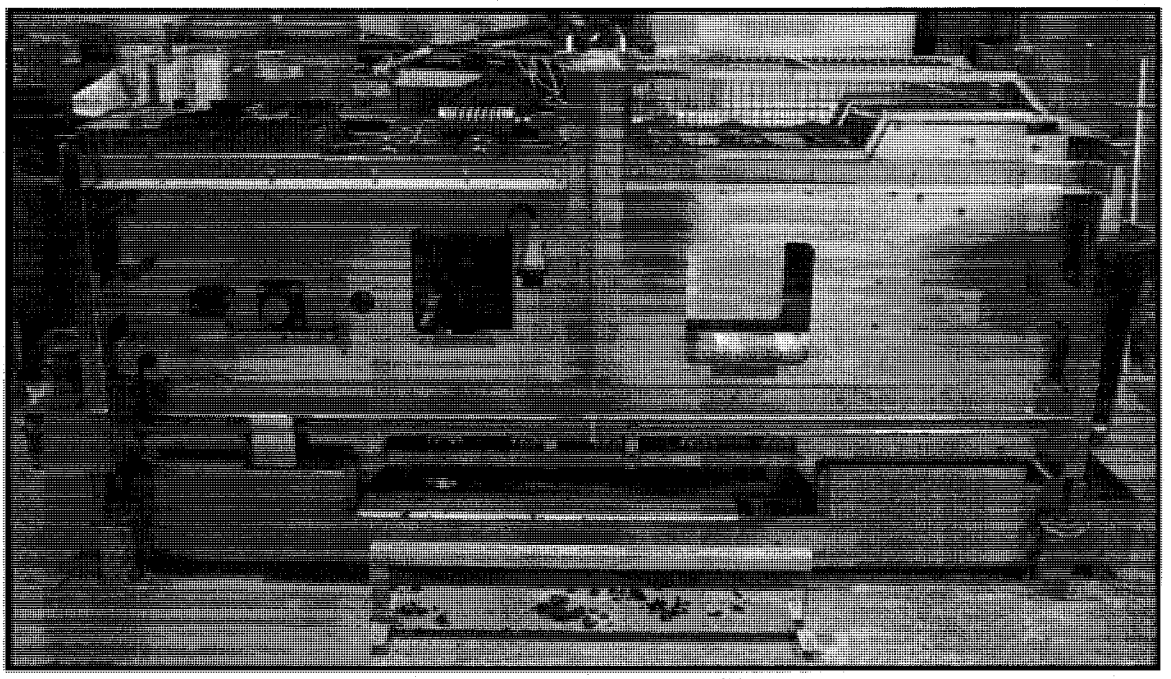

Figure 3.1: The MMLS3

Accelerated Pavement Testing

One of the main advantages of simulating real truck loads is that the expected behavior of the asphalt pavement in the road can be seen in the laboratory. Tests that use isolated loads, such as uniaxial loads, are good for testing certain single properties of an asphalt mix like dynamic modulus, strength, and resistance to fatigue failure. There are mathematical models that can use these properties to predict the pavement's resistance to certain types of damage under service loads in the field. However, a simulation is a good way to corroborate these separate tests. Additionally, the engineer can see which type of failure is most dominant under actual traffic loads.

Since asphalt pavement is meant to last for ten to twenty years, its resistance to damage from traffic loading over a short time is very high. Therefore, the rate of loading

in APT is greatly increased. Asphalt is viscoelastic and behaves differently depending on loading rate and temperature. A high loading rate will cause asphalt to behave more stiffly. However, a high temperature will cause asphalt to behave less stiffly. The combination of high temperature and high loading rate somewhat cancel each other. Therefore, the asphalt can be loaded at a high rate without the stiffening effect. There is research in developing mathematical models to convert the test results from accelerated testing under the MMLS3 into predicted behavior in the field. However, for this project the results from the MMLS3 were only used for comparison purposes; no prediction is made for actual behavior in the field.

Physical Structure and Capabilities

The basic structure of the MMLS3 is shown in Figure 3.2. Four inflated tires are run repeatedly over the asphalt. These tires are part of a looped wheel train that is made up of eight bogies, which are the cars of this train. The train is driven by a motor at one end that turns a large drive drum. Small guide wheels on each bogie are pinched between the drive drum and a guiding arc. As the drive drum turns, it forces the guide wheels to roll, thus moving the whole train along.

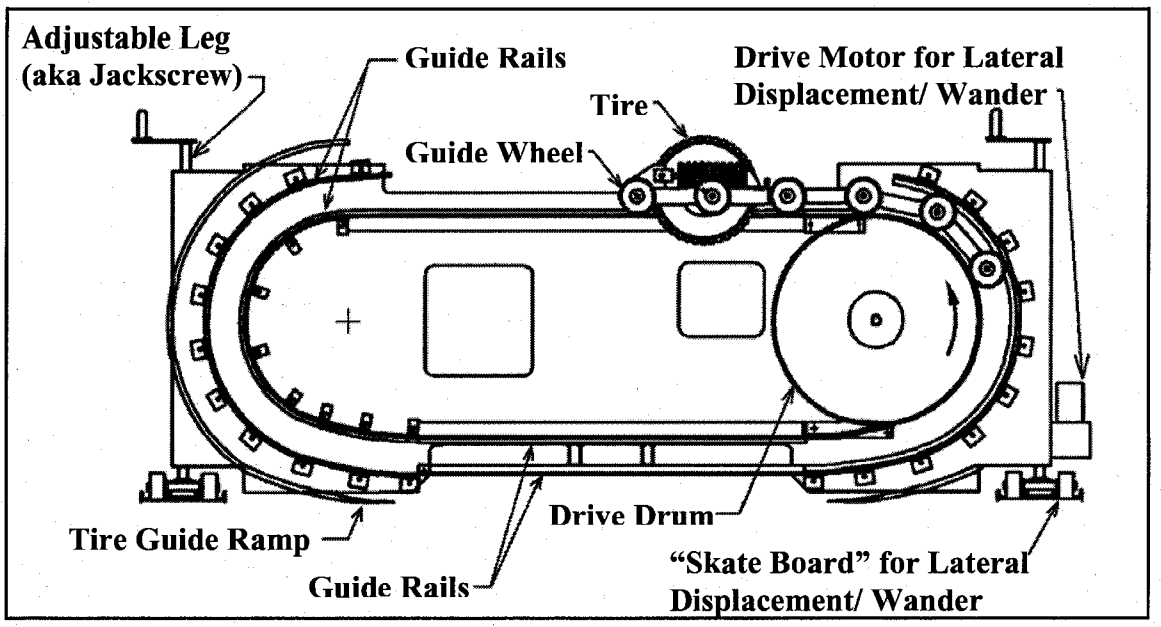

Figure 3.2: Basic Structure of MMLS3 (MMLS3 Operators Manual, p. 5)

A picture of a bogie with a tire and a schematic drawing, taken from the MMLS3 service manual, are shown in Figures 3.3 and 3.4 respectively. The tire is approximately 290 mm in diameter and approximately 80 mm wide. The tires are inflated with an inner tube to 700 kPa. The use of inflatable tires, and their internal pressure, were chosen by the MMLS3 designers to better simulate truck tires at one third scale.

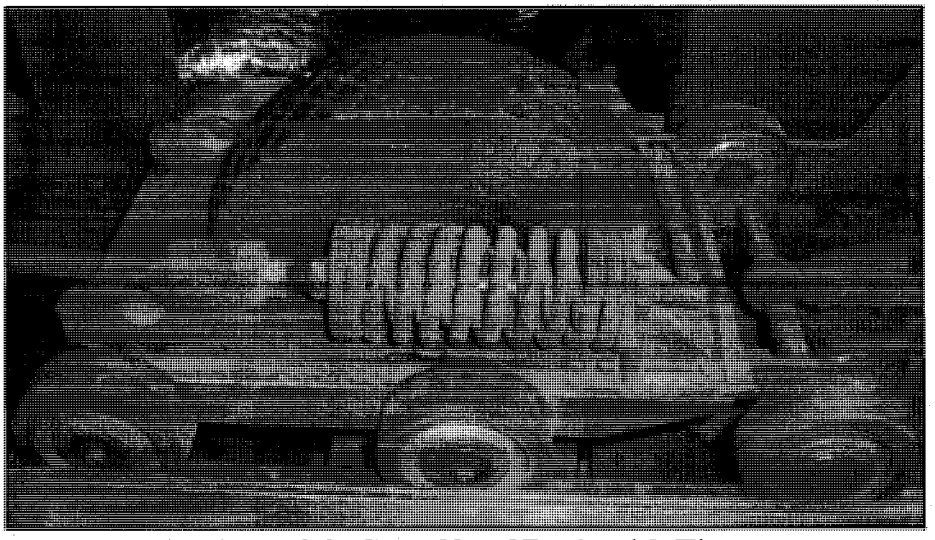

Figure 3.3: Close Up of Bogie with Tire

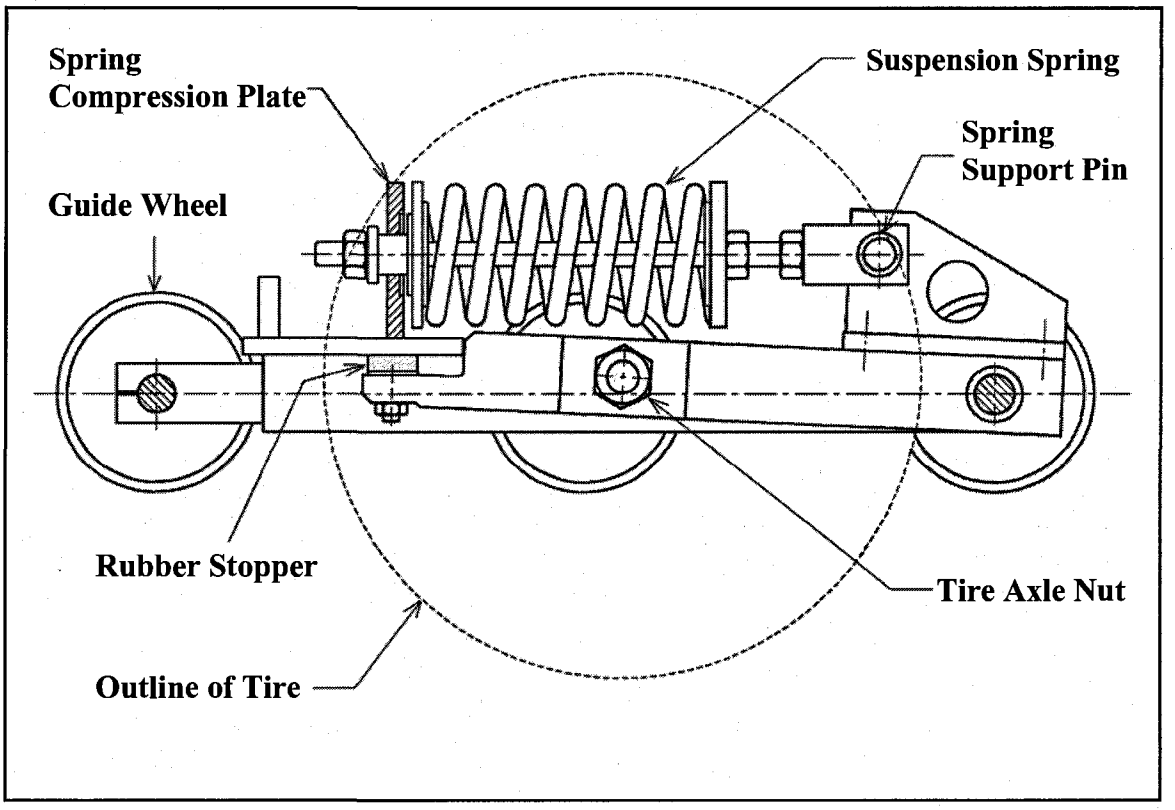

Figure 3.4: Schematic of Bogie with Tire and Suspension (MMLS3 Operators Manual, p. 10)

The guide track along the bottom of the machine keeps the tires running over the same locations at the same height throughout the test. As the asphalt ruts, the surface will slowly move away from the tires over the course of the test. The suspension system for the tires was designed to minimize the change in vertical force as the asphalt surface changes. This is achieved by converting large deflections in the tire to small deflections in the horizontal spring. The deflection is reduced by using a large lever arm to hold the tire axle and a small lever arm to connect to the spring, as illustrated in Figure 3.4. The force that the tires apply is adjusted to 2.7 kN by lengthening or shortening the springs and using a detachable load cell to monitor the force, shown in Figure 3.5. Note the deflection of the tire as indicated by the 10 mm gap between the rubber stopper and the metal frame of the bogie.

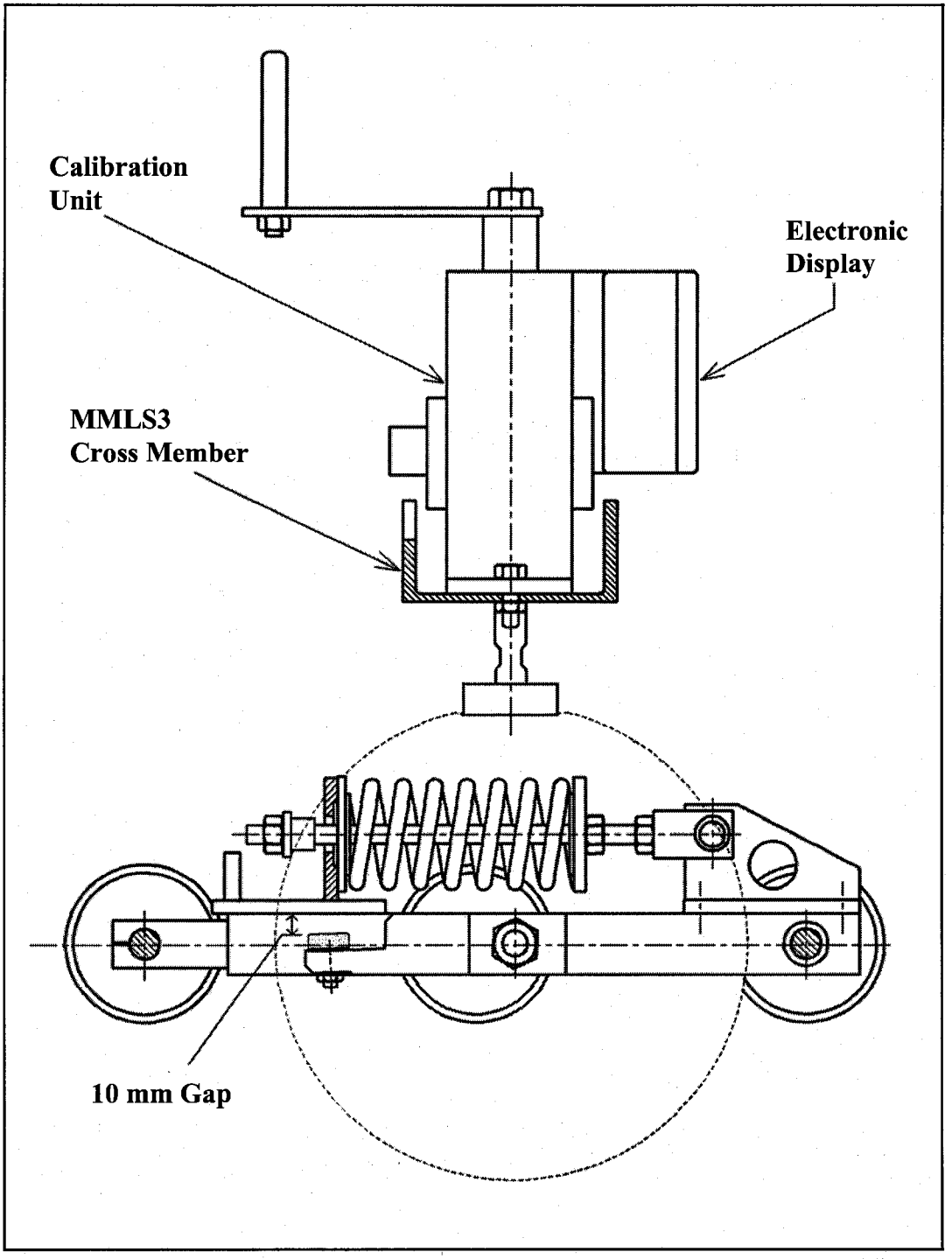

Figure 3.5: Load Calibration Unit (MMLS3 Operators Manual, p. 11)

The MMLS3 control unit supplies power to the machine and records its usage by means of a counter that shows how many tens of wheel loads have been run since it first began. A dial can adjust the speed of the machine from full stop up to two wheel loads

per second. The MMLS3 has the additional capacity to wander side to side to simulate traffic that does not always travel along the exact same path. The control unit has a separate power cord that connects to the wander motor on the side of the MMLS3. A user can input the magnitude of the wander from the display panel. Figure 3.6 shows the control unit for the MMLS3.

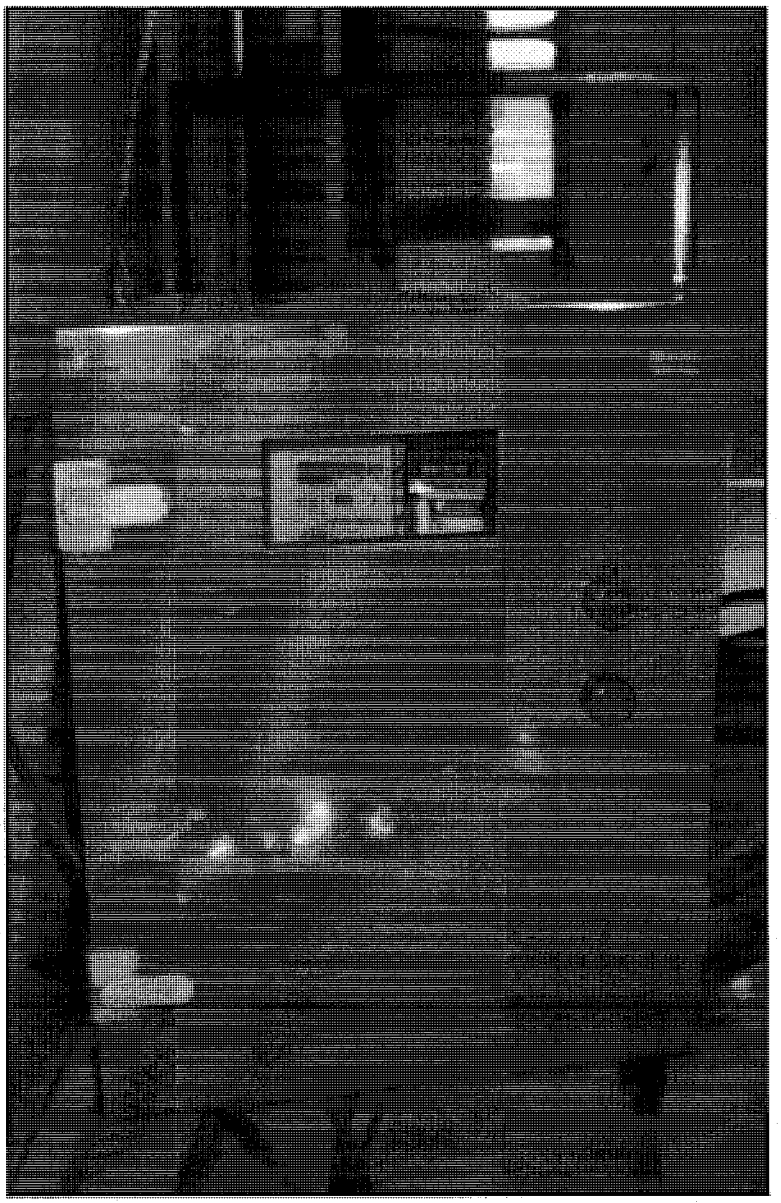

Figure 3.6: Control Unit for the MMLS3

There are several environmental simulation accessories that can be used with the MMLS3. The first is a dry air heating/ cooling unit. This unit blows air over the surface of the asphalt through two large vents that sit on each side of the MMLS3. One vent is at positive pressure and one is at negative so that the hot, or cold, air is recycled, reducing strain on the heating/ cooling unit. The dry air heater/ cooler is shown in Figure 3.7. The second item is a wet heater. This unit pumps hot water into the test bed or on the road surface. Much like the dry air unit, this heater recycles the hot water as much as possible. The wet heater is shown in Figure 3.8.

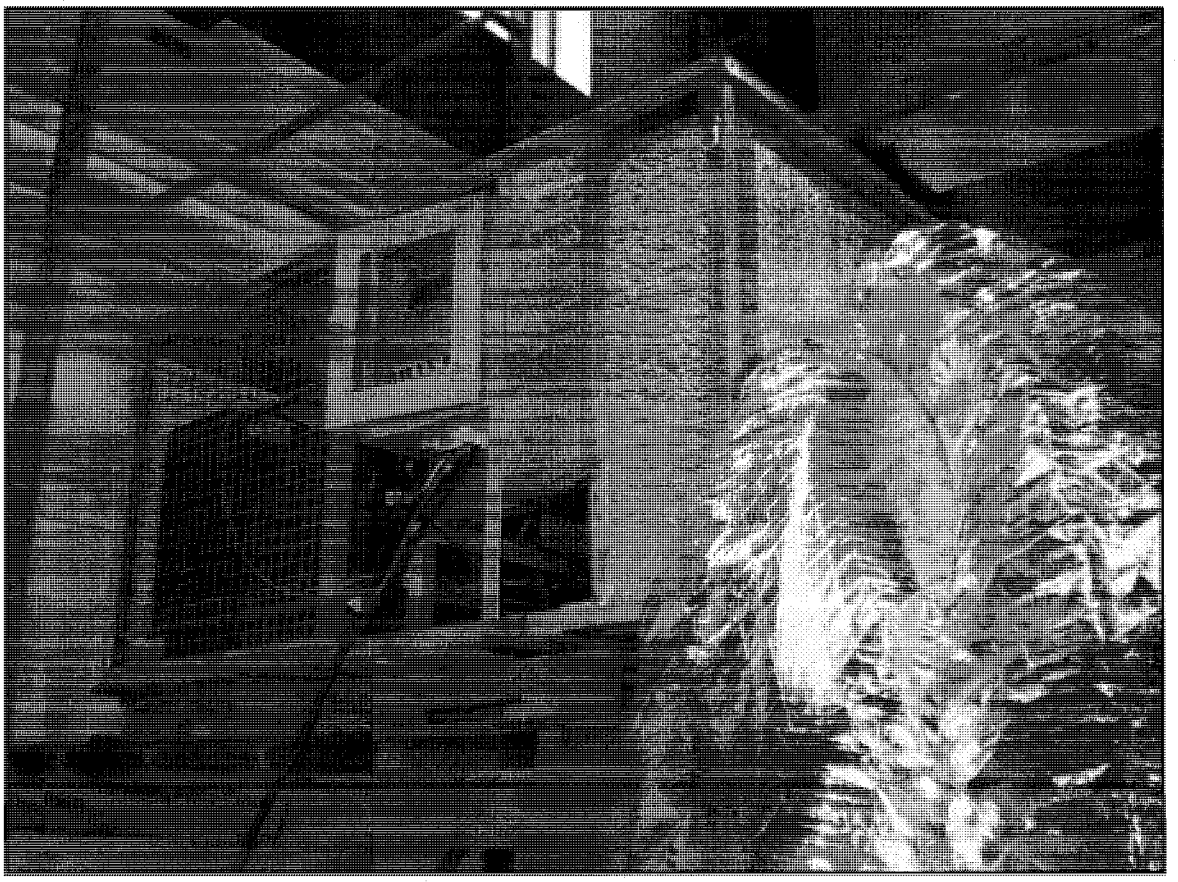

Figure 3.7: Dry Air Heating/ Cooling Unit

Figure 3.8: Wet Heating Unit

An environmental chamber can be assembled around the MMLS3 to preserve the asphalt temperature during testing. The chamber walls are made of thin sheets of metal with approximately 40 mm of insulating foam between them. They have spaces for the cables and dry air vents. Figure 3.9 shows the environmental chamber erected around the MMLS3.

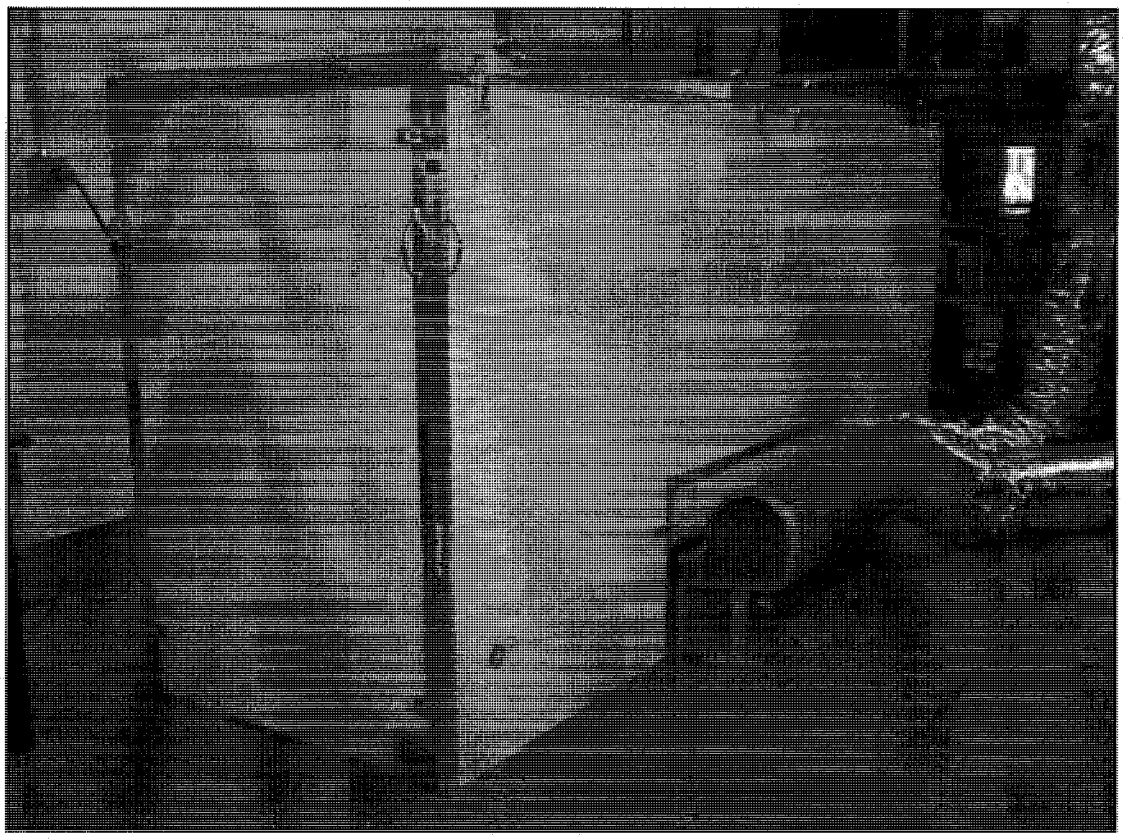

Figure 3.9: The Environmental Chamber

The MMLS3 test bed can hold nine bricks, each approximately 150 mm long, round face to round face, and 105 mm wide, cut face to cut face. Figure 3.10 shows a fabricated brick ready for testing. The test bed is 100 mm deep, so aluminum plates are used to raise the bricks to the top. On the bottom are the rectangular plates, 100 mm by 310 mm, that take up most of the height. On top of these are plates the same shape as the brick, but of varying thicknesses. These can be mixed and matched to bring the surfaces of all the bricks to the same level. The top plate is also the same shape as the sample brick and is 10 mm thick with a textured surface to keep the brick from slipping during the test. Figure 3.11 shows the test bed with the various plates and the asphalt bricks.

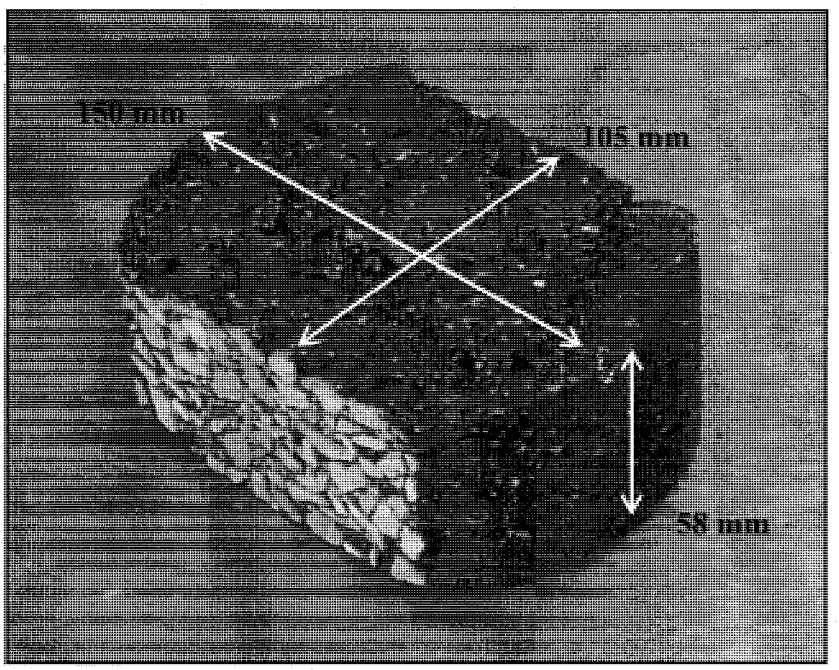

Figure 3.10: Sample Brick

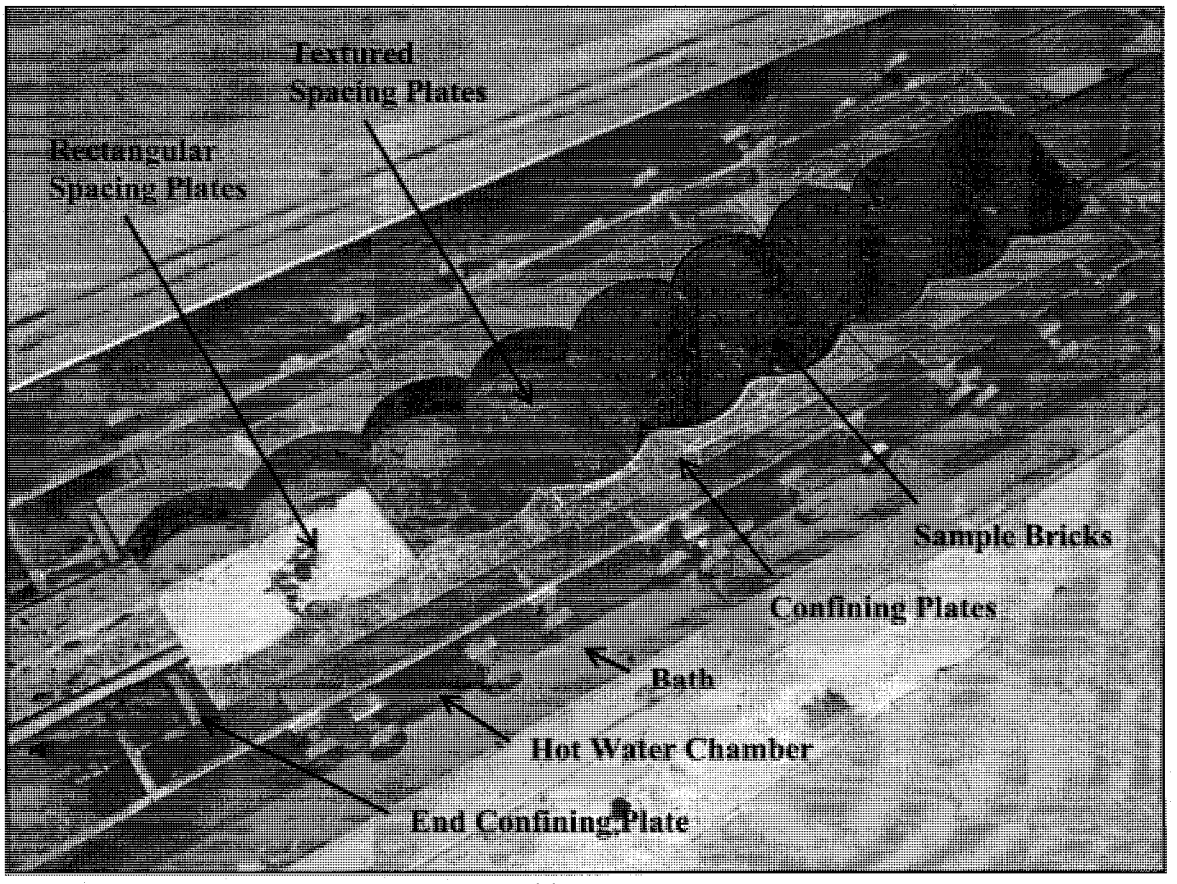

Figure 3.11: The Test Bed

On either side of each set of three bricks were thick, curved plates, shown in Figure 3.10, to keep the bricks in line and to simulate confining pressure that the asphalt would encounter in an actual road. Screws, set into the walls of the test bed, push and keep these confining plates in place. On one end of the test bed is a flat confining plate with two large screws to provide confinement along the long axis. Around the test bed is a large bath that can hold water for wet testing. Additionally, there is a chamber directly under the test bed that can hold hot water. This chamber is designed to help raise and preserve the temperature of the samples without wetting them.

In addition to performing tests in the lab, the MMLS3 can be taken into the field to perform APT directly on paved roads. The environmental chamber can be used outside, as well as the dry air heating/ cooling unit with its vents. The wet heater connects to a line of spray nozzles and suction vents to saturate the road with hot water.

The profile of the asphalt surface is measured with a tool called a profilometer. It is approximately one meter long and can measure ruts down to 40 mm from its set height with a sensitivity of 0.001 mm. The profilometer rests on two support rails that are permanently set in place during the course of a test. These support rails have grooves and dimples in them to ensure that the profiles are taken in the same places every time during testing. The height from which each profile is measured is kept constant by screws with locking wing nuts on the ends of the profilometer. The profilometer is connected, through its power supply unit, to a computer. A simple program on the computer allows the user to designate the file the data goes into and the measurement size and increments.

The profilometer drags a small metal wheel on a lever arm over the asphalt surface to measure the profile. Changes in the angle of the lever arm are converted to vertical displacement of the wheel. Figure 3.12 shows a diagram of the profilometer in place over rutted pavement. Figure 3.13 shows a close-up of the small wheel as a profile is being measured.

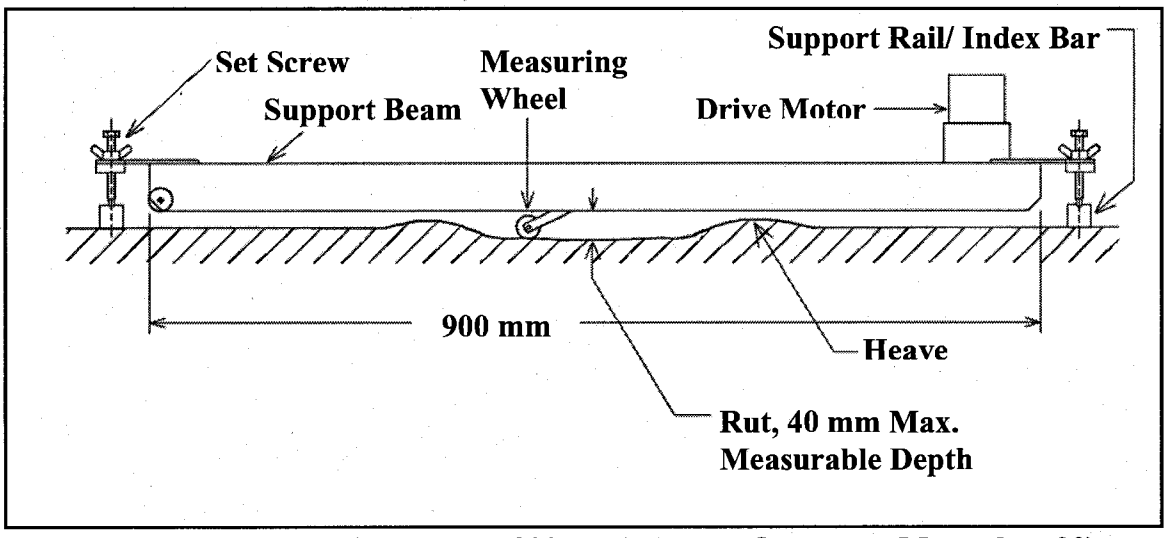

Figure 3.12: The Profilometer (P900 Profilometer Operators Manual, p. 20)

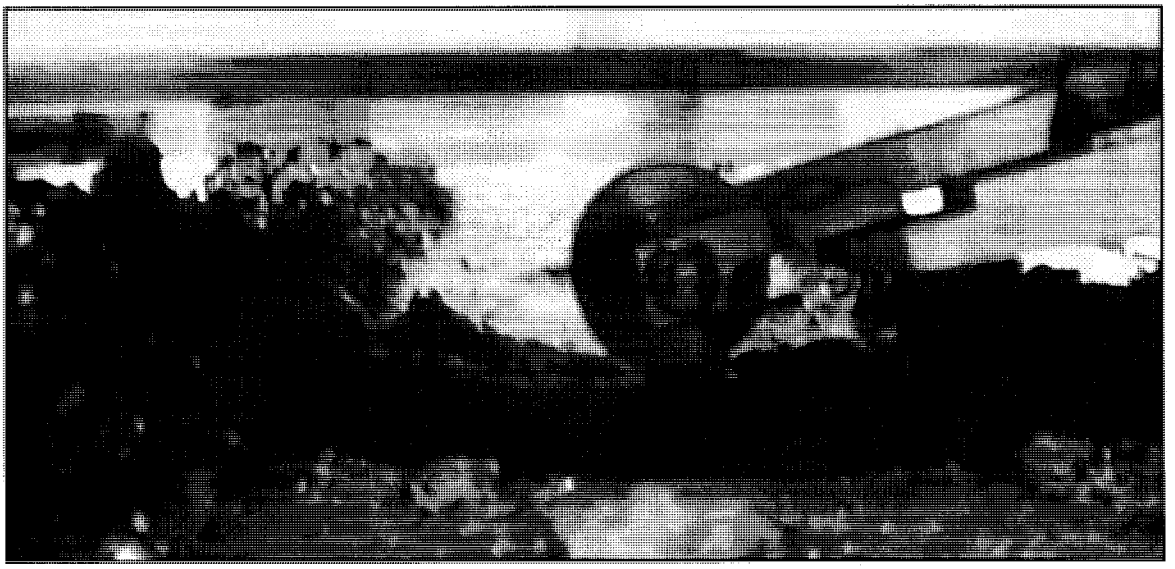

Figure 3.13: A Profile Being Measured

Advantages and Disadvantages

There are other kinds of APT machines in use including the Texas Model Load Simulator (TxMLS), the Hamburg Wheel Tester, and the Asphalt Pavement Analyzer. The Texas Model Load Simulator is a full scale model of truck tires driven over asphalt. The Hamburg Wheel Tester and the Asphalt Pavement Analyzer simulate wheel loads at a very small scale. The main advantage of the MMLS3 is that it is large enough to adequately simulate truck loads, yet small enough to be relatively portable. Additionally, the MMLS3, with its extra equipment, can simulate environmental conditions in addition to traffic loads.

When simulating loads on asphalt, it is easier to create a scale model of the loading structure, in this case large trucks, than of the pavement. The asphalt mix cannot be easily scaled because any changes in the aggregate particle sizes will change the performance properties. Even if the aggregate blend could be scaled with predictable results, the asphalt binder's reaction to force and interaction with the aggregate cannot be scaled. Therefore, it is desirable to create a simulation of truck loads as close to their true size as possible. A full scale simulation matches exactly with the scale of the tested asphalt mix. At any lower scale, there will be a discrepancy that must be accounted for by modeling mathematics. The advantage the MMLS3 has over small APT devices like the Hamburg Wheel Tester and the Asphalt Pavement Analyzer is that it is closer to the scale of the asphalt than they are and it is easier to make a prediction on actual road performance from its results.

Although the MMLS3 is large and sometimes difficult to move, accommodate, and work with, it may be easier than using a full scale tester like the TxMLS. Large scale simulations require more asphalt pavement than small scale models, thus requiring more sample fabrication in the lab or the movement of the machine to the field. Additionally, a large testing machine requires more powerful machinery to simulate environmental conditions like heat and cold.

One of the main disadvantages is using the MMLS3 in the field. While the MMLS3 is much smaller than the Texas Model Load Simulator, it is still very large and heavy making it difficult to move around. Additionally, its associated heaters each require a different kind of power supply that often necessitates separate generators. The wet heater, in particular, requires 50 Hz power, which is uncommon in the US. When using the wet heater in the field there is considerable water loss, meaning that the heater may have to run for a long time to get the wet asphalt up to the required temperature. Even if there were no problems whatsoever with the set up of the MMLS3 and its associated equipment, a normal test can run for a long time. At two wheel loads per second, a test of 100,000 wheel loads will take almost 14 hours to complete. Add to this the time for a number of profiles throughout the test, during which the MMLS3 is temporarily stopped. This would require a person to monitor the machine all day and into the night. Furthermore, testing schedules can be thrown off if parts need to be ordered and replaced due to mechanical wear and tear. Regular care and maintenance can help to prevent unexpected problems of that nature.

CHAPTER 4

MATERIALS AND METHODS

Overview

The New Hampshire Department of Transportation (NHDOT) provided six mix designs for this research project. These mix designs were chosen as representative asphalt mixes that are commonly used throughout New Hampshire. Half of these designs used gravel stone and half used fractured rock. In each half, one mix design incorporated RAP. Table 4.1 summarizes the six original mix designs. Full details for each is provided in Appendix 3. After testing the samples from these six mix designs, three were redesigned according to the Bailey Method. An additional two MMLS3 tests were run on field cores taken from Route 25, between Effingham and Freedom in New Hampshire, which used the Oss mix designs.

Table 4.1: Summary of Original Mix Designs

Mix Name	Aggregate	NMSA	Binder	AC*	RAP	Company, Location	Note
Oss 12.5	Gravel Stone	12.5 mm	PG 64-28	5.6		Pike, Ossipee	Redesigned
Oss 19	Gravel Stone	19 mm	PG 64-28	5.0		Pike, Ossipee	
Cont 12.5	Fractured Rock	12.5 mm	PG 64-28	5.5		Continental, Londonderry	
Cont 19	Fractured Rock	19 mm	PG 64-28	5.0		Continental, Londonderry	Redesigned
Farm	Gravel Stone	12.5 mm	PG 64-28	5.50	RAP	Pike, Farmington	Redesigned
Hook	Fractured Rock	12.5 mm	PG 64-28	5.60	RAP	Pike, Hooksett	

*This is total AC. The RAP AC and Virgin AC for the mixes containing RAP are detailed later.

Materials

The mix designs Oss 12.5, Oss 19, and Farm all used gravel stone as the virgin aggregate. This kind of aggregate generally has rounded, smooth faces with few flat and elongated particles even when crushed. The Cont 12.5, Cont 19, and Hook mix designs used fractured ledge rock as virgin aggregate. As opposed to gravel stone, this aggregate is angular and often rough with more flat and elongated particles. The Farm and Hook mix designs used 7/16" processed RAP. All known details about these aggregates stockpiles including grading, specific gravities, and unit weights are listed in Appendix 3.

Each of the four asphalt mixing plants, listed in Table 3.1, provided both aggregate and asphalt binder for the mix designs that were selected from those locations.

The majority of the materials were acquired in June and July of 2004, and additional materials were gathered in the subsequent years as needed. The additional aggregate appeared to have the same properties as the original aggregate. In accordance with AASHTO T-2-91, a loader laid mats of aggregate from scoops at various heights of the stockpiles and workers filled the barrels from the mats either by loader or by shovel. The aggregate from the Pike plants were stored in covered, plastic barrels while the aggregate from the Continental plant in Londonderry was stored in open-top, steel barrels. Rust and debris that collected in the steel barrels were removed as much as possible when the aggregate was used; any remaining amout of fine rust particles was assumed little enough to have a negligible effect on the final results. The binder was taken directly from the holding tanks connected to the plant mixers and stored indoors in lidded, steel buckets.

Methods

Overview

The project was carried out in two main stages. The first involved testing samples fabricated from the original mix designs provided by the NHDOT. The second involved redesigning three of the original mixes and testing samples fabricated from these new designs. In each stage, the fabrication process was the same with only a few changes over the course of the project. In stage two the mixes were redesigned according to the Bailey Method as described in Circular E-C044. After the aggregate blend was established, the asphalt content was determined according to Superpave. For both stages,

the samples were tested using the MMLS3. The method of testing was modified in a couple of ways over the course of the project.

Fabrication

For each mix design, both original and new, at least two small samples were fabricated for theoretical maximum specific gravity (Gmm) measurements, and at least seven samples were fabricated for testing in the MMLS3. The basic procedure of fabrication was as follows:

1. Aggregate Sieving
    a. Dry the unsieved aggregate for at least 8 hours.
    b. Sieve the aggregate.
    c. Store all the aggregate in buckets.
2. Sample Mixing
    a. Batch each sample according to their respective mix design recipes.
    b. Heat the aggregate at mixing temperature for at least 8 hours prior to mixing.
    c. If RAP was used
        i. Measure out required amounts for each sample in separate containers.
        ii. Put RAP in the oven at mixing temperature 2 hours before mixing.
    d. Measure out enough binder to mix all samples in one session.
    e. Heat binder to mixing temperature on a hot plate approximately 30 to 60 minutes before mixing.

f. Put aggregate in the mixing container and record its mass.

g. If using RAP, put RAP in the mixing container and record the new mass.

h. Calculate the required mass of binder.

i. Put the binder in the mixing container and record the mass of the binder alone.

j. Mix the sample.

k. Put the asphalt mix in a separate pan and record its final mass.

l. Put the completed mix in the oven for 2 hours at aging temperature.

m. If the sample was intended for Gmm measurement, this ends the fabrication.

3. Compaction and Cutting

a. Heat the compaction molds at aging temperature at least 2 hours prior to compacting.

b. Put the mix into the compaction mold.

c. Compact the asphalt in the IPC Servopac gyratory compactor.

d. Extract the sample and allow to cool.

e. Measure the air voids of the uncut sample.

f. Cut the sample into a usable brick for the MMLS3 test bed.

g. Measure the air voids of the cut brick.

There were several changes to the details of this process since the beginning of the project. These changes include the sample sizes used, the method of drawing a small portion of binder for mixing, the calculation of required binder mass for mixes with RAP, and the method of mixing. With regards to sample size, the original method of Gmm measurement used a pycnometer according to AASHTO T-209-05, and required a 2000g

sample. Later, the Gmm was measured using the CoreLok machine and required only a 1500g sample. The first several MMLS3 test bricks were made from large samples, batched to 4500g, that were cut in half. However, approximately 50% of these bricks had unacceptable air voids, so later bricks were batched to 2250g and compacted to nearly half the height of the original samples. By compacting each brick separately, the percentage of acceptable bricks increased.

The original method of separating out asphalt binder for mixing involved heating the whole bucket at approximately 100°C until enough binder, anywhere from 200g to 1500g, had melted and could be poured into a small can. Sometimes this took 2 hours. Since constant reheating endangered the binder properties, a new method was employed that involved using a couple of hot spoons to scoop cold asphalt into a can. Although there was no observed impact on the samples fabricated with the previous method, the change in measuring out binder was made in the interest of prudence.

Equation 4.1 was used to calculate the required mass of binder for a given mass of virgin aggregate:

$$M_b = M_a\left(\frac{P_b}{100 - P_b}\right) \tag{4.1}$$

Where:

M_b is the mass of the binder to add to the mix

M_a is the mass of the aggregate in the mixing bucket

P_b is the binder content

This formula is based on the assumption that the binder contents given on the mix design sheets provided by the NHDOT were a percentage of the final mix mass. The mix designs that contained RAP listed a total binder content ($P_{b,total}$) and a virgin binder content ($P_{b,v}$). It was assumed that both of these binder contents were also given as a percentage of the total mix mass. The mass of the virgin binder for each RAP mix was calculated with Equation 4.1 using the virgin binder content for P_b and the combined mass of the virgin aggregate and the total RAP, with its own aggregate and binder included, for M_a.

For the Farm-Bailey mix, the Superpave procedure was used to design the asphalt content. However, Superpave only gives calculations for virgin materials and makes no mention of how to design for a mix with RAP. Therefore, only the data for the virgin aggregate (Gsb, Gsa, and aggregate contributions) were used to calculate $P_{b,total}$. The mix designs for Farm and Hook were examined to learn the equation to calculate $P_{b,v}$ from $P_{b,total}$. It was discovered that the binder contents for these mixes were not percentages of the final mix mass, as previously assumed, rather percentages of the batched mass, which included the virgin aggregate and total RAP. Therefore, Equation 4.2 was used to calculate $P_{b,v}$ from $P_{b,total}$. Equation 4.3 was used to calculate the mass of the binder for each sample of the Farm-Bailey mix design.

$$P_{b,v} = P_{b,total} - P_{b,RAP}\left(\frac{P_{RAP}}{100}\right) \tag{4.2}$$

$$M_b = \left(M_a + M_{RAP}\right)\left(\frac{P_{b,v}}{100}\right) \tag{4.3}$$

Where:

$P_{b,total}$ is the total binder content

$P_{b,v}$ is the virgin binder content

$P_{b,RAP}$ is the RAP's binder content

P_{RAP} is the percent of RAP in the total blend

M_b is the mass of the binder to add to the mix

M_a is the mass of the virgin aggregate

M_{RAP} is the mass of the RAP

The method of mixing changed twice. In the beginning of the project, right after a sample was mixed a small amount of the material was removed until the final mass equaled the mass of the originally batched aggregate. This caused many fluctuations in volumetrics. The solution was to simply leave all the material in the sample after mixing. Thus a sample that started with 4500g of aggregate might end up as a 4720g sample after adding the binder. The second change was to use a dummy mix at the beginning of each session. Every time asphalt is mixed, material is unavoidably lost when it gets stuck in the grooves and sticks to the insides of the mixing bucket. Therefore the mass of the first sample mixed in each session ended up approximately 30g lower than all the other samples. The solution was to make the first sample a dummy sample that was then discarded.

Field Core Sample Preparation. The asphalt from which the cores were taken was paved in two layers. The surface layer used the Oss 12.5 mix and the base layer used the Oss 19

mix. Nine 150 mm diameter cores were sent by the NHDOT. One of these was too damaged to be used. Of the eight remaining cores, four separated into their respective layers of their own accord. The other four were cut with an asphalt saw at the interface of the two layers. The change in layers was determined by visually comparing the coarseness of the asphalt in the core. The bottom of each base layer was cut off to make a smooth face on each side. Finally the sides were cut off to make each sample into a brick that would fit in the MMLS3 test bed.

Volumetric Measurement

The Gmm was measured with a pycnometer, according to AASHTO T-209-05, for the Oss 12.5, Oss 19, Cont 12.5, and Cont 19 mix designs. The CoreLok machine, manufactured by InstroTek, Inc., was used to measure the Gmm for the Farm, Hook, Oss 12.5-Bailey, Cont 19-Bailey, and Farm-Bailey mix designs. The CoreLok was employed because it was much easier to work with and retained accuracy. The method outlined by the CoreLok manual is as follows:

1. Measure the combined mass of the 2 bags involved.
    a. The correction factor for the bags, C_{bag}, was given in the CoreLok manual as 0.903.
2. Measure the mass of the dry asphalt concrete.
    a. This was calculated as the difference between the mass of the asphalt in its pan and the mass of the pan alone.

3. Put the loose asphalt concrete into the smaller bag, which then goes in the larger bag, and lay in the CoreLok chamber.
4. The CoreLok vacuums the air out of the bags and seals the larger one.
5. Immerse the sealed bag in a water bath at 25°C and open them under water.
6. Record the mass of the asphalt concrete in the two bags under water.

Once the measurements were taken, the Gmm was calculated according to Equation 4.4:

$$G_{mm} = \frac{M_{asphalt,dry}}{\left(M_{bag,dry} + M_{asphalt,dry} - M_{total,sub}\right) - \left(\frac{M_{bag,dry}}{C_{bag}}\right)} \quad (4.4)$$

Where:

$M_{asphalt,dry}$ is the mass of the dry, loose mix

$M_{bag,dry}$ is the combined mass of the bags before they are used

$M_{total,sub}$ is the mass of the loose mix in the bags under water

C_{bag} is the correction factor for the bags

The bulk specific gravity (Gmb) was measured using the Saturated Surface Dry method, as detailed in the AASHTO T-166-05 test, for all samples. There was one change in the method of measuring the Gmb, although when this change took place is not recorded. In earlier measurements the water bath was left at room temperature, which was between 20°C and 28°C, whereas in later measurements the temperature of the water bath was checked and adjusted to 25±0.2°C. Since the density of water only changes by 0.002 g/cm^3 from 20°C to 28°C, the affect of not adjusting the water temperature on

previous samples was assumed to be insignificant. Appendix 4 lists the results from all of the volumetric measurements.

MMLS3 Testing

The asphalt sample bricks for the MMLS3 were compacted to cylinders 150 mm in diameter. Once the cylinders were ready, the sides were cut off using one of the spacing plates as a guide. The final result is shown in the Figure 4.1. The samples that were initially batched to 4500 g, the Oss 12.5, Oss 19, and Cont 12.5 mix designs, were also cut in half to make two samples approximately 58 mm tall. The bricks were oriented so only the compacted, uncut faces were driven on by the loading tire.

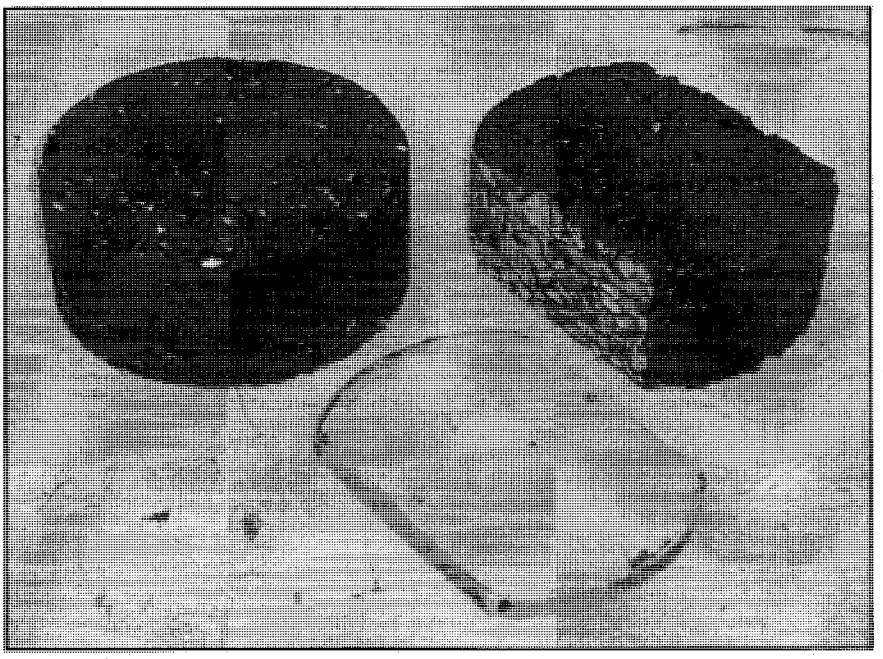

Figure 4.1: A Compacted Sample, a Brick, and the Cutting Template

In preparation for the tests, the MMLS3 was checked and calibrated. The belts were checked and bearings greased periodically. For load calibration, the tires were inflated fully to 700 kPa and locked in place under the calibration unit. The piston connected to the load cell was cranked down to push on the tire, deflecting it enough to make a 10 mm gap between its rubber stopper and metal frame as shown in Figure 3.5. If the force applied at this level of deflection was not 2.7 kN, the tire was released and the suspension springs were compressed more or less as needed to adjust the load. This load calibration was only done a couple of times a year, typically after replacing a tire, since the springs held their stiffness and moved little. After calibrating the load on all the wheel bogies, the MMLS3 was leveled to a proper height above the samples to ensure that 2.7 kN of force was applied evenly to all samples. This was done by lowering or raising the machine on its four adjustable legs until the measured gap between the rubber and steel was roughly 10 mm when the tire was at the ends and middle of the test bed. Stop nuts were placed on the bottoms of the legs to indicate the proper height of the MMLS3 each time it was lowered. Before each test, the tires were inflated to less than 700 kPa. The amount of inflation depended on the air temperature before the test and the target temperature during the test. The formula for tire inflation from the MMLS3 manual is shown in Equation 4.5.

$$P = 700\left(\frac{273+T_a}{273+T_t}\right) \tag{4.5}$$

Where:

P is tire pressure in kPa

T_a is the air temperature before the test in Celsius

T_t is the testing temperature in Celsius.

Although the MMLS3 test bed can hold nine bricks, only seven sample bricks were used. There is some abnormal loading on the first and last bricks in the test bed because the transition is not always smooth as the tires roll off and then on the metal guide ramps (personal communication with Fred Hugo). Therefore the end spaces were filled with dummy bricks only. The seven sample bricks were randomly ordered for some of the tests; for the other tests the bricks were kept in fabrication order to simplify record keeping. The top surfaces of the bricks were brought to a relatively even level with the tops of the confining plates on either side of the samples to within 3 mm over the length of the test bed.

The asphalt temperature was monitored with thermocouples connected to Hobo Type J data loggers that were imbedded in the dummy bricks and placed between the test bricks. Figure 4.2 shows an illustration of the samples in the test bed with the locations of the thermocouples. The dry heating unit had its own thermocouple to monitor and adjust the heating that was placed near the middle of the test bed. For the tests on the original six mixes, the heater's thermocouple and an additional thermocouple connected to a data logger were left in the air next to the sample bricks. The temperature for MMLS3 tests should not vary by more than 2°C above or below the target temperature (Kruger 2004). Therefore, during the tests for the redesigned mixes, the heater's thermocouple was put between the bricks in the middle of the test bed to reduce temperature variation over the course of the test. While this did reduce some of the temperature variation, it did not reduce it to the suggested level.

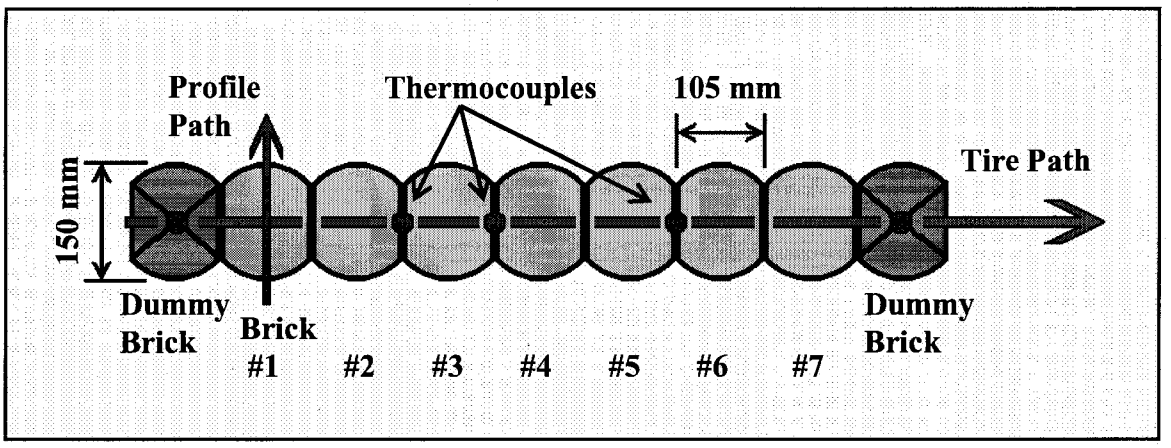

Figure 4.2: Test Bed Configuration

Once the samples were put into the test bed with the thermocouples installed, the confining screws were tightened. The confining screws on the sides were hand tightened only and set in place with locking nuts. The confining plate on the end was tightened by wrench and set in place with locking nuts. At this point, the samples were ready for initial profile measurements to be taken.

The profiles were measured close to the middle of each sample, parallel to the brick's long axis, which was perpendicular to the path of the loading wheels as shown in Figure 4.2. The profiles were measured over 200 mm at 5 mm increments. This took in the entire 150 mm length of each brick with 25 mm extra on each side to account for any heave and/ or over flow that might occur. The first profile was measured before any wheels were driven over the samples.

After looking at the profile data for tests run on the first few sample sets, the rutting that occurred within the first 1000 loading cycles seemed excessive. Therefore a seating load was applied to the bricks after the initial profile and before starting the first

1000 wheel loads. However, this observation and decision was made after the Oss 19 bricks had already been tested and new bricks from this mix design were not retested. Chapter 5 discusses the adjustment of the data for this test.

For the seating load, the MMLS3 was set in place over the test bed and lowered to allow the tires to apply their full force on the samples. The loading tires were slowly driven over the bricks between 10 and 20 times to fully seat them in place. While the samples may or may not have been heated at this point, no noticeable deformation occurred during this seating load but the bricks were pushed down and leveled out by a few millimeters. After the seating load was applied, the MMLS3 was raised up to make room for the profilometer. Profiles of the samples in their fully seated condition were used to normalize the rest of the profile data.

When it was time to heat the asphalt bricks, the environmental chamber was assembled around the MMLS3 and test bed. The air vents connected to the dry heater were inserted into the openings on the sides of the chamber. The dry heater was turned on and left to run for at least 5 hours to bring the sample bricks up to 60°C. This temperature was chosen to match other MMLS3 tests done (Epps 2001). During the initial heating, the MMLS3 was left raised up so that no force was applied to the samples.

Once the asphalt bricks had been heated and the seating load profile measured, the test began. The MMLS3 was first lowered onto the samples and then started up. The loading tires were driven over the samples at a rate of 2 tire passes per second. After

1000 wheel loads, the MMLS3 was stopped and raised up, the heater was turned off, and the blower vents were removed to make room for profilometer measurments. The total time for each of the profiles, from stopping the MMLS3 to starting it up again, was approximately 30 minutes. Since the heater was off during the profile measurements, there was some heat loss, but the temperature typically stayed above 45°C for the first several thousand cycles when the profiles measurements were closest together.

The MMLS3 applied 100,000 wheel loads in each test and profiles were taken at 1000, 2000, 4000, 8000, 16000, 30000, 50000, 75000, and 100,000 wheel loads. The profile measurements were more closely spaced at the beginning of each test because the asphalt deformed non-linearly at this phase. After approximately 16000 or 30000 wheel loads, the deformation became slower and more linear. At the end of the test, when the final profile after 100,000 wheel loads had been measured, the samples were allowed to cool and then removed from the test bed. Table 4.2 summarizes the test parameters for the MMLS3 tests.

Table 4.2: MMLS3 Test Parameters

Parameter	Value	
Target Temperature	60°C	
Vertical Force	~2.7 kN	
Loading Rate	2 Hz	
Total Applied Load	100,000 wheels	
Profile Measurements (wheels applied upto each measurement)	0 20 1,000 2,000 4,000 8,000	16,000 30,000 50,000 75,000 100,000

Bailey Method Design and Evaluation

The three mixes that were redesigned according to the Bailey Method were Oss 12.5, Cont 19, and Farm. The first step of the process involved collecting all of the relevant data for the aggregates used, including measuring the unit weights. The next step was to run through the design calculations to find a suitable aggregate blend. In the third step the asphalt contents were determined according to the Superpave method and, finally, bricks were fabricated for testing in the MMLS3. The aggregate data, Bailey calculations, Matlab programs, and mixing and design data are all listed in Appendix 1.

The Bailey Method requires the gradings for the aggregate stockpiles, the aggregate bulk specific gravities (Gsb), the loose and rodded unit weights of the coarse aggregate, and the rodded unit weights of the fine aggregate. The gradings and Gsb's were provided by the asphalt plants. The loose and rodded unit weights were measured by following the procedure in the AASHTO test T-19. The only deviation from T-19 was in preparing the samples for measurement. Instead of using a splitter, as called for in test T-248, which is referenced in section 6 of test T-19, the samples were simply batched to a size approximately 125% of what was needed to fill the measuring containers.

As described in Chapter 2, there are several input values for the Bailey calculations that must be chosen by the designer. These include the chosen unit weight (CUW) of the coarse aggregate, which is a percentage of the loose unit weights, the desired dust, and the relative proportions of the coarse and fine aggregate stockpiles. All

three mixes were meant to be designed as coarse, well graded mixes, so the CUW was kept between 95% and 105%. The design for Cont 19-Bailey was done manually on a spreadsheet, while the Oss 12.5-Bailey and Farm-Bailey aggregate blends were designed with a Matlab program that was written to make future designs easier. In each case the input values were altered until the best design was found. The best designs had gradings within their respective control points, out of their respective restricted zones, and were as close as possible to the target values for the Bailey weight ratios: CA, FAc, and FAf. The target values were the average of the upper and lower limits for each ratio, which were dictated by the NMSA of the mix design.

The Farm-Bailey mix was designed by choosing a set percentage of RAP, 15%, and running the Bailey calculations on the virgin aggregate only. The resulting contributions of the virgin aggregate were reduced by 15% to allow room for the RAP. The final combined grading was then tested against the control points, restricted zone, and target weight ratios. This process was slightly different from the one described in the Bailey Method, because the design program did not aim to keep the percent passing the PCS close to the same value both before and after adding RAP.

Once the aggregate blends were completed and the asphalt contents were determined, seven bricks were fabricated for each of the Oss 12.5-Bailey and Cont 19-Bailey mix designs. The completed bricks were stored in sealed, plastic bags until tested. No bricks were fabricated for Farm-Bailey because the final volumetrics for that mix design were out of range as dictated by Superpave.

The original mix designs, Oss 12.5, Cont 19, and Farm, were evaluated according to the Bailey Method as described in Chapter 2. In general, the percent aggregate contributions in the blend calculated by the Bailey Method are very close to the percent contributions used as input values. This meant that the input values for the aggregate contributions could be locked as constants to match those of the original blend, so only the CUW and desired dust would have to be varied. In this way, an approximate value for the CUW was calculated manually using a spread sheet before the Matlab programs were run. The Matlab program iterated through all possible combinations of input values from 10 below the initial estimates of CUW and aggregate contributions to 10 above. The optimum set of input values produced a calculated blend that closely matched the original blend, meaning sum of the absolute values of the differences between the calculated and original blends was the lowest it could possibly be. Appendix 1 shows the calculations for the Bailey evaluations including the gradings and weight ratios.

CHAPTER 5

RESULTS AND DISCUSSION

Results

Overview

A total of eight mixtures were tested using the MMLS3. Six of these mixtures are currently in use in New Hampshire. Three of the ones currently used were redesigned according to the Bailey Method; however, the redesigned RAP mix did not pass the Superpave criteria, thus was not tested under the MMLS3. Two sets of field cores were also tested with the MMLS3. These used the Oss 12.5 and Oss 19 mix designs. Table 5.1 summarizes the mixtures tested in this project.

Table 5.1: Summary of Mix Designs

Mix Designation	Aggregate	NMSA	AC
Original Mix Designs			
Oss 12.5	Gravel Stone	12.5 mm	5.6
Oss 19	Gravel Stone	19 mm	5.0
Cont 12.5	Fractured Rock	12.5 mm	5.5
Cont 19	Fractured Rock	19 mm	5.0
Farm	Gravel Stone w/ RAP	12.5 mm	5.50
Hook	Fractured Rock w/ RAP	12.5 mm	5.60
Bailey Redesigns			
Oss 12.5-Bailey	Gravel Stone	12.5 mm	5.1
Cont 19-Bailey	Fractured Rock	19 mm	5.6
Farm-Bailey	Gravel Stone w/ RAP	12.5 mm	4.85

Original Mix Designs

Figures 5.1 and 5.2 show the gradings for the original six mix designs. The horizontal axes show the the sieve sizes in millimeters, but are scaled to millimeters raised to the 0.45 power. The percent passing each sieve size is on the vertical axis. The higher a graphed line is on this chart, the finer the grading is. Full details, including blend and individual aggregate stockpile grading, for each mix design are given in Appendix 3.

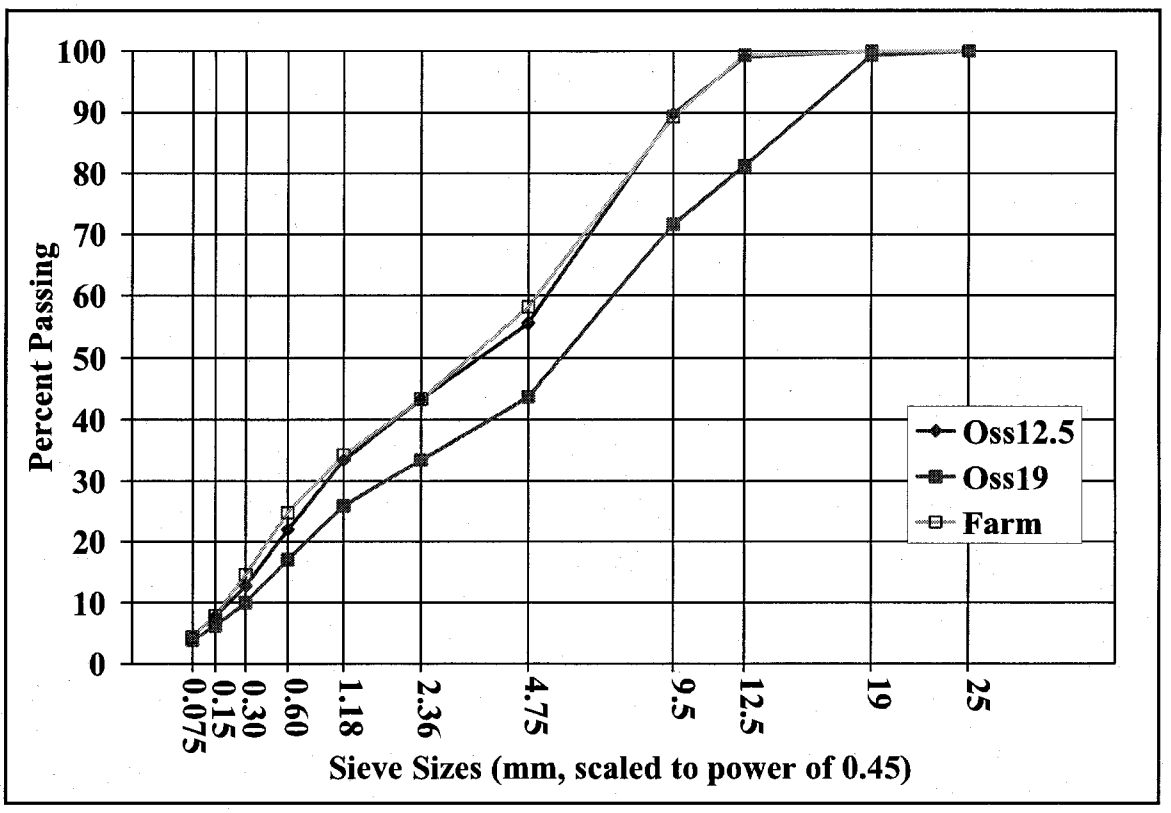

Figure 5.1: Gradings for Mixtures with Gravel Stone

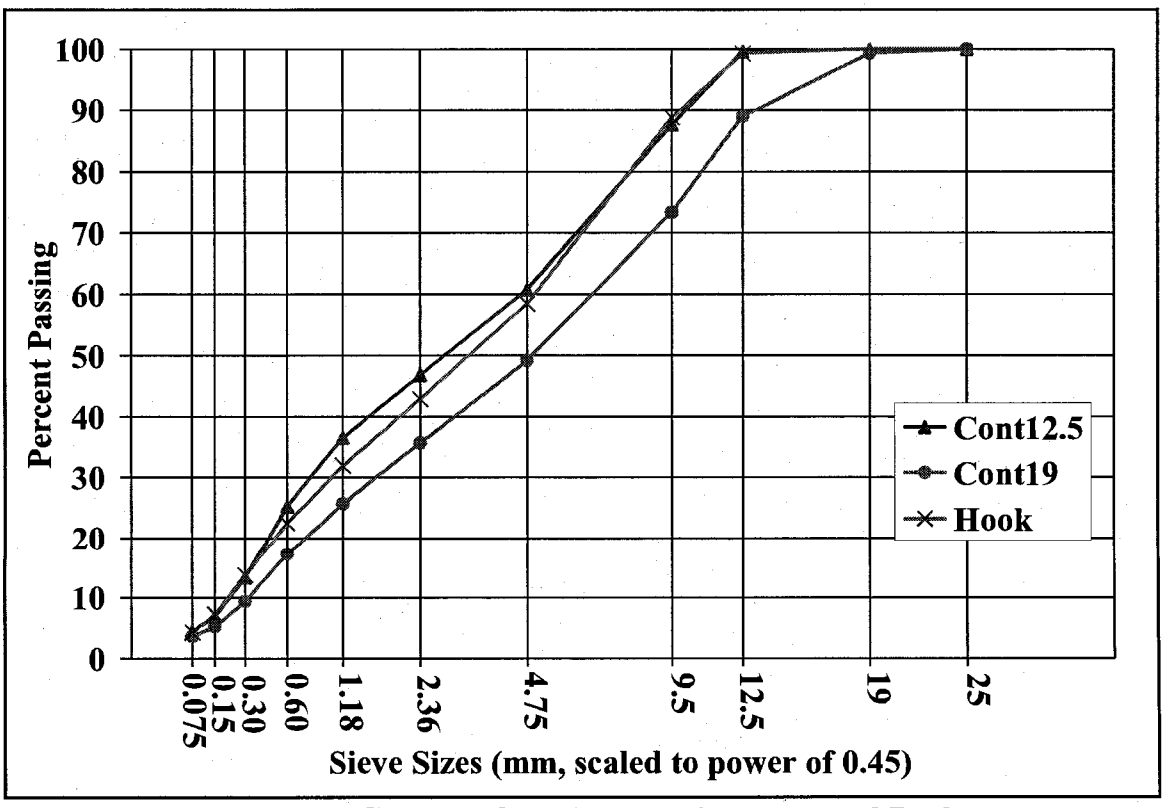

Figure 5.2: Gradings for Mixtures with Fractured Rock

Volumetrics. The theoretical maximum specific gravities (Gmm) for the Oss 12.5, Oss 19, Cont 12.5, and Cont 19 mix designs were measured with a pycnometer according to AASHTO T-209-05. The Gmm's for the Farm, Hook, Oss 12.5-Bailey, Cont 19-Bailey, and Farm-Bailey mix designs were measured with the CoreLok according to a different method, as discussed in Chapter 4. The bulk specific gravities (Gmb) for all the mix designs were measured according to the SSD method in AASHTO T-166-05. The bricks for the Oss 12.5, Oss 19, and Cont 12.5 mix designs came from large samples (batched to 4500g) that were cut in half. The T or B in the brick identification indicates whether it came from the top or bottom of the originally compacted sample. For all the other mix designs, there was only one brick from each compacted sample, which was batched to 2250g. Tables 5.2 through 5.7 list the Gmm, Gmb, the percent air voids (AV), the voids in the mineral aggregate (VMA), and the thickness of each of the seven sample bricks tested in the MMLS3 for each mix design. The sample bricks were chosen based on their AV, which had to be between 3.5% and 4.5%. The bricks are listed in the order in which they were laid in the test bed (meaning the first brick in the list was the first one to feel the tire).

Table 5.2: Volumetrics for Oss 12.5

Brick ID	Gmm	Gmb	AV	VMA	Thickness (mm)
O12.5M-7B	2.425	2.336	3.7	14.8	57.91
O12.5M-8T	2.425	2.333	3.8	14.9	57.32
O12.5M-6T	2.425	2.328	4.0	15.1	56.08
O12.5M-8B	2.425	2.338	3.6	14.7	55.78
O12.5M-5T	2.425	2.340	3.5	14.6	55.69
O12.5M-7T	2.425	2.324	4.2	15.2	55.39
O12.5M-4T	2.425	2.323	4.2	15.3	55.14
Average	2.425	2.332	3.9	15.0	56.19

Table 5.3: Volumetrics for Oss 19

Brick ID	Gmm	Gmb	AV	VMA	Thickness (mm)
O19M-11T	2.466	2.361	4.3	13.6	57.02
O19M-6B	2.466	2.366	4.0	13.4	56.95
O19M-7T	2.466	2.360	4.3	13.7	55.61
O19M-7B	2.466	2.375	3.7	13.1	55.18
O19M-6T	2.466	2.366	4.0	13.4	54.93
O19M-10B	2.466	2.363	4.1	13.5	54.39
O19M-11B	2.466	2.366	4.0	13.4	53.69
Average	2.466	2.365	4.1	13.5	55.40

Table 5.4: Volumetrics for Cont 12.5

Brick ID	Gmm	Gmb	AV	VMA	Thickness (mm)
C12.5M-2B	2.483	2.373	4.4	17.1	52.46
C12.5M-3B	2.483	2.385	3.9	16.7	51.81
C12.5M-4B	2.483	2.384	4.0	16.7	52.95
C12.5M-5B	2.483	2.390	3.7	16.5	52.76
C12.5M-6B	2.483	2.374	4.4	17.1	51.98
C12.5M-8T	2.483	2.377	4.2	17.0	52.67
C12.5M-8B	2.483	2.382	4.0	16.8	52.42
Average	2.483	2.381	4.1	16.8	52.44

Table 5.5: Volumetrics for Cont 19

Brick ID	Gmm	Gmb	AV	VMA	Thickness (mm)
C19M-1	2.514	2.409	4.2	15.4	56.77
C19M-2	2.514	2.413	4.0	15.3	56.80
C19M-4	2.514	2.424	3.6	14.9	56.60
C19M-5	2.514	2.414	4.0	15.2	56.80
C19M-6	2.514	2.424	3.6	14.9	56.99
C19M-7	2.514	2.408	4.2	15.4	*
C19M-9	2.514	2.419	3.8	15.1	56.99
Average	2.514	2.416	3.9	15.2	56.83

* Data file lost

Table 5.6: Volumetrics for Farm

Brick ID	Gmm	Gmb	AV	VMA*	Thickness (mm)
FM-7	2.467	2.366	4.1	14.1	57.28
FM-8	2.467	2.356	4.5	14.5	57.39
FM-10	2.467	2.365	4.1	14.2	57.42
FM-6	2.467	2.369	4.0	14.0	58.24
FM-11	2.467	2.367	4.0	14.1	57.46
FM-12	2.467	2.358	4.4	14.4	57.31
FM-9	2.467	2.363	4.2	14.2	57.18
Average	2.467	2.364	4.2	14.2	57.47

* Used VMA formula for AC as a percent of the total mix mass (SP-2, p. 43), because that's the way the bricks were fabricated.

Table 5.7: Volumetrics for Hook

Brick ID	Gmm	Gmb	AV	VMA*	Thickness (mm)
HM-11	2.439	2.346	3.8		58.11
HM-16	2.439	2.345	3.8		58.63
HM-17	2.439	2.339	4.1		58.59
HM-15	2.439	2.333	4.3		58.90
HM-19	2.439	2.337	4.2		58.67
HM-18	2.439	2.351	3.6		58.43
HM-20	2.439	2.335	4.2		58.24
Average	2.439	2.341	4.0		58.51

* No Gsb data available for the aggregate stockpiles, so VMA could not be calculated.

MMLS3 Test Results. The seven sample bricks for each mix were put in a line in the test bed under the MMLS3. Profiles were measured near the middle of each brick, perpendicular to the wheel path, as shown in Figure 4.2. The range of each profile was 200 mm, which covered the full 150 mm width of the brick plus 25 mm on each side to account for any heave or over flow during the test. The ruts in all the bricks developed in similar ways; a typical set of profile measurements is shown in Figure 5.3. Appendix 6 has the data and graphs for all the profile measurements for all the bricks in all the tests. The profile measurements were normalized to the seating load profile so that it lies along

a flat line at a height of 0 mm. The horizontal axis represents the transverse position along the brick in millimeters and was moved to the bottom of the graph for convenience. The vertical displacement in millimeters is represented on the vertical axis; a negative displacement is a rut and a positive displacement is a heave. The legend indicates the number of wheel loads that had been run up to each respective profile measurement. Generally, as more wheel loads were run, the rut got deeper and the heave got higher. Figure 5.3 shows the profile measurements for the middle brick, in the No. 5 position, for the Oss 12.5 MMLS3 test.

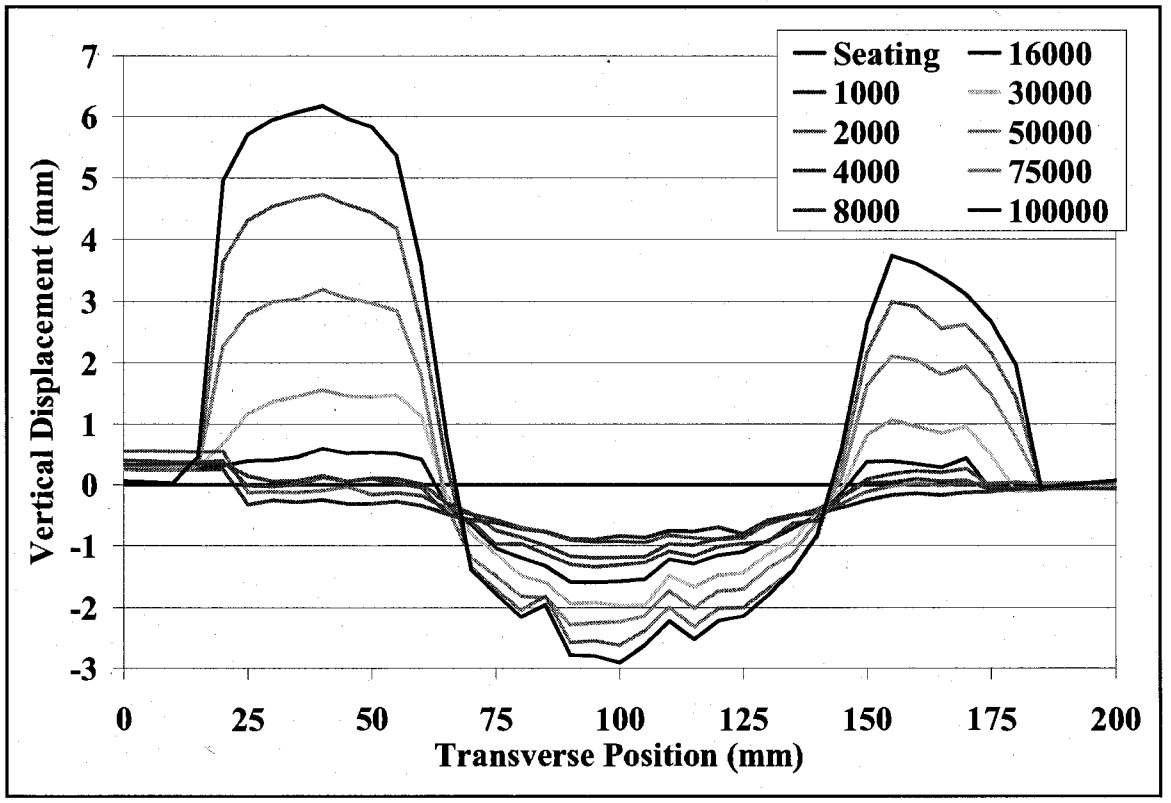

Figure 5.3: Surface Profile Measurements for O12.5M-8B

This graph is exaggerated in the vertical direction to clearly show the vertical displacements. The jaggedness of the profiles of the rut, especially in later profiles of the

test, is a result of large aggregate particles. Each time a wheel rolls over the asphalt it takes away a small amount of binder and whatever fine aggregate is stuck to that binder. Additionally, since the fine aggregate portion of the aggregate blend is the most deformable, the small particles are pushed down more than the large particles during rutting. The combination of wear and deformation result in the coarse aggregate being more and more exposed as the test continues.

The profiles after 30,000 loading cycles appear to have more material pushed up in the heave than pushed down in the rut. In reality, the volume of the asphalt pushed down is approximately equal to the volume pushed up because the brick is wider where the rut it and narrower where the heave is. This causes the heave to be larger than it would normally be in a field test.

There are three ways to condense the data from these profiles. The first is to average the measured rut depth over a certain range to minimize the effects of individual aggregate particles. The second is to use the maximum rut depth, meaning the deepest point of the graph. These first two methods measure the rut from the normalized base line, which is the seating load profile. The third is to measure the rut from the top of the heave. This last method uses the data normalized to the seating load profile, then measures the distance from the highest point to the lowest on the graph. The advantage of using one of the first two methods is that data can be easily compared between separate bricks and separate tests since all the measurements are taken from 0 mm vertical displacement. The advantage of the third method is that it better relates to

measurements of ruts in the field. There is no indication of the location of the original surface of the road after years of enduring traffic, so ruts are measured from the top of the heave. Since the heave that develops from testing bricks under the MMLS3 test is exaggerated, a correction factor should be used. Figure 5.4 illustrates the three methods of condensing the data from a profile measurement.

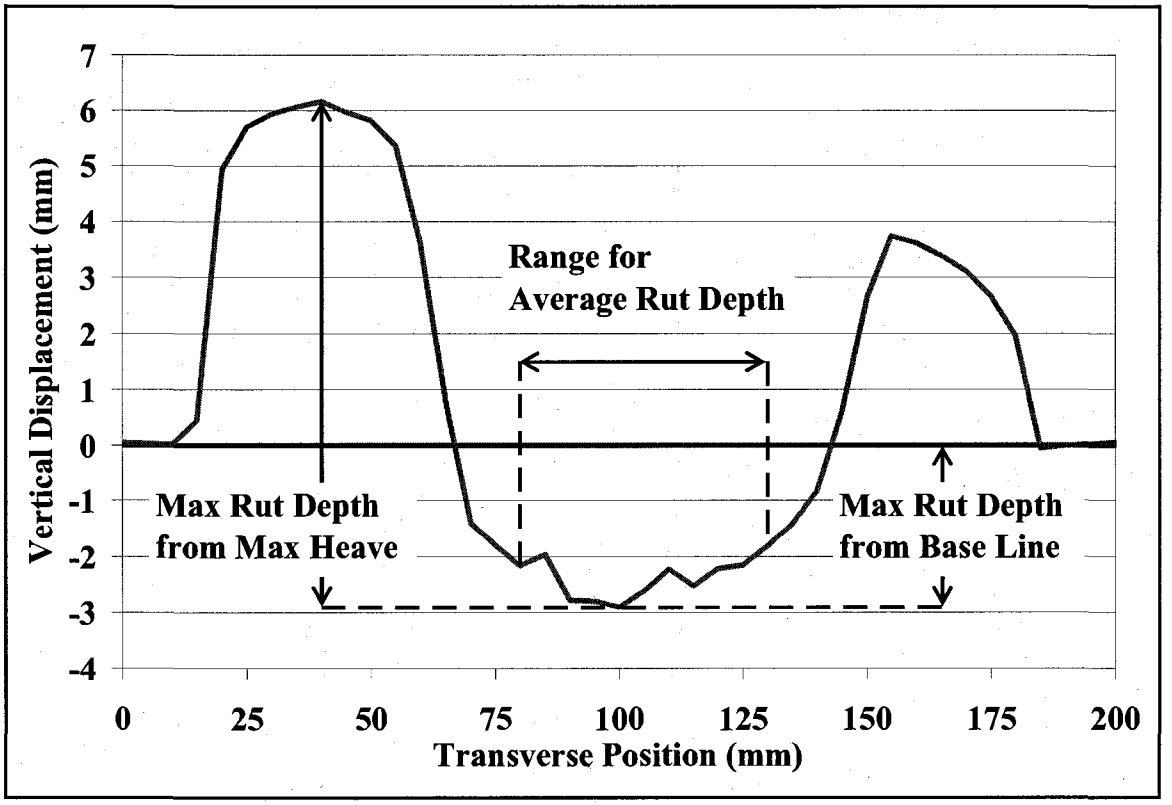

Figure 5.4: Three Methods of Condensing Rut Data from Profile

The range for the average rut depth is from 80 mm to 130 mm. This range was chosen by visual analysis of all the profile graphs. There appears to be a generally consistent shift to the right of the rut zones on all the profile graphs. This indicates that the tires were not rolling directly along the center of the bricks. The reason for this is most likely that the bricks were positioned slightly off center when the confining plates

were tightened in place. A width of 50 mm was chosen to exclude the steep slope on the sides of the rut for as many of the profiles as possible.

A few of the profiles were skewed when the ruts were very deep and the heaves were very large. The profilometer uses a small wheel on a comparatively long lever arm to measure the rut. When there is a large enough heave, the asphalt pushes the lever arm up, lifting the wheel off the surface of the asphalt. This shows up as a large hump that extends into the rut zone on the graph. For these profiles, a modified range was chosen for the average rut depth. Figure 5.5 shows an example of this case in the third brick from the Cont 12.5 test. The profile at 75,000 wheel loads is graphed to show the full range of the rut zone. The profile at 100,000 wheel loads was the anomalous case.

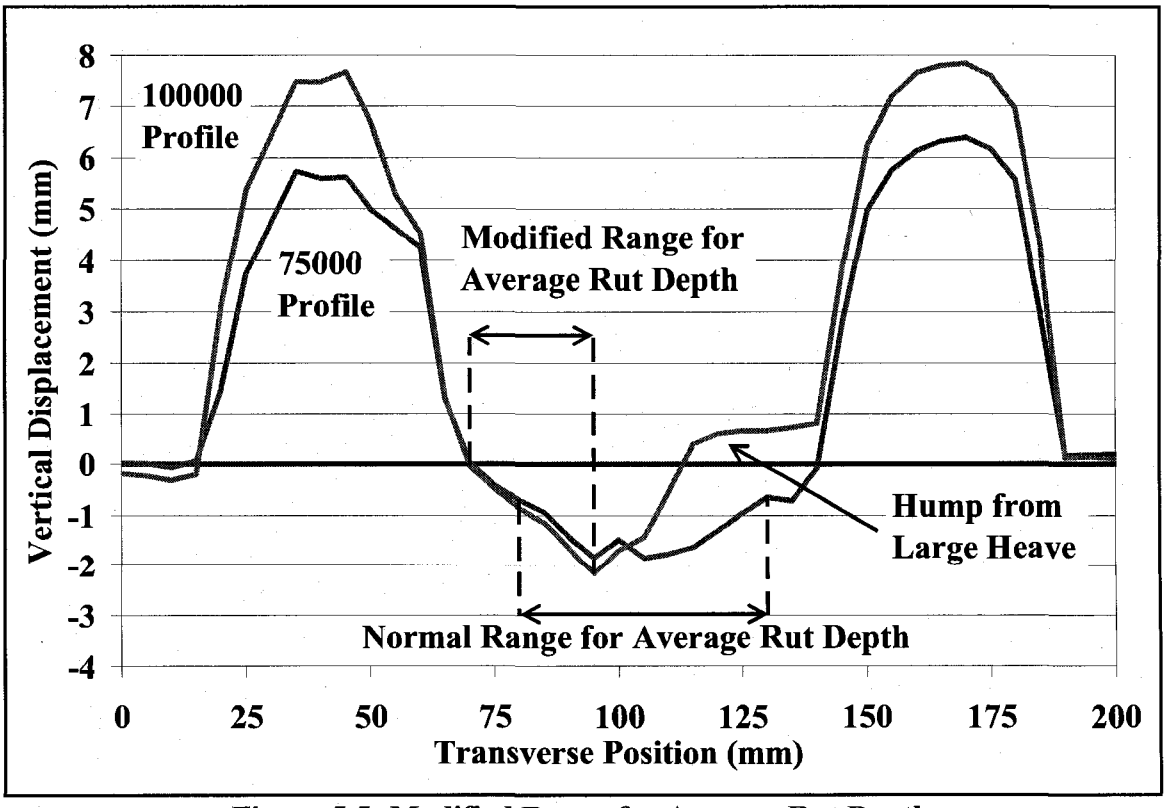

Figure 5.5: Modified Range for Average Rut Depth

The rut depth measurments from each transverse profile can be combined into a longitudinal profile showing how the rutting developes along the length of the test bed. The data and graphs for all the MMLS3 tests, using all three methods, are in Appendix 6. The absolute value of vertical displacement in millimeters is represented on the reversed vertical axis. The horizontal axis represents longitudinal position in millimeters measured from the end of the brick in position No. 1. The axis is divided into increments of 105 mm, to reflect the width of a brick. The locations of the data points are assumed to be exactly in the middle of each brick. No data is given for the bricks in positions No. 1 and No. 9 because they were filled with dummy samples. All the sample sets had similar longitudinal profiles. Figure 5.6 shows a typical graph: the Oss 12.5 profile using the maximum rut depths measured from the base line.

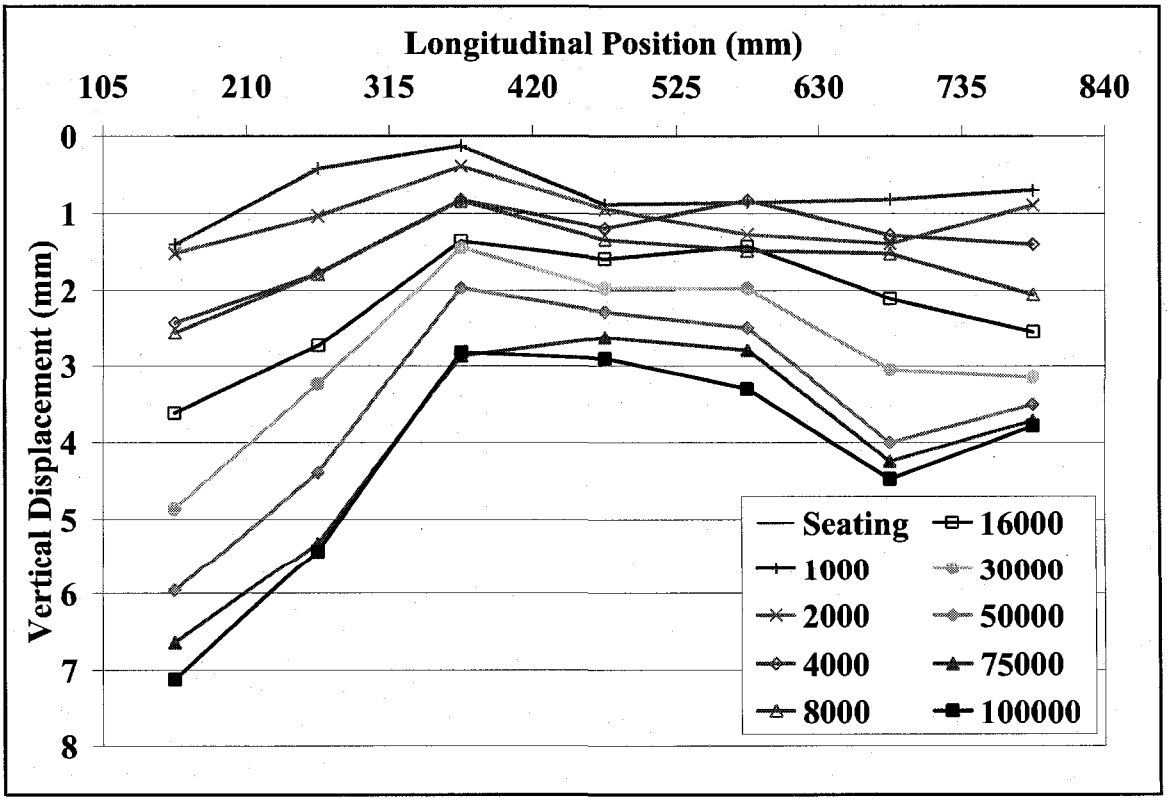

Figure 5.6: Longitudinal Profile of Oss 12.5 Bricks, Max Rut Depth

Each point on this graph represents the maximum rut depth one brick developed at one point in the test. A few general trends among the results from all the tests can best be seen from the longitudinal profiles. Firstly, the rutting in the first few samples was usually deeper than at the end. It is possible the MMLS3 delivered a particularly hard downward force when it first rolled onto the test bed, or there might have been some bouncing in the wheel as it came off the guide ramp. Another anomaly seen in the longitudinal profiles was comparatively little rutting in several samples in the middle of the test bed. This may have been due to shoving since a few of the longitudinal profile graphs show humps directly following a deep rut. Similar deformations can be seen on roads where truck wheels make a dent in the pavement, shoving the asphalt in front of it.

The longitudinal data can be further condensed into an average value for all bricks at a particular number of loading cycles in the test. The average rut values are plotted against the number of loading cycles. Figures 5.7 through 5.12 show the graphs of average rut depth verses loading cycles for the MMLS3 tests for all six of the original mix designs. The horizontal axes represent loading cycles, or wheel loads. The vertical axes represent rut depth in millimeters. All the vertical axes span the same range to make visual comparison easier. Each plot shows three graphed lines, each representing a different method of condensing the rut data from the transverse profiles: maximum rut measured from the maximum heave (the top line in each plot), the maximum rut measured from the base line (the middle line in each plot), and the average rut measured from the base line (the bottom line in each plot).

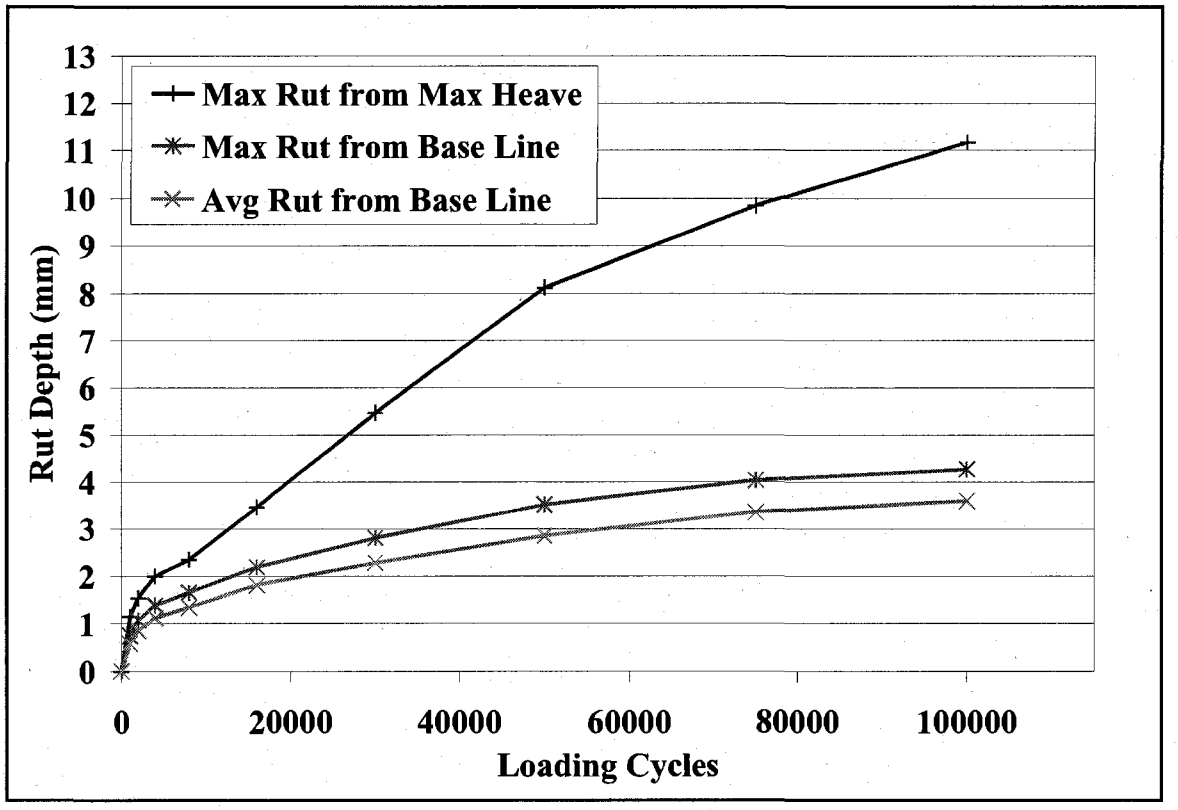

Figure 5.7: Rut Depth vs. Loading Cycles for Oss 12.5

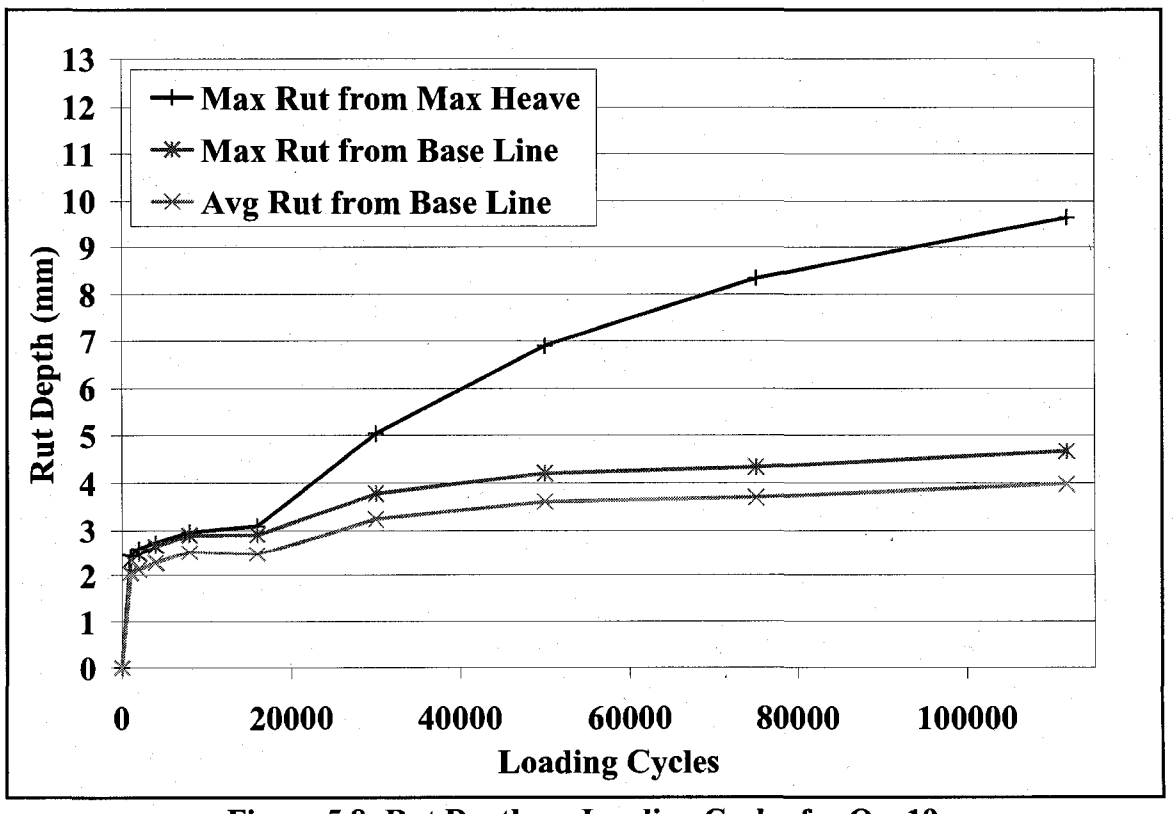

Figure 5.8: Rut Depth vs. Loading Cycles for Oss 19

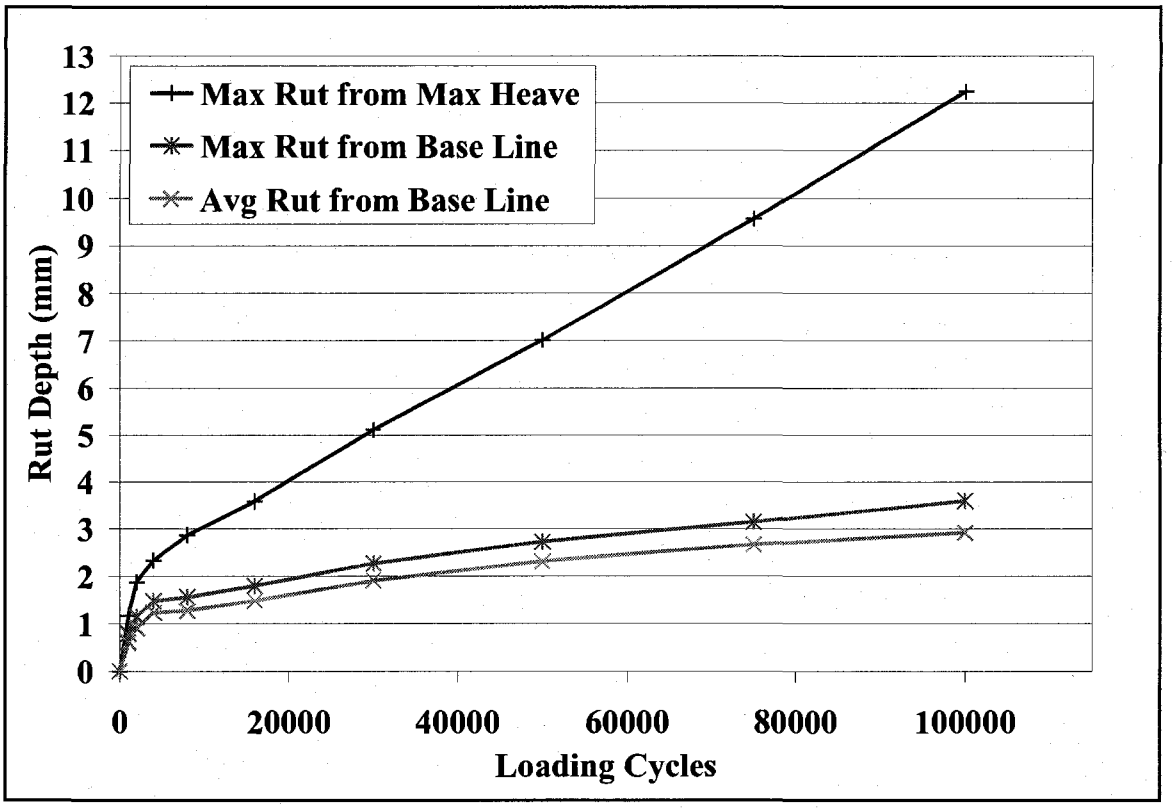

Figure 5.9: Rut Depth vs. Loading Cycles for Cont 12.5

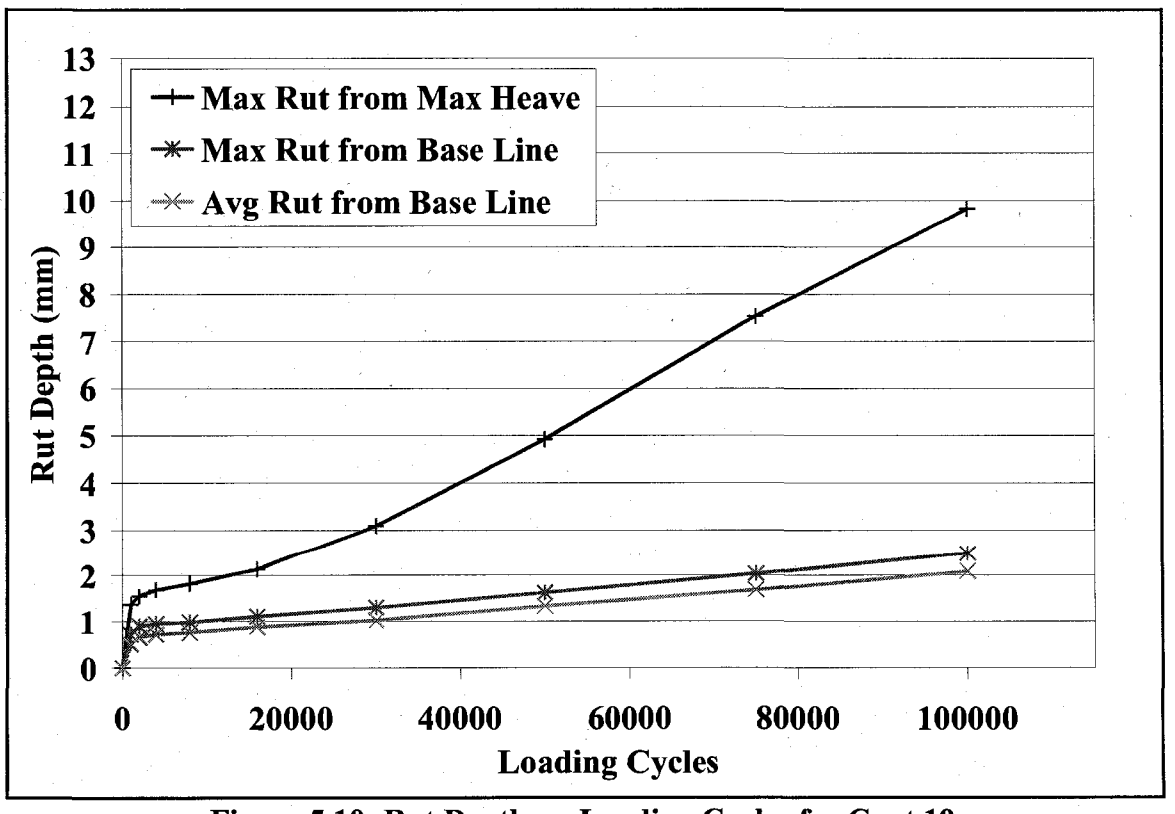

Figure 5.10: Rut Depth vs. Loading Cycles for Cont 19

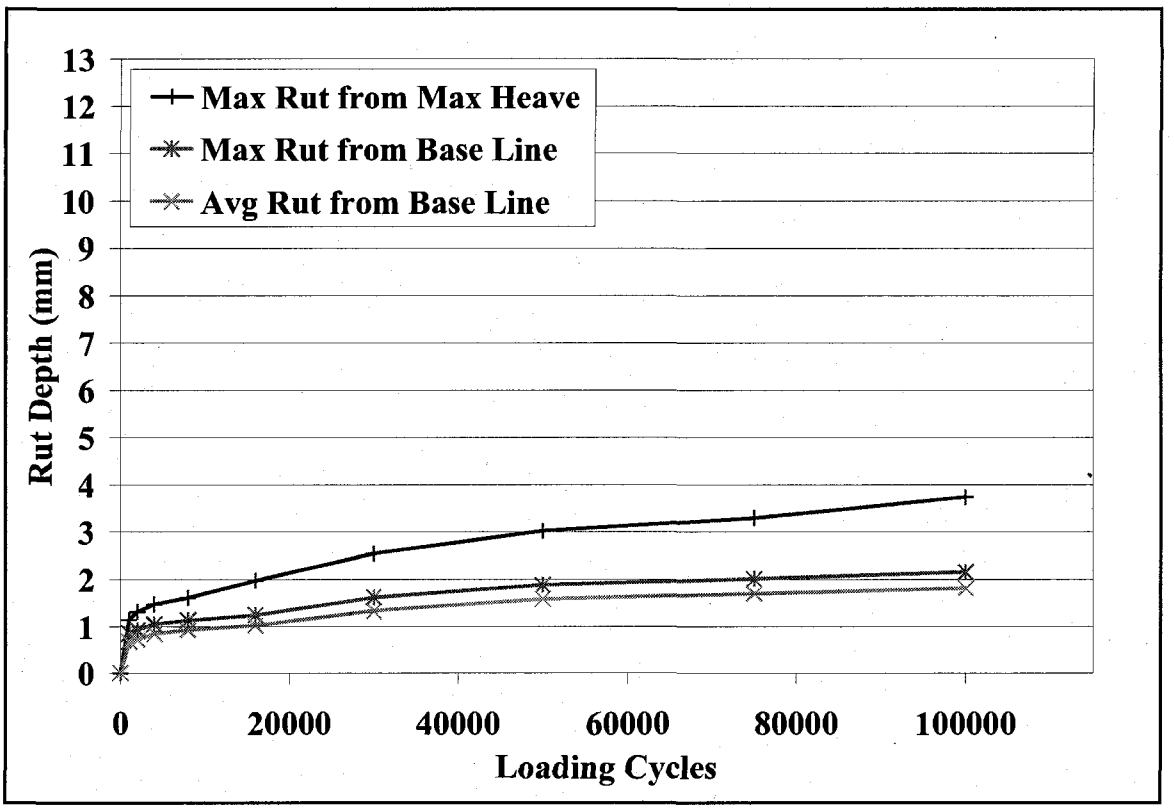

Figure 5.11: Rut Depth vs. Loading Cycles for Farm

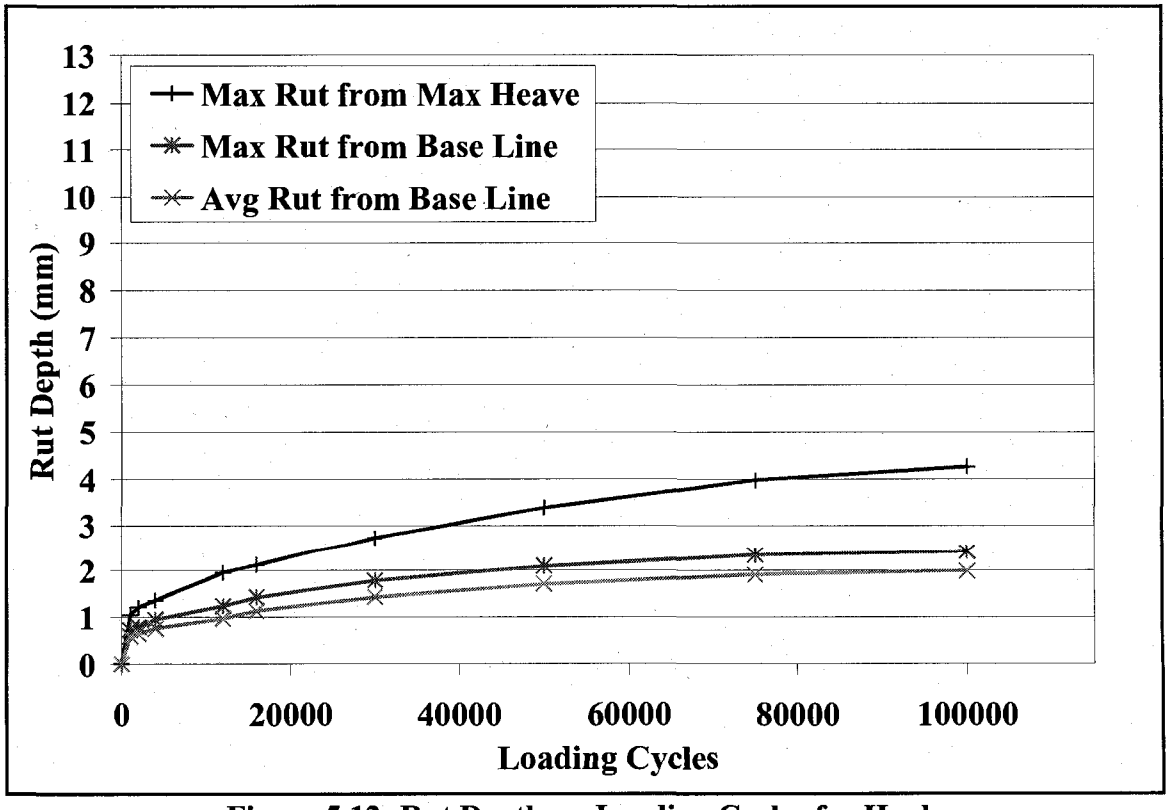

Figure 5.12: Rut Depth vs. Loading Cycles for Hook

The target temperature for each of these tests was 60°C. However, a consistent temperature was not maintained throughout each test for two reasons. Firstly, the dry heater's thermocouple wire was left in the open air rather than imbedded in the asphalt. This meant that the heating unit's control circuit only accounted for the hot air and not for the extra heating caused by the action of the MMLS3. Thus, some of the tests rose above 60°C during the last half. Leaving the thermocouple wire exposed also caused greater fluctuations in the temperature, causing the saw tooth pattern shown in Figure 5.13. Secondly, the bricks cool down during profile measurements because the heater is turned off and the environmental chamber is opened up to make room for the profilometer. After each set of profiles were measured, the samples were not brought back up to the target temperature before the next set of loading cycles were run. This caused the temperature during the first 16,000 loading cycles to be below average for the test. All of the temperature readings were similar; a typical graph is shown in Figure 5.13. The dark lines are the temperature readings from the thermocouples imbedded or between bricks. The light line is the air temperature that the heater's thermocouple was reading.

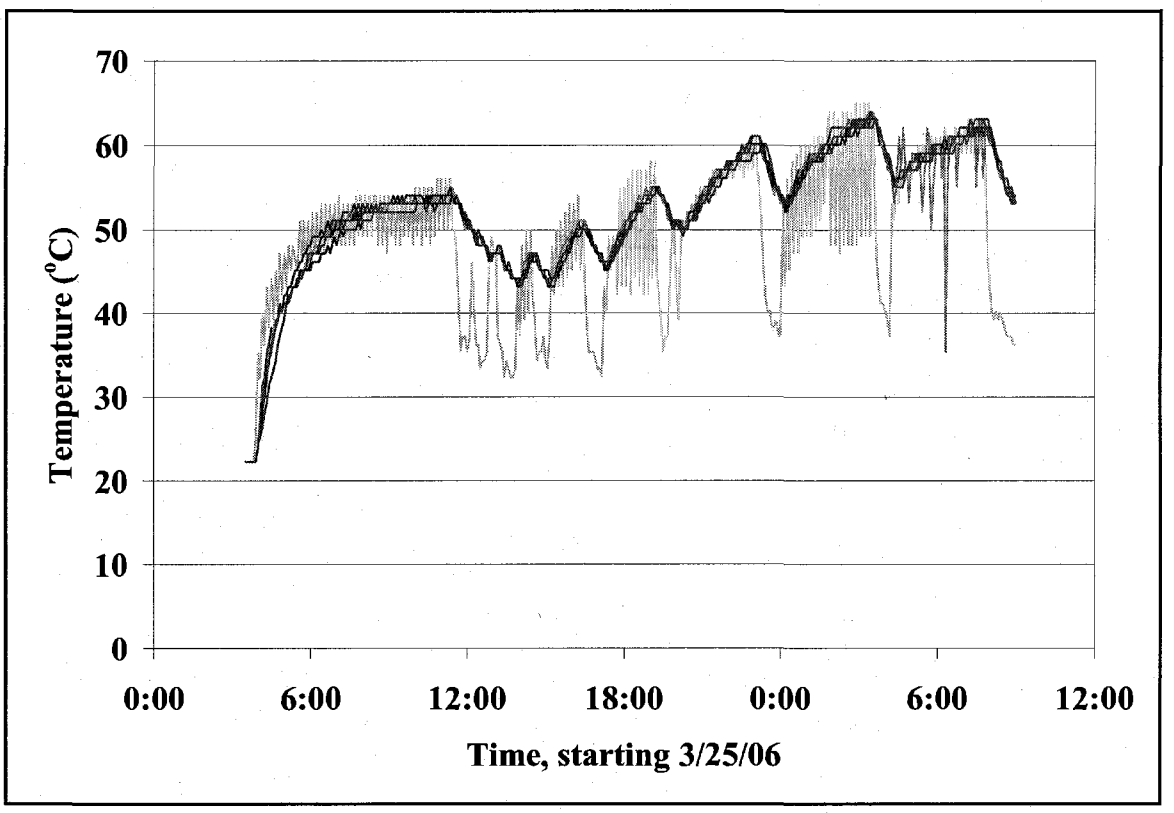

Figure 5.13: Temperature over the Course of the Cont 19 MMLS3 Test

Since the brick temperatures at each profile measurement varied within a single test, and since the brick temperatures at corresponding profile measurements varied from test to test, a method was developed to try to normalize the rut measurements with respect to temperature (Singh, 2007). This method uses a factor based on the modulus of the asphalt at the average brick temperature when the profiles were measured and the modulus of the asphalt at 50°C. The factors are applied to the additional rut depth from one point in the test to the next. However, this method uses calculated approximations for the shear modulus of the binder and the dynamic modulus of the mix instead of measured values. The adjusted rut depths were calculated for all of the tests except Hook because there were no VMA data for those samples. Figure 5.14 shows the adjusted performance, rut depth over the course of the test, for Cont 19, which corresponds to the

temperature graph shown above. All the calculated adjustments were of a similar magnitude, although not in the same direction. Furthermore, the relative positions of the adjusted graphs were the same as the original ones.

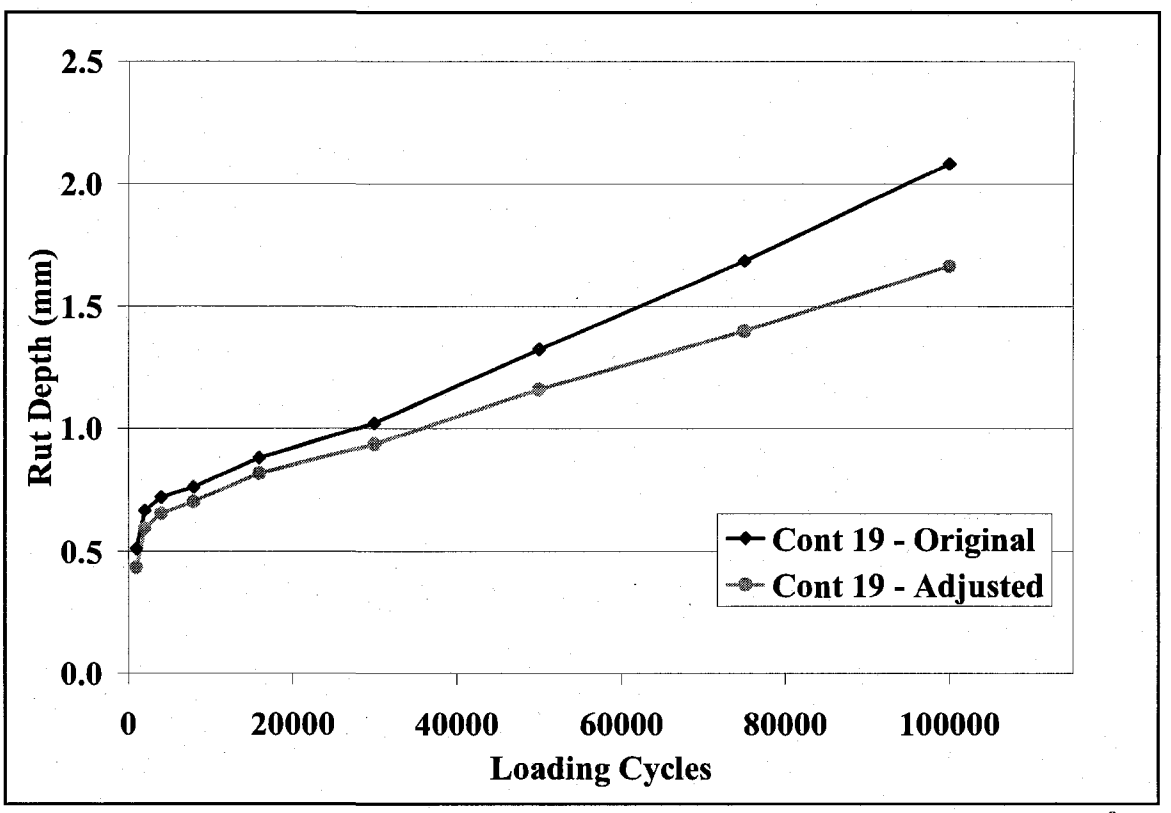

Figure 5.14: Performance of Cont 19 Adjusted to a Constant Temperature of 50°C

Rut Performance Comparisons. The original results from the MMLS3 tests were statistically compared using the Mann-Whitney/Wilcoxon Rank Sum Test. The statistical test compares the rut measurements for a pair of MMLS3 tests at a single point when profiles were measured. The rut depth values for both sets of data are arranged in order, from highest to lowest, in a single list. Each value is then given a rank, 1 for the highest and 14 for the lowest. The rut values, with their ranks, are separated again into their original two data sets. The ranks for each data set are numerically summed. The p-value

is the probability that one would get two sums of ranks as widely spaced as the real ones were by random chance.

For each pair of tests there were 18 comparisons: 9 using the maximum rut depths measured from the base line, and 9 using the average rut depths measured from the base line. The maximum rut depth measured from the maximum heave was not used because there was a high probability the heave was greatly exaggerated in any given test. Only the statistical comparisons using the average rut depths are shown here. The comparisons using the maximum rut depths yielded nearly identical results. A complete explanation of the statistical tests and the full results are shown in Appendix 7.

Figures 5.15 through 5.23 show graphs of the rut depths over the course of the tests for each pair of mix designs that were compared. The solid lines in the figures are the average of all the data for a particular sample set. The points spread around the line are the data points for the seven sample bricks. Tables 5.8 through 5.14 show p-values for the comparisons at each stage of the tests. Generally, a p-value of 0.05 or less means that the two sample sets are significantly different from a statistical standpoint.

Comparisons Based on NMSA: The comparisons between the results from these MMLS3 tests look at the effects of different NMSA, 12.5 mm verses 19 mm, while keeping other factors the same.

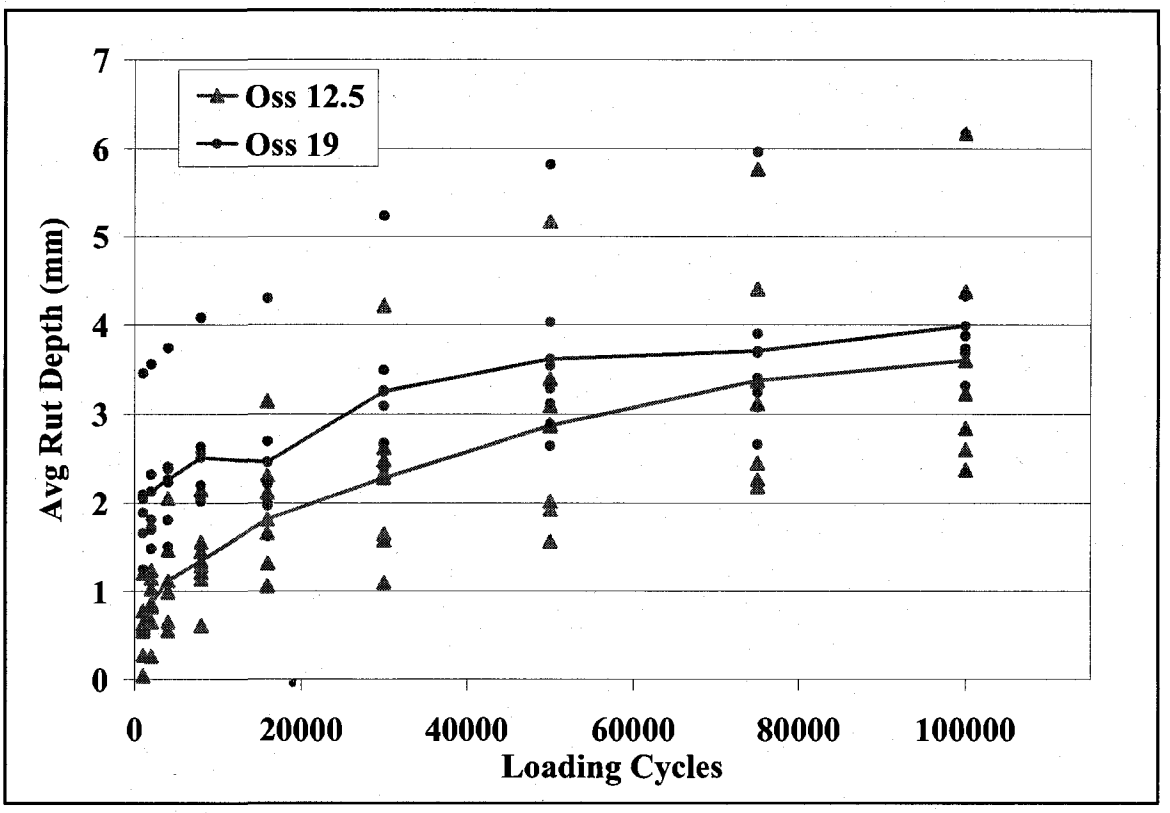

Figure 5.15: Comparison Graph of Oss 12.5 and Oss 19

Table 5.8: Comparison of Rut Depths of Oss 12.5 and Oss 19

	Thousands of Loading Cycles								
	1	2	4	8	16	30	50	75	100
P-Value	0.001	0.001	0.004	0.004	0.209	0.053	0.209	0.383	0.337
Significant Difference	Yes	Yes	Yes	Yes	No	*No?*	No	No	No

There are a couple of things to note about these data. As stated above, this comparison uses the rut depths averaged from the transverse profiles. The value for the third brick in the Oss 12.5 sample set, O12.5M-6T, developed a very large heave after

100,000 wheel loads, so a modified range for the average value was used, as described above. Secondly, the last profiles during the Oss 19 MMLS3 test were taken after 111,740 wheel loads, instead of right at 100,000. For simplicity in statistical comparison, the last profiles are assumed to have occurred at 100,000 loading cycles. Since the rate of rutting is low and linear after 50,000 loading cycles, as can be seen in Figure 5.8, this approximation for statistical testing is considered acceptable.

The limit of significant difference was set at 5%, a common limit for statistical `close to the limit and the result must be looked at in context to the rest of the values. The profiles at 16,000 cycles and 50,000 cycles are not significantly different, plus the points on the graph clearly overlap a great deal. Therefore, the initial result of no significant difference is accepted.

In general, a coarser mix is expected to rut less than a finer one, yet the Oss 19 mix rutted much more than Oss 12.5. More than half of the total average rutting in the Oss 19 bricks took place within the first 1,000 loading cycles. A possible reason for this is the lack of a seating load at the beginning of the Oss 19 test. The average seating displacement for all the tests was 0.57 mm. When this approximate seating is subtracted from the Oss 19 rut measurements the average rutting is still greater than the Oss 12.5 mix. However, when the rut measurement at 1,000 loading cycles is subtracted from each data set, the Oss 19 shows better performance, which is what was expected. This result is shown in Figure 5.16. It is possible that the rut data for the Oss 19 test is not a good representation of the strength of that mix.

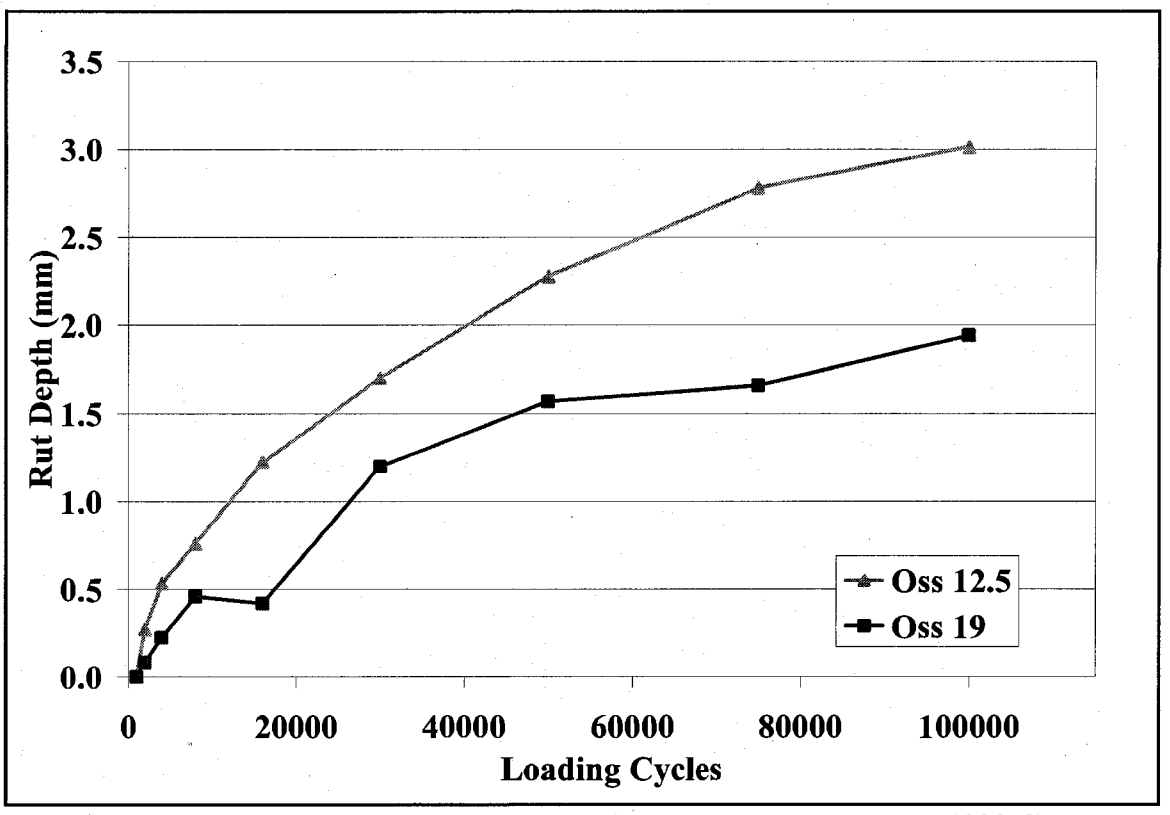

Figure 5.16: Oss 12.5 and Oss 19 Normalized to the Rut Depth at 1000 Cycles

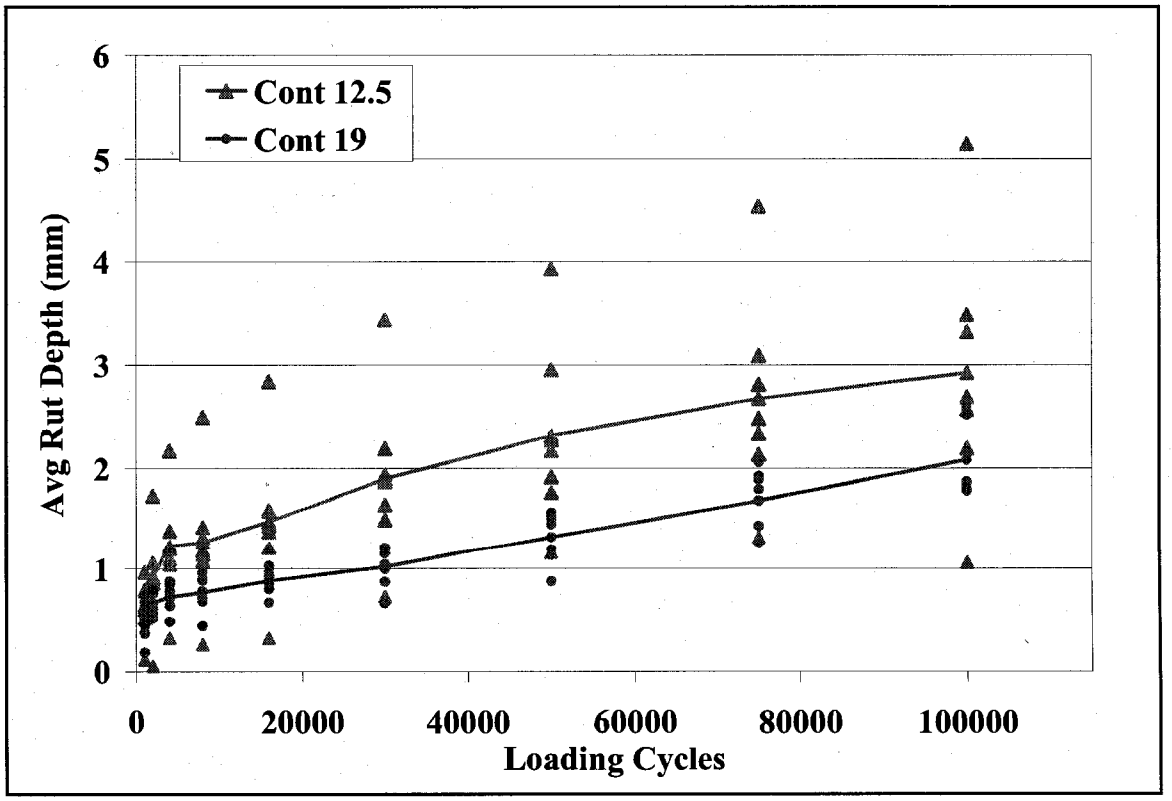

Figure 5.17: Comparison Graph of Cont 12.5 and Cont 19

Table 5.9: Comparison of Rut Depths of Cont 12.5 and Cont 19

	Thousands of Loading Cycles								
	1	2	4	8	16	30	50	75	100
P-Value	0.456	0.026	0.026	0.026	0.026	0.018	0.011	0.021	0.073
Significant Difference	No	Yes	Yes	Yes	Yes	Yes	Yes	Yes	No

The p-value at 100,000 cycles is above 5% indicating that there is no significant difference between these two sets of rut data at that point. However, this may be due to random error. In this comparison, the coarser mix has less rutting than the finer mix as expected. A solid, large stone is stronger and more resistant to deformation than a collection of smaller stones that take up the same volume. Therefore, a coarser mix is more resistant to rutting than a finer mix because it has a greater amount of larger aggregate particles.

Comparisons Based on Aggregate Type: These MMLS3 test results comparisons look at the effects of different aggregate type, gravel stone verses fractured rock, while keeping other factors the same.

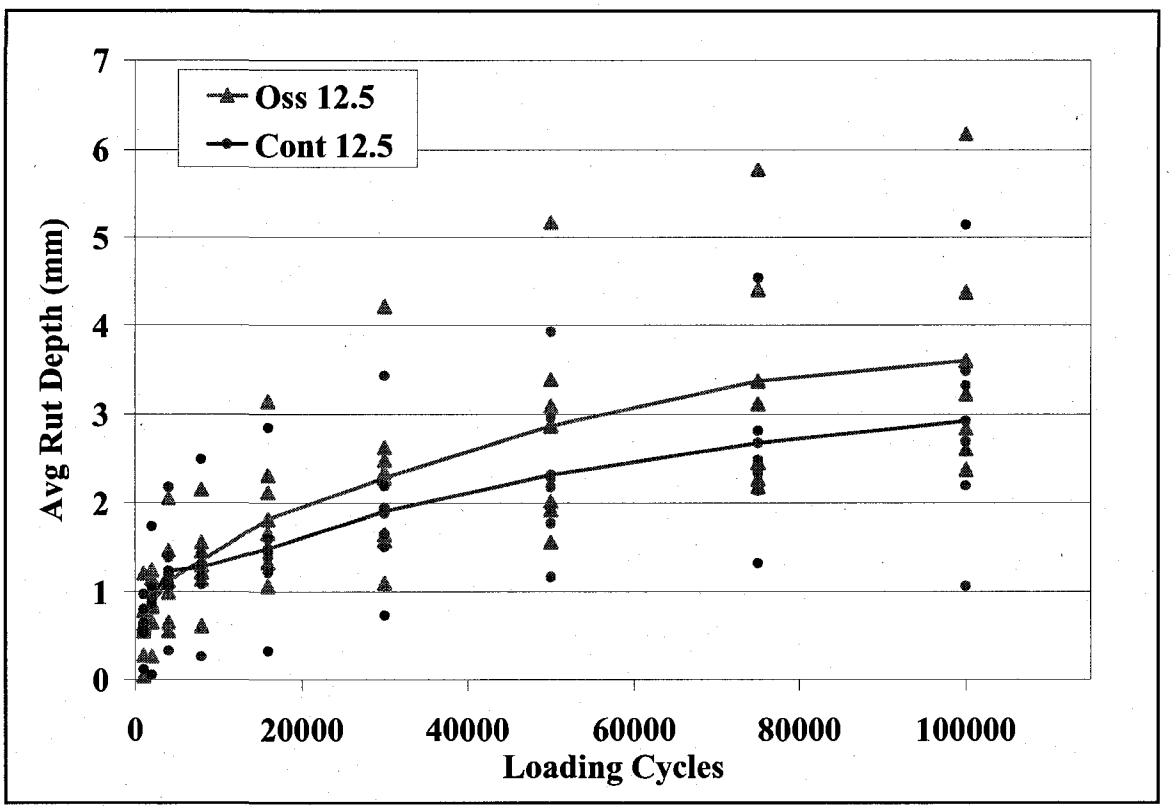

Figure 5.18: Comparison Graph of Oss 12.5 and Cont 12.5

Table 5.10: Comparison of Rut Depths of Oss 12.5 and Cont 12.5

	Thousands of Loading Cycles								
	1	2	4	8	16	30	50	75	100
P-Value	0.710	0.710	0.535	0.620	0.620	0.456	0.482	0.383	0.383
Significant Difference	No	No	No	No	No	No	No	No	No

Just as one of the Oss 12.5 bricks used a modified range to average the rut depth measurements, the third and fourth Cont 12.5 bricks used modified ranges after 100,000 wheel loads had been run. Although there is no significant difference between the test

results for these mix designs, the Cont 12.5 bricks generally out performed the Oss 12.5 bricks. This is expected because the Cont 12.5 mix uses fractured rock, which is rougher and more angular than the Oss 12.5 mix's gravel stone. These properties help the aggregate blend to lock up and resist deforming under a vertical load.

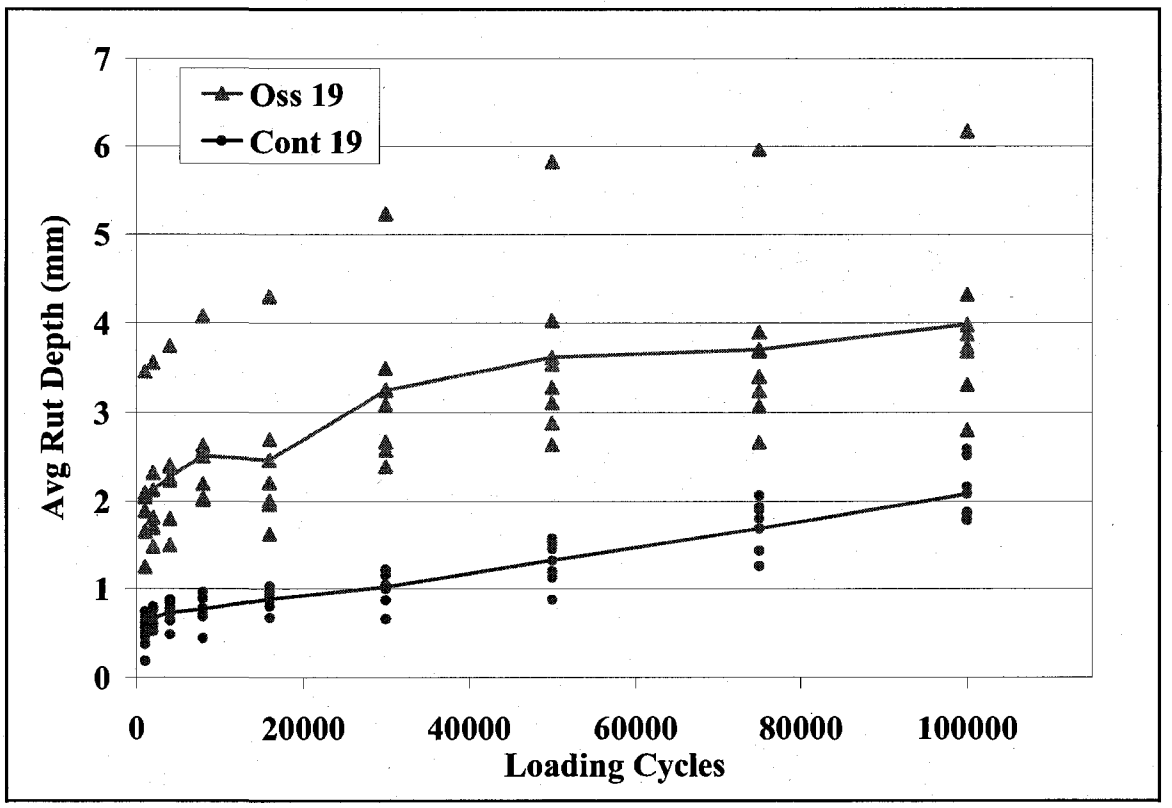

Figure 5.19: Comparison Graph of Oss 19 and Cont 19

Table 5.11: Comparison of Rut Depths of Oss 19 and Cont 19

	Thousands of Loading Cycles								
	1	2	4	8	16	30	50	75	100
P-Value	0.001	0.001	0.001	0.001	0.001	0.001	0.001	0.002	0.001
Significant Difference	Yes	Yes	Yes	Yes	Yes	Yes	Yes	Yes	Yes

The data points surrounding the average line for Cont 19 appear to have an unusually narrow spread mainly because the data for Oss 19 are much more spread out.

The Cont 19 mix performed better than the Oss 19 mix as expected for the same reason that the Cont 12.5 mix out performed the Oss 12.5 mix. Since most of the rutting in the Oss 19 samples occurred within the first 1,000 loading cycles, Figure 5.20 shows a comparison with Cont 19 with this rut measurement subtracted out. The graphs of the two sample sets are much closer, but the Cont 19 mix still out performs the Oss 19 mix.

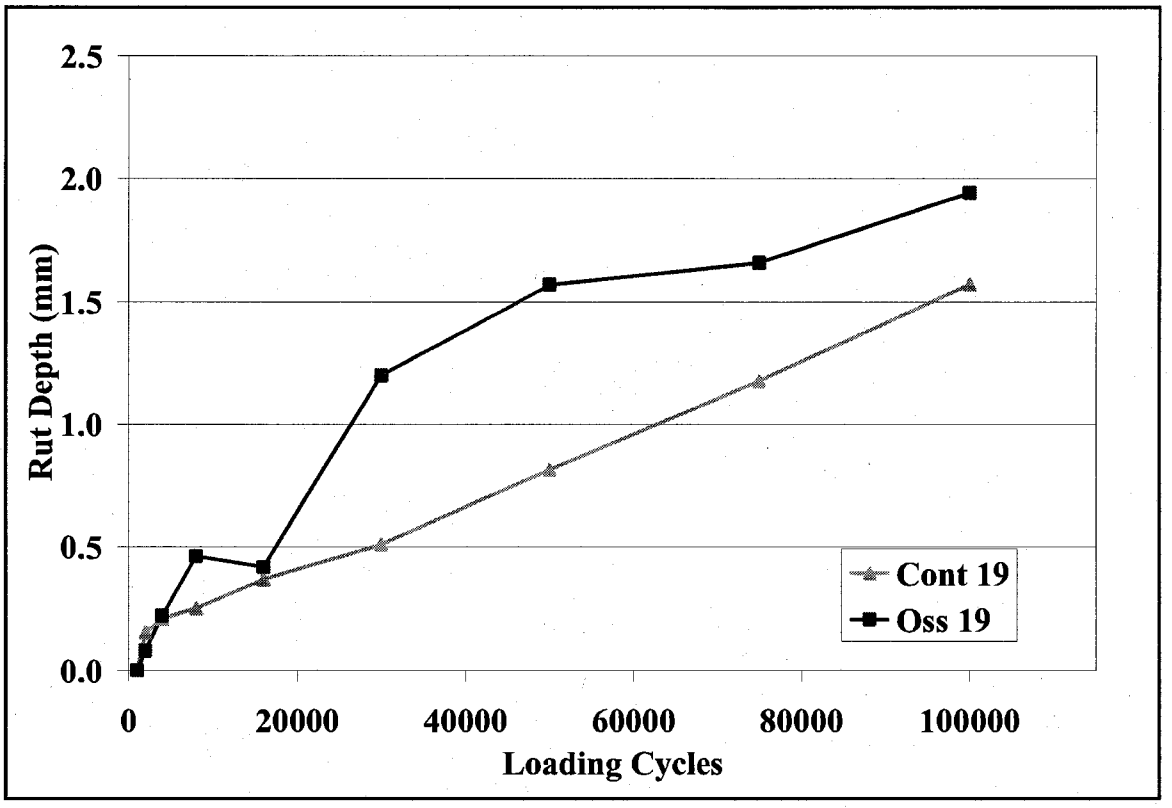

Figure 5.20: Oss 19 and Cont 19 Normalized to the Rut Depth at 1000 Cycles

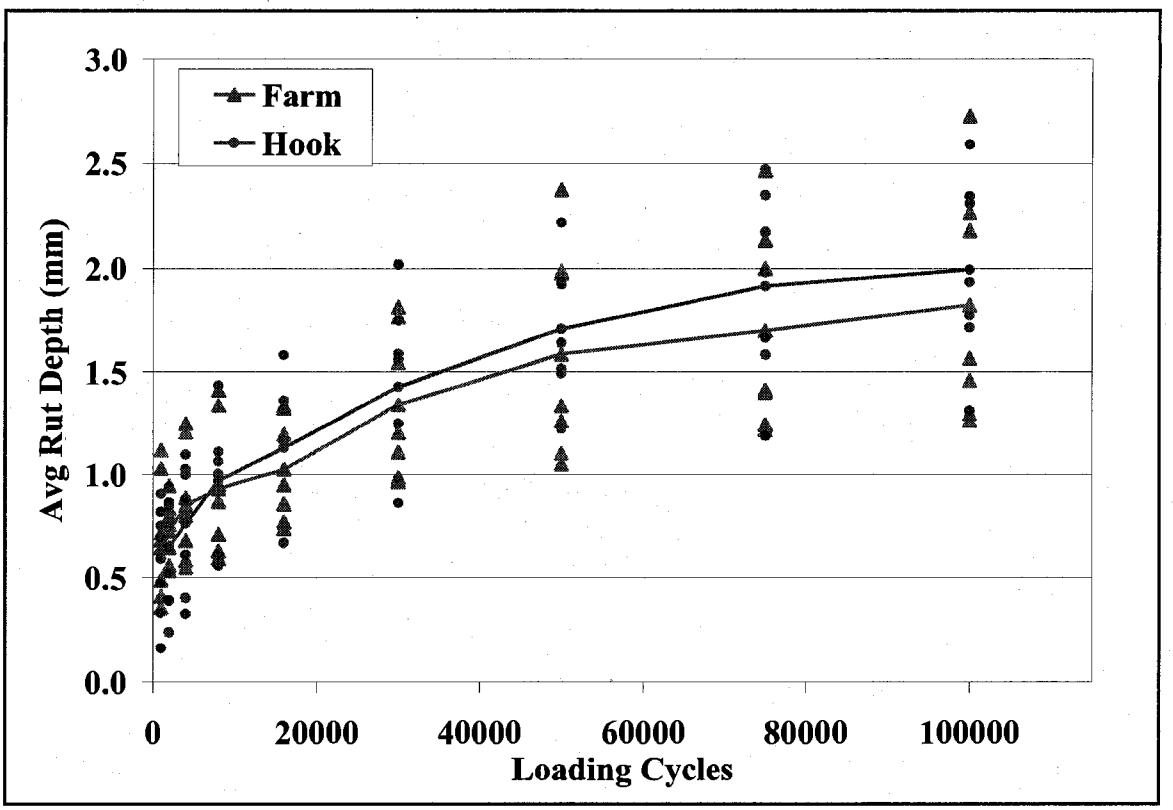

Figure 5.21: Comparison Graph of Farm and Hook

Table 5.12: Comparison of Rut Depths of Farm and Hook

	Thousands of Loading Cycles								
	1	2	4	8	16	30	50	75	100
P-Value	0.710	0.710	0.710	0.710	0.805	0.805	0.710	0.456	0.383
Significant Difference	No	No	No	No	No	No	No	No	No

Both mixes showed very strong resistance to rutting because they both contained RAP. The difference in aggregate suggests that the Hook mix with fractured rock would out perform the Farm mix with gravel stone. Although the average rutting in Farm was less, the difference in performance between these two mixes is very small and may be due to random error.

Comparisons Based on RAP Content: These comparisons look at the effects induced by including RAP, while keeping other factors the same.

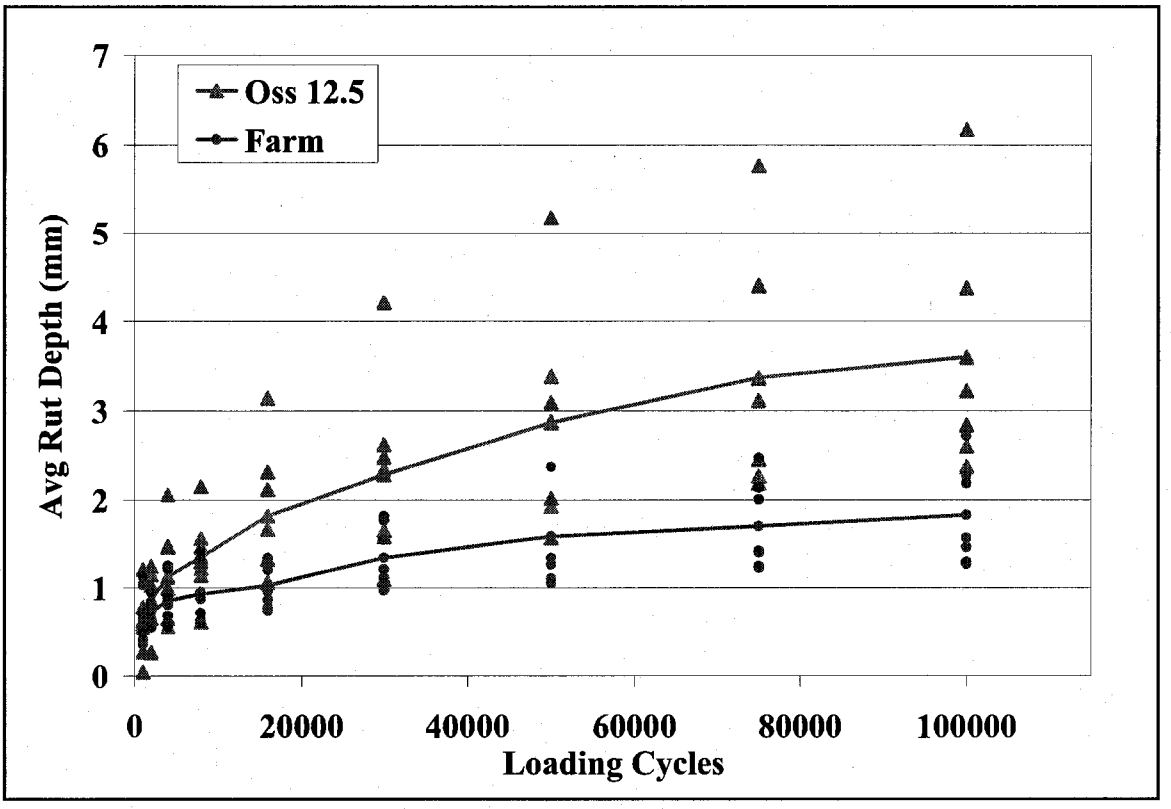

Figure 5.22: Comparison Graph of Oss 12.5 and Farm

Table 5.13: Comparison of Rut Depths of Oss 12.5 and Farm

	Thousands of Loading Cycles								
	1	2	4	8	16	30	50	75	100
P-Value	0.710	0.209	0.383	0.128	0.038	0.053	0.026	0.004	0.002
Significant Difference	No	No	No	No	Yes	*Yes?*	Yes	Yes	Yes

Just as for the comparison between Oss 12.5 and Oss 19, the p-value at 30,000 cycles is very close to the limit of 5%. In this case the surrounding p-values are all low, indicating there is a significant difference between the test results despite the slightly

higher p-value. This is supported by the statistical comparison between these mixes at 30,000 loading cycles using the maximum rut depth, which has a p-value less than 0.05.

The superior performance of the Farm bricks is expected because RAP is generally stiffer due to its age. As the pavement the RAP came from was exposed to the air, the binder lost some of its lighter components becoming stiffer over time. Additionally, if any of the RAP did not break down and blend with the virgin material it would have acted like a larger rock, effectively making the mix a little coarser and better at resisting rutting.

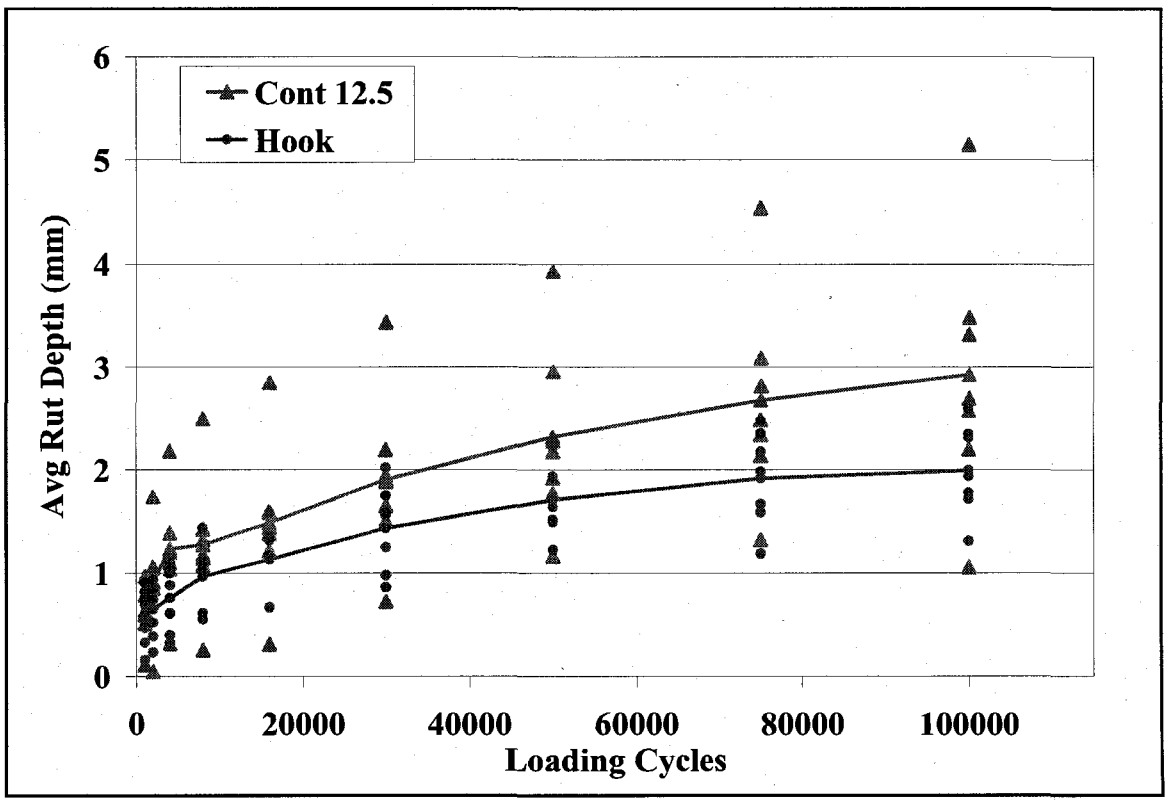

Figure 5.23: Comparison Graph of Cont 12.5 and Hook

Table 5.14: Comparison of Rut Depths of Cont 12.5 and Hook

	Thousands of Loading Cycles								
	1	2	4	8	16	30	50	75	100
P-Value	1.000	0.128	0.038	0.165	0.128	0.259	0.179	0.097	0.097
Significant Difference	No	No	Yes	No	No	No	No	No	No

This comparison between the Cont 12.5 mix and the Hook mix looks again at the effect of including RAP, this time with fractured rock. Just as for the comparison between Oss 12.5 and Farm, the superior performance of the Hook mix is expected because it contained RAP. The final average rut depth of the Hook bricks was 1 mm less than that of the Cont 12.5 bricks, which is well above the profilometer's sensitivity of 0.001 mm. However, the lack of significant difference between Cont 12.5 and Hook shows that the effect of the RAP on the performance of the Hook mix is clouded by random variation within the samples.

It should be noted that all of these statistical comparisons worked with data sets of seven observations each. This is a low number for statistical purposes because normal distributions cannot be established for the data sets. The Mann-Whitney/Wilcoxon Rank Sum Test was used because it does not require normal distributions. The graphs of the test results along with the statistical comparisons give a general idea of which mix designs performed better than others. Table 5.15 shows a summary of the comparisons including the parameters that were compared, the presence of significant difference overall, and which mix performed better, meaning shallower ruts. For those comparisons that had different p-values at the beginning and end of the tests, only the p-values for the

later part of the tests are considered important because that data indicates long term performance of the mix design.

Table 5.15: Summary of Statistical Comparisons

Compared Parameter	Mix Pair	Significant Difference	Better Performer
NMSA	Oss 12.5 vs. Oss 19	No	Oss 12.5
	Oss 12.5 vs. Oss 19, 1k Normalized		Oss 19
	Cont 12.5 vs. Cont 19	Yes	Cont 19
Aggregate Type	Oss 12.5 vs. Cont 12.5	No	Cont 12.5
	Oss 19 vs. Cont 19	Yes	Cont 19
	Oss 19 vs. Cont 19, 1k Normalized		Cont 19
	Farm vs. Hook	No	Farm
RAP	Oss 12.5 vs. Farm	Yes	Farm
	Cont 12.5 vs. Hook	No	Hook

MMLS3 Tests on Field Cores

A set of nine field cores were obtained by the NHDOT from the shoulder of Route 25, between the towns of Effingham and Freedom, although one was too damaged to be used. Each core contained both the surface layer and base layer from the road. The highway had beed paved approximately one year before using the Oss 12.5 mix for the surface layer and the Oss 19 mix for the base layer. The NHDOT provided the measured Gmm for the cores and the Gmb for each sample was measured in the UNH laboratory. Tables 5.16 and 5.17 summarize the volumetric data.

Table 5.16: Volumetrics for Field Core Surface Layer

Brick ID	Gmm	Gmb	AV	VMA	Thickness (mm)
EF12.5-1	2.429	2.234	8.0	18.5	39.02
EF12.5-2	2.429	2.274	6.4	17.0	38.68
EF12.5-6	2.429	2.262	6.9	17.5	38.84
EF12.5-8	2.429	2.256	7.1	17.7	37.17
EF12.5-3	2.429	2.281	6.1	16.8	35.28
EF12.5-4	2.429	2.271	6.5	17.2	35.24
EF12.5-5	2.429	2.253	7.3	17.8	30.71
EF12.5-7	2.429	2.248	7.4	18.0	28.83
Average	2.429	2.260	7.0	17.6	35.47

Table 5.17: Volumetrics for Field Core Base Layer

Brick ID	Gmm	Gmb	AV	VMA	Thickness (mm)
EF19-5	2.455	2.321	5.5	15.1	48.29
EF19-4	2.455	2.375	3.3	13.1	45.41
EF19-6	2.455	2.340	4.7	14.4	42.49
EF19-7	2.455	2.324	5.3	15.0	42.97
EF19-2	2.455	2.343	4.5	14.3	41.03
EF19-3	2.455	2.319	5.6	15.2	42.10
EF19-1	2.455	2.323	5.4	15.0	40.18
EF19-8	2.455	2.332	5.0	14.7	40.49
Average	2.455	2.335	4.9	14.6	42.87

The MMLS3 tests on the field cores had the same parameters as the tests on the laboratory compacted samples, except for the total number of cycles run. The field cores developed excessively large rutting and heave, so the tests were stopped after only 30,000 loading cycles. The rut depths from the top of the heave are not shown in Figures 5.24 and 5.25 because the heave was often so large that it had to be broken off to get any profile measurement. Furthermore, a modified range for the average rut depth was used for many of the measurements in both data sets.

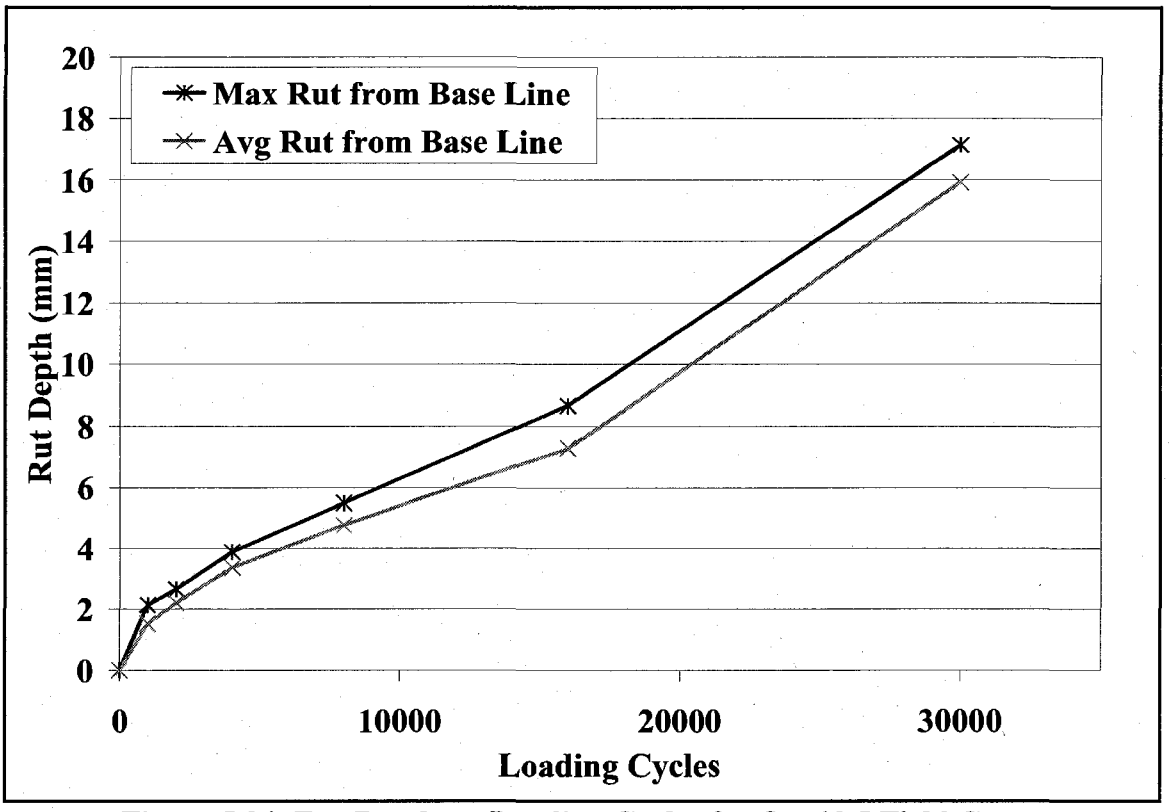

Figure 5.24: Rut Depth vs. Loading Cycles for Oss 12.5 Field Cores

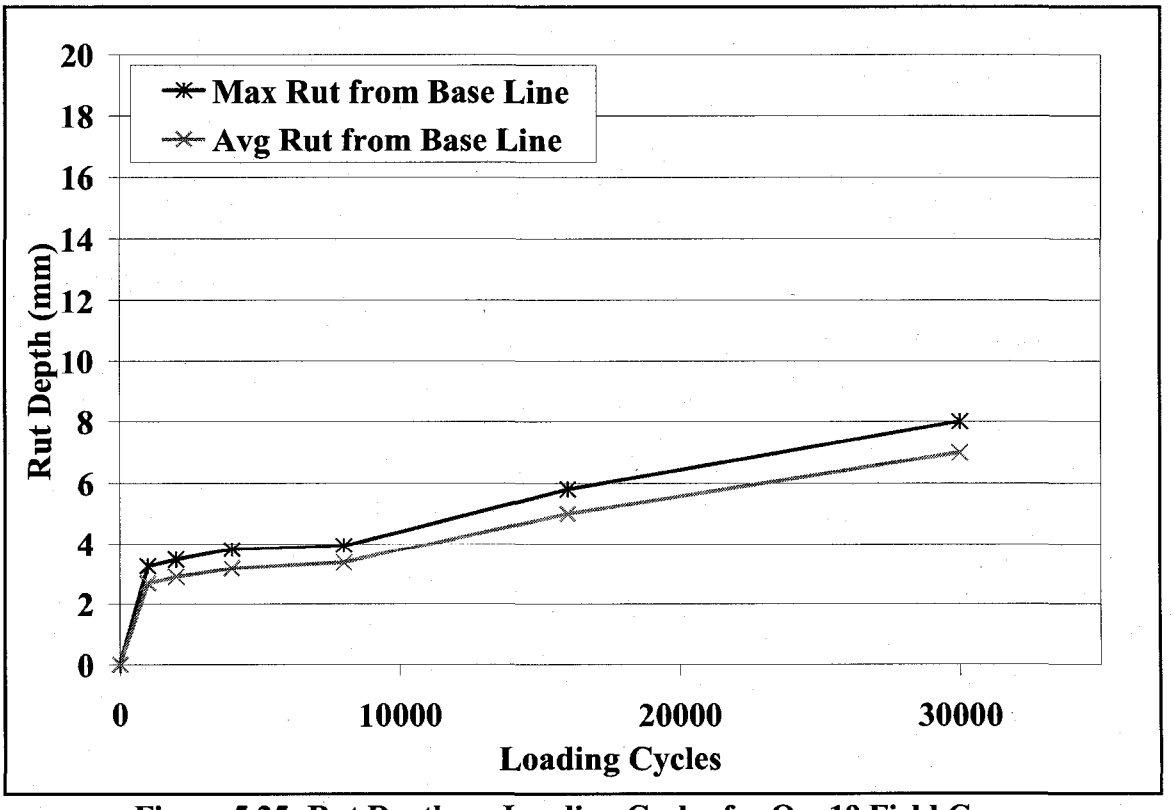

Figure 5.25: Rut Depth vs. Loading Cycles for Oss 19 Field Cores

The graphs in Figures 5.24 and 5.25 show that the Oss 19 field cores out performed the Oss 12.5 field cores, as is expected because of its coarser blend. Additionally, the rate of rutting in the Oss 12.5 field cores is much greater than the Oss 19 field cores. The reason for this could be the higher air void content in this layer, 7.0% verses 4.9%. More air voids mean the mix is less dense and will compact and deform more under vertical loads. Figures 5.26 and 5.27 show how the field cores compared to the laboratory fabricated samples.

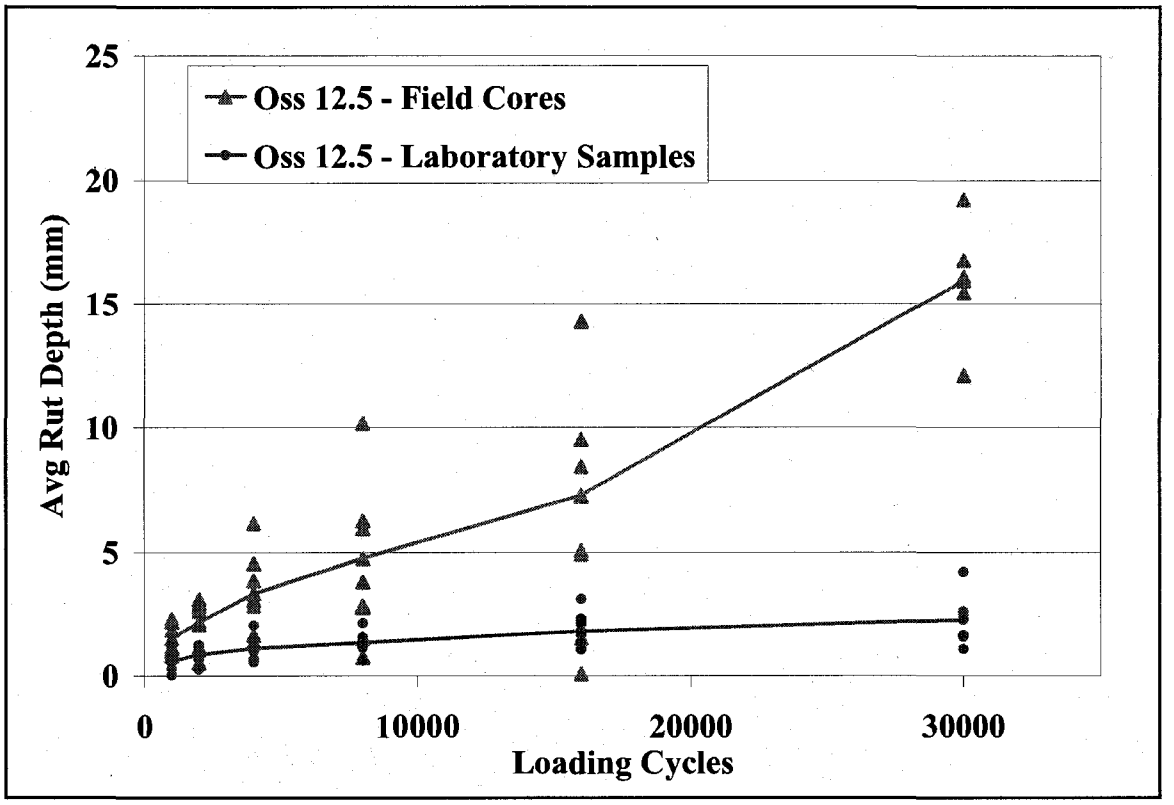

Figure 5.26: Comparison Graph of Oss 12.5 Lab Samples and Field Cores

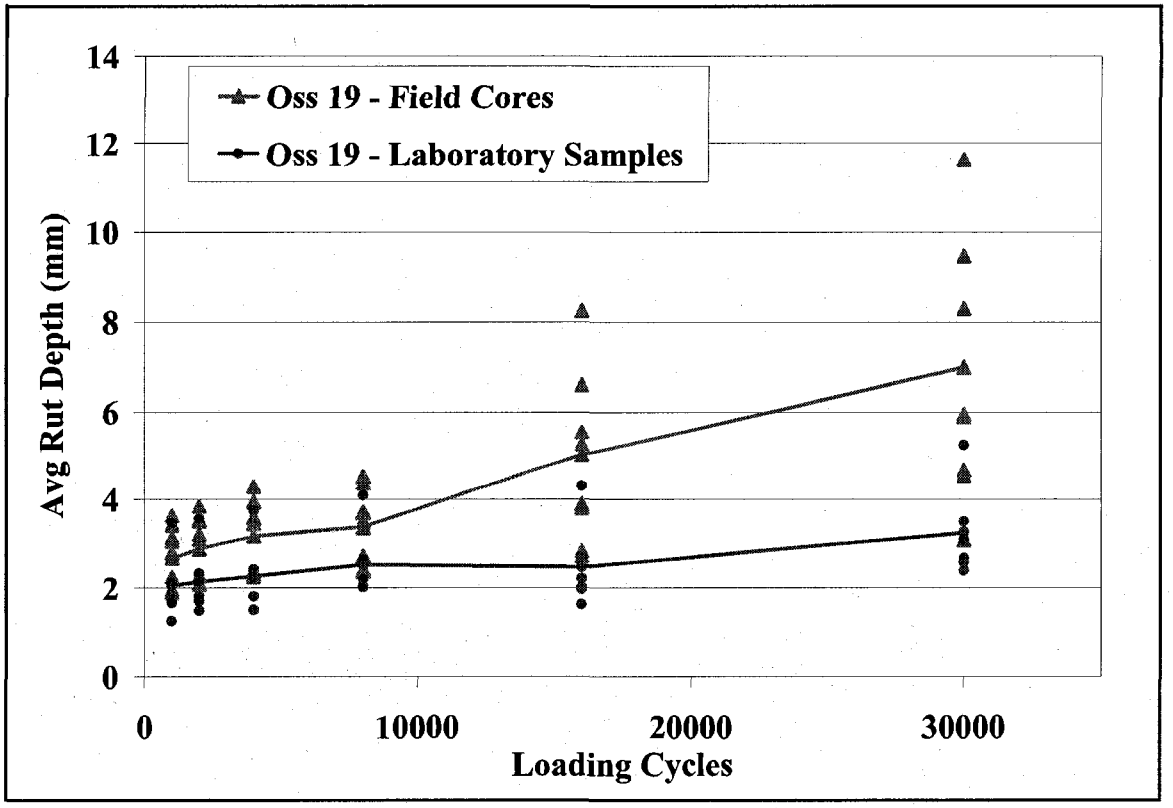

Figure 5.27: Comparison Graph of Oss 19 Lab Samples and Field Cores

In each comparison, the laboratory fabricated samples out performed the field cores, as was expected. It is likely that the reason for this is that the field cores had higher air voids and VMAs in each case. A higher percentage of voids in the brick volume allows more compaction and deformation than in bricks with less voids. The reason these samples had high percentages of voids is that they were paved only a year before and had experience very little traffic loading because they were from the shoulder.

Just as with the test on the Oss 19 laboratory samples, the tests on the field cores did not apply a seating load. Similarly, the Oss 19 field cores developed more rutting in the first 1,000 loading cycles than the Oss 12.5 field cores. As with the earlier

comparisons, the rut measurements can be renormalized to the rut depth at 1,000 loading cycles. Table 5.18 summarizes the increased rutting after 1,000 cycles in each test.

Table 5.18: Total Rut Depth Developed between 1,000 and 30,000 Loading Cycles

Test Run	Rut from 1k to 30k
Oss 12.5 Field Cores	14.4 mm
Oss 19 Field Cores	4.3 mm
Oss 12.5 Laboratory Samples	1.7 mm
Oss 19 Laboratory Samples	1.2 mm

Mixtures Redesigned According to the Bailey Method

The three redesigned mixes were Oss 12.5-Bailey, Cont 19-Bailey, and Farm-Bailey. Each redesigned mix has the same NMSA as the corresponding original mix. The Cont 19-Bailey mix was redesigned using a spreadsheet where the input values of CUW, desired dust, and aggregate contributions were adjusted manually to optimize the grading. The Oss 12.5-Bailey and Farm-Bailey mixes were designed using a Matlab program that iterated through all possible combinations of input values to optimize the gradings. An optimum grading was within the control points, out of the restricted zone, and closely matched the target values for the Bailey weight ratios, CA, FAc, and FAf. Figures 5.28 through 5.30 show the gradings of the three redesigned mixes and the original mixes. For clarity the Oss 12.5, Cont 19, and Farm mix designs will be called Oss 12.5-Original, Cont 19-Original, and Farm-Original in this section.

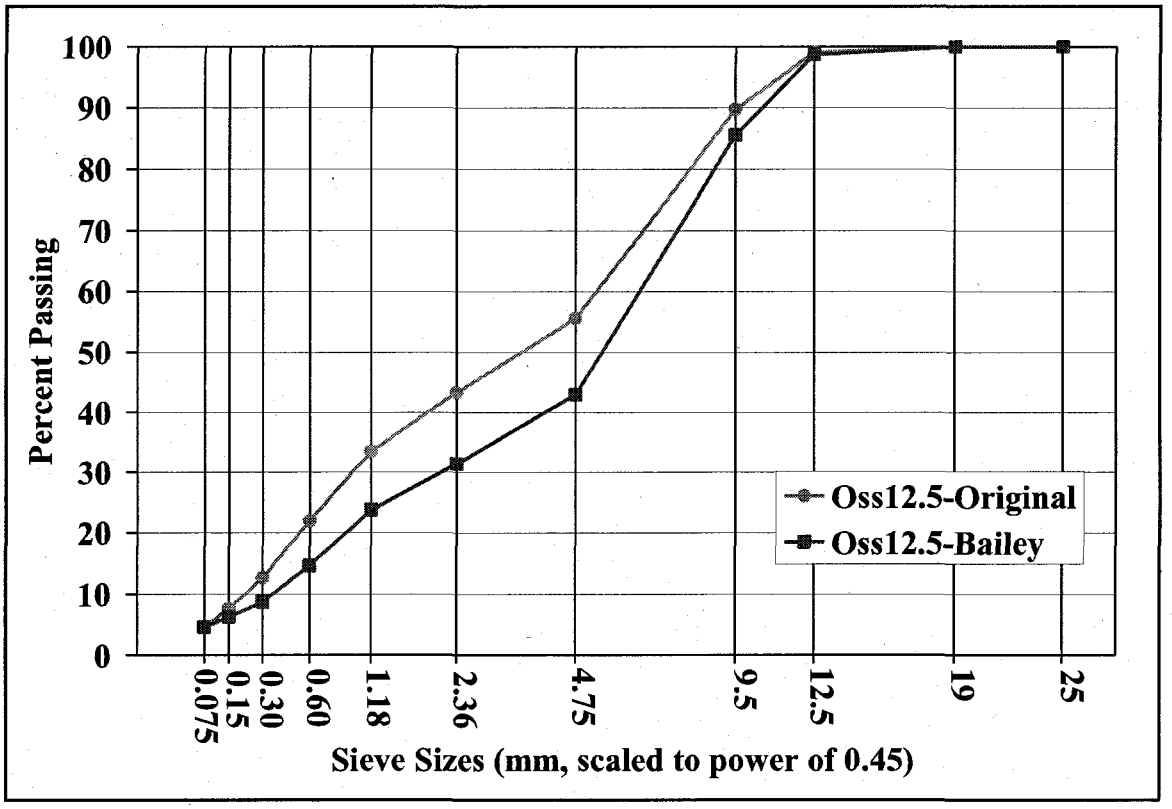

Figure 5.28: Oss 12.5-Original and Oss 12.5-Bailey Mix Design Gradings

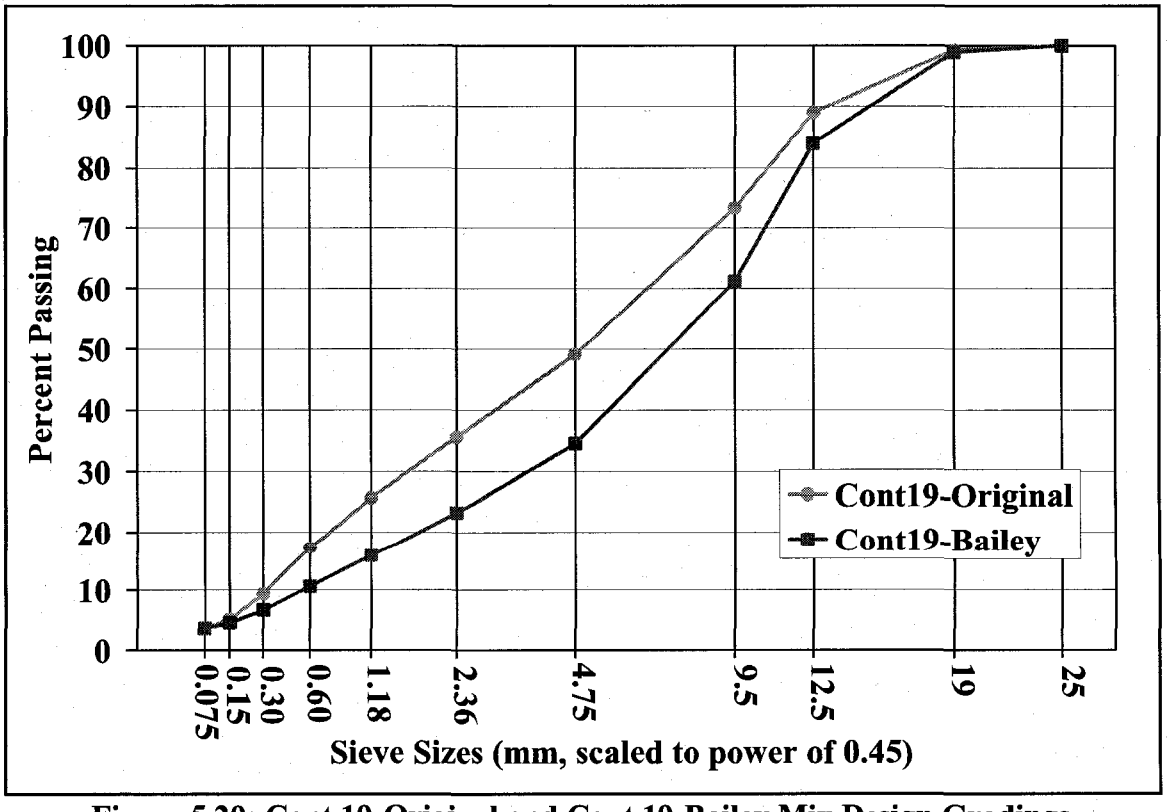

Figure 5.29: Cont 19-Original and Cont 19-Bailey Mix Design Gradings

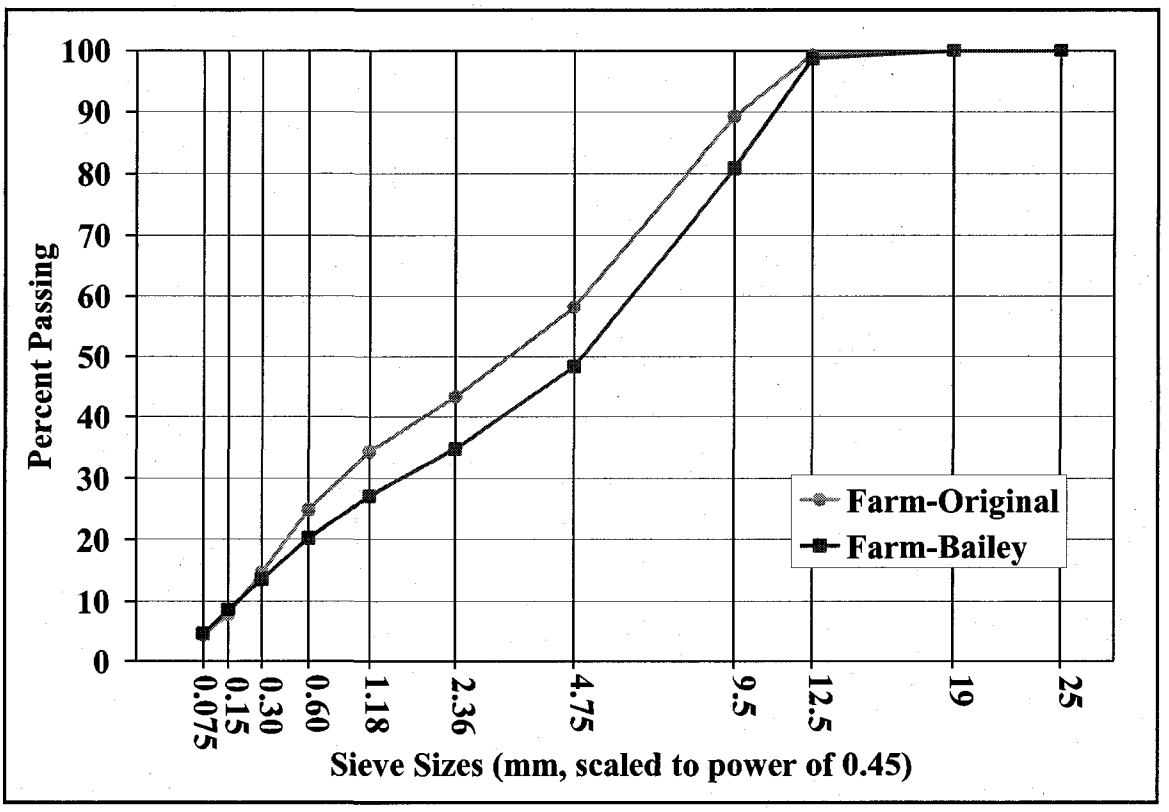

Figure 5.30: Farm-Original and Farm-Bailey Mix Design Gradings

Volumetrics and Bailey Parameters. Table 5.19 shows the Bailey parameters for the three new mix designs. The CUW for each was taken from the aggregate blend design calculations. The weight ratios are calculated from the gradings. Both the Oss 12.5-Bailey and Cont 19-Bailey mix designs had weight ratios close to their target values, which were the average of the upper and lower limit for each ratio. The Farm-Bailey mix had a very high FAc ratio. Several attempts were made to bring this ratio within limits without letting the grading out of the Superpave control points or into the restricted zone. No combination of input values achieved an acceptable FAc ratio without moving the other ratios out of range.

Table 5.19: Bailey Parameters for Redesigned Mixtures

Mix Design	Bailey Parameter	Parameter Value	Target Value	Limits
Oss 12.5	CUW	103		95% - 105%
	CA Ratio	0.57	0.58	0.50 – 0.65
	FAc Ratio	0.47	0.43	0.35 – 0.50
	FAf Ratio	0.42	0.43	0.35 – 0.50
Cont 19	CUW	101		95% - 105%
	CA Ratio	0.68	0.68	0.60 – 0.75
	FAc Ratio	0.46	0.43	0.35 – 0.50
	FAf Ratio	0.42	0.43	0.35 – 0.50
Farm	CUW	101%		95% - 105%
	CA Ratio	0.58	0.58	0.50 – 0.65
	FAc Ratio	0.58	0.43	0.35 – 0.50
	FAf Ratio	0.43	0.43	0.35 – 0.50

Tables 5.20 and 5.21 show the volumetric measurements of the MMLS3 sample bricks for the Oss 12.5-Bailey and Cont 19-Bailey mix designs. There were no bricks fabricated for the Farm-Bailey mix because it failed most of the Superpave criteria when the asphalt content was designed. The data files containing the volumetric measurements on most of the Oss 12.5-Bailey samples were lost. However, the volumetrics of each brick was measured right after fabrication and only those bricks with acceptable air voids, between 3.5% and 4.5%, were marked for testing; all other bricks were destroyed.

Table 5.20: Volumetrics for Oss 12.5-Bailey

Brick ID	Gmm	Gmb	AV	VMA	Thickness (mm)
OMB 2	2.456	2.366	3.7	13.3	58.39
OBM 4	2.456	2.365	3.7	13.3	58.69
OBM 5	2.456				58.80
OBM 6	2.456				58.70
OBM 7	2.456				58.69
OBM 8	2.456				58.80
OBM 9	2.456				58.78
Average	2.456	2.366	3.7	13.3	58.69

Table 5.21: Volumetrics for Cont 19-Bailey

Brick ID	Gmm	Gmb	AV	VMA	Thickness (mm)
CBM 13	2.511	2.416	3.8	15.8	58.89
CBM 14	2.511	2.414	3.9	15.9	58.87
CBM 16	2.511	2.421	3.6	15.6	58.88
CBM 17	2.511	2.415	3.8	15.8	58.89
CBM 19	2.511	2.408	4.1	16.1	58.99
CBM 23	2.511	2.403	4.3	16.2	59.98
CBM 25	2.511	2.410	4.0	16.0	59.98
Average	2.511	2.412	3.9	15.9	59.21

In all cases, the Bailey designs were coarser than the original designs. The reason for this is that the CUW for all the new mixes was chosen between 95% and 105%, which forces a greater density of coarse aggregate in the blend. Upon evaluation with the Bailey Method the original mix designs were found to have a CUW between 70% and 85%, which designates all of them as fine graded mixes. The change in CUW along with the changes in the CA, FAc, and FAf weight ratios influence the expected change in VMA (see Table 2.3 in Chapter 2). The Bailey Method does not mention any special considerations for comparing a fine graded mix to a coarse graded mix. Therefore the weight ratios were calculated twice: once as if both the original and Bailey mixes were coarse graded, and once as if they were fine graded. Tables 5.22 through 5.24 display the four Bailey parameters, calculated according to both the coarse and fine graded cases, for the original and redesigned mixes.

Table 5.22: Expected Change in VMA from Oss 12.5-Original

	CUW	CA	FAc	FAf	Total
Coarse Graded					
Oss 12.5 Original	80	0.68	0.51	0.35	
Oss 12.5 Bailey	103	0.57	0.47	0.42	
Change	23	-0.11	-0.04	0.08	
Predicted Effect on VMA	3.5	-0.4	0.5	-1.1	2.4
Fine Graded					
Oss 12.5 Original	80	1.18	0.35	NA	
Oss 12.5 Bailey	103	1.18	0.42	NA	
Change	23	0.01	0.08	0.00	
Predicted Effect on VMA	3.5	0.0	-1.1	0.0	2.3

Table 5.23: Expected Change in VMA from Cont 19-Original

	CUW	CA	FAc	FAf	Total
Coarse Graded					
Cont 19 Original	74	0.91	0.52	0.36	
Cont 19 Bailey	101	0.68	0.46	0.42	
Change	27	-0.23	-0.07	0.06	
Predicted Effect on VMA	4.1	-0.9	1.0	-0.9	3.3
Fine Graded					
Cont 19 Original	74	0.73	0.36	0.38	
Cont 19 Bailey	101	0.66	0.42	0.54	
Change	27	-0.07	0.06	0.16	
Predicted Effect on VMA	4.1	-0.3	-0.9	-2.3	0.6

Table 5.24: Expected Change in VMA from Farm-Original

	CUW	CA	FAc	FAf	Total
Coarse Graded					
Farm Original	81	0.77	0.57	0.32	
Farm Bailey	101	0.58	0.58	0.43	
Change	20	-0.20	0.01	0.11	
Predicted Effect on VMA	3.0	-0.7	-0.1	-1.6	0.5
Fine Graded					
Farm Original	81	1.06	0.32		
Farm Bailey	101	0.90	0.43		
Change	20	-0.16	0.11	0.00	
Predicted Effect on VMA	3.0	-0.6	-1.6	0.0	0.8

The Bailey Method gives a high and low expected change in VMA, 0.5% and 1.0%, for a given change in each parameter. Tables 5.22 through 5.24 use the average expected change, 0.75%. The fine graded analysis redesignates the original primary control sieve (PCS) as the fine NMSA from which the new, fine control sieves are calculated. For an original NMSA of 12.5mm, the fine tertiary control sieve (TCS) would need openings 0.033 mm in diameter. Since the smallest sieve used for asphalt engineering is the #200 with 0.075 mm openings, the TCS and the FAf ratio were ignored in the fine graded analysis for the Oss 12.5 and Farm calculations.

The actual changes in VMAs are summarized in Table 5.25. The values under VMA_{Design} are the voids measured during the design process for each mix. The values under VMA_{Brick} are the voids measured from the samples fabricated for the MMLS3 tests. Since no bricks were fabricated for the Farm-Bailey mix design, there are no values listed under VMA_{Brick} for the Farm mixes. Figure 5.31 compares the predicted changes in VMA to the actual changes in VMA.

Table 5.25: Measured VMAs

Mix Design	VMA_{Design}	VMA_{Brick}
Oss 12.5 Original	15.2	15.0
Oss 12.5 Bailey	13.7	13.3
Change	-1.5	-1.7
Cont 19 Original	15.2	15.2
Cont 19 Bailey	16.2	15.9
Change	1.0	0.7
Farm Original	15.2	
Farm Bailey	16.6	
Change	1.4	

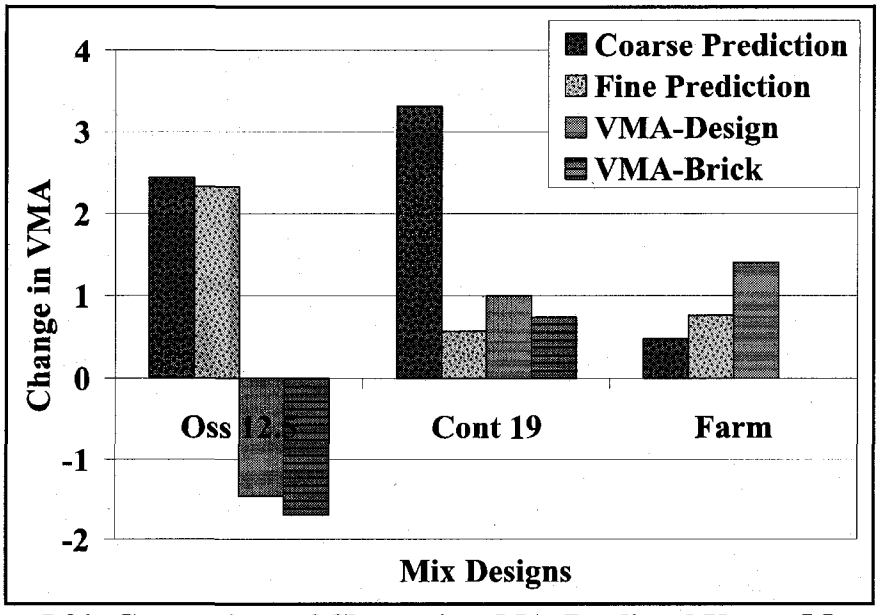

Figure 5.31: Comparison of Change in VMA, Predicted Verses Measured

The reason the predictions for the Farm mix designs were off could be that the RAP had an unpredictable effect on the blend properties. RAP does not always blend fully with the virgin material, so the actual grading may have been different from the grading calculated with the Bailey Method, which used a RAP grading after the RAP binder was extracted. The reason the Cont 19 fine graded prediction was much closer than the coarse graded prediction could be that fine aggregate greatly affected the compaction of the mix. The reason the Oss 12.5 predictions were completely wrong could be that the nature of the gravel stone countered the effect of a dense coarse aggregate skeleton.

MMLS3 Test Results. The MMLS3 tests on the redesigned mixes used the same test parameters as for the original mixes. The only difference in procedure was to imbed the thermocouple that controlled the dry air heater between two bricks. This reduced fluctuations in the temperature throughout the tests, although it did not prevent the

samples from cooling during the first several profile measurements. A graph of the temperature readings for the Cont 19-Bailey MMLS3 test is shown in Figure 5.32. Note the lack of the saw tooth pattern that was apparent in Figure 5.13. During this test the data loggers were set to a lower resolution than for the Cont 19-Original test.

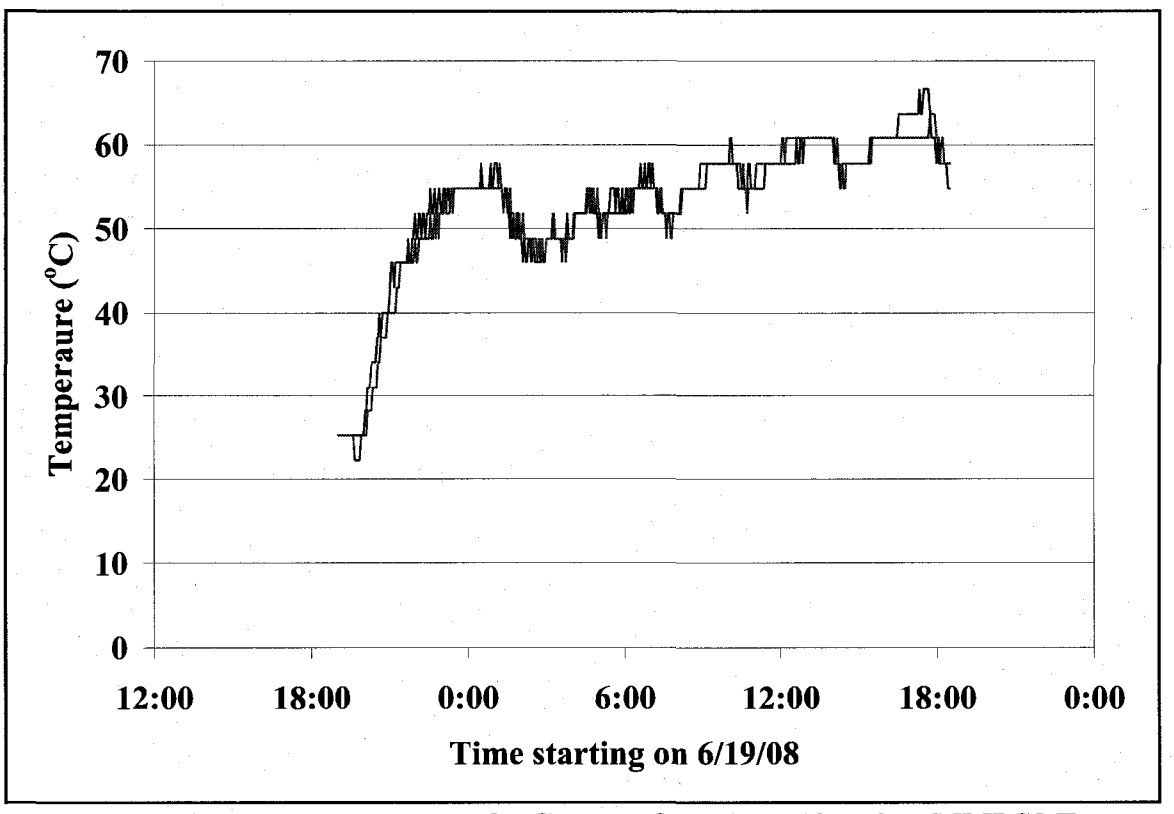

Figure 5.32: Temperature over the Course of the Cont 19-Bailey MMLS3 Test

The rutting over the course of each test is shown in Figures 5.33 and 5.34. In Figures 5.35 and 5.36, the results from the tests on the Bailey mixes are compared to the results from the original mixes. The Oss 12.5-Bailey mix performed better than the Oss 12.5-Original mix and the Cont 19-Bailey mix performed approximately as well as the Cont 19-Original mix. Tables 5.26 and 5.27 list the p-values for each statistical comparison.

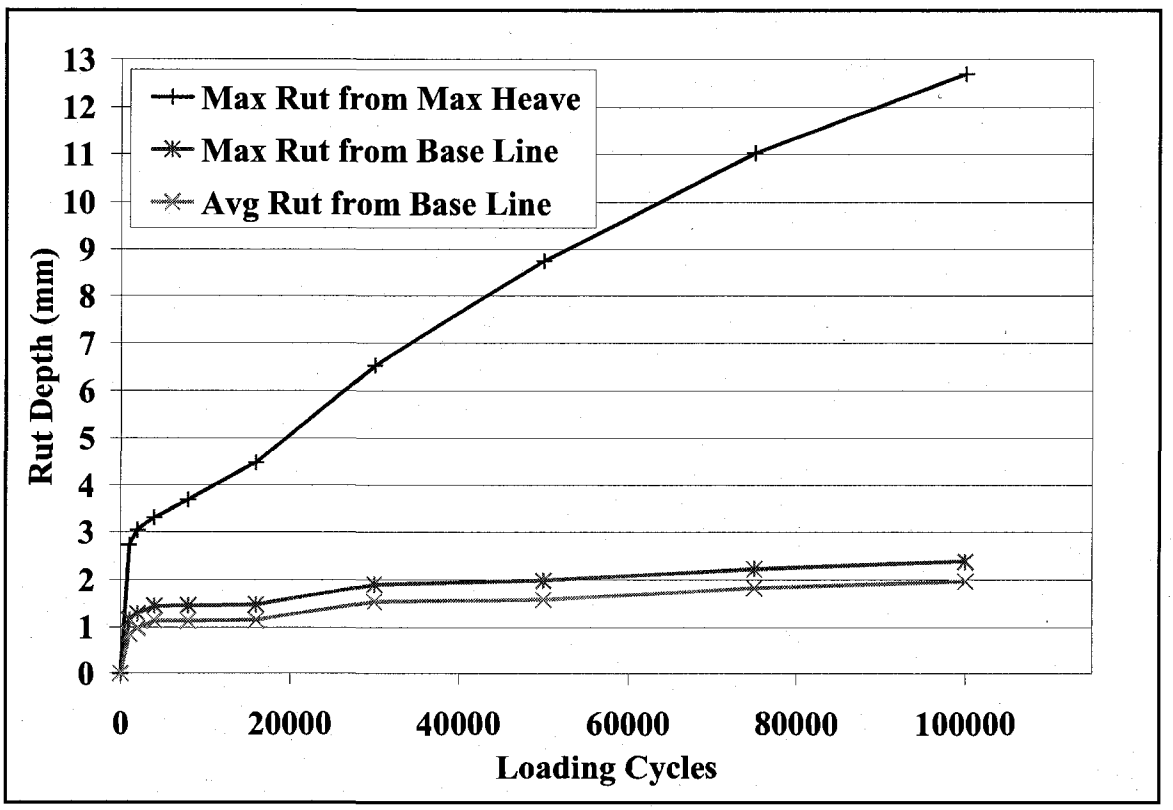

Figure 5.33: Rut Depth vs. Loading Cycles for Oss 12.5-Bailey

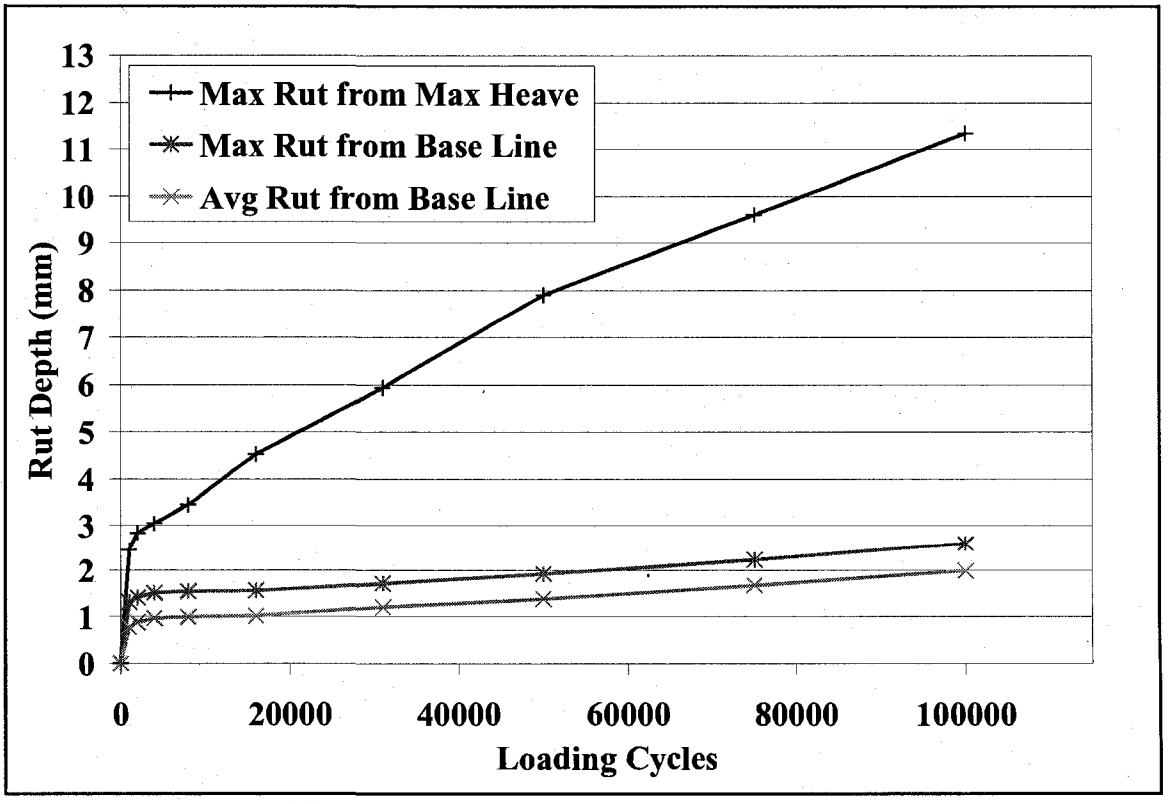

Figure 5.34: Rut Depth vs. Loading Cycles for Cont 19-Bailey

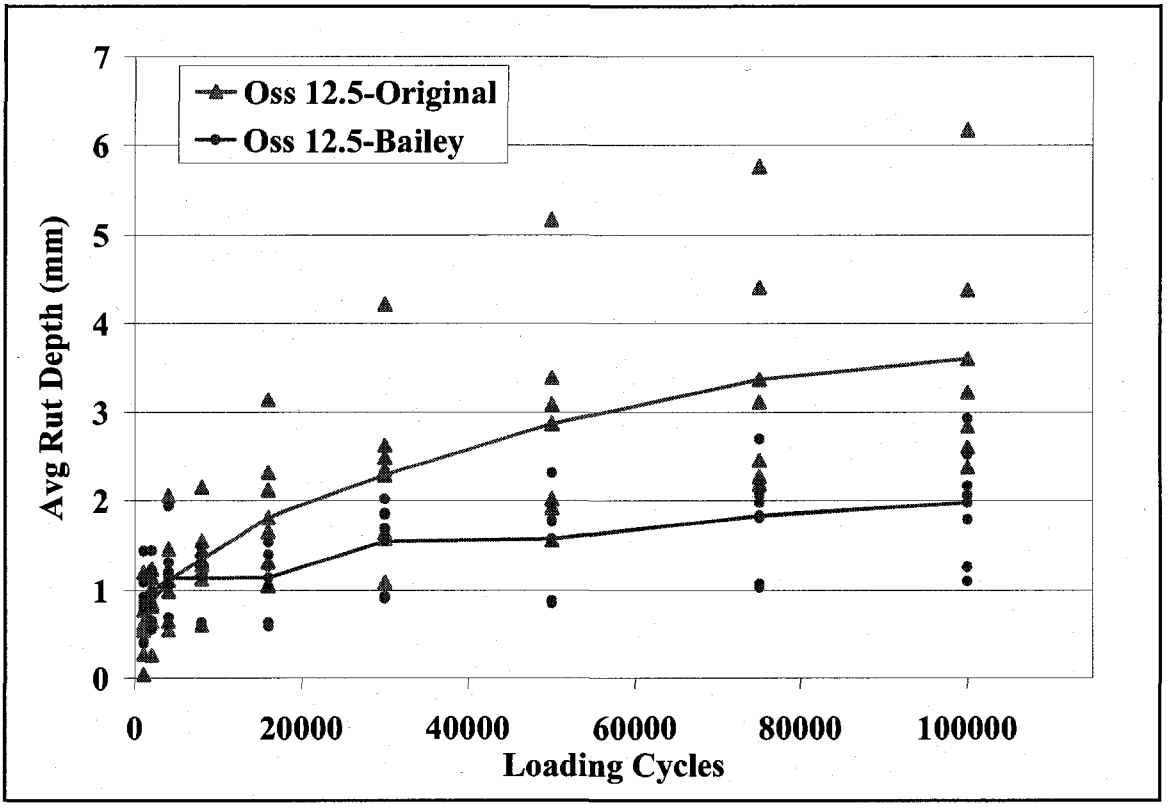

Figure 5.35: Comparison Graph of Oss 12.5-Original and Oss 12.5-Bailey

Table 5.26: Comparison of Rut Depths of Oss 12.5-Original and Oss 12.5-Bailey

	Thousands of Loading Cycles								
	1	2	4	8	16	30	50	75	100
P-Value	0.209	0.620	0.710	0.710	0.097	0.165	0.026	0.004	0.007
Significant Difference	No	No	No	No	No	No	Yes	Yes	Yes

Although the test results only become significantly different after 30,000 loading cycles, Figure 5.35 shows that the Oss 12.5-Bailey mix out performs the Oss 12.5-Original mix. There are several factors that contribute to the improved resistance to rutting. While both mixes have the same NMSA, the Bailey mix is coarser as shown in Figure 5.28. Additionally, the Bailey mix has less VMA, which means there is less room for the aggregate to compact under heavy loads. The value for voids filled with asphalt (VFA) is the percent difference between the air voids and the VMA. Since the VMA is

smaller and the air voids were maintained at approximately 4%, the VFA is smaller as well meaning there is less asphalt binder in the mix to lubricate the aggregate. This gives it more resistance to rutting.

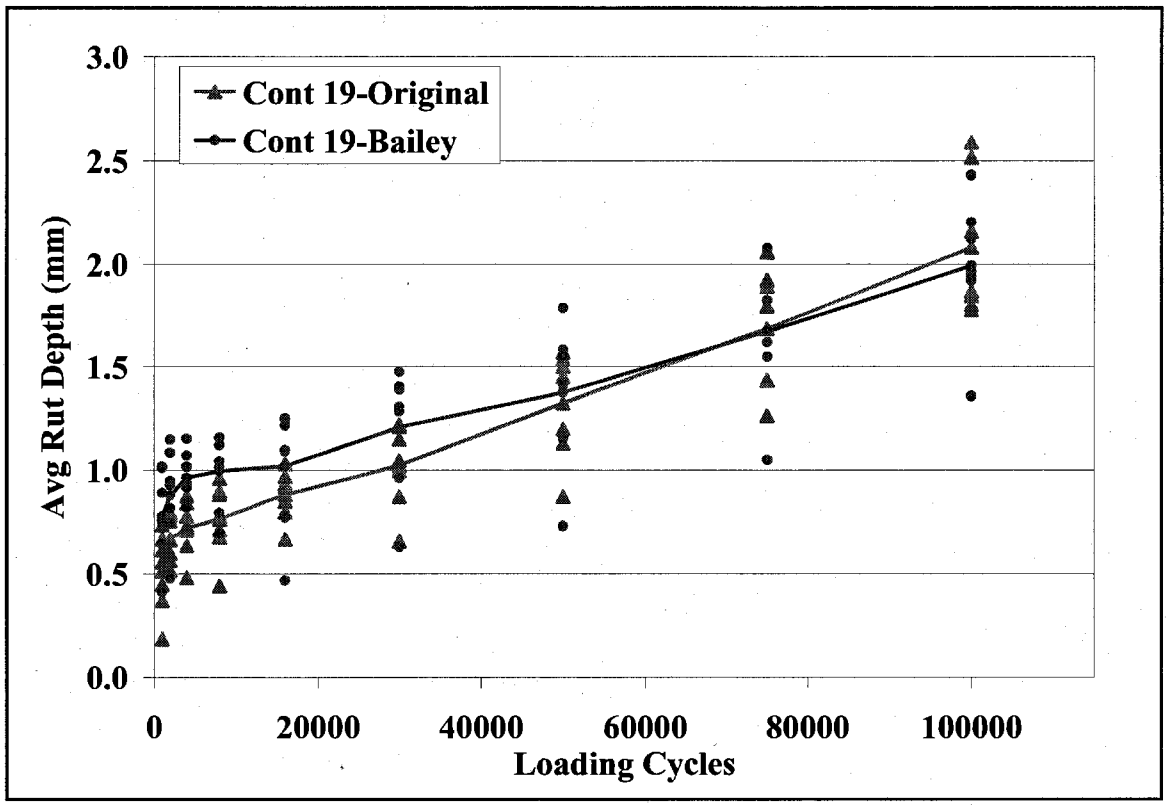

Figure 5.36: Comparison Graph of Cont 19-Original and Cont 19-Bailey

Table 5.27: Comparison of Rut Depths of Cont 19-Original and Cont 19-Bailey

	Thousands of Loading Cycles								
	1	2	4	8	16	30	50	75	100
P-Value	0.038	0.073	0.007	0.038	0.165	0.128	0.710	1.000	0.902
Significant Difference	Yes	No	Yes	Yes	No	No	No	No	No

The Cont 19-Bailey mix did not perform significantly better than the Cont 19-Original mix. Although the Bailey mix was coarser, as is shown in Figure 5.29, it also had greater VMA and, consequently, greater VFA. The greater VMA was predicted by

the Bailey Method because a coarser mix tends to resist compaction more than a finer one. Additionally, the rough and angular fractured rock aggregate probably helped the mix resist compaction even more than usual. While the coarse mix and rough aggregate would also help resist rutting, a greater amount of asphalt binder promotes rutting because it allows the aggregate particles to slide around more easily (Qiu 2006). These two factors seem to have off set each other making the net rutting resistance of the Bailey mix about the same as the original one.

Discussion

Both the Oss 12.5-Bailey and Farm-Bailey mix designs did not fully meet the Superpave criteria when the asphalt content was determined. For an NMSA of 12.5 mm, Superpave requires the VMA to be no lower than 14.0. The Oss 12.5-Bailey mix had a final VMA of 13.7. Since all the other requirements were met, the Oss 12.5-Bailey mix design was deemed acceptable. The Farm-Bailey mix design, however, had a final VMA of 12.2, a %Gmm@Nini of 89.6, and a dust proportion of 1.3. In addition to the VMA criteria, Superpave requires the %Gmm@Nini to be 89 or less and the dust proportion to be between 0.6 and 1.2. Because this mix had such a low VMA and failed two other criteria as well, it was deemed unacceptable for testing in the MMLS3 since it would never be paved in the field anyway.

In addition to failing the Superpave criteria, the Farm-Bailey mix did not have the FAc weight ratio within the recommended limits. According to the Bailey Method, an

FAc ratio above the limit means that the voids are over filled with fine aggregate. This would account for the small VMA because the majority of the voids between the coarse aggregate were filled with fine aggregate. This also accounts for the high dust proportion in the mix. In addition to adversely affecting the volumetrics in the mix, over filled voids can reduce rut resistance. On the other hand, a small VMA would mean a small VFA and asphalt content, which might improve rut resistance. The net result might be no real gain in performance, as with the Cont 19-Bailey mix.

The VMA predictions for Cont 19 mixes were better under the fine graded evaluation. This suggests that the fine aggregate is important in influencing voids in the mixture. The coarse aggregate was so densely packed that it kept the voids between the coarse particles large by resisting compaction. The Bailey fine weight ratios suggested that there was enough fine aggregate to adequately fill those voids and act as dry lubrication to help the mix compact more easily. However, the weight ratios are derived from a model that assumes that the coarse particles are adequately compacted. The Cont 19-Bailey mix may not have compacted enough, leaving voids too large to be filled by the fine aggregate present. If the blend had been designed so the fine aggregate ratios were at the upper end of their limits, instead of in the middle, then the mix might have compacted more and the voids might have been filled more completely. This would have lowered the VMA, which in turn would have lowered the VFA and raised the rutting resistance.

The Bailey Method predictions on compactability state that a higher CUW and CA ratio values mean greater resistance to compaction. If the values stay within the recommended range, then the increased resistance should be too small to hinder paving operations. Additionally, similar effects occur with lowered FAc ratio and FAf ratio values. Figure 5.37 shows the average compaction for both the Cont 19-Original and Cont 19-Bailey samples. The Bailey samples require approximately 3 times the number of gyrations as the original ones to reach the same height. Figure 5.38 shows the average density of both sets of samples over the course of compaction. The Bailey samples required about 2 times the number of gyrations to reach the same density as the original ones. As it is, the Cont 19-Bailey mix would be difficult to compact in the field.

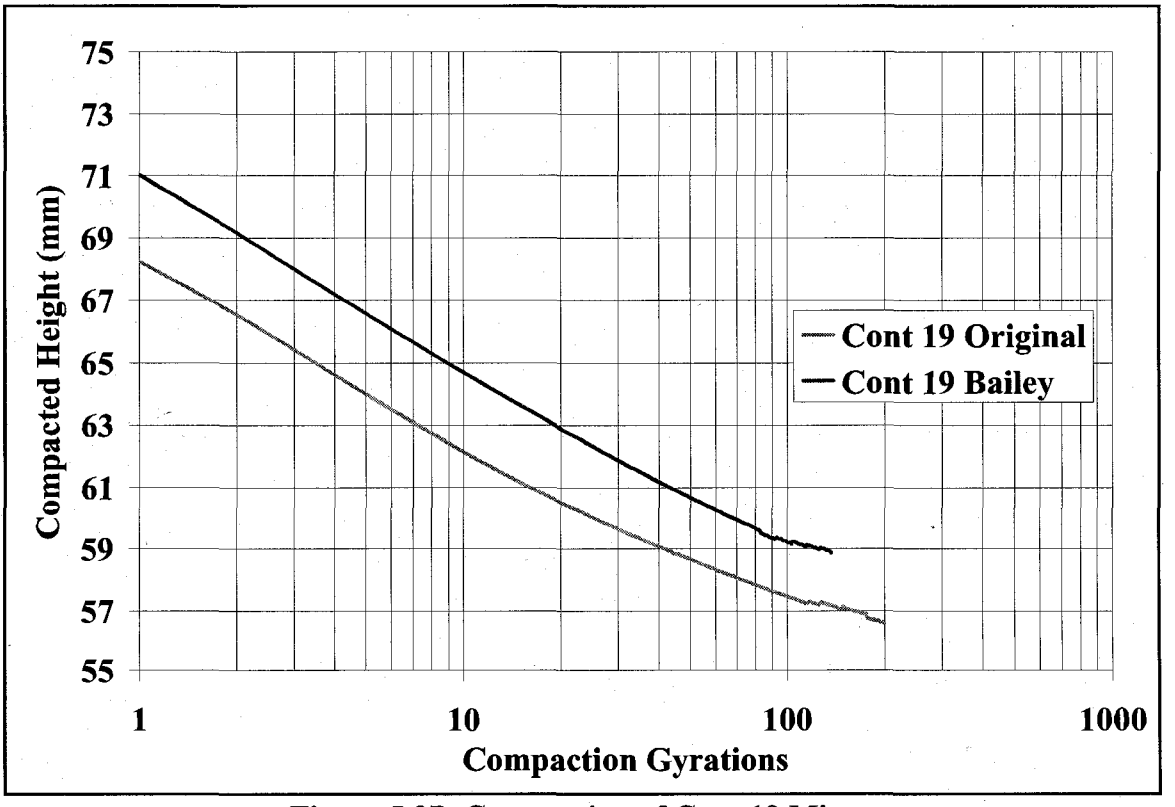

Figure 5.37: Compaction of Cont 19 Mixes

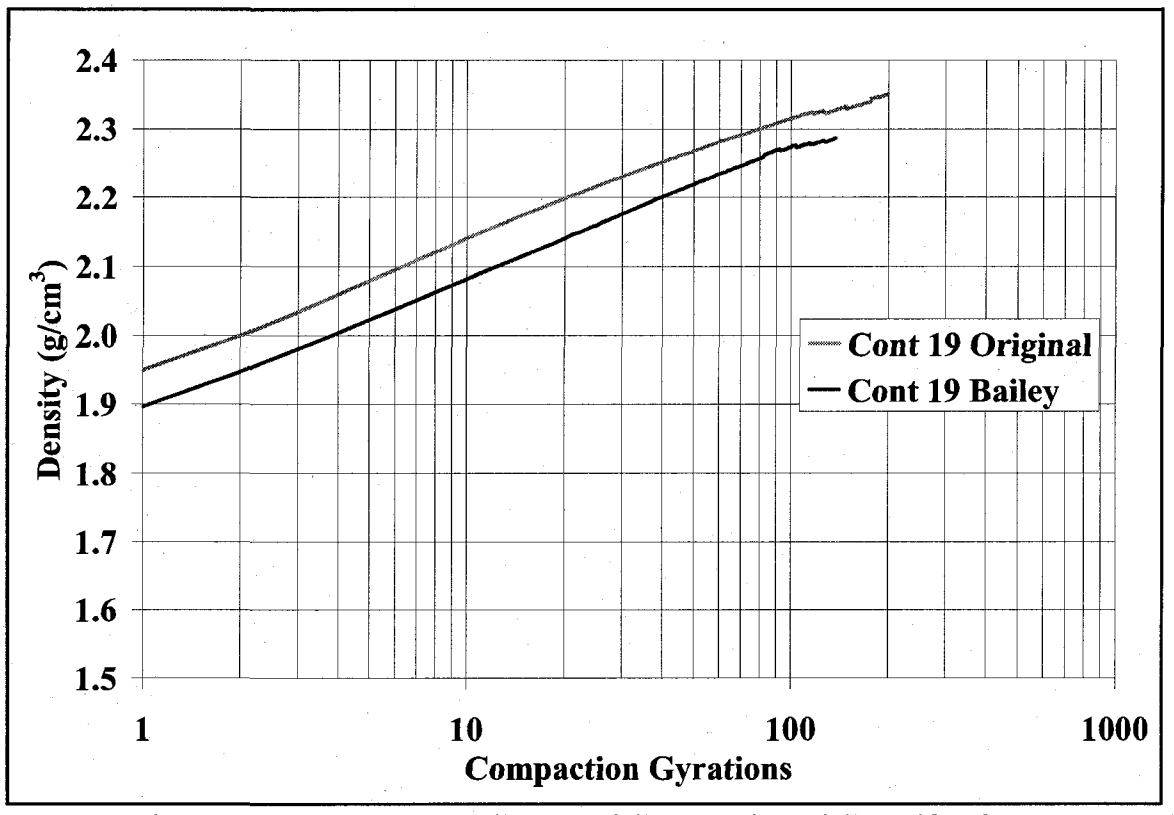

Figure 5.38: Density over Course of Compaction of Cont 19 Mixes

The Oss 12.5-Bailey mix was expected to have a greater VMA than the Oss 12.5-Original mix because the Bailey Method predicts that the greater density in coarse aggregate will resist compaction causing an increase in VMA. While the rough, angular fractured rock in the Cont 19-Bailey mix most likely supported this resistance to compaction, the smooth, rounded gravel stone in the Oss 12.5-Bailey mix may have countered the resistance to compaction. The Bailey Method assumes there will be enough compaction so its model of particle packing applies. However, if there was extra compaction, then voids between the coarse aggregate were smaller than expected and most of the space was taken up by fine aggregate instead of air or binder, thus resulting in a lower VMA. The lower VMA, lower asphalt content, and a coarser blend seem to be the greatest factors that improved the rut resistance over the original design.

The increased CUW for the Oss 12.5-Bailey mix also meant that this mix would have greater resistance to compaction than the original mix. Although the samples for the original mix design were batched to 4500g and the samples for the Bailey design were batched to 2250g, the densities can be compared. Figure 5.39 shows the comparison of the average densities of the two mixes over the course of compaction. The Oss 12.5-Bailey samples require approximately 3 times the number of gyrations to reach the same density as the original samples. This confirms the Bailey Method prediction. The compaction data do not indicate whether the aggregate shape and texture had any effect on the mixture's resistance to compaction.

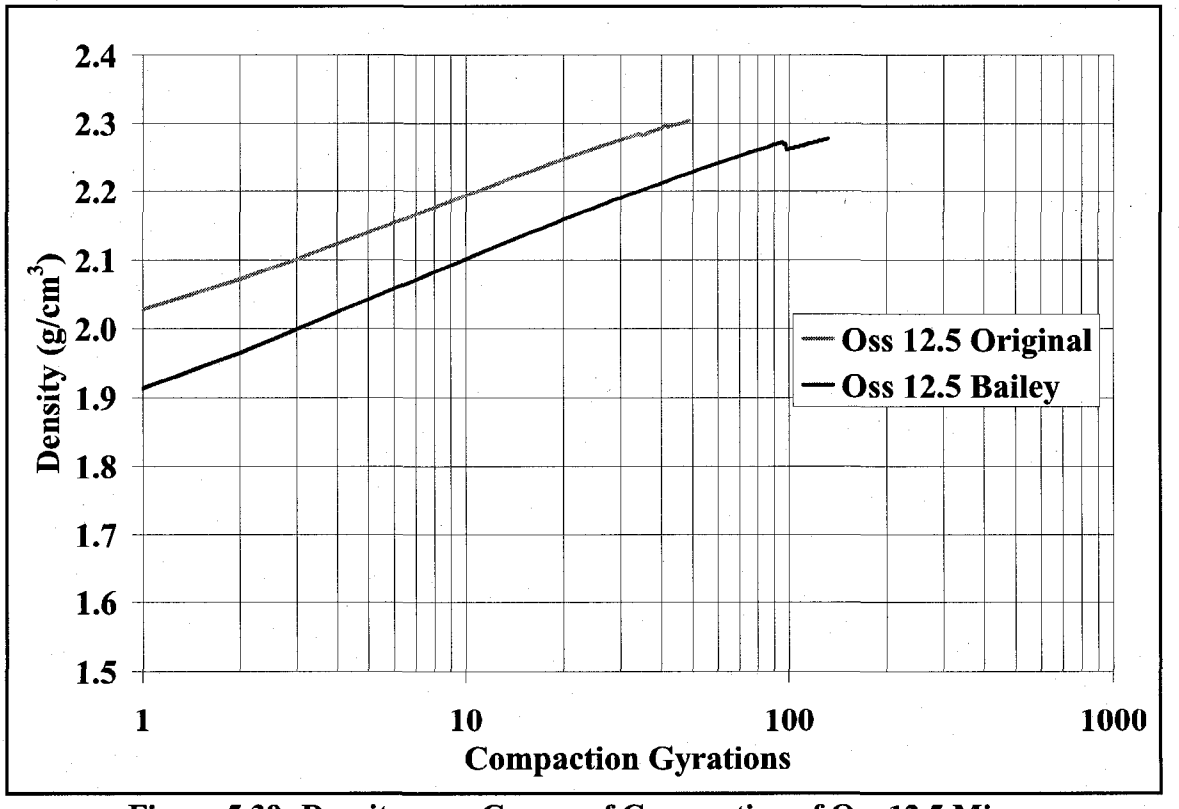

Figure 5.39: Density over Course of Compaction of Oss 12.5 Mixes

CHAPTER 6

SUMMARY AND CONCLUSIONS

Summary of Final Results

This project's objective was to determine the effectiveness of the Bailey Method as a tool to design more rut resistant mixtures using New Hampshire aggregate. Six mix designs currently used in New Hampshire, representing different mixture properties, were tested for rutting performance using the MMLS3. Three of these mixes were redesigned according to the Bailey Method and two were tested under the MMLS3. Finally, two sets of laboratory samples were compared to pavement cores of the same mix designs taken from a highway in New Hampshire.

The results from the performance tests on the original six mix designs were compared based on NMSA, aggregate type, and use of RAP. The mixtures with a higher NMSA had coarser aggregate blends and were, therefore, expected to develop less rutting. However, the Oss 19 mix showed inferior rutting resistance to the Oss 12.5 mix, although the former had a higher NMSA. Most of the rutting in the Oss 19 samples developed between 0 and 1,000 cycles, only 1% of the total load applied. From 1,000 to 100,000 loading cycles, the Oss 19 samples developed less additional rutting than the Oss 12.5 samples. The MMLS3 test results for the Oss 19 mix may not be an accurate

representation of that mix design's rutting resistance because the bricks were not properly seated in the test bed, or because the samples experienced excessive preheating. Conversely, the comparison between the Cont 12.5 and Cont 19 mixes showed superior performance in the Cont 19 mix design, which was the expected result.

The mixtures with fractured rock aggregate were expected to out perform the mixtures with gravel. The comparisons between the Oss 12.5 and Cont 12.5 mix designs and the Oss 19 and Cont 19 mix designs supported this expectation. Both Cont mixtures with fractured rock did have superior performance to the Oss mixtures with gravel stone. However, between the mixtures with RAP, the Hook mix with fractured rock had approximately equal rut resistance to the Farm mix with gravel stone. It is likely that the influence of the RAP overpowered any influence of differing aggregate.

The mixtures that included RAP were expected to have superior performance to those that did not because RAP is generally stiffer thanks to its aged binder. Between the mixes using gravel stone, the Farm mix with RAP out performed the Oss 12.5 mix without RAP. Between the mixes with fractured rock, the Hook mix with RAP out performed the Cont 12.5 mix without RAP, which supports the expectation.

The field cores were taken from the shoulder of Route 25 in NH, between Effingham and Freedom, which had been paved approximately a year before with the Oss 19 mix for the base layer and the Oss 12.5 mix for the surface layer. The field cores had higher average air voids than the laboratory fabricated samples: and 7.0% verses 3.9% for

the Oss 12.5 mix and 4.9% verses 4.1% for the Oss 19 mix. The MMLS3 tests on these field cores were only run up to 30,000 loading cycles because the bricks rutted too deeply to continue. When compared with each other, the Oss 19 field cores out performed the Oss 12.5 field cores as was expected. In each case the laboratory fabricated bricks out performed the field cores, most likely due to their lower air voids.

The three mixes that were redesigned according to the Bailey Method were the Oss 12.5 mix, the Cont 19 mix, and the Farm mix, chosen to represent different aggregate type, NMSA, and RAP content. All three new aggregate blends were coarser than the original ones. After the asphalt content was determined according to Superpave, the Oss 12.5-Bailey mix had a VMA 0.3 below the Superpave minimum value of 14.0. However, this was deemed acceptable and the mix was tested in the MMLS3. The Farm-Bailey mix, on the other hand, had even lower VMA, 12.2, and failed on two other Superpave criteria and thus was unacceptable for further testing.

The Bailey Method predictions on the VMA of the redesigned Oss 12.5 mix were completely wrong because they estimated a positive change in VMA when there was actually a negative change. A possible reason for this is that the smooth, rounded gravel stone allowed aggregate blend to compact more than the Bailey Method accounted for. The coarse graded prediction for the Cont 19 mix was much too high, although the fine graded prediction was quite close to the actual changes. This suggests that the reduction of the fine aggregate, and not the addition of the coarse aggregate, was the main factor in the change in VMA from the original mix design. The predicted change in VMA in the

Farm mixes were about half of the actual change. The RAP in the Farm mix may have been too unpredictable to allow a more accurate estimate of the change in VMA.

The performance of the Bailey designs was expected to be superior to the original designs. The Oss 12.5-Bailey samples met this expectation and developed much less rutting than the Oss 12.5-Original samples. This was probably due to a combination of a coarser aggregate blend, a lower VMA, and lower asphalt content. The Cont 19-Bailey samples performed about as well as the Cont 19-Original samples. Although the Bailey mix was coarser it had a larger value for VMA, which requires a greater asphalt content to keep the air voids at approximately 4%. The rut resistance gained by a coarser mix and the rut resistance lost by a greater asphalt content combined to a net result of no significant change in performance.

Conclusions from the Results

- The Bailey Method is a useful tool in redesigning and evaluating aggregate blends, especially when combined with judgement based on engineering experience.
- The Bailey Method has two main limitations: First, it only looks at aggregate size and pays little attention to other aggregate properties. Second, it has limited procedures in working with RAP.
- In its current form, the Bailey Method does not accurately predict the VMA of the NH mixtues evaluated in this study.
- The MMLS3 is a useful tool for comparing the performance of various mix designs.

- Users should be fully familiarized with the MMLS3 workings and testing procedures to save time and material in the long run. This can best be achieved by running several practice tests first.
- The MMLS3 results are a good indication of rutting resistance when measured from the original, undeformed profile.
- The MMLS3 does not give accurate results when the rut is measured from the top of the heave for test run on bricks held in the test bed.

Suggested Areas of Further Research

Additional mixes could be designed or redesigned with the Bailey Method. Particularly, it might be useful to use the Bailey Method with mixes that contain RAP to help develop more detailed procedures for working with RAP. Additionally, several different target values for the CUW and weight ratios could be tried to see which yield optimum results when using New Hampshire aggregate. This could also be done by simply evaluating existing mixes with the Bailey Method and comparing their performances based on the differences in Bailey parameters.

Additional MMLS3 tests could be run on the mix designs used in this project or with new mixes that use similar aggregate. An MMLS3 test in the wet condition looks at the effect of stripping and rutting by submerging the samples in hot water prior to and during testing. Such a test would indicate whether the Oss 12.5-Bailey mix is adversely

affected by its low VMA, or if the Cont 19-Bailey mix is prone to stripping and raveling because of its large voids.

Another type of comparison could be done to measure the effects of air voids and/or sample thickness in the MMLS3 sample bricks. Several sample sets of the same mix design and asphalt content could be compacted to different heights or levels of air voids and then tested. If an approximate mathematical model could be derived from the test results, then it might help when comparing laboratory fabricated samples to field cores tested in the MMLS3.

After samples have been testing under the MMLS3, they could be analyzed for changes in density and strength. The samples could be cut and polished to look for any indication of how they deformed. Cutting the samples might also show whether or not the RAP fully integrated into the mix and whether or not the coarse aggregate skeleton was uniformly distributed as the Bailey Method assumes.

Final Remarks

Although only one of the two mix designs that was redesigned according to the Bailey Method and tested in the MMLS3 showed significantly improved rutting resistance, I believe that the Bailey Method can be a useful tool to engineers in New Hampshire. Some work would need to be done to fine tune the limits and procedures in the Bailey Method to account for properties of New Hampshire aggregates. Plus,

additional testing would be needed to make sure the redesigned mixes can maintain superior rut resistance under adverse weather conditions common in this state. Such work should utilize the experiential knowledge of engineers who have worked on the highways of New Hampshire for years. Once this work is done, I think that new mixes can be designed that have superior performance and longer life times.

REFERENCES

AASHTO T-2-91 (2000), "Sampling of Aggregates." Standard Specifications for Transportation Materials and Methods of Sampling and Testing, Part 2A: Tests, 25th Edition, American Association of State Highway and Transportation Officials, 2005

AASHTO T-19M/ T-19-00 (2004), "Bulk Density (Unit Weight) and Voids in Aggregate." Standard Specifications for Transportation Materials and Methods of Sampling and Testing, Part 2A: Tests, 25th Edition, American Association of State Highway and Transportation Officials, 2005

AASHTO T-166-05, "Bulk Specific Gravity of Compacted Hot-Mix Asphalt Using Saturated Surface-Dry Specimens." Standard Specifications for Transportation Materials and Methods of Sampling and Testing, Part 2A: Tests, 25th Edition, American Association of State Highway and Transportation Officials, 2005

AASHTO T-209-05, "Theoretical Maximum Specific Gravity and Density of Hot-Mix Asphalt Paving Mixtures." Standard Specifications for Transportation Materials and Methods of Sampling and Testing, Part 2A: Tests, 25th Edition, American Association of State Highway and Transportation Officials, 2005

AASHTO T-248-02, "Reducing Samples of Aggregate to Testing Size." Standard Specifications for Transportation Materials and Methods of Sampling and Testing, Part 2B: Tests, 25th Edition, American Association of State Highway and Transportation Officials, 2005

Epps, A. L.; T. Ahmed; D. C. Little; F. Hugo. "Performance Prediction with the MMLS3 at Westrack." Texas Department of Transportation, Research Report FHWA/TX-01/2134-1, May 2001

Gierhart, D. "Analysis of Oklahoma Mix Designs for the National Center for Asphalt Technology Test Track Using the Bailey Method." *Practical Approaches to Hot-Mix Asphalt Mix Design and Production Quality Control Testing,* Transportation Research E-Circular No. E-C124, December 2007

Khosla, N.P.; S. Sadasivam. "Determination of Optimum Gradation for Resistance to Permeability, Rutting and Fatigue Cracking." North Carolina Department of Transportation, Final Report FHWA/NC/2004-12, February 2005

Mohammad, L.N.; K. Al Shamsi. "A Look at the Bailey Method and Locking Point Concept in Superpave Mixture Design." *Practical Approaches to Hot-Mix Asphalt Mix Design and Production Quality Control Testing,* Transportation Research E-Circular No. E-C124, December 2007

Qiu, Y.F.; K.M. Lum. "Design and Performance of Stone Mastic Asphalt." *Journal of Transportation Engineering*. December 2006

Roberts, F.L.; P.W. Kandhal; E.R. Brown; D. Lee; T.W. Kennedy. "Hot Mix Asphalt Materials, Mixture Design, and Construction." 2nd Edition. National Asphalt Pavement Association Research and Education Foundation, Lanham MD, 1996

Smit, A. F.; F. Hugo; D. Rand; B. Powell. "MMLS3 Testing at the NCAT Test Track." TRB Annual Meeting, Transportation Research Board, Washington D. C., January 2003

Smit, A.F.; F. Hugo, A. Epps. "Report on the First Jacksboro MMLS Tests." Texas Department of Transportation, Research Report FHWA/TX-00/0-1814-2, December 1999

Superpave Mix Design, Superpave Series No. 2 (SP-2), 3rd Edition, Asphalt Institute, 2001 Printing

Thompson, G. "Investigation of the Bailey Method for the Design and Analysis of Dense-Graded HMAC Using Oregon Aggregates." Oregon Department of Transporation, Federal Highway Administration, Final Report FHWA-OR-DF-07-02, September 2006

Vavrik, W. R.; G. Huber, W. J. Pine, S. H. Carpenter, R. Bailey. "Bailey Method for Gradation Selection in Hot-Mix Asphalt Mixture Design." Transportation Research E-Circular No. E-C044. Transportation Research Board, Washington D.C., October 2002

APPENDIX 1

BAILEY METHOD CALCULATIONS

Design Calculations

The calculations shown here use the Oss 12.5 mix design as an example. These calculations were used for both design and evaluation. For design, the input values were varied until the weight ratios were as close to their target values as possible. For evaluation, the input values were varied until the calculated blend matched the original blend as closely as possible. At each step in the calculations, the general equation is shown followed by the calculations using the numerical values for Oss 12.5.

Abbreviations:

CA_1: Coarse Aggregate 1
FA_1: Fine Aggregate 1
MF: Mineral Filler Aggregate
PCS: Percent Passing the Primary Control Sieve
#200: Percent Passing the #200 Sieve
Gsb_i: Bulk Specific Gravity of Aggregate i
LUW_i: Loose Unit Weight of Aggregate i (kg/m^3)
RUW_i: Rodded Unit Weight of Aggregate i (kg/m^3)
CUW: Chosen Unit Weight
Dust: Desired Amount Passing the #200 Sieve for the Final Gradation
CA_iW_c: Contributed Weight for Coarse Aggregate i
FA_iW_c: Contributed Weight for Fine Aggregate i
VCA: Voids in the Coarse Aggregate
TUW: Total Unit Weight
CA_iB_{in}: Initial Contribution of Coarse Aggregate i as a Percentage of the Total Blend
CA_iB_f: Final Contribution of Coarse Aggregate i as a Percentage of the Total Blend
FA_iB_{in}: Initial Contribution of Fine Aggregate i as a Percentage of the Total Blend
FA_iB_{adj}: Adjusted Contribution of Fine Aggregate i as a Percentage of the Total Blend
FA_iB_f: Final Contribution of Fine Aggregate i as a Percentage of the Total Blend
MFB_f: Final Contribution of Mineral Filler as a Percentage of the Total Blend
$FAinCA_i$: Percent of Fine Aggregate in Coarse Aggregate i
$CAinFA_i$: Percent of Coarse Aggregate in Fine Aggregate i
$MFinCA_i$: Percent of Mineral Filler in Coarse Aggregate i
$MFinFA_i$: Percent of Mineral Filler in Fine Aggregate i

Table A1.1: Aggregate Data

Aggregate	Name	PCS	#200	Gsb	LUW	RUW
CA_1	1/2 Gravel	3	0.9	2.619	1501.6	1625.8
CA_2	3/8 Gravel	9	1.0	2.588	1510.6	1616.5
FA_1	Grits	83	3.1	2.556	1573.6	1713.6
FA_2	Dust	85	13.0	2.607	1502.6	1772.6
FA_3	Scr. Sand	91	2.2	2.543	1541.5	1691.3
MF	BHF	100	80.0			

Table A1.2: Input Values

Input	Value	Limits
CUW	103	95 – 105
Dust	4.7	3.5 – 6.0
Coarse Agg. Contributions		
CA1	41	
CA2	59	
Fine Agg. Contributions		
FA1	100	
FA2	0	
FA3	0	

Calculations:

Step 1

$CUW_i = LUW_i \times CUW / 100$

$CUW_1 = 1501.6 \times 103 / 100 = 1546.6$

$CUW_2 = 1510.6 \times 103 / 100 = 1555.9$

Step 2

$CA_iW_c = CUW_i \times CA_i \text{ Contribution} / 100$

$CA_1W_c = 1546.6 \times 41 / 100 = 634.1$

$CA_2W_c = 1555.6 \times 59 / 100 = 918.0$

Step 3

$VCA_i = CA_i \text{ Contribution} \times (1 - (CUW_i / (1000 \times Gsb_i)))$

$VCA_1 = 41 \times (1 - (1546.6 / (1000 \times 2.619))) = 16.8$

$VCA_2 = 59 \times (1 - (1555.6 / (1000 \times 2.588))) = 23.5$

Step 4

$VCA_T = \sum VCA_i$

$VCA_T = 16.8 + 23.5 = 40.3$

Step 5

$FA_iW_c = RUW_i \times (FA_i \text{ Contribution} / 100) \times (VCA_T / 100)$

$FA_1W_c = 1713.6 \times (100 / 100) \times (40.3 / 100) = 690.9$

$FA_2W_c = 1772.6 \times (0 / 100) \times (40.3 / 100) = 0$

$FA_3W_c = 1691.3 \times (0 / 100) \times (40.3 / 100) = 0$

Step 6

$TUW = \sum CA_i W_c + \sum FA_i W_c$

$TUW = 634.1 + 918.0 + 690.9 = 2243.0$

Step 7

$CA_iB_{in} = 100 \times CA_iW_c / TUW$

$CA_1B_{in} = 100 \times 634.1 / 2243.0 = 28.3$

$CA_2B_{in} = 100 \times 918.0 / 2243.0 = 40.9$

Step 8

$CA_TB_{in} = \sum CA_iB_{in}$

$CA_TB_{in} = 28.3 + 40.9 = 69.2$

Step 9

$FA_iB_{in} = 100 \times FA_iW_c / TUW$

$FA_1B_{in} = 100 \times 690.9 / 2243.0 = 30.8$

$FA_2B_{in} = 100 \times 0 / 2243.0 = 0$

$FA_3B_{in} = 100 \times 0 / 2243.0 = 0$

Step 10

$FA_TB_{in} = \sum FA_iB_{in}$

$FA_TB_{in} = 30.8 + 0 + 0 = 30.8$

Step 11

$FAinCA_i = CA_iB_{in} \times PCS_i / 100$

$FAinCA_1 = 28.3 \times 3 / 100 = 0.8$

$FAinCA_2 = 40.9 \times 9 / 100 = 3.7$

Step 12

$FAinCA_T = \sum FAinCA_i$

$FAinCA_T = 0.8 + 3.7 = 4.5$

Step 13

$CAinFA_i = FA_iB_{in} \times (100 - PCS_i) / 100$

$CAinFA_1 = 30.8 \times (100 - 83) / 100 = 5.2$

$CAinFA_2 = 0 \times (100 - 85) / 100 = 0$

$CAinFA_3 = 0 \times (100 - 91) / 100 = 0$

Step 14

$CAinFA_T = \sum CAinFA_i$

$CAinFA_T = 5.2 + 0 + 0 = 5.2$

Step 15

$CA_iB_f = CA_iB_{in} + FAinCA_i - (CA_iB_{in} \times CAinFA_T / CA_TB_{in})$

$CA_1B_f = 28.3 + 0.8 - (28.3 \times 5.2 / 69.2) = 27.0$

$CA_2B_f = 40.9 + 3.7 - (40.9 \times 5.2 / 69.2) = 41.5$

Step 16

$FA_iB_{adj} = FA_iB_{in} + CAinFA_i - (FA_iB_{in} \times FAinCA_T / FA_TB_{in})$

$FA_1B_{adj} = 30.8 + 5.2 - (30.8 \times 4.5 / 30.8) = 31.5$

$FA_2B_{adj} = 0 + 0 - (0 \times 4.5 / 30.8) = 0$

$FA_3B_{adj} = 0 + 0 - (0 \times 4.5 / 30.8) = 0$

Step 17

$MFinCA_i = CA_iB_f \times \#200 / 100$

$MFinCA_1 = 27.0 \times 0.9 / 100 = 0.2$

$MFinCA_2 = 41.5 \times 1.0 / 100 = 0.4$

Step 18

$MFinFA_i = FA_iB_{adj} \times \#200 / 100$

$MFinFA_1 = 31.5 \times 3.1 / 100 = 1.0$

$MFinFA_2 = 0 \times 13.0 / 100 = 0$

$MFinFA_3 = 0 \times 2.2 / 100 = 0$

Step 19

$MF_T = \sum MFinCA_i + \sum MFinFA_i$

$MF_T = 0.2 + 0.4 + 1.0 + 0 + 0 = 1.6$

Step 20

$MFB_f = (Dust - MF_T) / (\#200_{MF} / 100)$

$MFB_f = (4.7 - 1.6) / (80.0 / 100) = 3.8$

Step 21

$FA_iB_f = FA_iB_{adj} - (FA_iB_{adj} \times MFB_f / \sum FA_iB_{adj})$

$FA_1B_f = 31.5 - (31.5 \times 3.8 / 31.5) = 27.7$

$FA_2B_f = 0 - (0 \times 3.8 / 31.5) = 0$

$FA_3B_f = 0 - (0 \times 3.8 / 31.5) = 0$

Table A1.3: Output Values

Aggregate	% Blend
1/2 Gravel	27.0
3/8 Gravel	41.5
Grits	27.67
Dust	0
Scr. Sand	0
BHF	3.83

Weight Ratio Calculations

The formulas for the weight ratios are the same for both the coarse graded analysis and the fine graded analysis. Only the gradations and the size of the control sieves change from one analysis to the next. The gradations are listed for each mix design along with labels telling which sieves are the control sieves.

Abbreviations:

NMSA: Nominal Maximum Size Aggregate, one sieve higher than the first sieve to retain 10% or more

Half: Percent passing the Half Sieve, the closest sieve to 0.5 times the NMSA

PCS: Percent passing the Primary Control Sieve, the closest sieve to 0.22 times the NMSA

SCS: Percent passing the Secondary Control Sieve, the closest sieve to 0.22 times the PCS

TCS: Percent passing the Tertiary Control Sieve, the closest sieve to 0.22 times the SCS

CA: Coarse Aggregate weight ratio

FAc: Coarse part of the Fine Aggregate weight ratio

FAf: Fine part of the Fine Aggregate weight ratio

$Diff_T$: Total difference between calculated gradation and original blend

Calculations:

CA = (Half – PCS) / (100 – Half)

FAc = SCS / PCS

FAf = TCS / SCS

Half = %Pass 3/8 – (%Pass 3/8 – %Pass #4) x (9.5 – 6.25) / (9.5 – 4.75); for NMSA of 12.5

$Diff_T = \sum|Blend_{i,original} - Blend_{i,calculated}|$

Oss 12.5 Original

Table A1.4: Oss 12.5 Original Gradation

	Coarse Graded Analysis		Fine Graded Analysis	
Sieve (mm)	% Pass	Control Sieves	% Pass	Control Sieves
25.0	100.0		100.0	
19.0	100.0		100.0	
12.5	99.1	NMSA	100.0	
9.5	89.8		100.0	
6.25	66.3	Half	100.0	
4.75	55.5		100.0	
2.36	43.3	PCS	100.0	NMSA
1.18	33.5		77.3	Half
0.600	21.9	SCS	50.7	PCS
0.300	12.7		29.4	
0.150	7.6	TCS	17.7	SCS
0.075	4.5		10.5	

Table A1.5: Input Values for Oss 12.5 Original Evaluation

Input	Value	Limits
CUW	80	95 – 105
Dust	4.6	3.5 – 6.0
Coarse Agg. Contributions		
CA1	37	
CA2	63	
Fine Agg. Contributions		
FA1	35	
FA2	42	
FA3	23	

Table A1.6: Output Values for Oss 12.5 Original Evaluation

	Coarse Graded Analysis		Fine Graded Analysis	
Parameter	Value	Limits	Value	Limits
CUW	80	95 - 105	80	<90
CA	0.68	0.50 - 0.65	1.18	0.60 - 1.00
FAc	0.51	0.35 - 0.50	0.35	0.35 - 0.50
FAf	0.35	0.35 - 0.50	NA	0.35 - 0.50
$Diff_T$	0.60		0.60	

Oss 12.5 Bailey

Table A1.7: Oss 12.5 Bailey Gradation

	Coarse Graded Analysis		Fine Graded Analysis	
Sieve (mm)	% Pass	Control Sieves	% Pass	Control Sieves
25.0	100.0		100.0	
19.0	100.0		100.0	
12.5	98.7	NMSA	100.0	
9.5	85.6		100.0	
6.25	56.4	Half	100.0	
4.75	43.0		100.0	
2.36	31.3	PCS	100.0	NMSA
1.18	23.7		75.7	Half
0.600	14.7	SCS	47.1	PCS
0.300	8.8		28.0	
0.150	6.3	TCS	20.0	SCS
0.075	4.6		14.6	

Table A1.8: Input Values for Oss 12.5 Bailey Design

Input	Value	Limits
CUW	103	95 – 105
Dust	4.7	3.5 – 6.0
Coarse Agg. Contributions		
CA1	41	
CA2	59	
Fine Agg. Contributions		
FA1	100	
FA2	0	
FA3	0	

Table A1.9: Output Values for Oss 12.5 Bailey Design

	Coarse Graded Analysis		Fine Graded Analysis	
Parameter	Value	Limits	Value	Limits
CUW	103	95 - 105	103	<90
CA	0.57	0.50 - 0.65	1.18	0.60 - 1.00
FAc	0.47	0.35 - 0.50	0.42	0.35 - 0.50
FAf	0.42	0.35 - 0.50	NA	0.35 - 0.50

Cont 19 Original

Table A1.10: Cont 19 Original Gradation

	Coarse Graded Analysis		Fine Graded Analysis	
Sieve (mm)	**% Pass**	**Control Sieves**	**% Pass**	**Control Sieves**
25.0	100.0		100.0	
19.0	99.3	NMSA	100.0	
12.5	89.0		100.0	
9.5	73.4	Half	100.0	
4.75	49.1	PCS	100.0	NMSA
2.36	35.6		72.5	Half
1.18	25.7	SCS	52.4	PCS
0.600	17.2		35.0	
0.300	9.3	TCS	19.0	SCS
0.150	5.2		10.5	
0.075	3.6		7.3	TCS

Table A1.11: Input Values for Cont 19 Original Evaluation

Input	**Value**	**Limits**
CUW	74	95 – 105
Dust	3.6	3.5 – 6.0
Coarse Agg. Contributions		
CA1	31	
CA2	38	
CA3	31	
Fine Agg. Contributions		
FA1	55	
FA2	45	

Table A1.12: Output Values for Cont 19 Original Evaluation

	Coarse Graded Analysis		Fine Graded Analysis	
Parameter	**Value**	**Limits**	**Value**	**Limits**
CUW	74	95 - 105	74	<90
CA	0.91	0.60 - 0.75	0.73	0.60 - 1.00
FAc	0.52	0.35 - 0.50	0.36	0.35 - 0.50
FAf	0.36	0.35 - 0.50	0.38	0.35 - 0.50
$Diff_T$	0.28		0.28	

Cont 19 Bailey

Table A1.13: Cont 19 Bailey Gradation

	Coarse Graded Analysis		Fine Graded Analysis	
Sieve (mm)	% Pass	Control Sieves	% Pass	Control Sieves
25.0	100.0		100.0	
19.0	98.9	NMSA	100.0	
12.5	84.0		100.0	
9.5	61.1	Half	100.0	
4.75	34.6	PCS	100.0	NMSA
2.36	23.3		67.4	Half
1.18	15.8	SCS	45.7	PCS
0.600	10.6		30.8	
0.300	6.7	TCS	19.2	SCS
0.150	4.6		13.2	
0.075	3.6		10.4	TCS

Table A1.14: Input Values for Cont 19 Bailey Design

Input	Value	Limits
CUW	101	95 – 105
Dust	3.7	3.5 – 6.0
Coarse Agg. Contributions		
CA1	35	
CA2	45	
CA3	20	
Fine Agg. Contributions		
FA1	75	
FA2	25	

Table A1.15: Output Values for Cont 19 Bailey Design

	Coarse Graded Analysis		Fine Graded Analysis	
Parameter	Value	Limits	Value	Limits
CUW	101	95 - 105	101	<90
CA	0.68	0.60 - 0.75	0.66	0.60 - 1.00
FAc	0.46	0.35 - 0.50	0.42	0.35 - 0.50
FAf	0.42	0.35 - 0.50	0.54	0.35 - 0.50

Farm Original

Table A1.16: Farm Original Gradation

	Coarse Graded Analysis		Fine Graded Analysis	
Sieve (mm)	% Pass	Control Sieves	% Pass	Control Sieves
25.0	100.0		100.0	
19.0	100.0		100.0	
12.5	99.3	NMSA	100.0	
9.5	89.3		100.0	
6.25	68.0	Half	100.0	
4.75	58.1		100.0	
2.36	43.3	PCS	100.0	NMSA
1.18	34.3		79.2	Half
0.600	24.8	SCS	57.4	PCS
0.300	14.6		33.7	
0.150	7.8	TCS	18.1	SCS
0.075	4.4		10.1	

Table A1.17: Input Values for Farm Original Evaluation

Input	Value	Limits
CUW	81	95 – 105
Dust	3.6	3.5 – 6.0
Coarse Agg. Contributions		
CA1	38	
CA2	62	
Fine Agg. Contributions		
FA1	56	
FA2	24	
FA3	20	
RAP	14.4	

Table A1.18: Output Values for Farm Original Evaluation

	Coarse Graded Analysis		Fine Graded Analysis	
Parameter	Value	Limits	Value	Limits
CUW	81	95 - 105	81	<90
CA	0.77	0.50 - 0.65	1.06	0.60 - 1.00
FAc	0.57	0.35 - 0.50	0.32	0.35 - 0.50
FAf	0.32	0.35 - 0.50	NA	0.35 - 0.50
$Diff_T$	0.55		0.55	

Farm Bailey

Table A1.19: Farm Bailey Gradation

	Coarse Graded Analysis		Fine Graded Analysis	
Sieve (mm)	% Pass	Control Sieves	% Pass	Control Sieves
25.0	100.0		100.0	
19.0	100.0		100.0	
12.5	98.7	NMSA	100.0	
9.5	80.9		100.0	
6.25	58.6	Half	100.0	
4.75	48.3		100.0	
2.36	34.8	PCS	100.0	NMSA
1.18	27.1		78.0	Half
0.600	20.3	SCS	58.3	PCS
0.300	13.6		39.1	
0.150	8.6	TCS	24.8	SCS
0.075	4.6		13.3	

Table A1.20: Input Values for Farm Bailey Design

Input	Value	Limits
CUW	101	95 – 105
Dust	3.8	3.5 – 6.0
Coarse Agg. Contributions		
CA1	58	
CA2	42	
Fine Agg. Contributions		
FA1	19	
FA2	81	
FA3	0	
RAP	15.0	

Table A1.21: Output Values for Farm Bailey Design

	Coarse Graded Analysis		Fine Graded Analysis	
Parameter	Value	Limits	Value	Limits
CUW	101	95 - 105	101	<90
CA	0.58	0.50 - 0.65	0.90	0.60 - 1.00
FAc	0.58	0.35 - 0.50	0.43	0.35 - 0.50
FAf	0.43	0.35 - 0.50	NA	0.35 - 0.50

Matlab Programs

These Matlab programs iterate through all possible combinations of input values to find the best aggregate blend, whether that means a blend with optimum weight ratios or one that matches a target blend. Baileydesign.m is the main program for designing new aggregate blends. It is set up to work with the Oss 12.5 and Farm mixes because Cont 19 was done manually before hand. The program calls Bailey.m and Baileylimits.m. The first one contains the full Bailey calculations and the second outputs a list of limiting values for both the Bailey Method and Superpave. Baileyevaluation.m is the main program for evaluation and finds the input values to match a target blend.

BAILEYDESIGN.M

```
function inputs=baileydesign(Agg,NMSA,RAP);

% This matlab function determines the input values to acheive the
% optimum bailey parameters given a set of aggregate, a PCS, and a
% desired amount of RAP.  "Optimum" is defined as the minimum sum of
% the deviations from the target values
% INPUT
%    Agg = aggregate info in matrix format (see osspiee.m for example)
%    NMSA = Nominal Maximum Size Aggegate, enter as mm
%    RAP = percentage of aggregate blend that is RAP
% OUTPUT
%    input = a matrix of seven sets of input values, one in each row

% Define variables for comparison and set targets
currentinput=zeros(1,9);
prevTotal=100;
lim=baileylimits(NMSA);
CAtarget=(lim(5)+lim(6))/2;
FActarget=(lim(7)+lim(8))/2;
FAftarget=(lim(9)+lim(10))/2;

% Iterate through all possible inputs
n=0;
for cuw=95:105
   for dd=3.5:0.1:6.0
      for ca2=0:100
         for fa1=0:100
            for fa2=0:100-fa1
               currentinput(1)=cuw;
               currentinput(2)=dd;
               currentinput(3)=0;
               currentinput(4)=ca2;
               currentinput(5)=100-ca2;
               currentinput(6)=fa1;
               currentinput(7)=fa2;
               currentinput(8)=100-fa1-fa2;
               currentinput(9)=RAP;
               [blend,grad,ratios,tests]=bailey(Agg,NMSA,currentinput);
               blendOK=1;
               for stockpile=1:8
```

```
                    if blend(stockpile)<0;
                        blendOK=0;
                    end
                end
                if (tests(1)==1)&&(blendOK==1)
                    n=n+1;
                    CAdiff=abs(ratios(1)-CAtarget);
                    FAcdiff=abs(ratios(2)-FActarget);
                    FAfdiff=abs(ratios(3)-FAftarget);
                    Totaldiff=CAdiff+FAcdiff+FAfdiff;
                    if (Totaldiff<=prevTotal)
                        inputbest=currentinput;
                        prevTotal=Totaldiff;
                    end
                end
            end
        end
    end
end

% Output results.  If n=0 at the end, something went wrong
if (n==0)
    inputs=3.14159;
else
    inputs=zeros(1,9);
    inputs=inputbest;
end

disp('cool beans');

return
```

BAILEY.M

```
function [blend,gradation,ratios,tests]=bailey(Agg,NMSA,Input)

% This matlab function calculates the aggregate blend of an asphalt mix
% using the Bailey Method given a set of aggregate, a PCS, and a set of
% input values.
% INPUT
%    Agg = aggregate info in matrix format (see osspiee.m for example)
%    NMSA = Nominal Maximum Size Aggegate, enter as mm
%    Input = the input values to perform the calculations
% OUTPUT
%    blend = the percentages required from each stockpile
%    gradation = the final gradation of the aggregate blend
%    ratios = the calculated bailey parameters for this blend
%    tests = the results of testing if the blend meets requirements

% blend=0;
% gradation=0;
% ratios=0;
% tests=0;

% DETERMINING LIMITS FOR GIVEN NMSA
```

```
lim=baileylimits(NMSA);

% CALCULATING AGGREGATE BLEND
CUW=Input(1);
DD=Input(2);
CA1=Input(3);
CA2=Input(4);
CA3=Input(5);
FA1=Input(6);
FA2=Input(7);
FA3=Input(8);
RAP=Input(9);

% chosen unit weight
cauw1=Agg(12,1)*CUW/100;
cauw2=Agg(12,2)*CUW/100;
cauw3=Agg(12,3)*CUW/100;

% ca contrubution weight
cacw1=cauw1*CA1/100;
cacw2=cauw2*CA2/100;
cacw3=cauw3*CA3/100;

% voids in ca
cav1=(1-(cauw1/(Agg(11,1)*1000)))*CA1;
cav2=(1-(cauw2/(Agg(11,2)*1000)))*CA2;
cav3=(1-(cauw3/(Agg(11,3)*1000)))*CA3;

% total voids
vt=cav1+cav2+cav3;

% fa contribution weight
facw1=Agg(13,4)*(FA1/100)*(vt/100);
facw2=Agg(13,5)*(FA2/100)*(vt/100);
facw3=Agg(13,6)*(FA3/100)*(vt/100);

% total unit weight
tuw=cacw1+cacw2+cacw3+facw1+facw2+facw3;

% initial blend percentage, ca and fa
caib1=100*cacw1/tuw;
caib2=100*cacw2/tuw;
caib3=100*cacw3/tuw;
faib1=100*facw1/tuw;
faib2=100*facw2/tuw;
faib3=100*facw3/tuw;

% ca percent pass pcs
PCS=lim(2);
cappcs1=Agg(PCS,1);
cappcs2=Agg(PCS,2);
cappcs3=Agg(PCS,3);

% fa percent retain pcs
farpcs1=100-Agg(PCS,4);
farpcs2=100-Agg(PCS,5);
farpcs3=100-Agg(PCS,6);
```

```
% percent fa in ca
fainca1=caib1*(cappcs1/100);
fainca2=caib2*(cappcs2/100);
fainca3=caib3*(cappcs3/100);

% total fa in ca
tfainca=fainca1+fainca2+fainca3;

% percent ca in fa
cainfa1=faib1*(farpcs1/100);
cainfa2=faib2*(farpcs2/100);
cainfa3=faib3*(farpcs3/100);

% total ca in fa
tcainfa=cainfa1+cainfa2+cainfa3;

% adjusted blens for ca and fa
caab1=caib1+fainca1-(caib1*tcainfa/(caib1+caib2+caib3));
caab2=caib2+fainca2-(caib2*tcainfa/(caib1+caib2+caib3));
caab3=caib3+fainca3-(caib3*tcainfa/(caib1+caib2+caib3));
faab1=faib1+cainfa1-(faib1*tfainca/(faib1+faib2+faib3));
faab2=faib2+cainfa2-(faib2*tfainca/(faib1+faib2+faib3));
faab3=faib3+cainfa3-(faib3*tfainca/(faib1+faib2+faib3));

% percent dust (passing #200) in ca and fa
dinca1=caab1*(Agg(10,1)/100);
dinca2=caab2*(Agg(10,2)/100);
dinca3=caab3*(Agg(10,3)/100);
dinfa1=faab1*(Agg(10,4)/100);
dinfa2=faab2*(Agg(10,5)/100);
dinfa3=faab3*(Agg(10,6)/100);

% total dust
td=dinca1+dinca2+dinca3+dinfa1+dinfa2+dinfa3;

% mf blend
mfb=(DD-td)/(Agg(10,7)/100);

% final blend for ca and fa
cafb1=caab1*((100-RAP)/100);
cafb2=caab2*((100-RAP)/100);
cafb3=caab3*((100-RAP)/100);
fafb1=(faab1-(faab1*mfb/(faab1+faab2+faab3)))*((100-RAP)/100);
fafb2=(faab2-(faab2*mfb/(faab1+faab2+faab3)))*((100-RAP)/100);
fafb3=(faab3-(faab3*mfb/(faab1+faab2+faab3)))*((100-RAP)/100);
mffb=mfb*((100-RAP)/100);

% final total blend
blend=[cafb1,cafb2,cafb3,fafb1,fafb2,fafb3,mffb,RAP];

% CALCULATING GRADATION OF AGGREGATE BLEND
gradation=zeros(1,10);
for seive=1:10
    for stockpile=1:8
        gradation(seive)=gradation(seive)+...
        (Agg(seive,stockpile)*blend(stockpile)/100);
```

```
    end
end

% CALCULATING BAILEY AGGREGATE RATIOS
half=lim(1);
SCS=lim(3);
TCS=lim(4);
if (half==6.25)
    halfseive=gradation(3)-(gradation(3)-gradation(4))*...
    (9.5-6.25)/(9.5-4.75);
else
    halfseive=gradation(half);
end
CA=(halfseive-gradation(PCS))/(100-halfseive);
FAc=gradation(SCS)/gradation(PCS);
FAf=gradation(TCS)/gradation(SCS);
ratios=[CA,FAc,FAf];

% TESTING FOR COMPLIANCE TO REQUIREMENTS
% control points
cpOK=1;
if (gradation(1)<lim(11))||(gradation(1)>lim(12))
    %disp('outside of control points at 3/4" seive');
    cpOK=0;
end
if (gradation(2)<lim(13))||(gradation(2)>lim(14))
    %disp('outside of control points at 1/2" seive');
    cpOK=0;
end
if (gradation(3)<lim(15))||(gradation(3)>lim(16))
    %disp('outside of control points at 3/8" seive');
    cpOK=0;
end
if (gradation(4)<lim(17))||(gradation(4)>lim(18))
    %disp('outside of control points at #4 seive');
    cpOK=0;
end
if (gradation(5)<lim(19))||(gradation(5)>lim(20))
    %disp('outside of control points at #8 seive');
    cpOK=0;
end
if (gradation(10)<lim(21))||(gradation(10)>lim(22))
    %disp('outside of control points at #200 seive');
    cpOK=0;
end
%disp('within control points');

% restricted zone
rz16OK=1;
rz30OK=1;
if (gradation(6)>lim(25))&&(gradation(6)<lim(26))
    %disp('in restricted zone at #16 seive');
    rz16OK=0;
end
if (gradation(7)>lim(27))&&(gradation(7)<lim(28))
    %disp('in restricted zone at #30 seive');
    rz30OK=0;
```

```
end

% bailey ratios
CAOK=1;
FAcOK=1;
FAfOK=1;
if (CA<lim(5))||(CA>lim(6))
    %disp('CA outside of recomended range');
    CAOK=0;
end
if (FAc<lim(7))||(FAc>lim(8))
    %disp('FAc outside of recomended range');
    FAcOK=0;
end
if (FAf<lim(9))||(FAf>lim(10))
    %disp('FAf outside of recomended range');
    FAfOK=0;
end

tests=[cpOK,rz16OK,rz30OK,CAOK,FAcOK,FAfOK];

return
```

BAILEYLIMITS.M

```
function limits=baileylimits(NMSA)

% This matlab function returns a list of the limits for the weight
% ratios for the Bailey Method, the gradation control points for
% Superpave, and the restricted zone points for Superpave

FAc_lower=0.35;
FAc_upper=0.50;
FAf_lower=0.35;
FAf_upper=0.50;

if (NMSA==19)
    CA_lower=.6;
    CA_upper=.75;
    Half=3;
    PCS=4;
    SCS=6;
    TCS=8;
    CP19_lower=90;
    CP19_upper=100;
    CP12p5_lower=0;
    CP12p5_upper=90;
    CP9p5_lower=0;
    CP9p5_upper=100;
    CP4_lower=0;
    CP4_upper=100;
    CP8_lower=23;
    CP8_upper=49;
    CP200_lower=2;
    CP200_upper=8;
    RZ8_lower=34.6;
```

```
    RZ8_upper=34.6;
    RZ16_lower=22.3;
    RZ16_upper=28.3;
    RZ30_lower=16.7;
    RZ30_upper=20.7;
    RZ50_lower=13.7;
    RZ50_upper=13.7;
end
if (NMSA==12.5)
    CA_lower=.5;
    CA_upper=.65;
    Half=6.25;
    PCS=5;
    SCS=7;
    TCS=9;
    CP19_lower=100;
    CP19_upper=100;
    CP12p5_lower=90;
    CP12p5_upper=100;
    CP9p5_lower=0;
    CP9p5_upper=90;
    CP4_lower=0;
    CP4_upper=100;
    CP8_lower=28;
    CP8_upper=58;
    CP200_lower=2;
    CP200_upper=10;
    RZ8_lower=39.1;
    RZ8_upper=39.1;
    RZ16_lower=25.6;
    RZ16_upper=31.6;
    RZ30_lower=19.1;
    RZ30_upper=23.1;
    RZ50_lower=15.5;
    RZ50_upper=15.5;
end
if (NMSA==9.5)
    CA_lower=.4;
    CA_upper=.55;
    Half=4;
    PCS=5;
    SCS=7;
    TCS=9;
    CP19_lower=0;
    CP19_upper=100;
    CP12p5_lower=100;
    CP12p5_upper=100;
    CP9p5_lower=90;
    CP9p5_upper=100;
    CP4_lower=0;
    CP4_upper=90;
    CP8_lower=32;
    CP8_upper=67;
    CP200_lower=2;
    CP200_upper=10;
    RZ8_lower=47.2;
    RZ8_upper=47.2;
```

```
    RZ16_lower=31.6;
    RZ16_upper=37.6;
    RZ30_lower=23.5;
    RZ30_upper=27.5;
    RZ50_lower=18.7;
    RZ50_upper=18.7;
end

control_seives=[Half,PCS,SCS,TCS];
ratio_limits=[CA_lower,CA_upper,FAc_lower,FAc_upper,...
    FAf_lower,FAf_upper];
control_points=[CP19_lower,CP19_upper,CP12p5_lower,CP12p5_upper,...
    CP9p5_lower,CP9p5_upper,CP4_lower,CP4_upper,CP8_lower,CP8_upper,...
    CP200_lower,CP200_upper];
restricted_zone=[RZ8_lower,RZ8_upper,RZ16_lower,RZ16_upper,...
    RZ30_lower,RZ30_upper,RZ50_lower,RZ50_upper];
limits=[control_seives,ratio_limits,control_points,restricted_zone];

return
```

OSSIPEE.M

```
function M=ossipee(x)

% This matlab function makes a 13 row by 8 column matrix of aggregate
% info.
% Aggregate origin: Pike Industries in Ossipee, NH
% Each line makes a column for one stockpile with percent passing in
% rows 1-10, Gsb in row 11, loose unit weight in 12, and rodded unit
% wt. in 13
% INPUTS
%    x = anything; without some input, I could not get this to work
% OUTPUT
%    M = the 13x8 matrix of aggregate information

% agg=  [3/4";1/2";3/8';4;8;16;30;50;100;200;Gsb;Loose;Rodded]

three4= [100;100;100;100;100;100;100;100;100;100;1   ;1      ;1      ];
half=   [100;95;48;5 ;3  ;2  ;2  ;1  ;1   ;0.9 ;2.619;1501.57;1625.78];
three8= [100;100;99;27;9 ;6  ;3  ;2  ;1   ;1.0 ;2.588;1510.61;1616.49];
grits=  [100;100;100;96;83;61;33 ;14 ;7.0 ;3.1 ;2.556;1573.60;1713.62];
dust=   [100;100;100;100;85;67;51;36 ;23.0;13.0;2.607;1502.65;1772.63];
scrsand=[100;100;100;97;91;75;45 ;17 ;6.0 ;2.2 ;2.543;1541.50;1691.32];
bhf=    [100;100;100;100;100;100;100;99 ;95.0;80.0;1   ;1     ;1     ];
rap=    [100;100;100;100;100;100;100;100;100 ;100 ;1   ;1     ;1     ];

M=[three4,half,three8,grits,dust,scrsand,bhf,rap];

return
```

CONTINENTAL.M

```
function M=continental(x)

% This matlab function makes a 13 row by 8 column matrix of aggregate
% info.
% Aggregate origin: Continental Paving in Londonderry, NH
% Each line makes a column for one stockpile with percent passing in
% rows 1-10, Gsb in row 11, loose unit weight in 12, and rodded unit
% wt. in 13
% INPUTS
%    x = anything; without some input, I could not get this to work
% OUTPUT
%    M = the 13x8 matrix of aggregate information

% agg=  [3/4";1/2";3/8";4;8;16;30;50;100;200;Gsb;Loose;Rodded]

three4=
[95.4;33.6;9.6;1.1;0.8;0.8;0.8;0.7;0.7;0.6;2.691;1492.53;1636.28];
half=
[100;98.0;42.7;1.4;0.9;0.8;0.7;0.7;0.6;0.5;2.722;1518.89;1638.49];
three8=
[100;100;96.7;34.0;7.0;2.8;1.4;1.1;0.8;0.7;2.707;1556.70;1667.15];
WMS=
[100;100;100;98.0;68.1;38.0;20.9;11.0;6.6;4.9;2.710;1567.40;1740.43];
DSS=
[100;100;100;97.9;93.2;80.3;55.7;24.5;7.6;2.3;2.687;1548.24;1696.35];
none=   [100;100;100;100;100;100;100;100;100;100;1   ;1      ;1      ];
bhf=    [100;100;100;100;100;100;100;99.8;96.7;87.1;1;1      ;1      ];
rap=    [100;100;100;100;100;100;100;100;100;100;1   ;1      ;1      ];

M=[three4,half,three8,WMS,DSS,none,bhf,rap];

return
```

FARMINGTON.M

```
function M=farmington(x)

% This matlab function makes a 13 row by 8 column matrix of aggregate
% info.
% Aggregate origin: Pike Industries in Farmington, NH
% Each line makes a column for one stockpile with percent passing in
% rows 1-10, Gsb in row 11, loose unit weight in 12, and rodded unit
% wt. in 13
% INPUTS
%    x = anything; without some input, I could not get this to work
% OUTPUT
%    M = the 13x8 matrix of aggregate information

% agg=  [3/4";1/2";3/8';4;8;16;30;50;100;200;Gsb;Loose;Rodded]

three4= [100;100;100;100;100;100;100;100;100;100;1   ;1      ;1      ];
half=   [100;96;43;4 ;3  ;2  ;2  ;2  ;2   ;0.7 ;2.645;1580.38;1689.01];
three8= [100;100;99;32;5 ;3  ;3  ;2  ;2   ;0.9 ;2.616;1615.78;1691.25];
wasand= [100;100;100;100;91;72;49;21 ;5.0 ;2.0 ;2.565;1544.39;1686.94];
dust=   [100;100;100;100;85;67;51;36 ;23.0;12.0;2.598;1609.88;1809.01];
```

```
scrsand=[100;100;100;94;86;71;50 ;29 ;12.0;5.1 ;2.566;1604.48;1797.73];
bhf=    [100;100;100;100;100;100;100;99;95.0;80.0;1   ;1     ;1      ];
rap=    [100;100;100;81 ;63 ;50 ;35 ;23 ;14 ;9.3 ;1   ;1     ;1      ];

M=[three4,half,three8,wasand,dust,scrsand,bhf,rap];

return
```

BAILEYEVALUATION.M

```
function bestinput=baileyevaluation(Agg,NMSA,TargetBlend)

% This Matlab function finds the input values that generate a blend
that is closest to
% the target blend.  "Closest" means the sum of the absolute
differences between the
% calculated and target blends is as small as possible.
% Adjust the limits on the for loops as needed to cut down run time.


currentinput=zeros(1,9);
bestinput=currentinput;
prevTotal=100;

n=0;
for cuw=75:85
   for dd=3.5:0.1:6.0
      for ca2=27:47
         for fa1=43:63
            for fa2=16:36
               currentinput(1)=cuw;
               currentinput(2)=dd;
               currentinput(3)=0;
               currentinput(4)=ca2;
               currentinput(5)=100-ca2;
               currentinput(6)=fa1;
               currentinput(7)=fa2;
               currentinput(8)=100-fa1-fa2;
               currentinput(9)=14.4;
               [blend,grad,ratios,tests]=bailey(Agg,NMSA,currentinput);
               n=n+1;
               CA1=abs(TargetBlend(1)-blend(1));
               CA2=abs(TargetBlend(2)-blend(2));
               CA3=abs(TargetBlend(3)-blend(3));
               FA1=abs(TargetBlend(4)-blend(4));
               FA2=abs(TargetBlend(5)-blend(5));
               FA3=abs(TargetBlend(6)-blend(6));
               MF=abs(TargetBlend(7)-blend(7));
               Totaldiff=CA1+CA2+CA3+FA1+FA2+FA3+MF;
               if (Totaldiff<prevTotal)
                  bestinput=currentinput;
                  prevTotal=Totaldiff;
               end
               if (Totaldiff<0.3)
                  bestinput=currentinput;
                  disp('cool beans');
```

```
                    disp('Total difference =');
                    disp(Totaldiff);
                    disp('number of itterations =');
                    disp(n);
                    return
                end
            end
        end
    end
end

disp('GOOD ENOUGH!');
disp('Total difference =');
disp(prevTotal);
disp('number of itterations =');
disp(n);

return
```

APPENDIX 2

SUPERPAVE ASPHALT CONTENT DESIGN RESULTS

Oss 12.5 Bailey

NMSA: 12.5 mm (0.5 in.)
Binder: Gb = 1.026

Table A2.1: Oss 12.5-Bailey Aggregate Data

Aggregate	Blend %	Gsb	Gsa
1/2" Gravel	27.0	2.619	2.686
3/8" Gravel	41.5	2.588	2.666
Grits	27.7	2.556	2.618
Dust	0	2.607	2.651
Scr. Sand	0	2.543	2.62
BHF	3.8	2.607	2.651
Total	100	2.588	2.657

Table A2.2: Oss 12.5-Bailey Calculation Results for Pbi and Pb,est

Pbi		Pb,est	
Gse	2.643	Gmm	2.444
Vba	0.0181	Gmb - 1	2.351
Vbe	0.101	Gmb - 2	2.355
Ws	2.235	%Gmm@Nini, avg	88.8
Pbi	5.2	%Gmm@Ndes, avg	96.3
		Va	3.7
		VMA	13.8
		Pb,est	5.1

Table A2.3: Oss 12.5-Bailey Volumetrics of Design Specimens

Parameter	Pb,est – 1.0	Pb,est – 0.5	Pb,est	Pb,est + 0.5
Pb	4.6	5.1	5.6	6.1
Gmm	2.470	2.452	2.434	2.417
Gmb #1	2.330	2.365	2.376	2.377
Gmb #2	2.319	2.349	2.370	2.375
Gse	2.650	2.650	2.650	2.650
%Gmm@Nini avg	86.8	88.5	89.7	90.4
%Gmm@Ndes avg	94.1	96.1	97.5	98.3
Va	5.9	3.9	2.5	1.7
VMA	14.3	13.6	13.4	13.8
VFA	58.7	71.3	81.3	87.8
Pbe	3.7	4.2	4.7	5.2
DP	1.2	1.1	1.0	0.9

Table A2.4: Oss 12.5-Bailey Final Volumetrics

Parameter	Value	Limits	Pass/Fail
Pb	5.1		
Gmm	2.456		
Gmb - 1	2.347		
Gmb - 2	2.358		
Gse	2.655		
%Gmm@Nini avg	88.0	<89	OK
%Gmm@Ndes avg	95.8		
Va	4.2	=4.0	IN LIMITS
VMA	13.7	>14.0	UNDER LIMIT
VFA	69.4	65 - 75	OK
Pbe	4.2		
DP	1.1	0.6 - 1.2	OK

Cont 19 Bailey

NMSA: 19 mm (0.75 in.)
Binder: Gb = 1.020

Table A2.5: Cont 19-Bailey Aggregate Data

Aggregate	Blend %	Gsb	Gsa
3/4" Frac	23.1	2.691	2.749
1/2" Frac	30.4	2.722	2.768
3/8" Frac	18.3	2.707	2.756
WMS	19.5	2.71	2.825
DSS	6.3	2.687	2.707
BHF	2.4	2.763	2.763
Total	100	2.708	2.768

Table A2.6: Cont 19-Bailey Calculation Results for Pbi and Pb,est

Pbi		Pb,est	
Gse	2.756	Gmm	2.551
Vba	0.0148	Gmb - 1	2.408
Vbe	0.089	Gmb - 2	2.403
Ws	2.317	%Gmm@Nini, avg	86.2
Pbi	4.4	%Gmm@Ndes, avg	94.3
		Va	5.7
		VMA	15.1
		Pb,est	5.1

Table A2.7: Cont 19-Bailey Volumetrics of Design Specimens

Parameter	Pb,est – 1.0	Pb,est – 0.5	Pb,est	Pb,est + 0.5
Pb	4.6	5.1	5.6	6.1
Gmm	2.547	2.527	2.508	2.488
Gmb #1	2.385	2.391	2.409	2.415
Gmb #2	2.383	2.378	2.409	2.427
Gse	2.745	2.745	2.745	2.745
%Gmm@Nini avg	85.3	86.1	88.0	88.6
%Gmm@Ndes avg	93.6	94.4	96.1	97.3
Va	6.4	5.6	3.9	2.7
VMA	16.0	16.4	16.0	16.1
VFA	60.1	65.8	75.5	83.1
Pbe	4.1	4.6	5.1	5.6
DP	0.9	0.8	0.7	0.6

Table A2.8: Cont 19-Bailey Final Volumetrics

Parameter	Value	Limits	Pass/Fail
Pb	5.6		
Gmm	2.511		
Gmb - 1	2.401		
Gmb - 2	2.407		
Gse	2.750		
%Gmm@Nini avg	87.0	<89	OK
%Gmm@Ndes avg	95.7		
Va	4.3	=4.0	IN LIMITS
VMA	16.2	>13.0	OK
VFA	73.7	65 - 75	OK
Pbe	5.1		
DP	0.7	0.6 - 1.2	OK

Farm Bailey

NMSA: 12.5 mm (0.5 in.)
Binder: Gb = 1.026

Table A2.9: Farm-Bailey Aggregate Data

Aggregate	Blend %	Gsb	Gsa
1/2" Gravel	33.13	2.645	2.617
3/8" Gravel	25.04	2.616	2.703
Wa. Sand	4.59	2.565	2.625
Dust	22.23	2.598	2.68
Scr. Sand	0	2.566	2.642
BHF	0.02	2.607	2.651
RAP	15		
Total	100	2.620	2.659

Table A2.10: Farm-Bailey Calculation Results for Pbi and Pb,est

Pbi		Pb,est	
Gse	2.651	Gmm	2.508
Vba	0.0101	Gmb - 1	2.402
Vbe	0.101	Gmb - 2	2.406
Ws	2.240	%Gmm@Nini, avg	89.3
Pbi	4.85	%Gmm@Ndes, avg	95.9
		Va	4.1
		VMA	12.7
		Pb,est	4.90

Table A2.11: Farm-Bailey Volumetrics of Design Specimens

Parameter	Pb,est – 1.0	Pb,est – 0.5	Pb,est	Pb,est + 0.5
Pb	4.40	4.90	5.40	5.90
Gmm	2.526	2.507	2.488	2.470
Gmb #1	2.387	2.408	2.426	2.439
Gmb #2	2.399	2.413	2.437	2.439
Gse	2.709	2.709	2.709	2.709
%Gmm@Nini avg	88.4	89.4	88.0	92.2
%Gmm@Ndes avg	94.7	96.1	97.7	98.8
Va	5.3	3.9	2.3	1.2
VMA	12.7	12.5	12.2	12.4
VFA	58.3	69.2	81.3	89.9
Pbe	3.2	3.7	4.2	4.7
DP	1.5	1.3	1.1	1.0

Table A2.12: Farm-Bailey Final Volumetrics

Parameter	Value	Limits	Pass/Fail
Pb	4.85		
Gmm	2.506		
Gmb - 1	2.415		
Gmb - 2	2.418		
Gse	2.705		
%Gmm@Nini avg	89.6	<89	OVER LIMIT
%Gmm@Ndes avg	96.4		
Va	3.6	=4.0	IN LIMITS
VMA	12.2	>14.0	UNDER LIMIT
VFA	70.8	65 - 75	OK
Pbe	3.7		
DP	1.3	0.6 - 1.2	OUTSIDE LIMITS

APPENDIX 3

AGGREGATE DATA AND MIX DESIGNS

Aggregate Stockpile Data

Table A3.1: Ossipee Aggregates

	3/4"	1/2"	3/8"	Grits	Dust	Scr. Sand	BHF
Sieve Size							
25.0	100	100	100	100	100	100	100
19.0	97	100	100	100	100	100	100
12.5	24	95	100	100	100	100	100
9.5	7	48	99	100	100	100	100
4.75	3	5	27	96	100	97	100
2.36	2	3	9	83	85	91	100
1.18	2	2	6	61	67	75	100
0.600	2	2	3	33	51	45	100
0.300	1	1	2	14	36	17	99
0.150	1	1	1	7	23	6	95
0.075	1	0.9	1	3.1	13	2.2	80
Gsb	2.629	2.619	2.588	2.556	2.607	2.543	2.607
Gsa	2.694	2.686	2.666	2.618	2.651	2.62	2.651
% Abs	0.92	0.95	1.13	0.93	0.64	1.15	
LUW		1501.6	1510.6	1573.6	1502.6	1541.5	
RUW		1625.8	1616.5	1713.6	1772.6	1691.3	
Source	OssAgg	OssAgg	OssAgg	OssAgg	#618	Madison	Baghouse

Table A3.2: Continental Aggregates

	3/4"	1/2"	3/8"	WMS	DSS	BHF
Sieve Size						
25.0	100.0	100.0	100.0	100.0	100.0	100.0
19.0	95.4	100.0	100.0	100.0	100.0	100.0
12.5	33.6	98.0	100.0	100.0	100.0	100.0
9.5	9.6	42.7	96.7	100.0	100.0	100.0
4.75	1.1	1.4	34.0	98.0	97.9	100.0
2.36	0.8	0.9	7.0	68.1	93.2	100.0
1.18	0.8	0.8	2.8	38.0	80.3	100.0
0.600	0.8	0.7	1.4	20.9	55.7	100.0
0.300	0.7	0.7	1.1	11.0	24.5	99.8
0.150	0.7	0.6	0.8	6.6	7.6	96.7
0.075	0.6	0.5	0.7	4.9	2.3	87.1
Gsb	2.691	2.722	2.707	2.71	2.687	2.763
Gsa	2.749	2.768	2.756	2.825	2.707	2.763
% Abs	0.8	0.5	0.7	1.2	0.8	
LUW	1492.5	1518.9	1556.7	1567.4	1548.2	
RUW	1636.3	1638.5	1667.1	1740.4	1696.4	
Source	West Road	West Road	West Road	West Road	BOW	Baghouse

Table A3.3: Farmington Aggregates

	1/2"	3/8"	Wa. Sand	Dust	Scr. Sand	BHF	RAP (7/16)
Sieve Size							
25.0	100	100	100	100	100	100	100
19.0	100	100	100	100	100	100	100
12.5	96	100	100	100	100	100	100
9.5	43	99	100	100	100	100	100
4.75	4	32	100	100	94	100	81
2.36	3	5	91	85	86	100	63
1.18	2	3	72	67	71	100	50
0.600	2	3	49	51	50	100	35
0.300	2	2	21	36	29	99	23
0.150	2	2	5.0	23.0	12.0	95.0	14
0.075	0.7	0.9	2.0	12.0	5.1	80.0	9.3
Gsb	2.645	2.616	2.565	2.598	2.566	2.607	2.607
Gsa	2.617	2.703	2.625	2.680	2.642	2.651	2.651
% Abs	0.98	1.24	0.89	1.17	1.11		
LUW	1580.4	1615.8	1544.4	1609.9	1604.5		
RUW	1689.0	1691.3	1686.9	1809.0	1797.7		
Source	#618	#618	#618	#618	#618	Baghouse	Farmington

Table A3.4: Hooksett Aggregates

	1/2"	3/8"	WMS	Dust	Wa. Sand	BHF	RAP
Sieve Size							
25.0	100	100	100	100	100	100	100
19.0	100	100	100	100	100	100	100
12.5	100	100	100	100	100	100	100
9.5	97	100	100	100	100	100	100
4.75	55	100	100	100	100	100	100
2.36	5	36	100	99	99	100	80
1.18	4	8	77	76	86	100	62
0.600	3	6	47	53	67	100	49
0.300	3	5	29	40	46	99	35
0.150	2	4	16	30	24	99	23
0.075	2	3	8	20.6	7.5	95	13
Source	#607	#607	#607	#607	Michie	#803	Marcou

Mix Designs and Batching Recipes

After the aggregate was sieved, stockpiles from the same source were stored in the same buckets. For example, the Ossipee 3/4", 1/2", 3/8", and Grits stockpiles all came from OssAgg and were stored together in a single set of buckets labeled "Gravel". The Dust and the Scr. Sand came from two separate sources, so they were each stored in their own sets of buckets. Each bucket in each set contained the aggregate retained on one sieve tray.

Oss 12.5

Table A3.5: Oss 12.5 Blend

Stockpile	3/4"	1/2"	3/8"	Grits	Dust	Scr. Sand	BHF
% Agg.	0	19.0	34.9	16.14	19.36	9.60	1.00

Table A3.6: Oss 12.5 Batching Recipes

	Gmm Sample			MMLS3 Sample		
Bucket	Gravel	Dust	Scr Sand	Gravel	Dust	Scr Sand
25.0	0	0	0	0	0	0
19.0	0	0	0	0	0	0
12.5	19.0	0	0	42.8	0	0
9.5	185.6	0	0	417.6	0	0
4.75	678.9	0	5.8	1527.5	0	13.0
2.36	175.2	58.1	11.5	394.2	130.7	25.9
1.18	95.8	69.7	30.7	215.5	156.8	69.1
0.600	111.3	62.0	57.6	250.5	139.4	129.6
0.300	72.1	58.1	53.8	162.3	130.7	121.0
0.150	29.6	50.3	21.1	66.5	113.3	47.5
0.075	13.0	38.7	7.3	29.2	87.1	16.4
Pan	20.4	50.3	4.2	45.9	113.3	9.5
BHF	20.0			45.0		
Total	2000			4500		

Oss 19

Table A3.7: Oss 19 Blend

Stockpile	3/4"	1/2"	3/8"	Grits	Dust	Scr. Sand	BHF
% Agg.	24.0	11.0	30.0	14.00	14.00	5.98	1.02

Table A3.8: Oss 19 Batching Recipes

	Gmm Sample			MMLS3 Sample		
Bucket	Gravel	Dust	Scr Sand	Gravel	Dust	Scr Sand
25.0	0	0	0	0	0	0
19.0	14.4	0	0	32.4	0	0
12.5	361.4	0	0	813.2	0	0
9.5	191.0	0	0	429.8	0	0
4.75	557.0	0	3.6	1253.3	0	8.1
2.36	153.6	42.0	7.2	345.6	94.5	16.1
1.18	81.8	50.4	19.1	184.1	113.4	43.1
0.600	96.4	44.8	35.9	216.9	100.8	80.7
0.300	66.2	42.0	33.5	149.0	94.5	75.3
0.150	25.6	36.4	13.2	57.6	81.9	29.6
0.075	11.1	28.0	4.5	25.1	63.0	10.2
Pan	21.5	36.4	2.6	48.3	81.9	5.9
BHF	20.4			45.9		
Total	2000			4500		

Cont 12.5

Table A3.9: Cont 12.5 Blend

Stockpile	3/4"	1/2"	3/8"	WMS	DSS	BHF
% Agg.	0	20.0	28.0	16.0	33.0	3.0

Table A3.10: Cont 12.5 Batching Recipes

	Gmm Sample		MMLS3 Sample	
Bucket	Frac	DSS	Frac	DSS
25.0	0	0	0	0
19.0	0	0	0	0
12.5	8.0	0	18.0	0
9.5	221.2	0	497.7	0
4.75	541.2	13.9	1217.7	31.2
2.36	248.9	31.0	560.0	69.8
1.18	120.2	85.1	270.5	191.6
0.600	63.0	162.4	141.7	365.3
0.300	33.4	205.9	75.1	463.3
0.150	16.2	111.5	36.4	251.0
0.075	6.4	35.0	14.4	78.7
Pan	21.6	15.2	48.6	34.2
BHF	60.0		135.0	
Total	2000		4500	

Cont 19

Table A3.11: Cont 19 Blend

Stockpile	3/4"	1/2"	3/8"	WMS	DSS	BHF
% Agg.	16.0	20.0	22.0	22.0	18.0	2.0

Table A3.12: Cont 19 Batching Recipes

	Gmm Sample		MMLS3 Sample	
Bucket	Frac	DSS	Frac	DSS
25.0	0.0	0	0.0	0
19.0	14.7	0	16.6	0
12.5	205.8	0	231.5	0
9.5	298.0	0	335.3	0
4.75	491.6	7.6	553.1	8.5
2.36	253.3	16.9	285.0	19.0
1.18	151.3	46.4	170.2	52.2
0.600	81.8	88.6	92.0	99.6
0.300	45.2	112.3	50.9	126.4
0.150	21.1	60.8	23.7	68.4
0.075	8.6	19.1	9.7	21.5
Pan	28.6	8.3	32.1	9.3
BHF	40.0		45.0	
Total	2000		2250	

Farm

Table A3.13: Farm Blend

Stockpile	1/2"	3/8"	Wa. Sand	Dust	Scr. Sand	BHF	RAP
% Agg.	18.2	31.2	18.82	9.05	7.35	0.98	14.4

Table A3.14: Farm Batching Recipes

	Gmm Sample	MMLS3 Sample
Bucket	Gravel	Gravel
19.0	0	0
12.5	10.9	16.4
9.5	149.4	224.1
4.75	426.6	640.0
2.36	183.7	275.5
1.18	106.7	160.0
0.600	109.8	164.7
0.300	127.2	190.9
0.150	81.6	122.3
0.075	39.7	59.6
Pan	33.7	50.5
BHF	14.7	22.1
RAP	216.0	324.0
Total	1500	2250

Hook

Table A3.14: Hook Blend

Stockpile	1/2"	3/8"	WMS	Dust	Wa. Sand	BHF	RAP
% Agg.	25	23	13.14	1.88	21.4	1.13	14.5

Table A3.15: Hook Batching Recipes

	Gmm Sample		MMLS3 Sample	
Bucket	Frac	Wa. Sand	Frac	Wa. Sand
19.0	0	0	0	0
12.5	11.3	0	16.9	0
9.5	157.5	0	236.3	0
4.75	408.6	3.2	612.9	4.8
2.36	152.2	41.7	228.3	62.6
1.18	76.3	61.0	114.4	91.5
0.600	42.6	67.4	63.9	101.1
0.300	35.6	70.6	53.5	105.9
0.150	21.9	53.0	32.8	79.4
0.075	13.2	18.0	19.7	27.0
Pan	26.3	6.1	39.4	9.1
BHF	17.0		25.4	
RAP	217.5		326.3	
Total	1500.8*		2251.1*	

*The blend for the Hook mix design totaled to 100.05%.

Oss 12.5 Bailey

Table A3.15: Oss 12.5-Bailey Blend

Stockpile	3/4"	1/2"	3/8"	Grits	Dust	Scr. Sand	BHF
% Agg.	0	27.0	41.5	27.67	0	0	3.83

Table A3.16: Oss 12.5-Bailey Batching Recipes

	Gmm Sample	Superpave Sample	MMLS3 Sample
Bucket	Gravel	Gravel	Gravel
19.0	0	0	0
12.5	20.2	60.7	30.4
9.5	196.4	589.3	294.7
4.75	639.0	1916.9	958.5
2.36	174.1	522.4	261.2
1.18	114.1	342.2	171.1
0.600	134.9	404.7	202.4
0.300	89.1	267.4	133.7
0.150	35.3	105.9	52.9
0.075	16.6	49.8	24.9
Pan	22.7	68.2	34.1
BHF	57.5	172.4	86.2
Total	1500	4500	2250

Cont 19 Bailey

Table A3.17: Cont 19-Bailey Blend

Stockpile	3/4"	1/2"	3/8"	WMS	DSS	BHF
% Agg.	23.1	30.4	18.3	19.5	6.3	2.4

Table A3.18: Cont 19-Bailey Batching Recipes

	Gmm Sample		Superpave Sample		MMLS3 Sample	
Bucket	Frac	DSS	Frac	DSS	Frac	DSS
25.0	0	0	0	0	0	0
19.0	16.0	0	23.9	0	47.9	0
12.5	223.5	0	335.3	0	670.6	0
9.5	335.1	0	502.7	0	1005.3	0
4.75	404.8	2.0	607.1	3.0	1214.3	6.0
2.36	164.8	4.5	247.2	6.7	494.5	13.4
1.18	99.9	12.3	149.9	18.4	299.7	36.8
0.600	54.2	23.4	81.4	35.1	162.7	70.1
0.300	30.1	29.6	45.1	44.5	90.3	88.9
0.150	14.1	16.1	21.2	24.1	42.4	48.2
0.075	6.0	5.0	9.1	7.6	18.1	15.1
Pan	20.6	2.2	30.9	3.3	61.8	6.6
BHF	35.8		53.7		107.4	
Total	1500		2250		4500	

Farm Bailey

Table A3.19: Farm-Bailey Blend

Stockpile	1/2"	3/8"	Wa. Sand	Dust	Scr. Sand	BHF	RAP
% Agg.	33.1	25.0	4.59	22.23	0	0.02	15.0

Table A3.20: Farm-Bailey Batching Recipes

	Gmm Sample	Superpave Sample
Bucket	Gravel	Gravel
19.0	0	0
12.5	19.9	59.6
9.5	267.2	801.5
4.75	445.4	1336.3
2.36	162.6	487.7
1.18	85.6	256.7
0.600	69.2	207.5
0.300	73.0	219.1
0.150	54.4	163.1
0.075	49.3	148.0
Pan	48.2	144.7
BHF	0.2	0.7
RAP	225.0	675.0
Total	1500	4500

APPENDIX 4

VOLUMETRIC MEASUREMENTS

Gmm Measurements

Table A4.1: Gmm Measurements Using Pycnometer

Sample	Pyc	Pyc+H2O	Pan+Mix	Pan	Mix	Total	Gmm
OSS-12.5-20-3	1571.3	11758.8	2866.2	774.5	2091.7	12988.4	2.426
OSS-12.5-20-4	1571.3	11758.8	2880.3	777.0	2103.3	12994.5	2.424
OSS-19-20-3	1571.3	11758.8	2857.7	780.4	2077.3	12993.2	2.464
OSS-19-20-4	1571.3	11758.8	2844.3	770.0	2074.3	12992.2	2.467
CONT-12.5-20-1	1571.3	11758.8	2884.3	775.9	2108.4	13017.2	2.480
CONT-12.5-20-3	1571.3	11758.8	2848.1	774.0	2074.1	12998.2	2.485
CONT-19-20-1	1571.3	11758.8	2900.6	809.3	2091.3	13018.5	2.515
CONT-19-20-3	1571.3	11758.8	2846.4	782.5	2063.9	13001.7	2.514

Table A4.2: Gmm Measurements Using CoreLok

Sample	Bags	Pan+ Mix	Pan	Mix	Mix in H_2O	V_T	Vbag	Vmix	Gmm
Farm-15-2	73.2	2345.4	771.2	1574.2	927.0	720.4	81.1	639.3	2.462
Farm-15-4	73.5	2344.5	768.5	1576.0	930.4	719.1	81.4	637.7	2.471
Hook-15-3	75.7	2333.5	771.3	1562.2	913.3	724.6	83.8	640.8	2.438
Hook-15-4	75.5	2344.1	771.9	1572.2	920.6	727.1	83.6	643.5	2.443
Hook-15-5	75.7	2349.5	768.9	1580.6	923.3	733.0	83.8	649.2	2.435
O-B-Pbf-1	73.6	2341.0	770.3	1570.7	922.9	721.4	81.5	639.9	2.455
O-B-Pbf-2	72.6	2343.4	769.8	1573.6	925.3	720.9	80.4	640.5	2.457
C-B-Pbf-1	73.0	2360.3	774.2	1586.1	946.1	713.0	80.8	632.2	2.509
C-B-Pbf-2	72.9	2349.7	772.1	1577.6	942.1	708.4	80.7	627.7	2.513
F-B-Pbf-1	72.0	2314.1	767.1	1547.0	921.3	697.7	79.7	618.0	2.503
F-B-Pbf-2	72.5	2351.3	804.9	1546.4	922.1	696.8	80.3	616.5	2.508

Gmb, VA, and VMA Measurements

Table A4.3 Oss 12.5 Volumetrics

	Weights			Volumetrics					
Sample	Dry	Sub	SSD	Gmb	Gmm	Va	Pb	Gsb	VMA
OSS-12.5-45-4-T	1777.3	1014.5	1779.7	2.323	2.425	4.2	5.6	2.588	15.3
OSS-12.5-45-5-T	1829.3	1050.2	1831.8	2.340	2.425	3.5	5.6	2.588	14.6
OSS-12.5-45-6-T	1837.4	1051.8	1841.1	2.328	2.425	4.0	5.6	2.588	15.1
OSS-12.5-45-7-T	1785.2	1020.5	1788.6	2.324	2.425	4.2	5.6	2.588	15.2
OSS-12.5-45-7-B	1868.4	1071.8	1871.6	2.336	2.425	3.7	5.6	2.588	14.8
OSS-12.5-45-8-T	1864.4	1068.4	1867.6	2.333	2.425	3.8	5.6	2.588	14.9
OSS-12.5-45-8-B	1817.7	1043.5	1821.1	2.338	2.425	3.6	5.6	2.588	14.7

Table A4.4 Oss 19 Volumetrics

	Weights			Volumetrics					
Sample	Dry	Sub	SSD	Gmb	Gmm	Va	Pb	Gsb	VMA
OSS-19-45-6-T	1842.5	1066.8	1845.6	2.366	2.466	4.0	5.0	2.597	13.4
OSS-19-45-6-B	1894.3	1100.2	1900.7	2.366	2.466	4.0	5.0	2.597	13.4
OSS-19-45-7-T	1871.4	1082.7	1875.6	2.360	2.466	4.3	5.0	2.597	13.7
OSS-19-45-7-B	1844.2	1076.8	1853.2	2.375	2.466	3.7	5.0	2.597	13.1
OSS-19-45-10-B	1795.3	1040.5	1800.1	2.363	2.466	4.1	5.0	2.597	13.5
OSS-19-45-11-T	1904.5	1102.9	1909.7	2.361	2.466	4.3	5.0	2.597	13.6
OSS-19-45-11-B	1782.3	1036.0	1789.3	2.366	2.466	4.0	5.0	2.597	13.4

Table A4.5 Cont 12.5 Volumetrics

	Weights			Volumetrics					
Sample	Dry	Sub	SSD	Gmb	Gmm	Va	Pb	Gsb	VMA
Cont-12.5-45-2-B	1844.9	1071.1	1848.6	2.373	2.483	4.4	5.5	2.705	17.1
Cont-12.5-45-3-B	1821.6	1063.7	1827.6	2.385	2.483	3.9	5.5	2.705	16.7
Cont-12.5-45-4-B	1868.8	1091.8	1875.7	2.384	2.483	4.0	5.5	2.705	16.7
Cont-12.5-45-5-B	1862.2	1085.9	1865.1	2.390	2.483	3.7	5.5	2.705	16.5
Cont-12.5-45-6-B	1821.2	1061.3	1828.6	2.374	2.483	4.4	5.5	2.705	17.1
Cont-12.5-45-8-T	1851.4	1074.4	1853.2	2.377	2.483	4.2	5.5	2.705	17.0
Cont-12.5-45-8-B	1851.7	1077.2	1854.5	2.382	2.483	4.0	5.5	2.705	16.8

Table A4.6 Cont 19 Volumetrics

	Weights			Volumetrics					
Sample	Dry	Sub	SSD	Gmb	Gmm	Va	Pb	Gsb	VMA
Cont-19-2250-1	1905.4	1117.4	1908.5	2.409	2.514	4.2	5.0	2.706	15.4
Cont-19-2250-2	1896.5	1115.3	1901.4	2.413	2.514	4.0	5.0	2.706	15.3
Cont-19-2250-4	1898.1	1119.3	1902.5	2.424	2.514	3.6	5.0	2.706	14.9
Cont-19-2250-5	1904.7	1119.5	1908.6	2.414	2.514	4.0	5.0	2.706	15.2
Cont-19-2250-6	1915.8	1127.5	1917.9	2.424	2.514	3.6	5.0	2.706	14.9
Cont-19-2250-7	1912.7	1122.5	1916.7	2.408	2.514	4.2	5.0	2.706	15.4
Cont-19-2250-9	1919.9	1129.5	1923.2	2.419	2.514	3.8	5.0	2.706	15.1

Table A4.7 Farm Volumetrics

	Weights			Volumetrics					
Sample	**Dry**	**Sub**	**SSD**	**Gmb**	**Gmm**	**Va**	**Pb**	**Gsb**	**VMA**
FARM-6	1957.4	1136.2	1962.5	2.369	2.467	4.0	5.5	2.604	14.0
FARM-7	1894.1	1100.2	1900.6	2.366	2.467	4.1	5.5	2.604	14.1
FARM-8	1898.8	1098.6	1904.5	2.356	2.467	4.5	5.5	2.604	14.5
FARM-9	1917.0	1112.3	1923.4	2.363	2.467	4.2	5.5	2.604	14.2
FARM-10	1923.5	1116.8	1930.1	2.365	2.467	4.1	5.5	2.604	14.2
FARM-11	1925.1	1117.5	1930.8	2.367	2.467	4.0	5.5	2.604	14.1
FARM-12	1911.6	1106.7	1917.3	2.358	2.467	4.4	5.5	2.604	14.4

Table A4.8 Hook Volumetrics

	Weights			Volumetrics					
Sample	**Dry**	**Sub**	**SSD**	**Gmb**	**Gmm**	**Va**	**Pb**	**Gsb**	**VMA**
HOOK-11	1888.2	1088.8	1893.7	2.346	2.439	3.8			
HOOK-15	1920.1	1102.8	1925.9	2.333	2.439	4.3			
HOOK-16	1915.0	1102.3	1918.8	2.345	2.439	3.8			
HOOK-17	1912.3	1099.8	1917.5	2.339	2.439	4.1			
HOOK-18	1911.0	1102.6	1915.4	2.351	2.439	3.6			
HOOK-19	1916.2	1102.9	1922.9	2.337	2.439	4.2			
HOOK-20	1900.4	1094.3	1908.1	2.335	2.439	4.2			

Table A4.9 Oss 12.5-Bailey Volumetrics*

	Weights			Volumetrics					
Sample	**Dry**	**Sub**	**SSD**	**Gmb**	**Gmm**	**Va**	**Pb**	**Gsb**	**VMA**
O-B-MMLS-2	1914.5	1108.1	1917.4	2.366	2.456	3.7	5.1	2.588	13.3
O-B-MMLS-4	1928.1	1118.7	1933.8	2.365	2.456	3.7	5.1	2.588	13.3

*The data files for the last five samples were lost.

Table A4.10 Cont 19-Bailey Volumetrics

	Weights			Volumetrics					
Sample	**Dry**	**Sub**	**SSD**	**Gmb**	**Gmm**	**Va**	**Pb**	**Gsb**	**VMA**
C-B-MMLS-13	1951.8	1147.5	1955.3	2.416	2.511	3.8	5.6	2.708	15.8
C-B-MMLS-14	1957.7	1149.6	1960.5	2.414	2.511	3.9	5.6	2.708	15.9
C-B-MMLS-16	1954.0	1149.2	1956.4	2.421	2.511	3.6	5.6	2.708	15.6
C-B-MMLS-17	1941.8	1141.3	1945.4	2.415	2.511	3.8	5.6	2.708	15.8
C-B-MMLS-19	1948.4	1141.9	1951.2	2.408	2.511	4.1	5.6	2.708	16.1
C-B-MMLS-23	1937.0	1134.7	1940.8	2.403	2.511	4.3	5.6	2.708	16.2
C-B-MMLS-25	1930.8	1134.7	1935.9	2.410	2.511	4.0	5.6	2.708	16.0

APPENDIX 5

COMPACTION GRAPHS

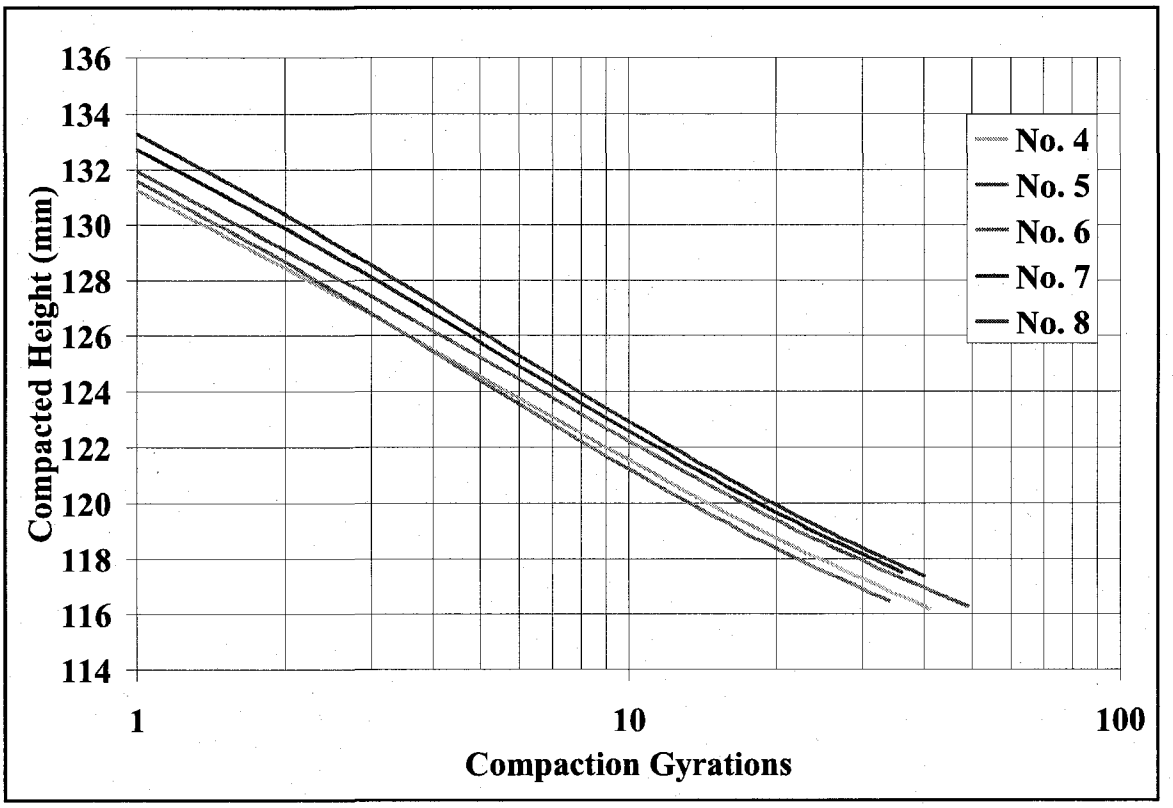

Figure A5.1: Oss 12.5 Compaction Graphs

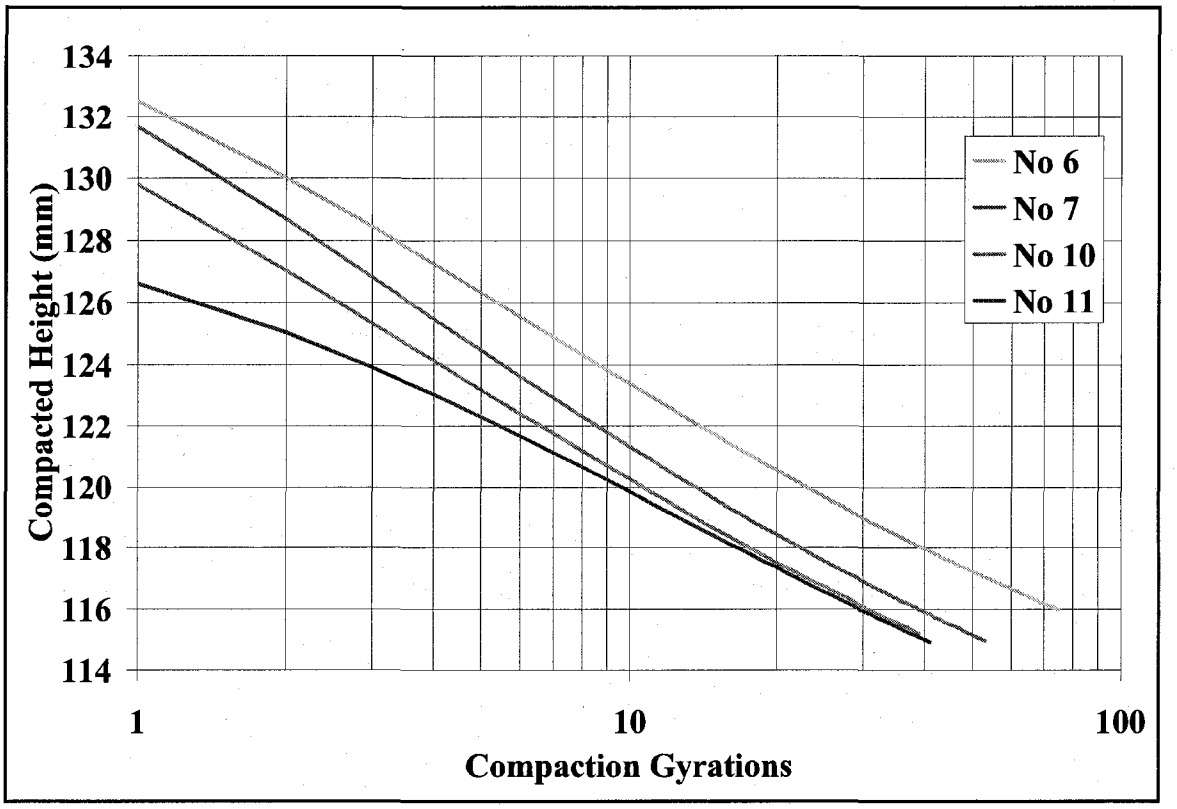

Figure A5.2: Oss 19 Compaction Graphs

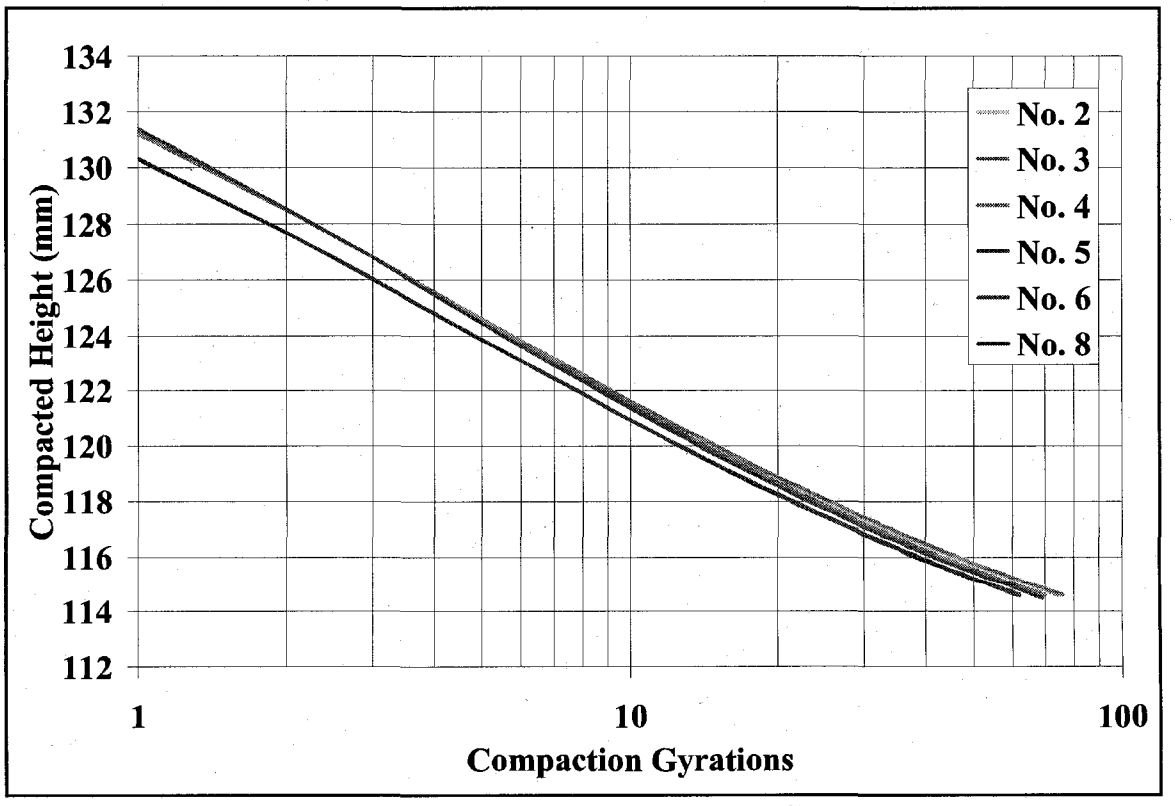

Figure A5.3: Cont 12.5 Compaction Graphs

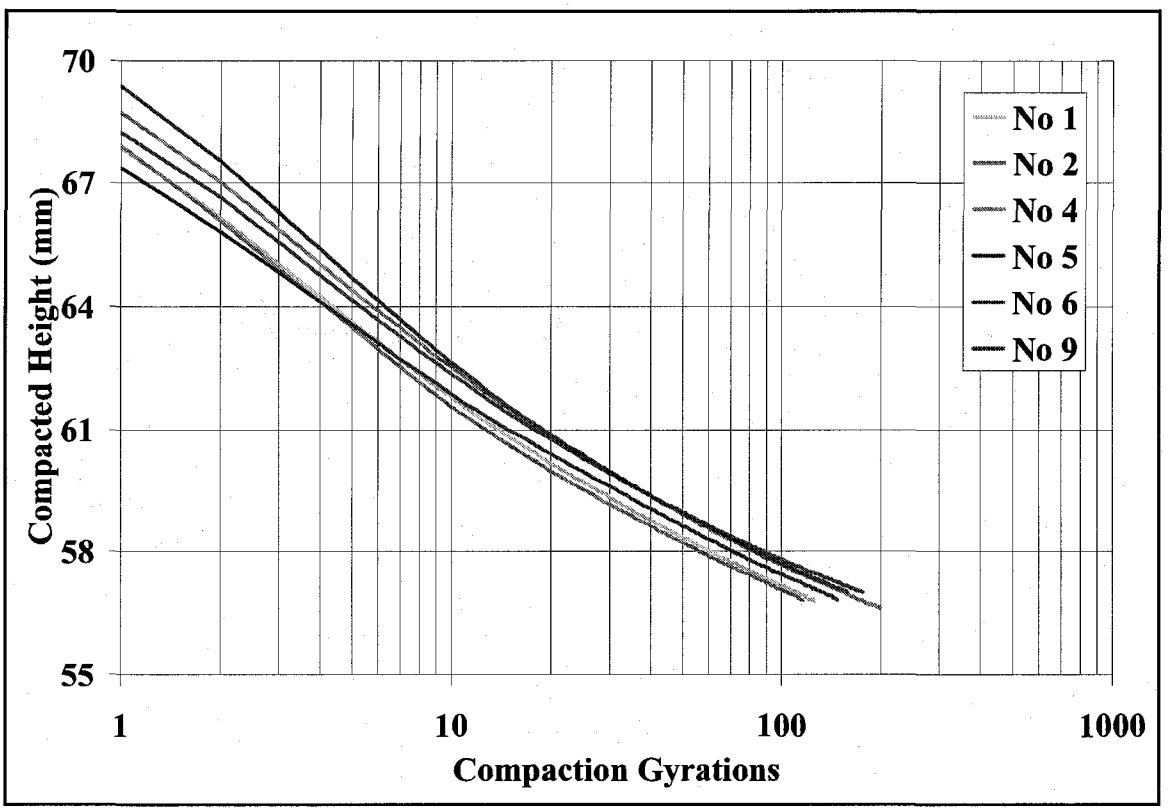

Figure A5.4: Cont 19 Compaction Graphs

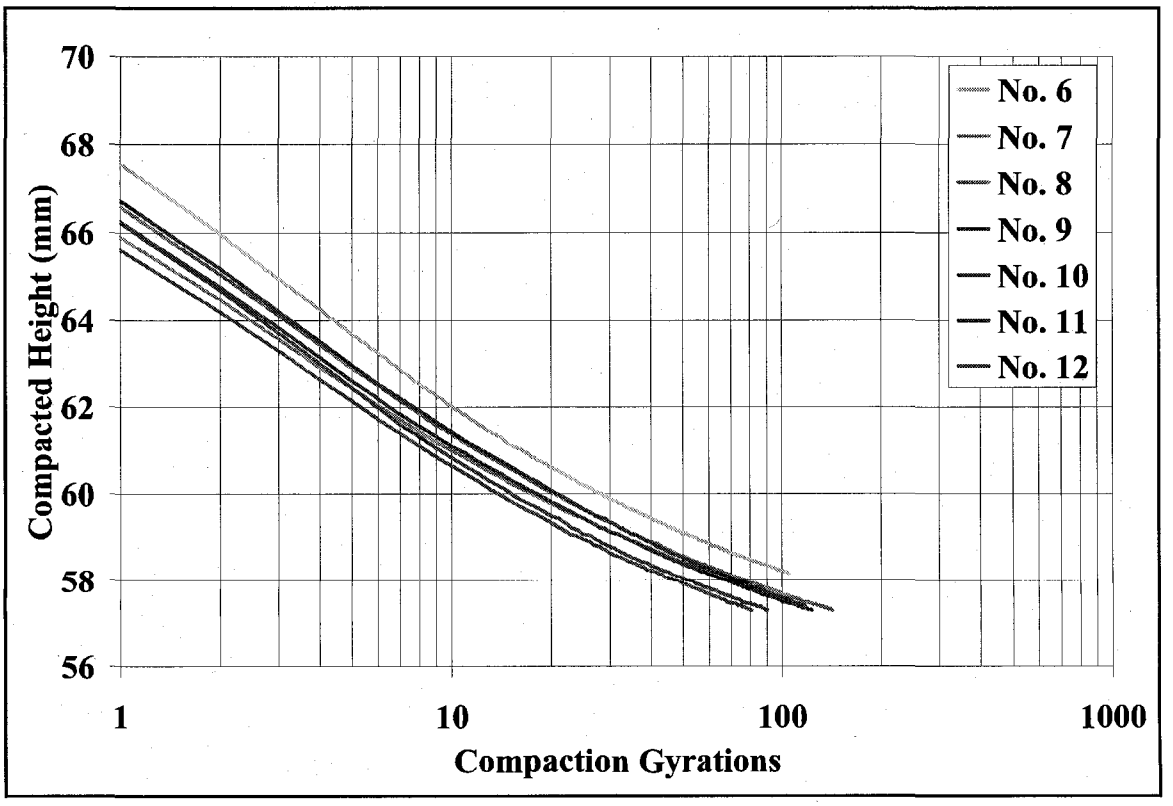

Figure A5.5: Farm Compaction Graphs

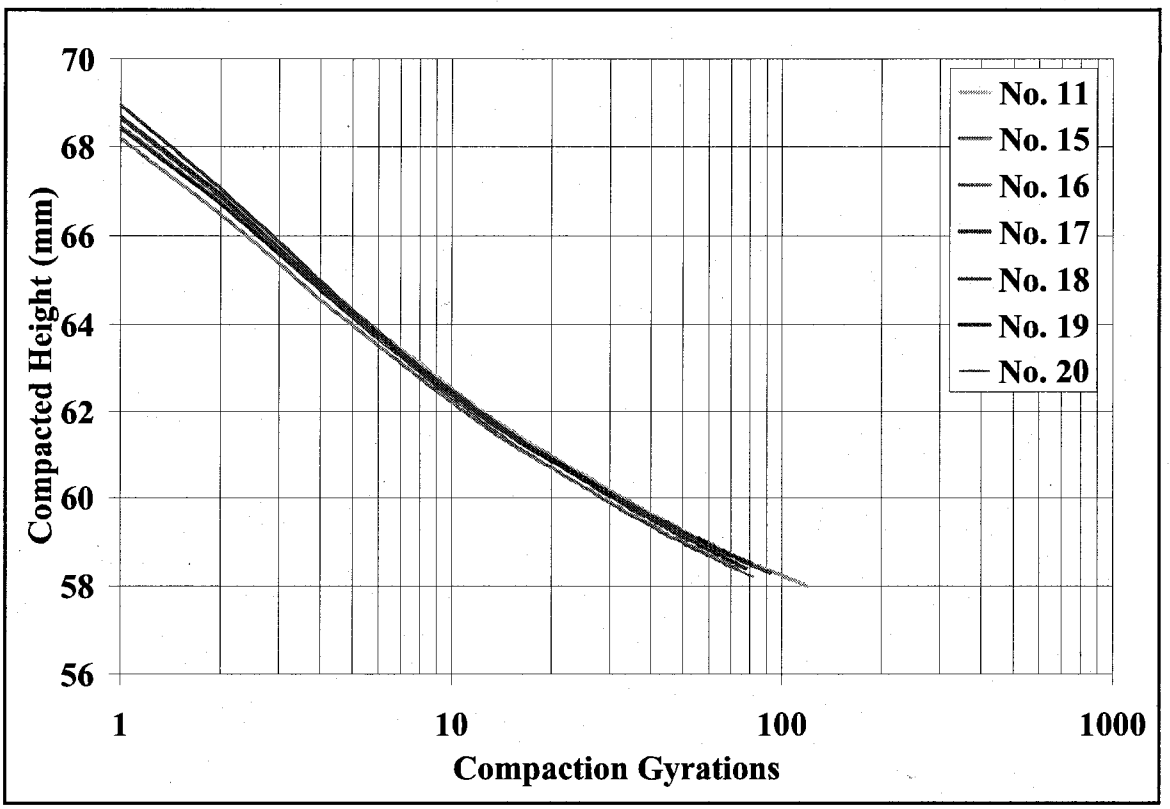

Figure A5.6: Hook Compaction Graphs

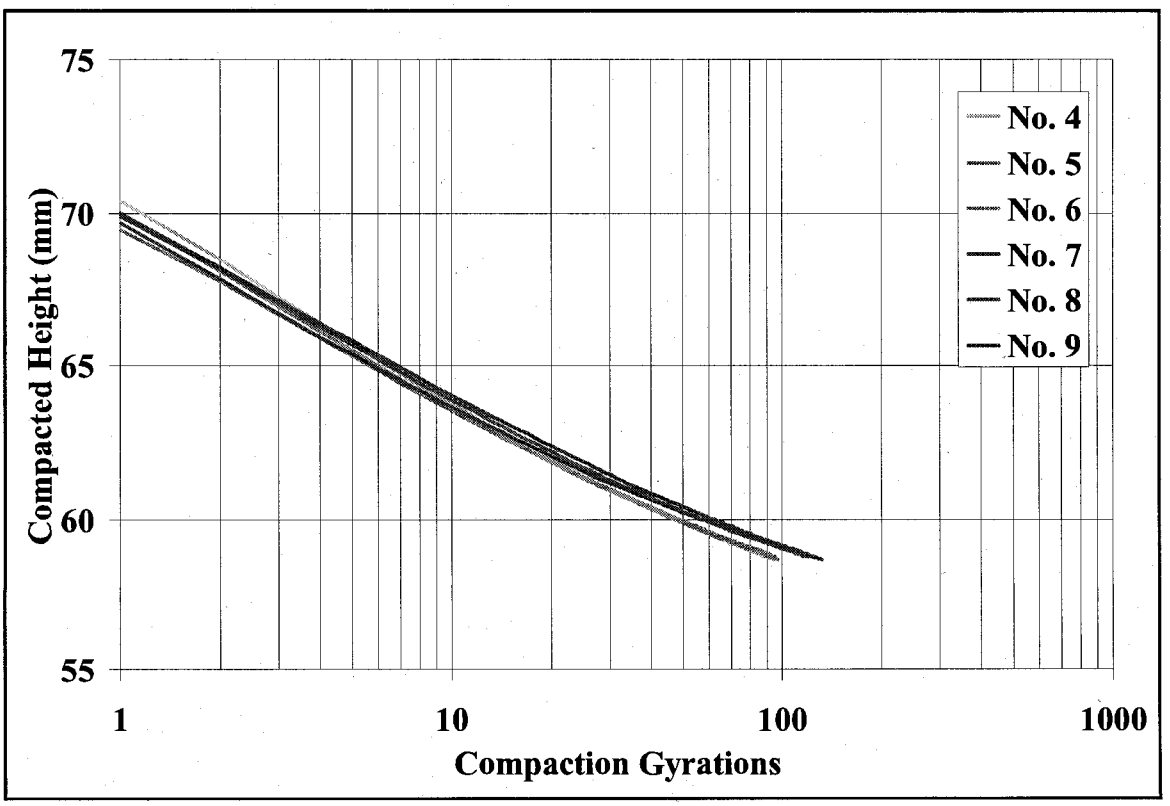

Figure A5.7: Oss 12.5 Bailey Compaction Graphs

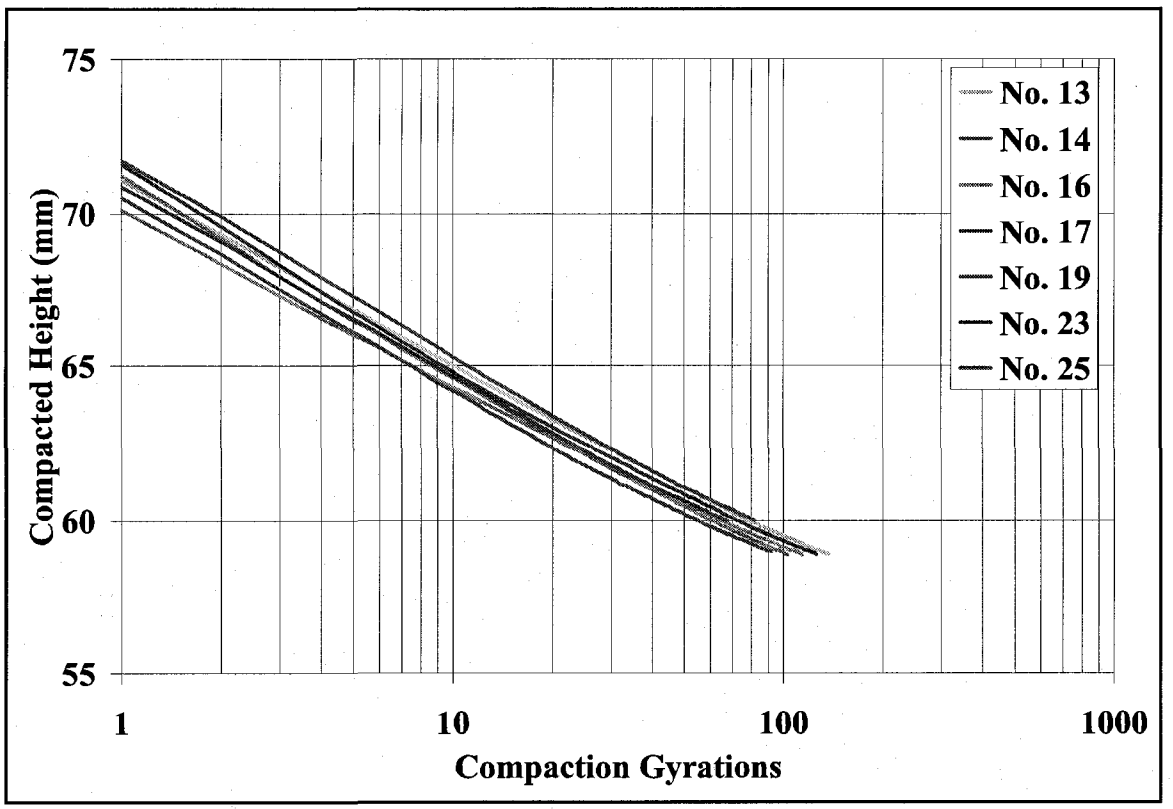

Figure A5.8: Cont 19 Bailey Compaction Graphs

APPENDIX 6

MMLS3 TEST RESULTS

Profile Data

Oss 12.5

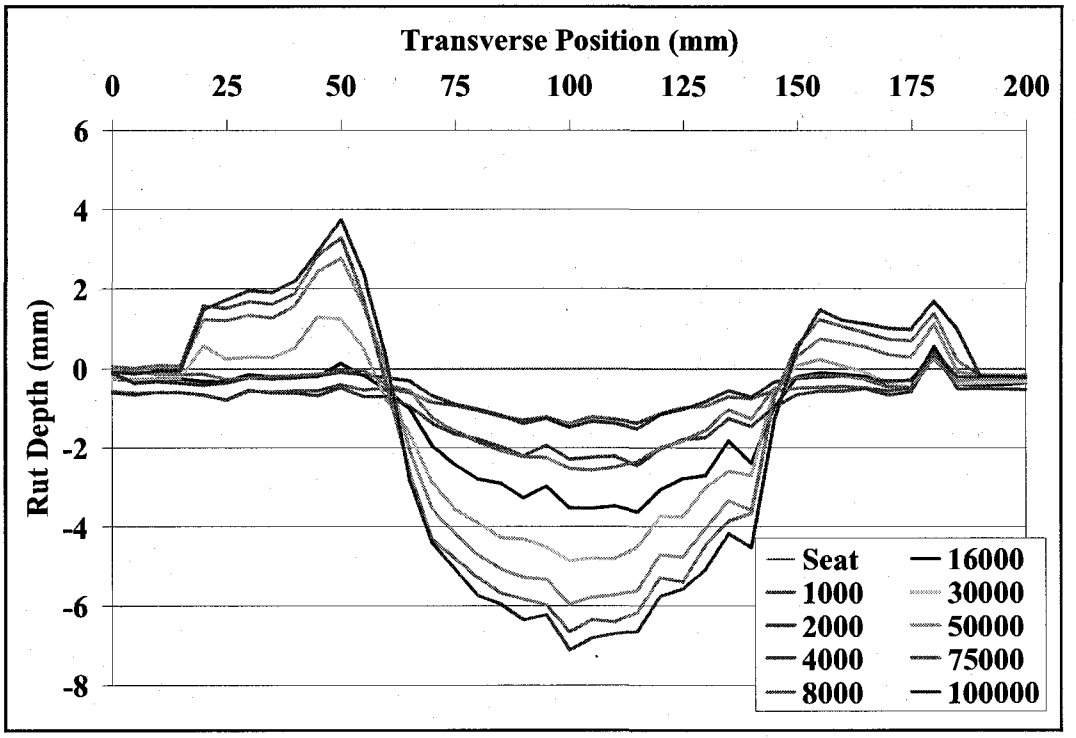

Figure A6.1: Oss 12.5 Brick 1 Transverse Profiles

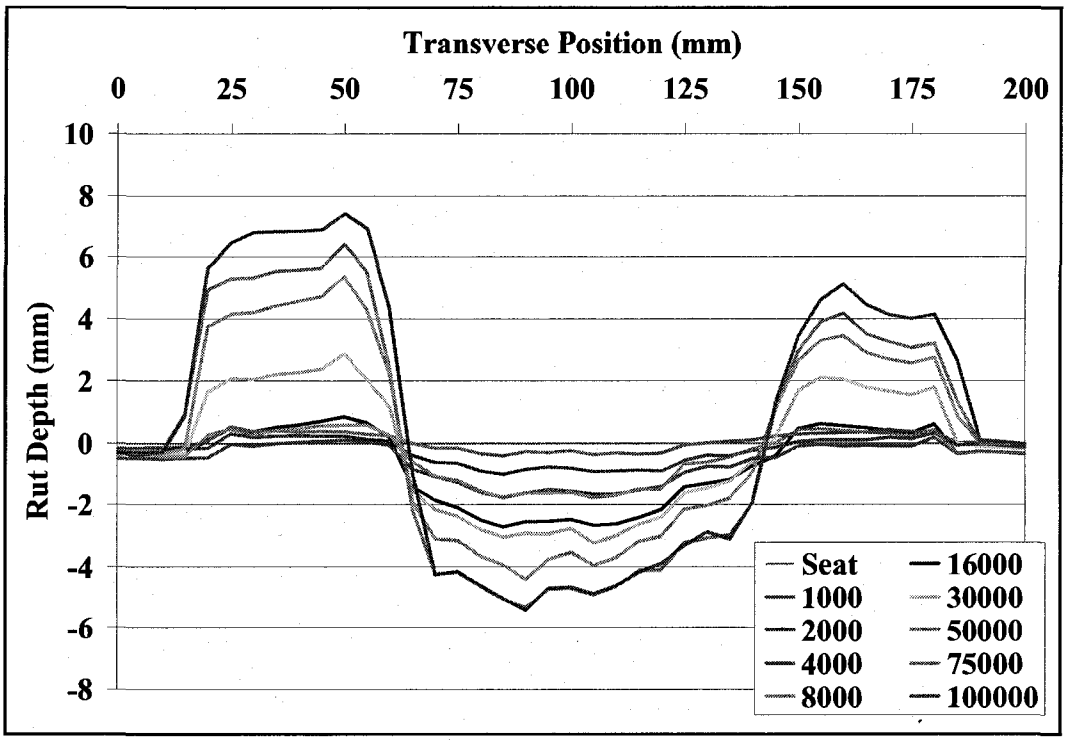

Figure A6.2: Oss 12.5 Brick 2 Transverse Profiles

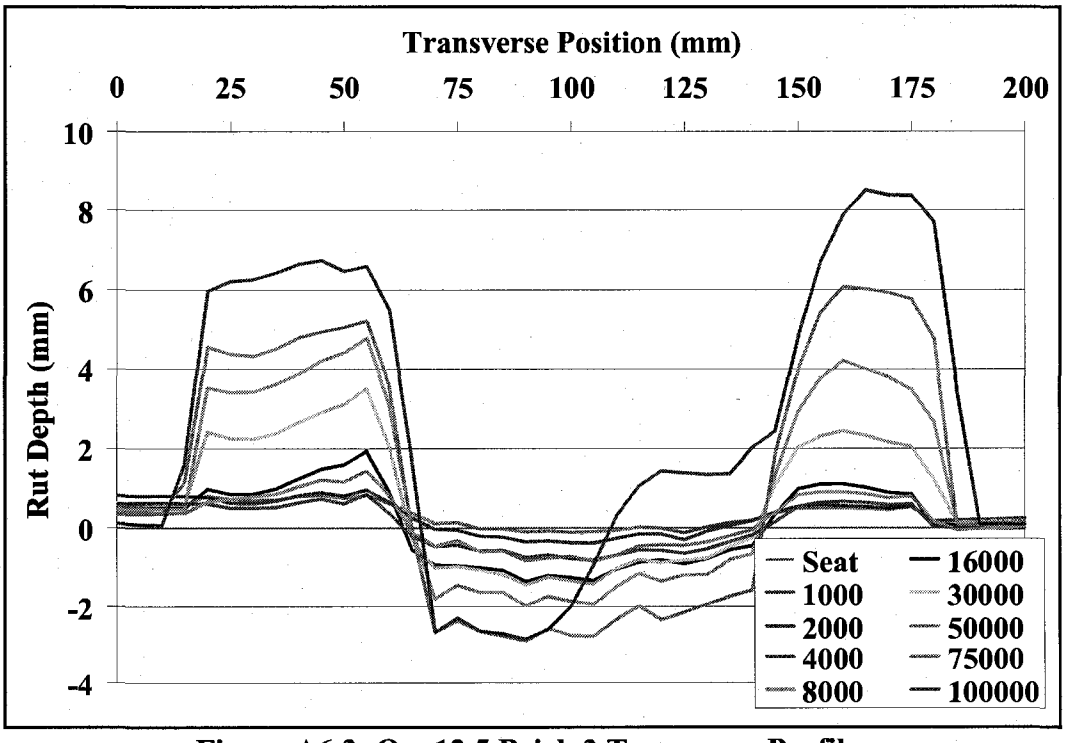

Figure A6.3: Oss 12.5 Brick 3 Transverse Profiles

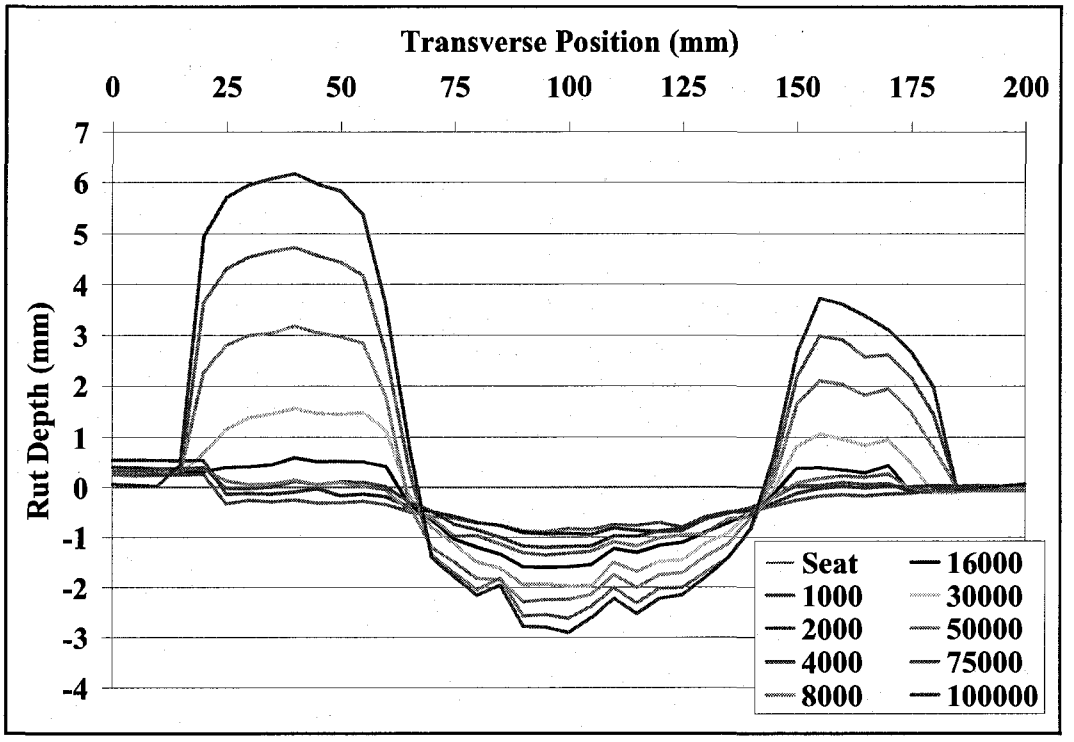

Figure A6.4: Oss 12.5 Brick 4 Transverse Profiles

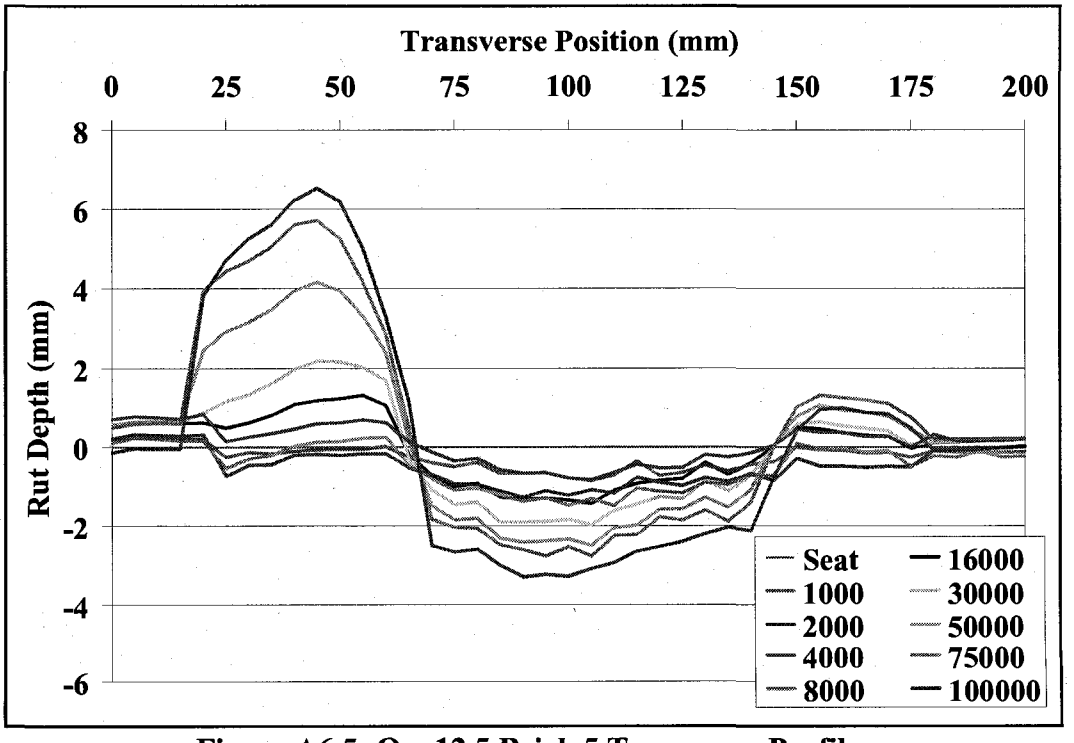

Figure A6.5: Oss 12.5 Brick 5 Transverse Profiles

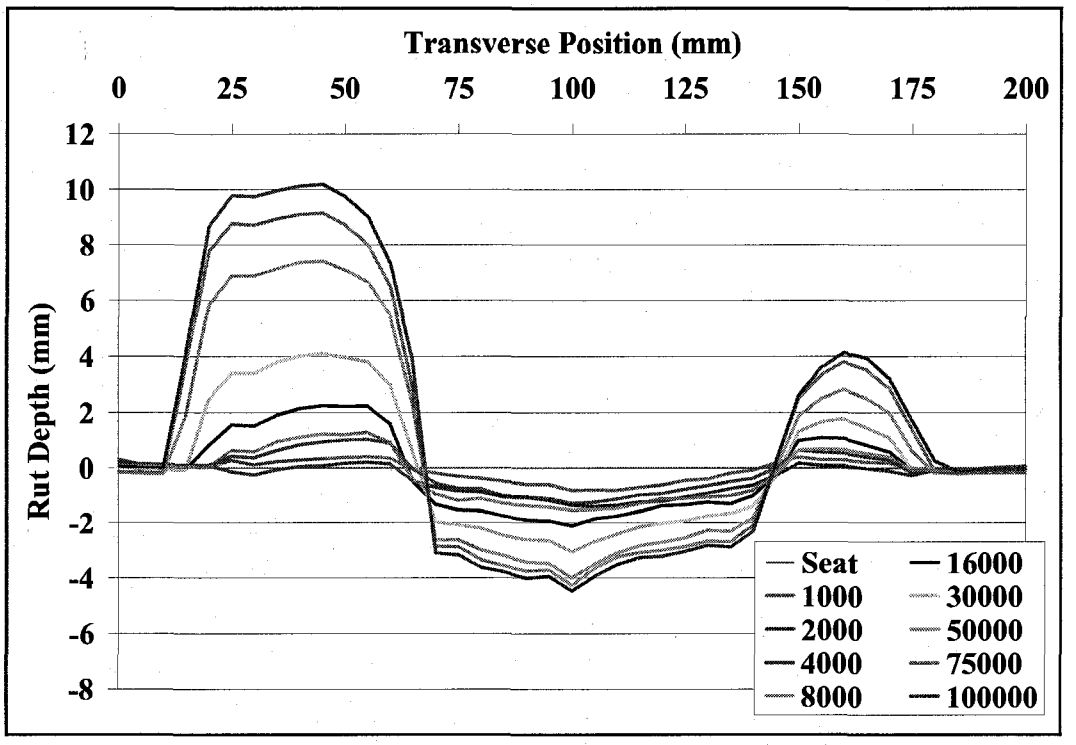

Figure A6.6: Oss 12.5 Brick 6 Transverse Profiles

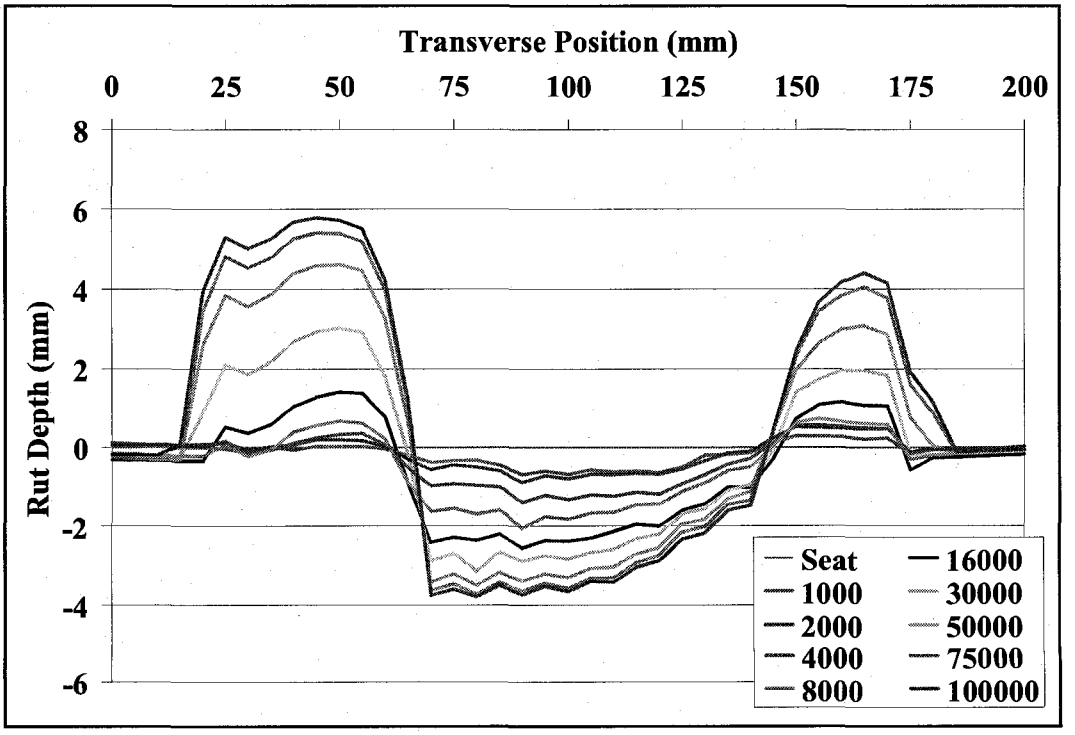

Figure A6.7: Oss 12.5 Brick 7 Transverse Profiles

Table A6.1: Oss 12.5 Avg Rut Depth from Base Line

Brick	Long Pos	Thousands of Loading Cycles								
		1	2	4	8	16	30	50	75	100
1	157.5	1.20	1.24	2.06	2.15	3.14	4.22	5.17	5.77	6.18
2	262.5	0.27	0.82	1.47	1.46	2.31	2.63	3.39	4.41	4.38
3	367.5	0.05	0.26	0.65	0.61	1.06	1.10	1.56	2.45	2.61*
4	472.5	0.78	0.84	0.99	1.14	1.32	1.65	1.92	2.18	2.38
5	577.5	0.63	1.03	0.55	1.22	1.06	1.58	2.02	2.27	2.84
6	682.5	0.62	1.15	0.99	1.29	1.66	2.35	3.09	3.37	3.60
7	787.5	0.55	0.65	1.12	1.56	2.12	2.48	2.88	3.11	3.22
Avg		0.58	0.86	1.12	1.35	1.81	2.29	2.86	3.37	3.60

* Brick 3 used a modified range for the average rut at 100,000 cycles

Table A6.2: Oss 12.5 Max Rut Depth from Base Line

Brick	Long Pos	Thousands of Loading Cycles								
		1	2	4	8	16	30	50	75	100
1	157.5	1.41	1.53	2.43	2.56	3.62	4.87	5.96	6.65	7.12
2	262.5	0.42	1.04	1.78	1.79	2.73	3.24	4.40	5.32	5.42
3	367.5	0.13	0.39	0.82	0.84	1.36	1.45	1.97	2.87	2.82
4	472.5	0.89	0.94	1.20	1.35	1.60	1.97	2.29	2.62	2.91
5	577.5	0.86	1.27	0.83	1.49	1.43	1.98	2.49	2.79	3.30
6	682.5	0.81	1.39	1.28	1.52	2.11	3.05	4.00	4.25	4.48
7	787.5	0.70	0.89	1.40	2.05	2.54	3.15	3.51	3.72	3.79
Avg		0.74	1.07	1.39	1.66	2.20	2.82	3.52	4.03	4.26

Table A6.3: Oss 12.5 Max Rut Depth from Max Heave

Brick	Long Pos	Thousands of Loading Cycles								
		1	2	4	8	16	30	50	75	100
1	157.5	1.71	1.95	2.83	2.79	4.16	6.16	8.74	9.93	10.86
2	262.5	0.93	1.36	1.97	2.38	3.57	6.11	9.75	11.73	12.83
3	367.5	0.95	1.35	1.66	2.29	3.29	4.97	6.74	8.95	11.33
4	472.5	1.13	1.50	1.59	1.69	2.19	3.54	5.48	7.35	9.08
5	577.5	1.09	1.59	1.66	1.72	2.76	4.16	6.64	8.51	9.82
6	682.5	1.21	1.58	2.32	2.80	4.37	7.15	11.43	13.40	14.67
7	787.5	0.98	1.41	1.97	2.78	3.95	6.17	8.12	9.12	9.58
Avg		1.14	1.53	2.00	2.35	3.47	5.46	8.13	9.85	11.17

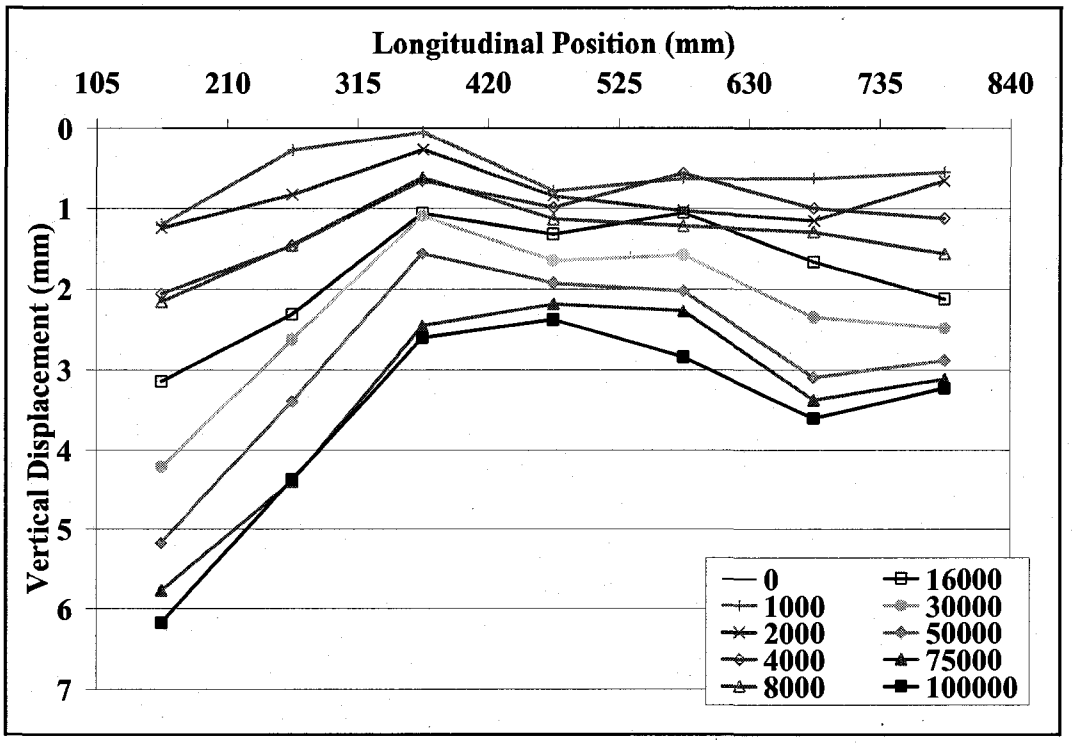

Figure A6.8: Oss 12.5 Avg Rut from Base Line Longitudinal Profiles

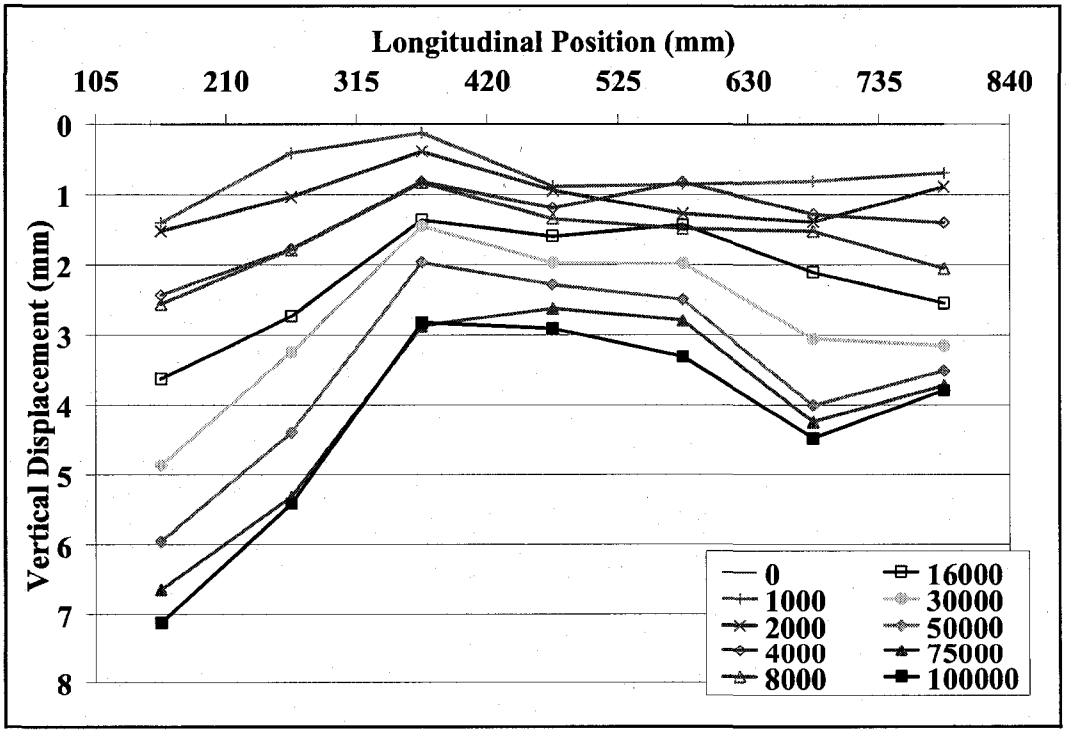

Figure A6.9: Oss 12.5 Max Rut from Base Line Longitudinal Profiles

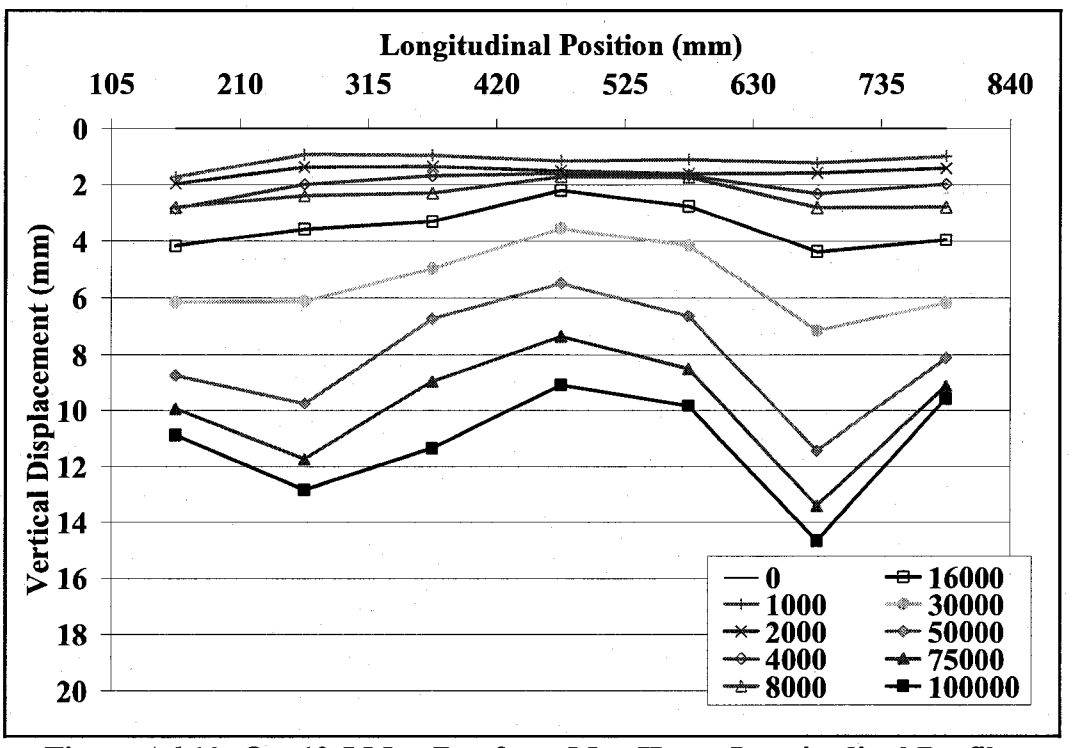

Figure A6.10: Oss 12.5 Max Rut from Max Heave Longitudinal Profiles

Oss 19

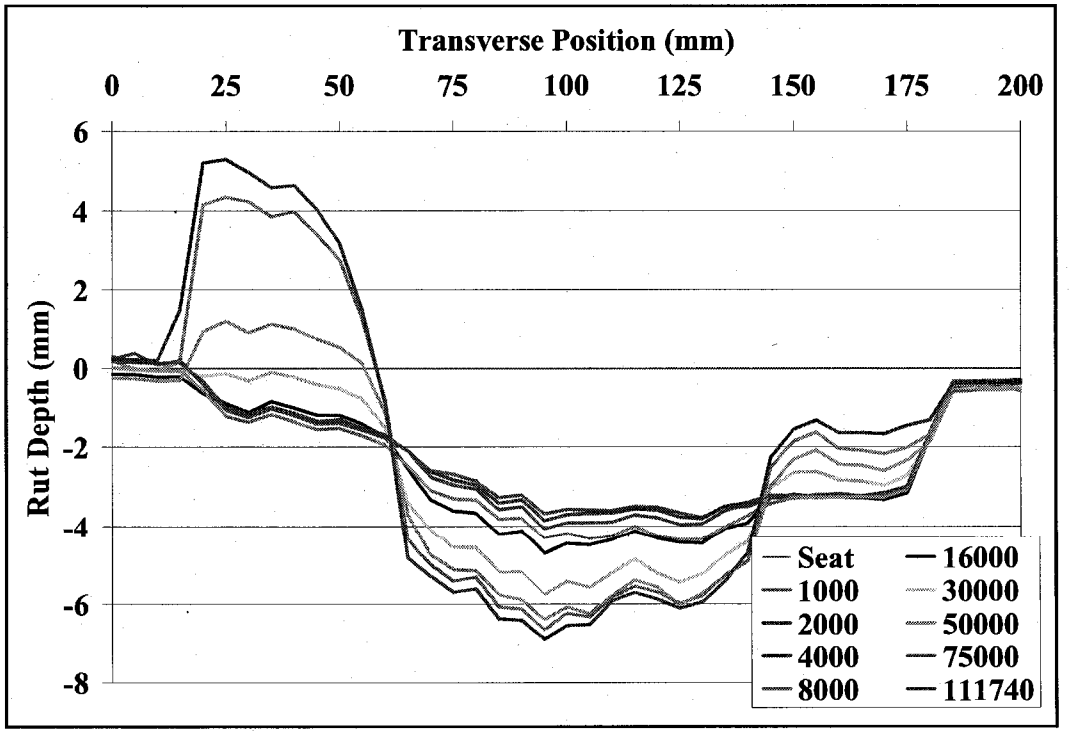

Figure A6.11: Oss 19 Brick 1 Transverse Profiles

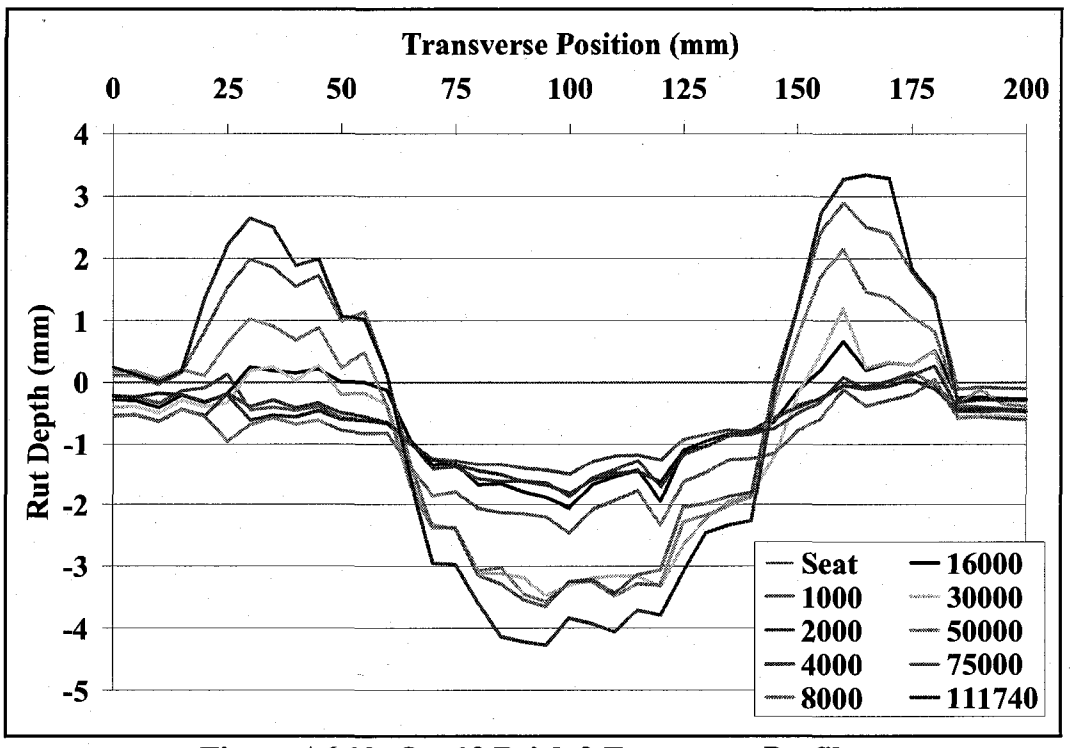

Figure A6.12: Oss 19 Brick 2 Transverse Profiles

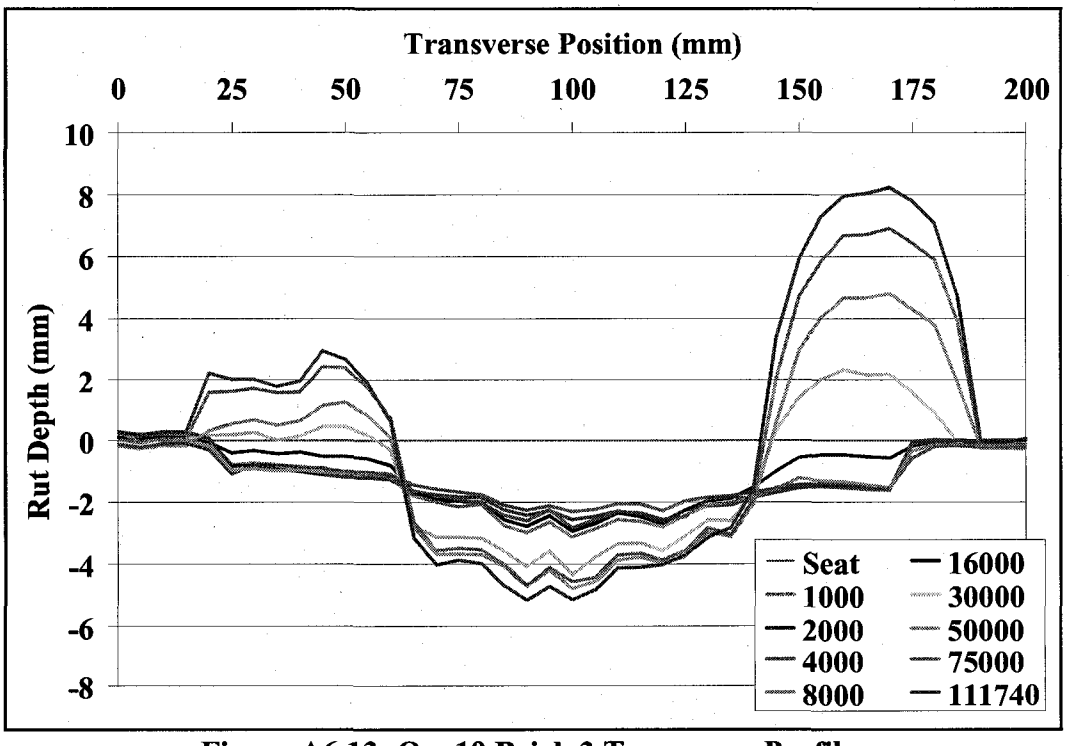

Figure A6.13: Oss 19 Brick 3 Transverse Profiles

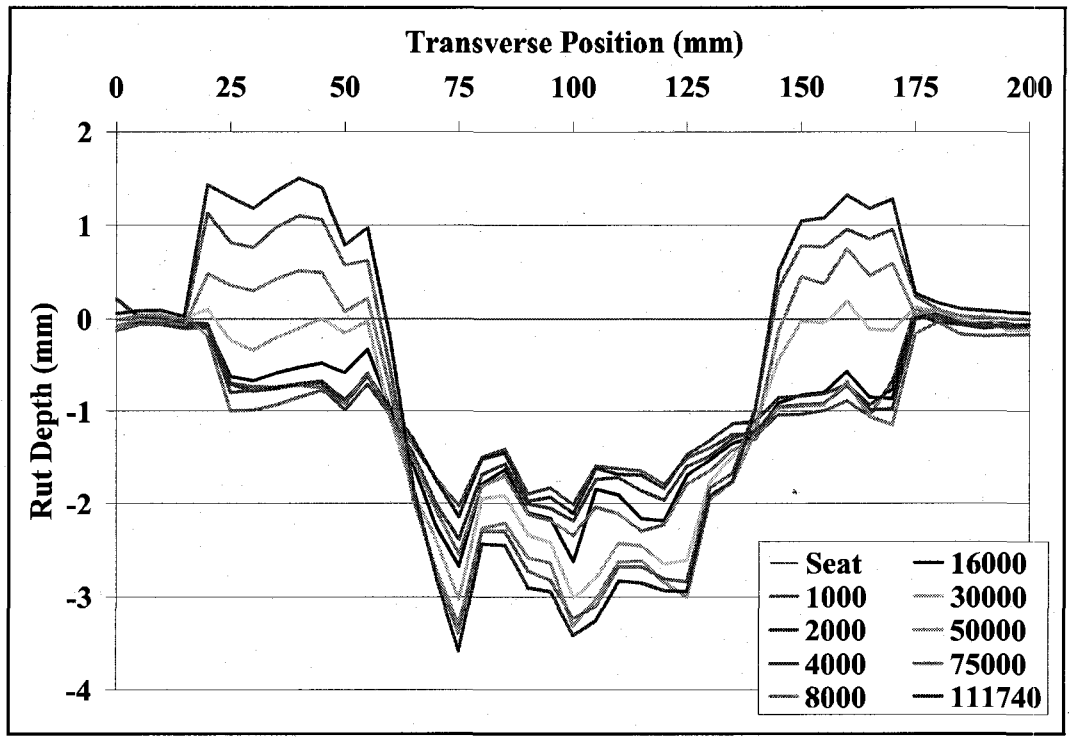

Figure A6.14: Oss 19 Brick 4 Transverse Profiles

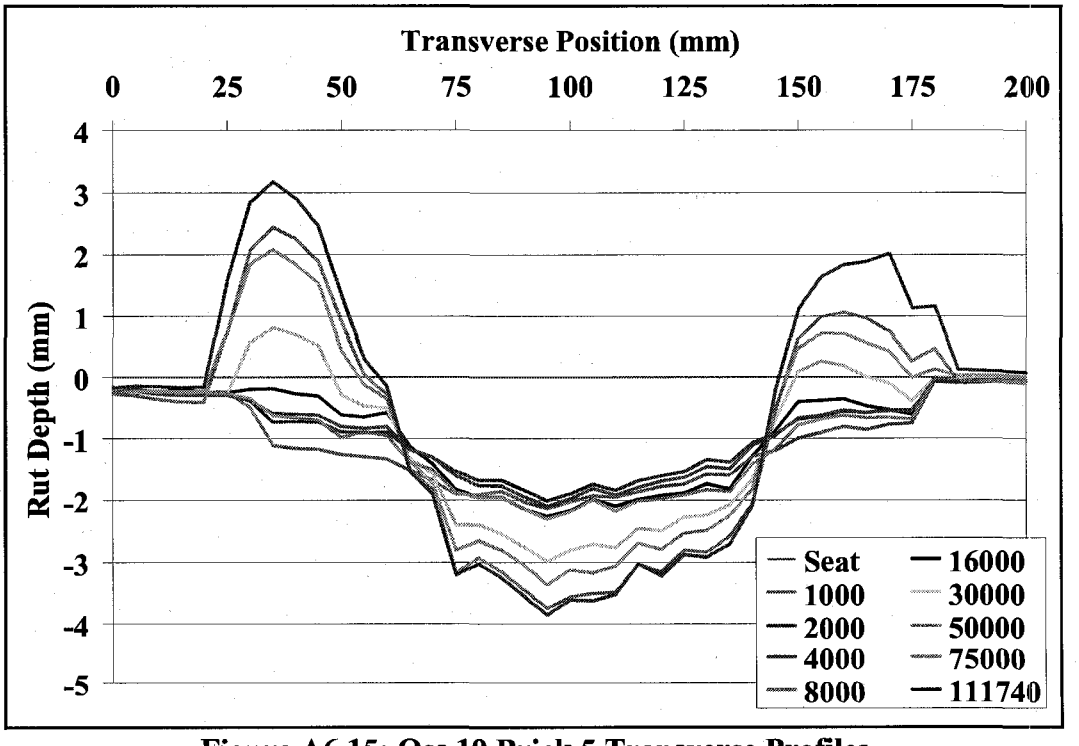

Figure A6.15: Oss 19 Brick 5 Transverse Profiles

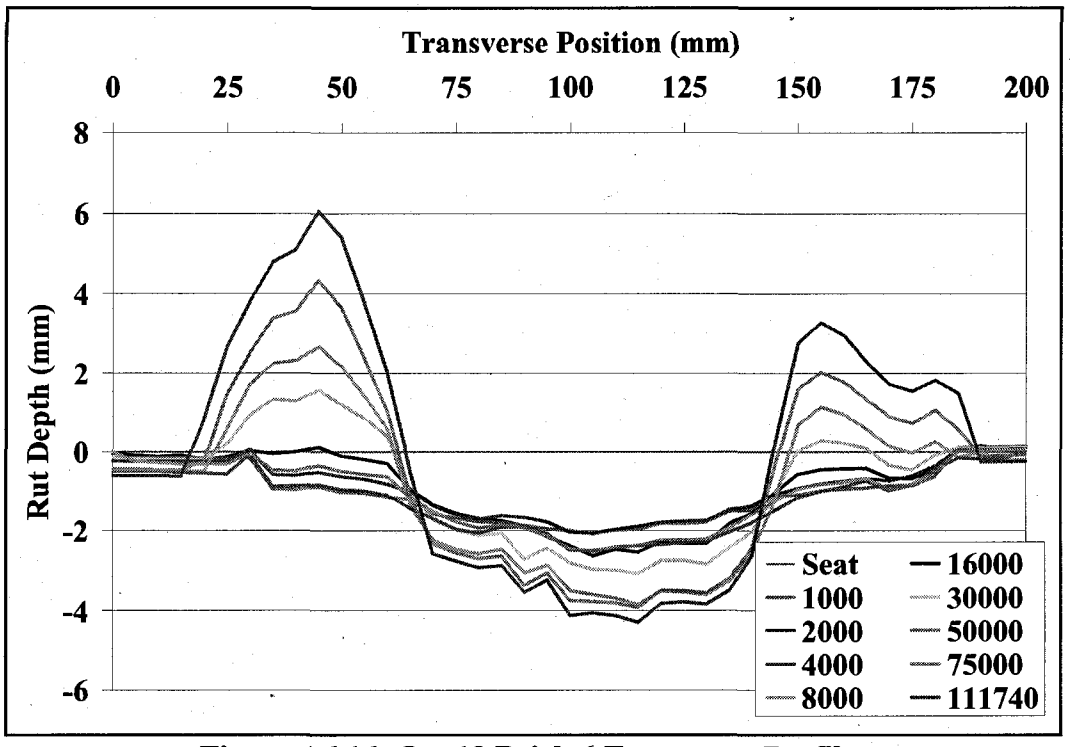

Figure A6.16: Oss 19 Brick 6 Transverse Profiles

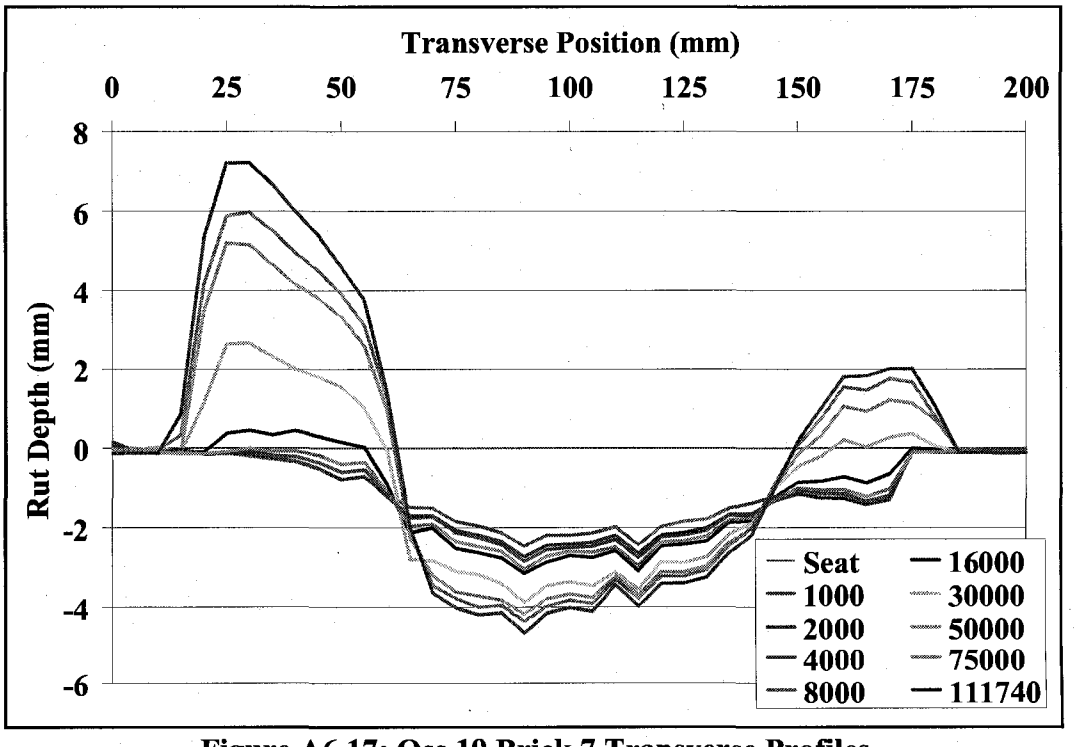

Figure A6.17: Oss 19 Brick 7 Transverse Profiles

Table A6.4: Oss 19 Avg Rut Depth from Base Line

Brick	Long Pos	Thousands of Loading Cycles								
		1	2	4	8	16	30	50	75	100
1	157.5	3.46	3.56	3.74	4.08	4.30	5.24	5.82	5.96	6.18
2	262.5	1.25	1.48	1.50	2.02	1.62	3.09	3.11	3.07	3.73
3	367.5	2.09	2.32	2.39	2.63	2.46	3.49	4.03	3.90	4.33
4	472.5	1.66	1.69	1.81	2.02	1.97	2.39	2.64	2.66	2.80
5	577.5	1.89	1.71	1.80	2.04	2.00	2.58	2.88	3.24	3.31
6	682.5	1.89	1.81	2.23	2.20	2.21	2.67	3.28	3.40	3.68
7	787.5	2.09	2.32	2.41	2.57	2.69	3.26	3.54	3.68	3.88
Avg		2.05	2.13	2.27	2.51	2.47	3.25	3.61	3.70	3.99

Table A6.5: Oss 19 Max Rut Depth from Base Line

Brick	Long Pos	Thousands of Loading Cycles								
		1	2	4	8	16	30	50	75	100
1	157.5	3.76	3.84	4.07	4.36	4.70	5.75	6.39	6.65	6.90
2	262.5	1.50	1.81	1.86	2.45	2.05	3.48	3.58	3.65	4.27
3	367.5	2.31	2.64	2.84	3.13	2.94	4.34	4.78	4.66	5.14
4	472.5	2.03	2.14	2.38	2.55	2.67	3.03	3.32	3.40	3.58
5	577.5	2.13	2.00	2.09	2.30	2.26	2.98	3.36	3.74	3.85
6	682.5	2.08	2.05	2.50	2.51	2.62	3.06	3.84	3.91	4.29
7	787.5	2.46	2.72	2.84	3.05	3.14	3.88	4.18	4.36	4.64
Avg		2.32	2.46	2.65	2.91	2.91	3.79	4.21	4.34	4.67

Table A6.6: Oss 19 Max Rut Depth from Max Heave

Brick	Long Pos	Thousands of Loading Cycles								
		1	2	4	8	16	30	50	75	100
1	157.5	3.92	4.12	4.44	4.36	4.55	5.75	7.58	10.99	12.20
2	262.5	1.67	1.86	2.13	2.50	2.71	4.67	5.74	6.54	7.61
3	367.5	2.54	2.93	2.75	3.41	3.09	6.66	9.59	11.57	13.38
4	472.5	2.14	2.36	2.42	2.59	2.73	3.22	4.06	4.52	5.09
5	577.5	2.07	1.93	2.05	2.28	2.26	3.80	5.44	6.18	7.03
6	682.5	2.21	2.12	2.52	2.57	2.78	4.63	6.51	8.26	10.34
7	787.5	2.53	2.88	2.88	3.04	3.58	6.52	9.39	10.33	11.87
Avg		2.44	2.60	2.74	2.96	3.10	5.04	6.90	8.34	9.64

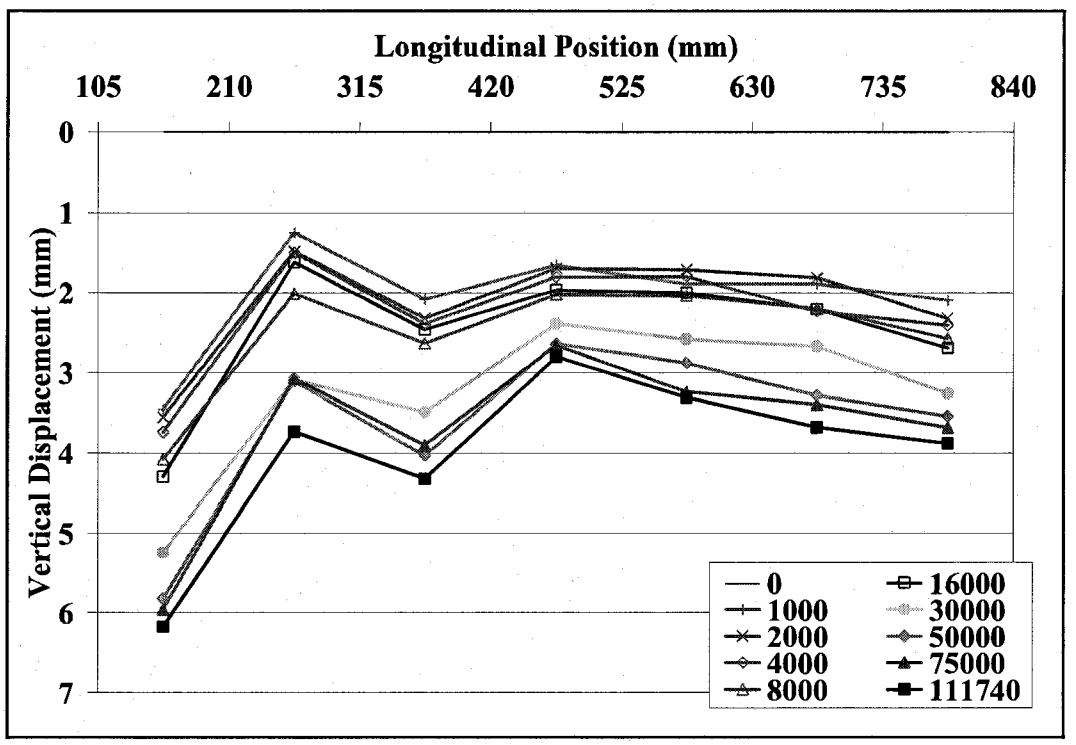

Figure A6.18: Oss 19 Avg Rut from Base Line Longitudinal Profiles

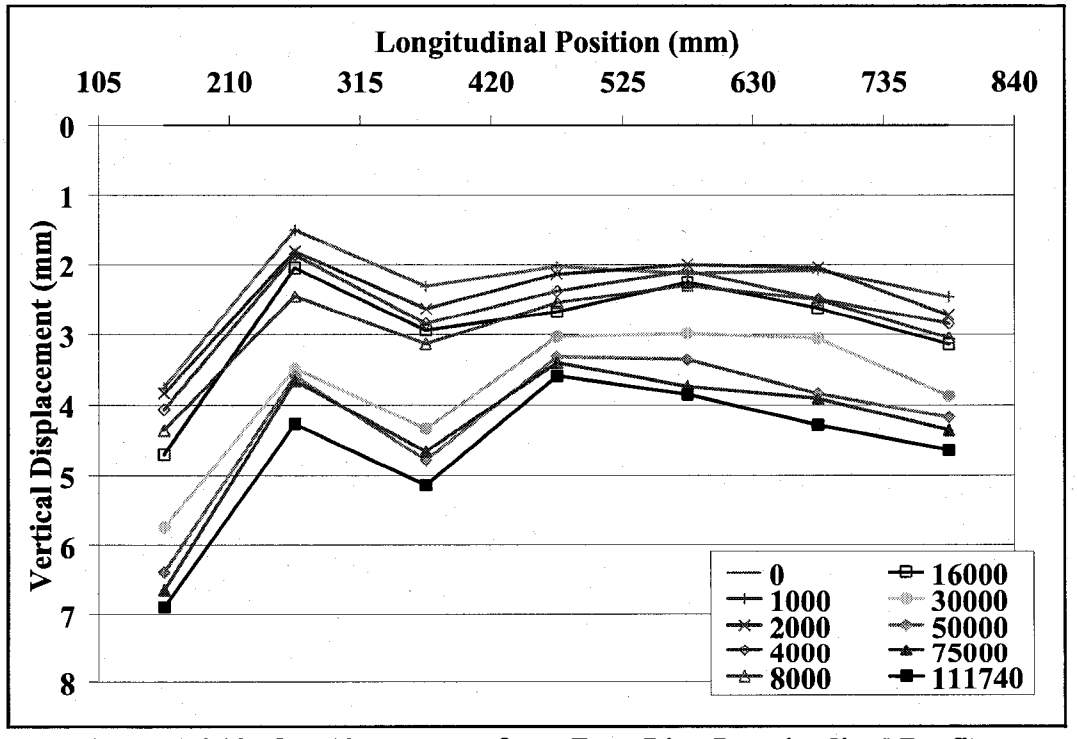

Figure A6.19: Oss 19 Max Rut from Base Line Longitudinal Profiles

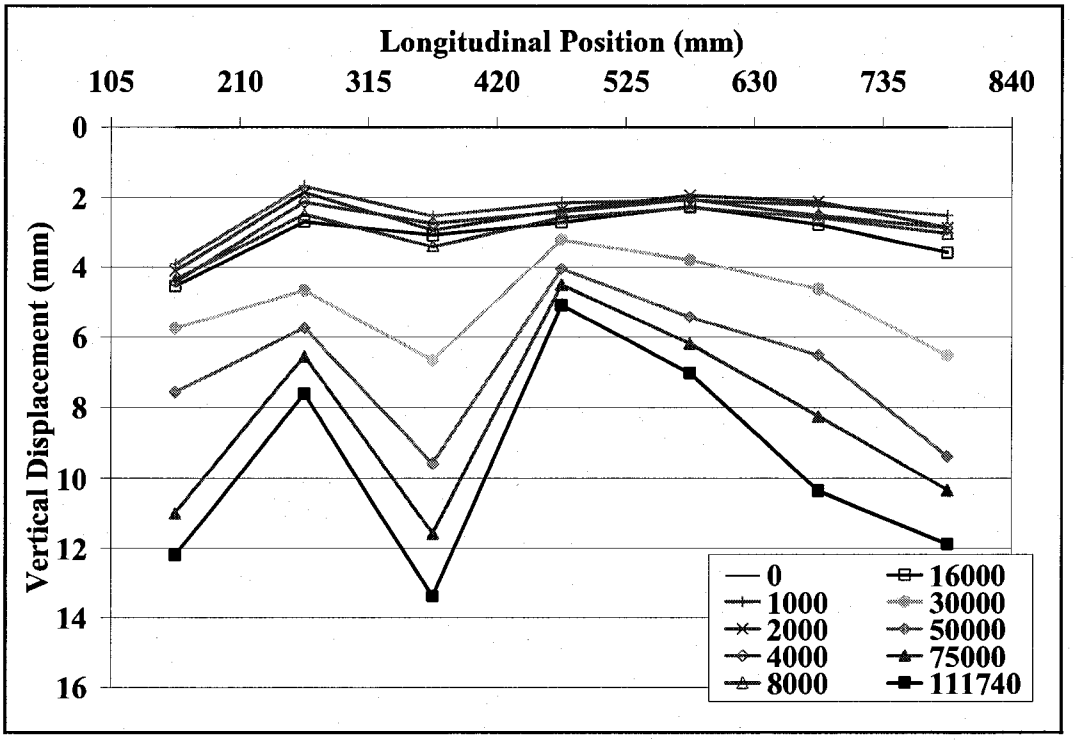

Figure A6.20: Oss 19 Max Rut from Max Heave Longitudinal Profiles

Cont 12.5

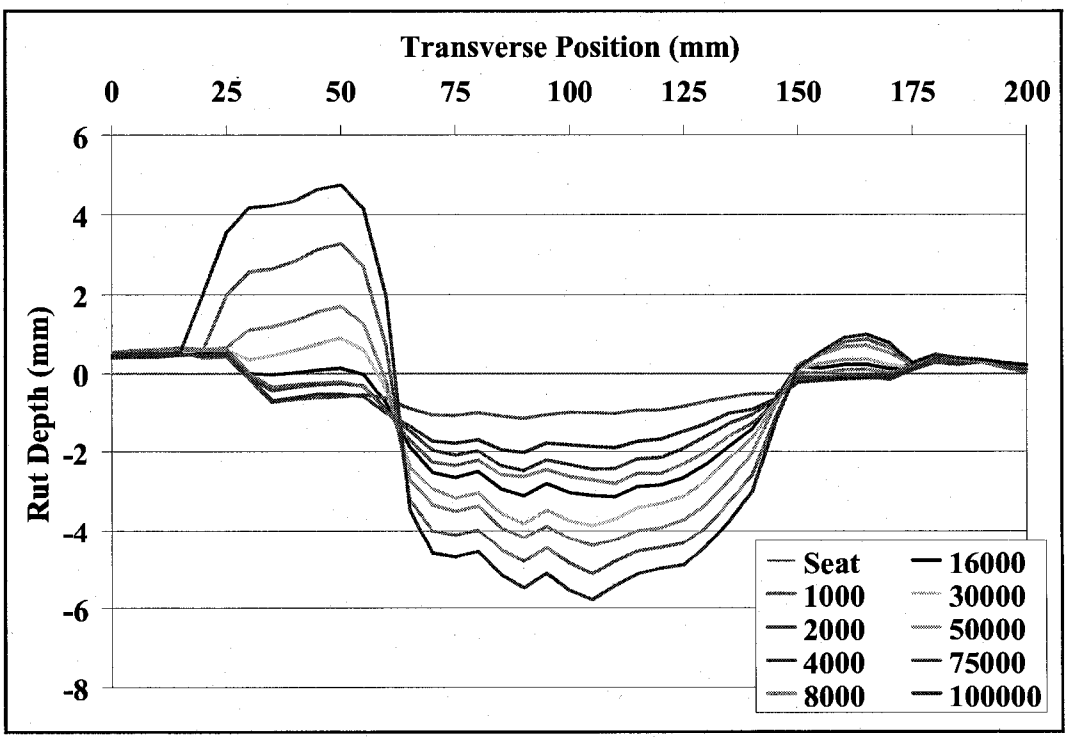

Figure A6.21: Cont 12.5 Brick 1 Transverse Profiles

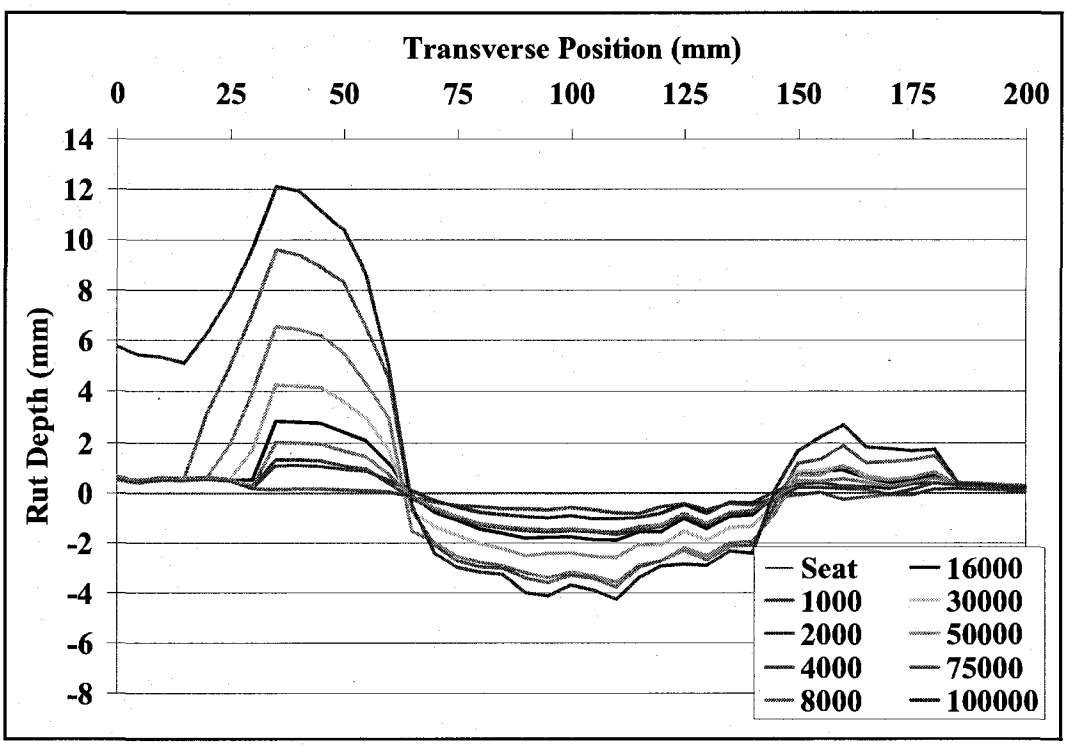

Figure A6.22: Cont 12.5 Brick 2 Transverse Profiles

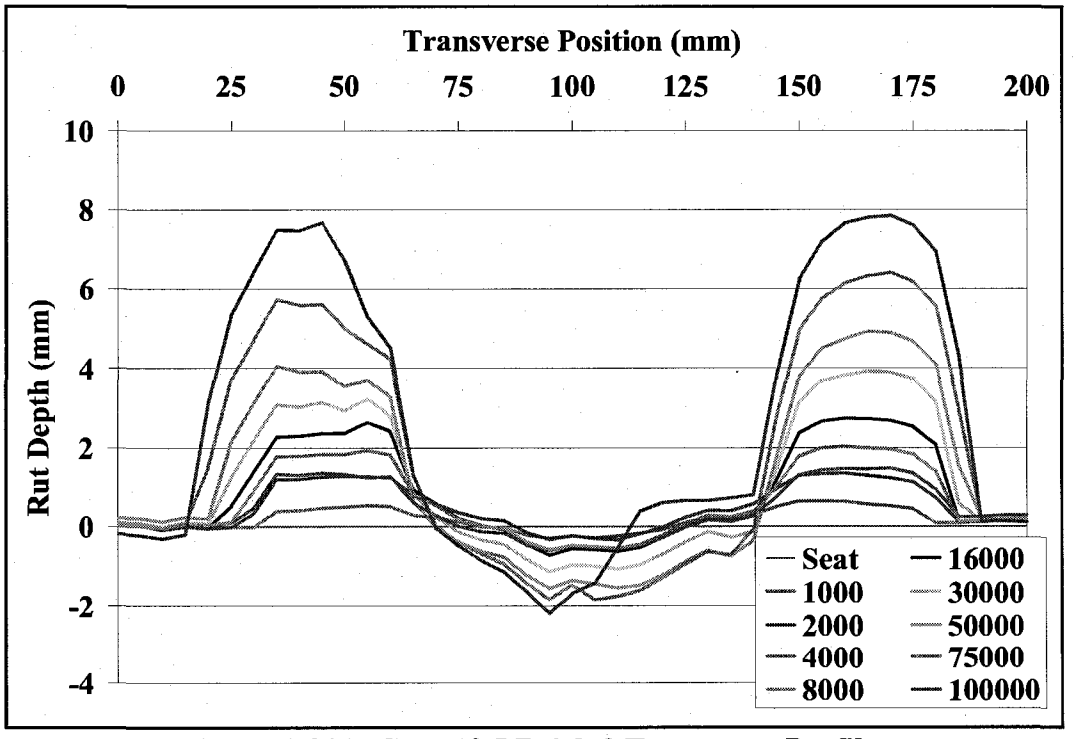

Figure A6.23: Cont 12.5 Brick 3 Transverse Profiles

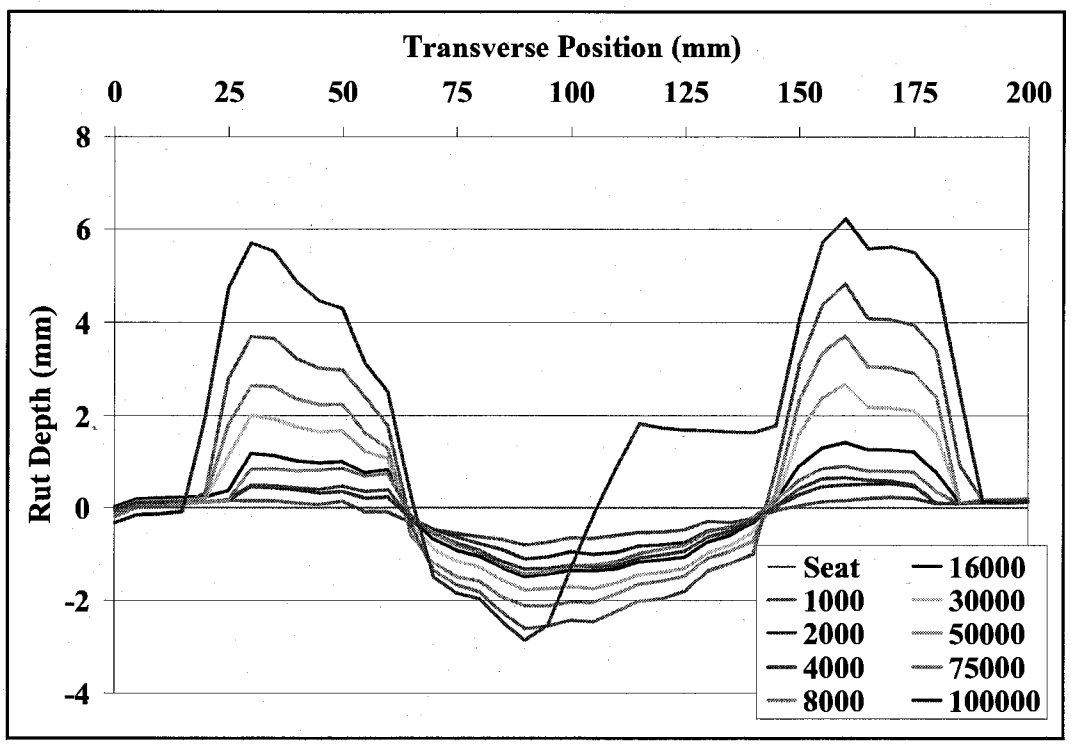

Figure A6.24: Cont 12.5 Brick 4 Transverse Profiles

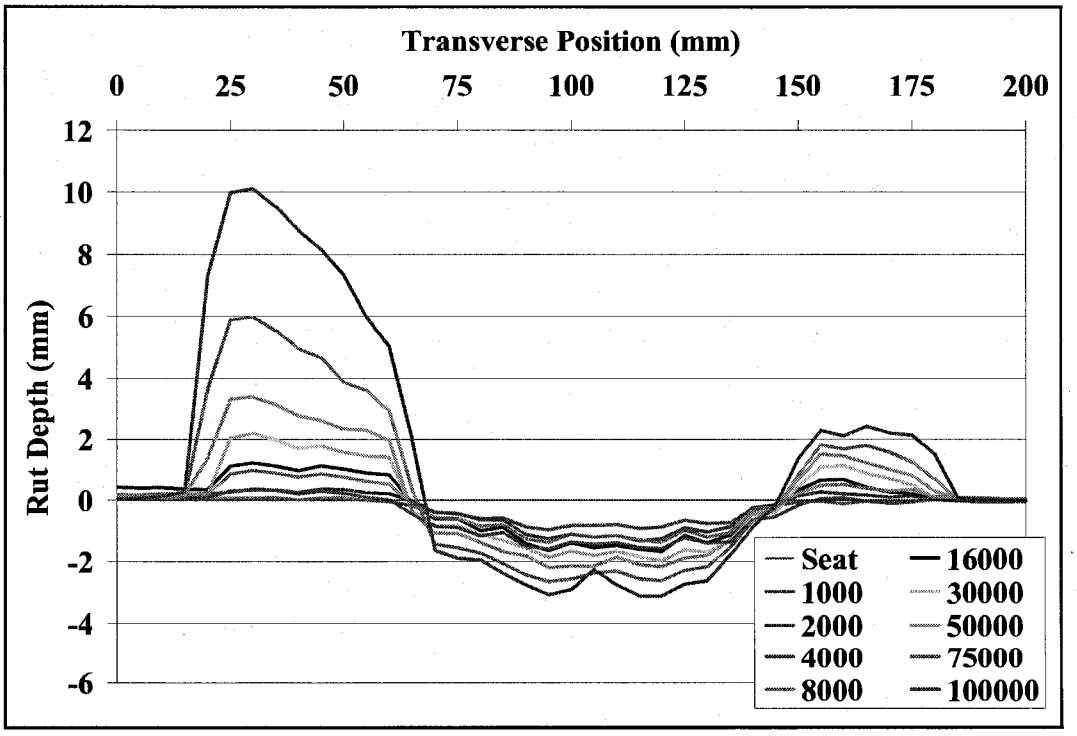

Figure A6.25: Cont 12.5 Brick 5 Transverse Profiles

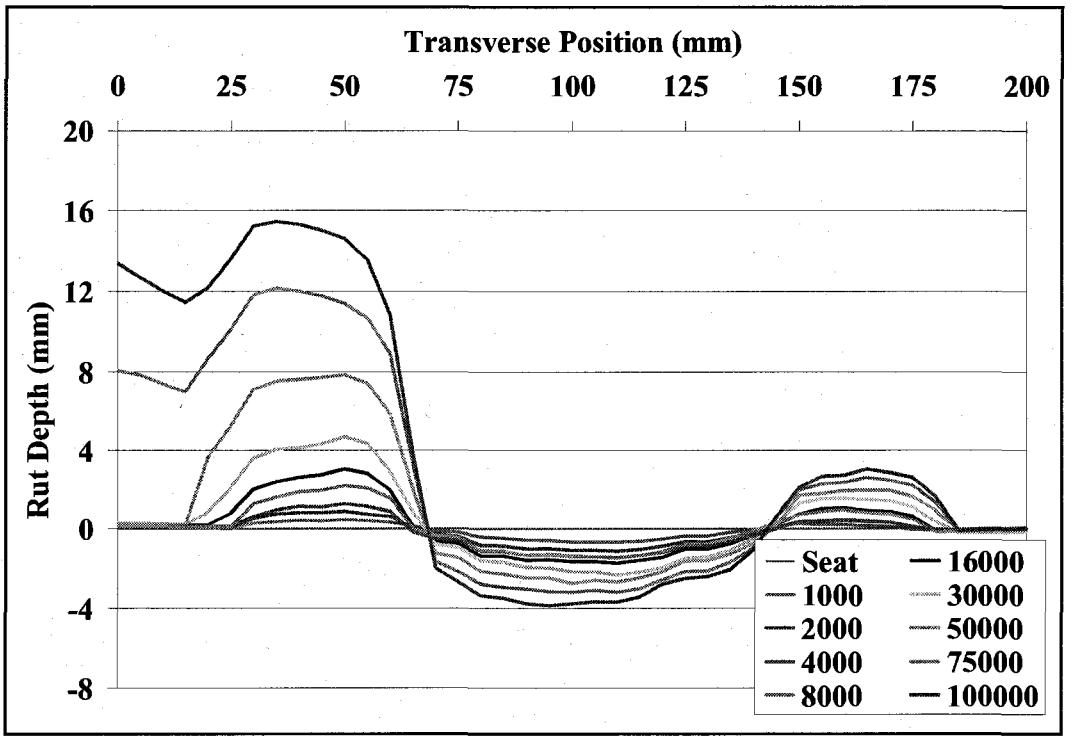

Figure A6.26: Cont 12.5 Brick 6 Transverse Profiles

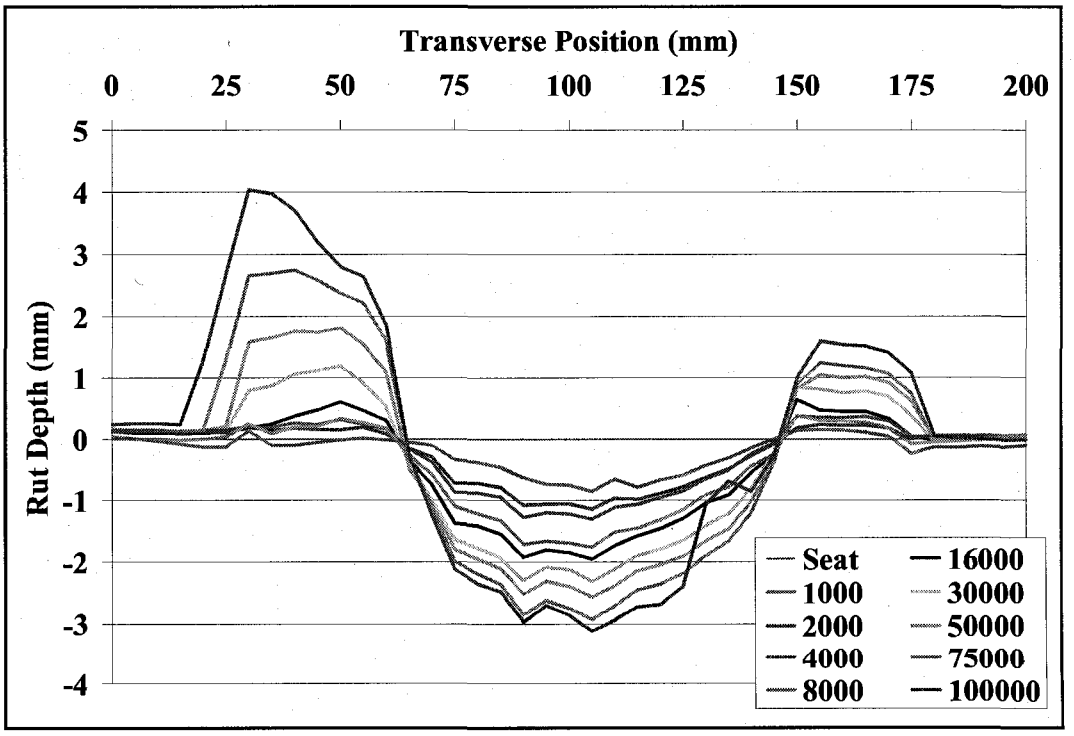

Figure A6.27: Cont 12.5 Brick 7 Transverse Profiles

Table A6.7: Cont 12.5 Avg Rut Depth from Base Line

Brick	Long Pos	Thousands of Loading Cycles								
		1	2	4	8	16	30	50	75	100
1	157.5	0.97	1.74	2.18	2.49	2.84	3.43	3.93	4.53	5.15
2	262.5	0.64	0.86	1.39	1.32	1.59	2.19	2.96	3.09	3.48
3	367.5	0.11	0.05	0.32	0.26	0.32	0.73	1.16	1.32	1.06*
4	472.5	0.60	0.87	1.10	1.08	1.21	1.50	1.77	2.14	2.20*
5	577.5	0.79	1.06	1.38	1.14	1.38	1.65	1.92	2.33	2.69
6	682.5	0.52	0.91	1.20	1.18	1.44	1.88	2.28	2.81	3.32
7	787.5	0.63	0.92	1.04	1.43	1.60	1.94	2.18	2.48	2.57
Avg		0.61	0.91	1.23	1.27	1.48	1.90	2.31	2.67	2.92

* Bricks 3 and 4 used a modified range for the average rut at 100,000 cycles

Table A6.8: Cont 12.5 Max Rut Depth from Base Line

Brick	Long Pos	Thousands of Loading Cycles								
		1	2	4	8	16	30	50	75	100
1	157.5	1.14	2.01	2.47	2.80	3.13	3.86	4.41	5.14	5.80
2	262.5	0.80	1.02	1.63	1.56	1.88	2.56	3.57	3.74	4.25
3	367.5	0.30	0.34	0.61	0.58	0.72	1.14	1.56	1.85	2.18
4	472.5	0.81	1.10	1.33	1.43	1.48	1.77	2.12	2.61	2.87
5	577.5	0.96	1.33	1.59	1.38	1.67	1.99	2.19	2.63	3.11
6	682.5	0.66	1.10	1.42	1.45	1.71	2.29	2.71	3.17	3.84
7	787.5	0.85	1.14	1.30	1.76	1.96	2.32	2.57	2.93	3.12
Avg		0.79	1.15	1.48	1.57	1.79	2.27	2.73	3.15	3.60

Table A6.9: Cont 12.5 Max Rut Depth from Max Heave

Brick	Long Pos	Thousands of Loading Cycles								
		1	2	4	8	16	30	50	75	100
1	157.5	1.69	2.53	2.98	3.42	3.77	4.76	6.11	8.41	10.54
2	262.5	1.36	2.13	2.95	3.59	4.73	6.81	10.12	13.33	16.38
3	367.5	0.94	1.71	2.09	2.61	3.46	5.06	6.48	8.25	10.03
4	472.5	1.04	1.63	1.98	2.34	2.91	4.46	5.85	7.45	9.09
5	577.5	1.04	1.70	1.95	2.37	2.89	4.17	5.57	8.60	13.21
6	682.5	1.12	2.02	2.69	3.64	4.75	6.99	10.55	15.32	19.30
7	787.5	1.00	1.37	1.68	2.14	2.60	3.51	4.37	5.68	7.15
Avg		1.17	1.87	2.33	2.87	3.59	5.11	7.01	9.58	12.24

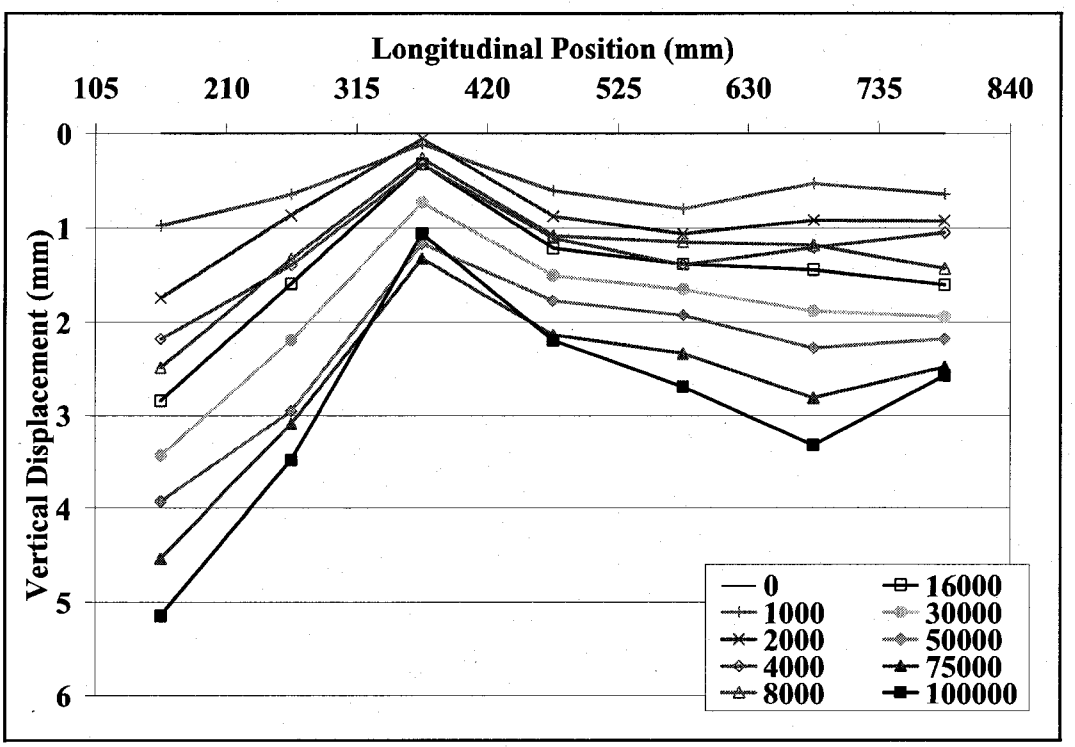

Figure A6.28: Cont 12.5 Avg Rut from Base Line Longitudinal Profiles

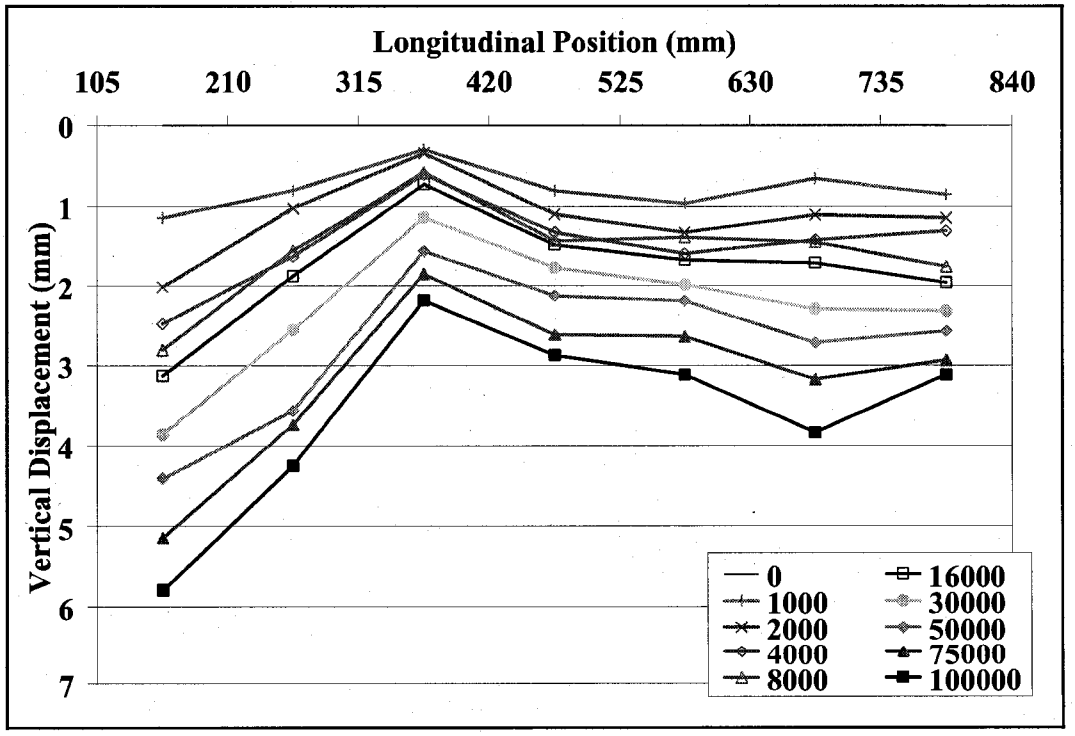

Figure A6.29: Cont 12.5 Max Rut from Base Line Longitudinal Profiles

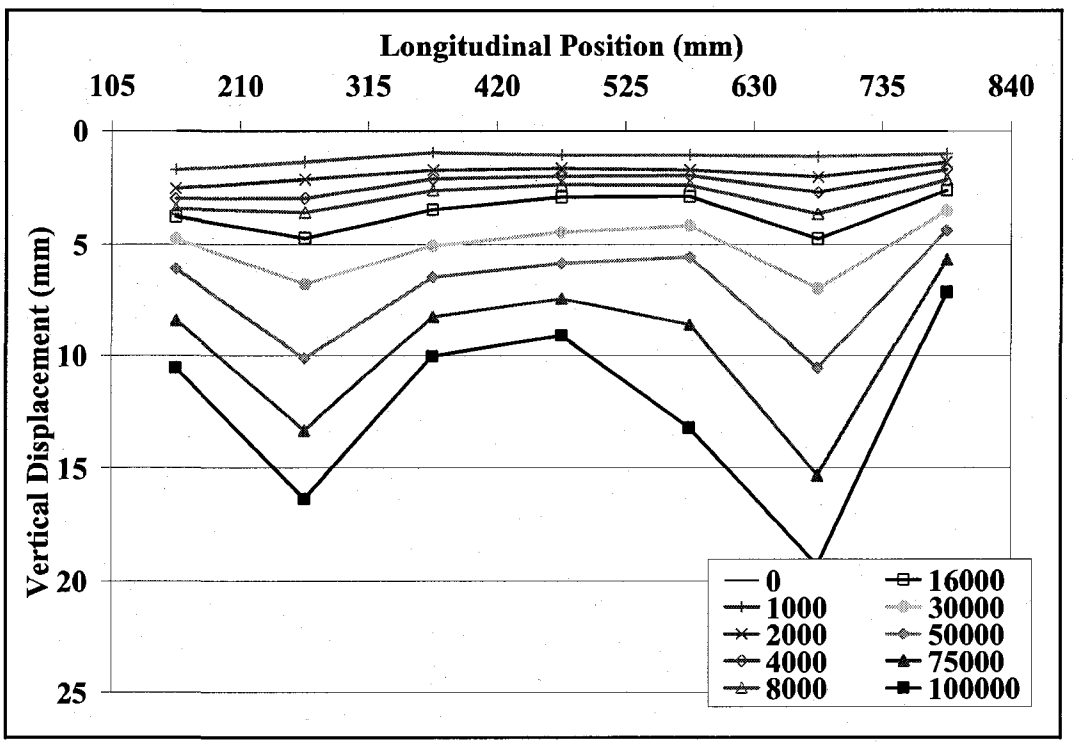

Figure A6.30: Cont 12.5 Max Rut from Max Heave Longitudinal Profiles

Cont 19

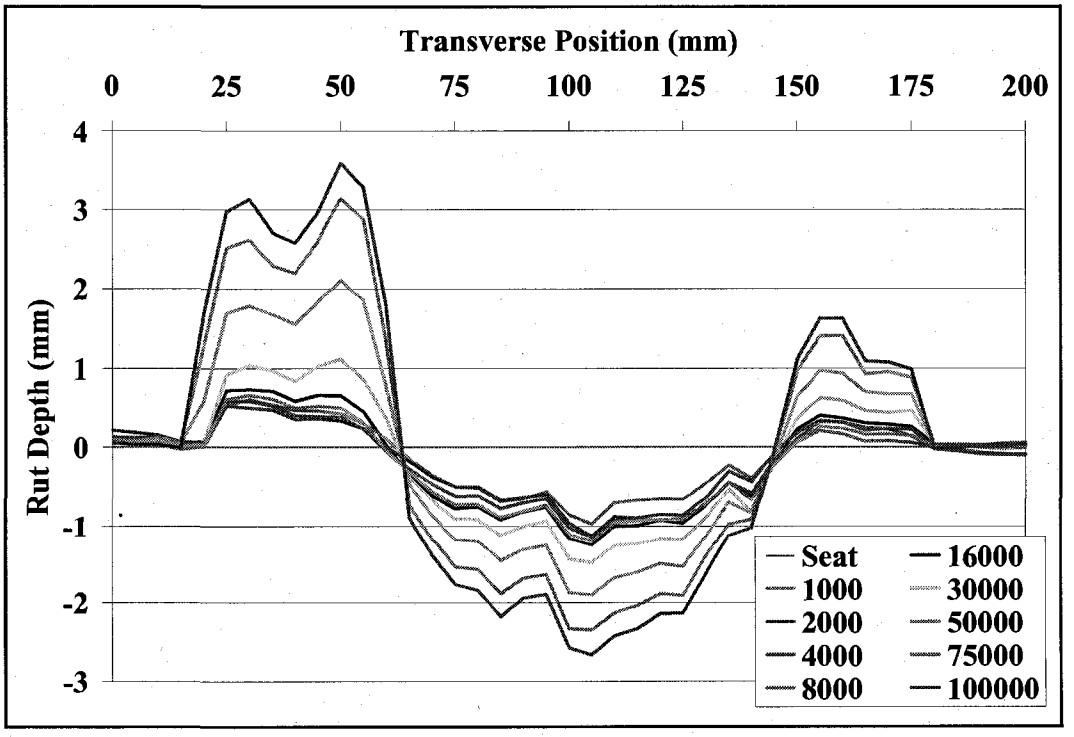

Figure A6.31: Cont 19 Brick 1 Transverse Profiles

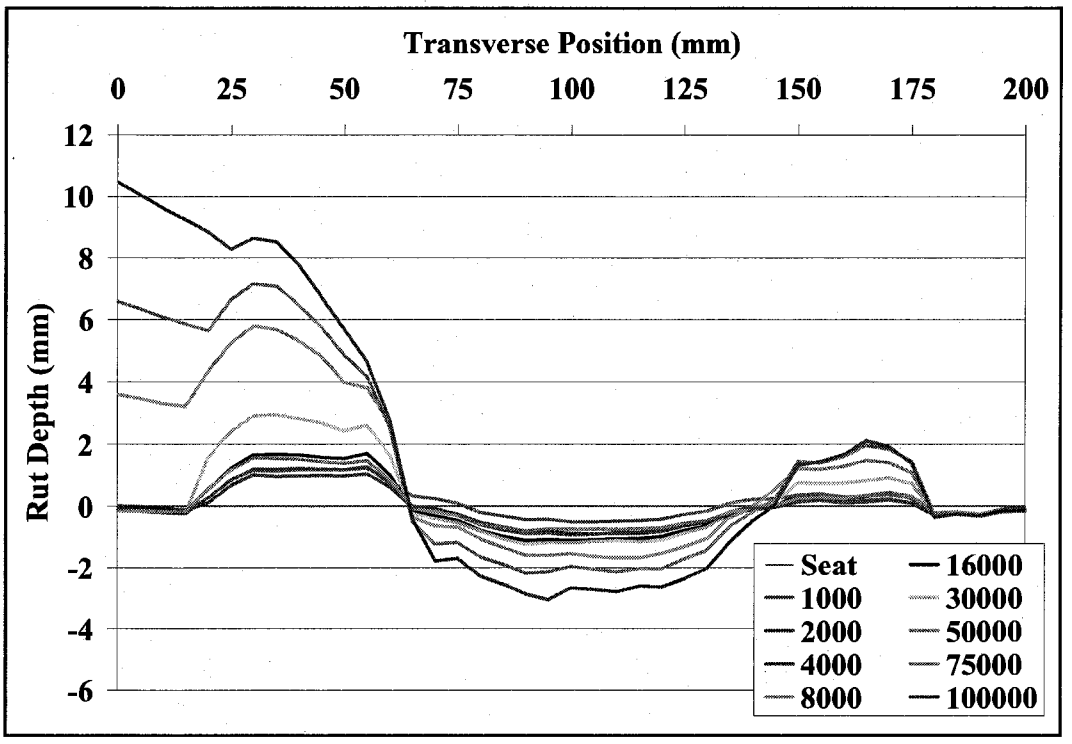

Figure A6.32: Cont 19 Brick 2 Transverse Profiles

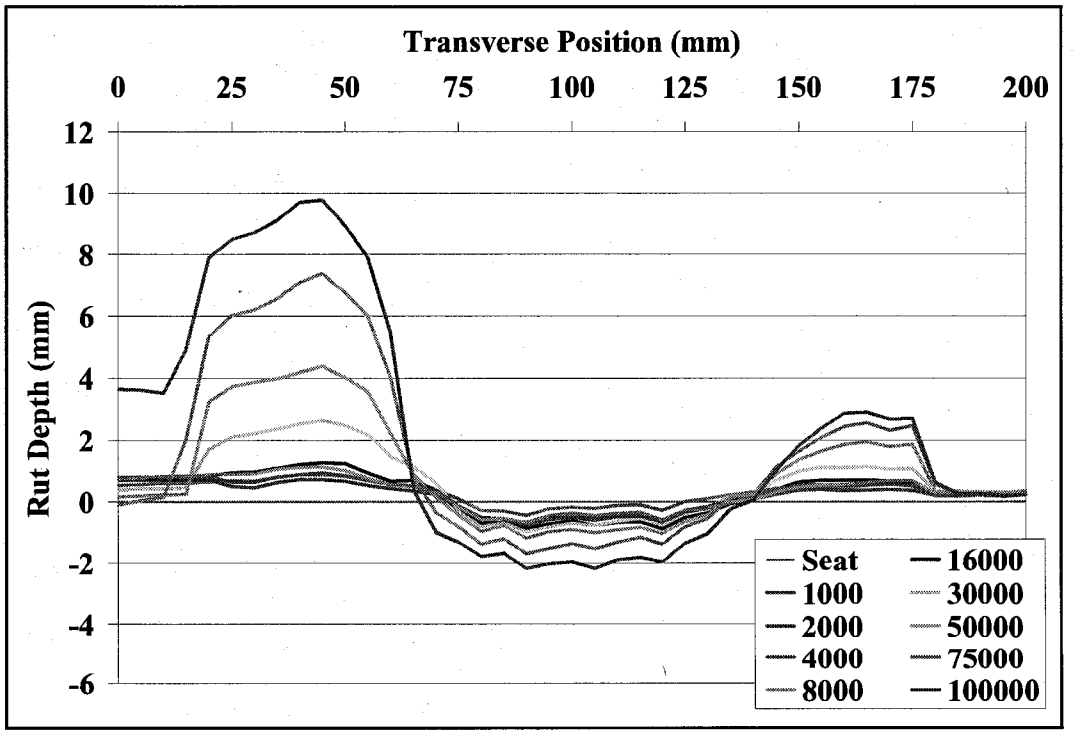

Figure A6.33: Cont 19 Brick 3 Transverse Profiles

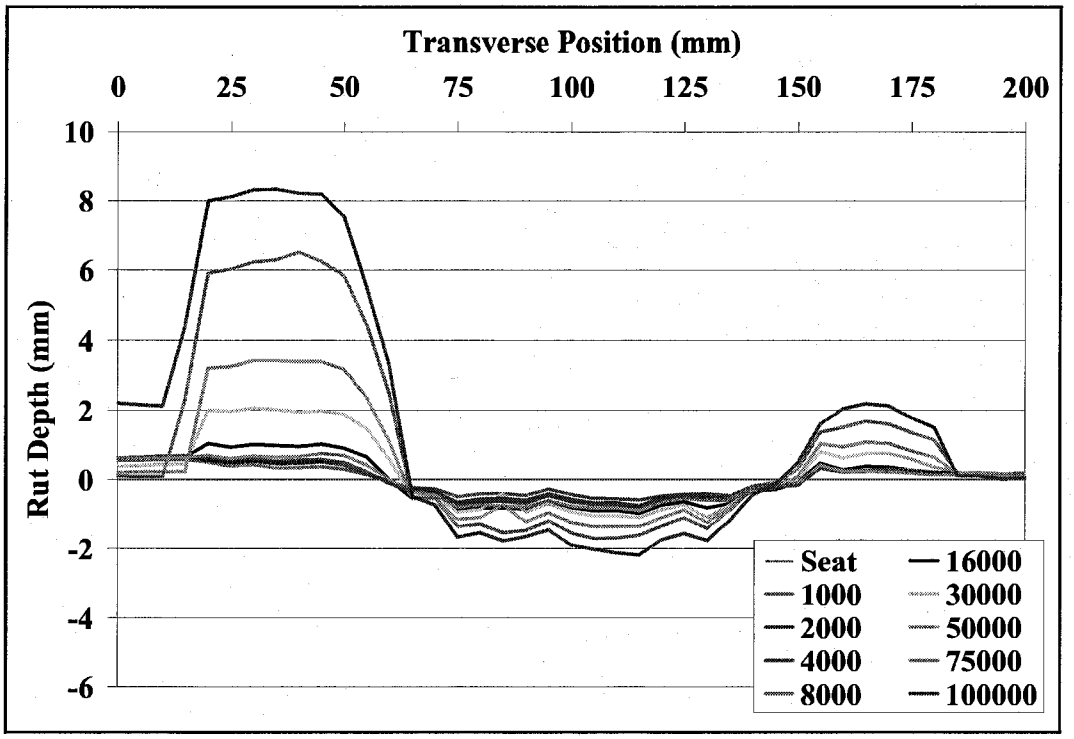

Figure A6.34: Cont 19 Brick 4 Transverse Profiles

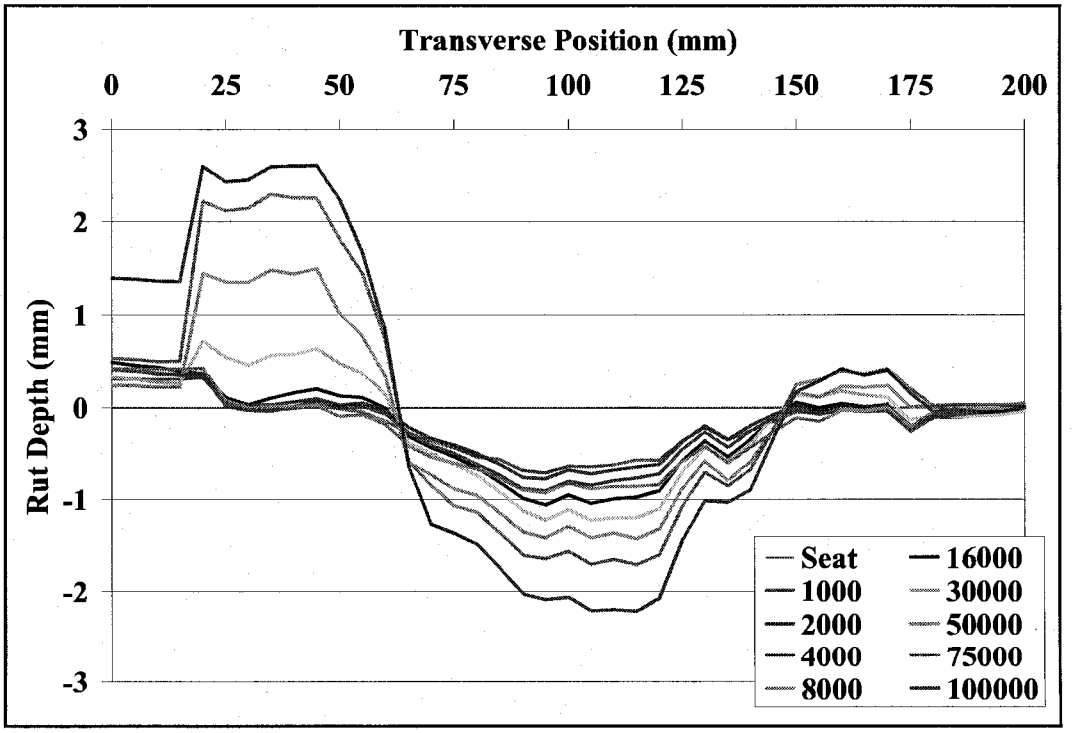

Figure A6.35: Cont 19 Brick 5 Transverse Profiles

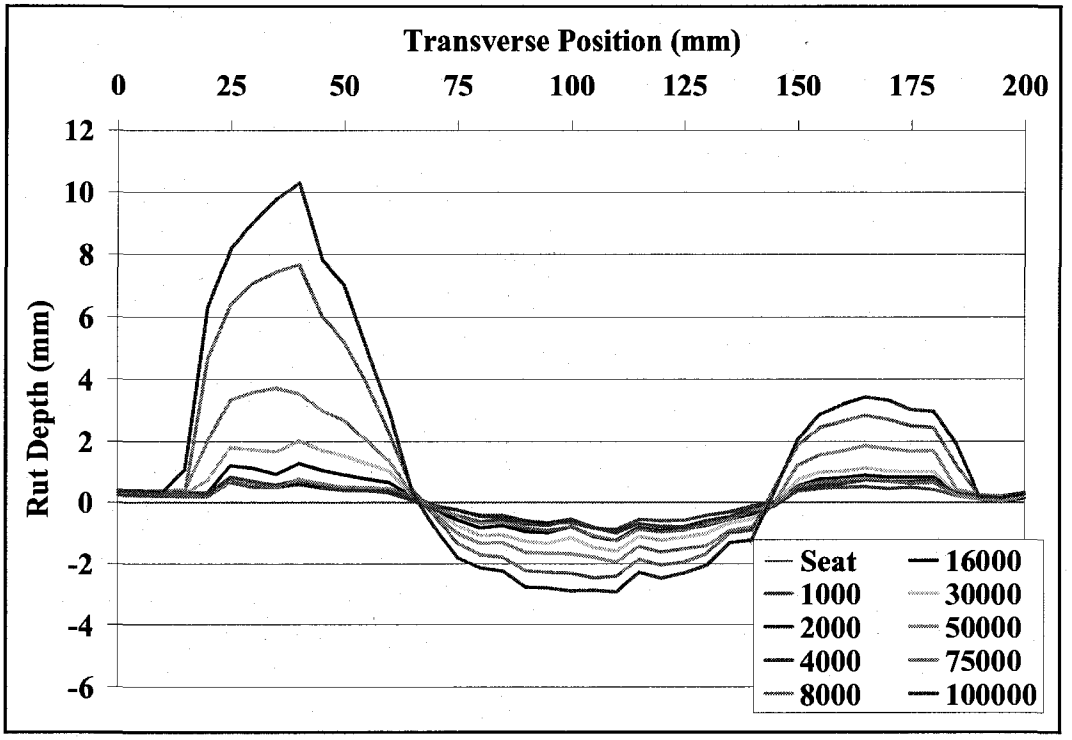

Figure A6.36: Cont 19 Brick 6 Transverse Profiles

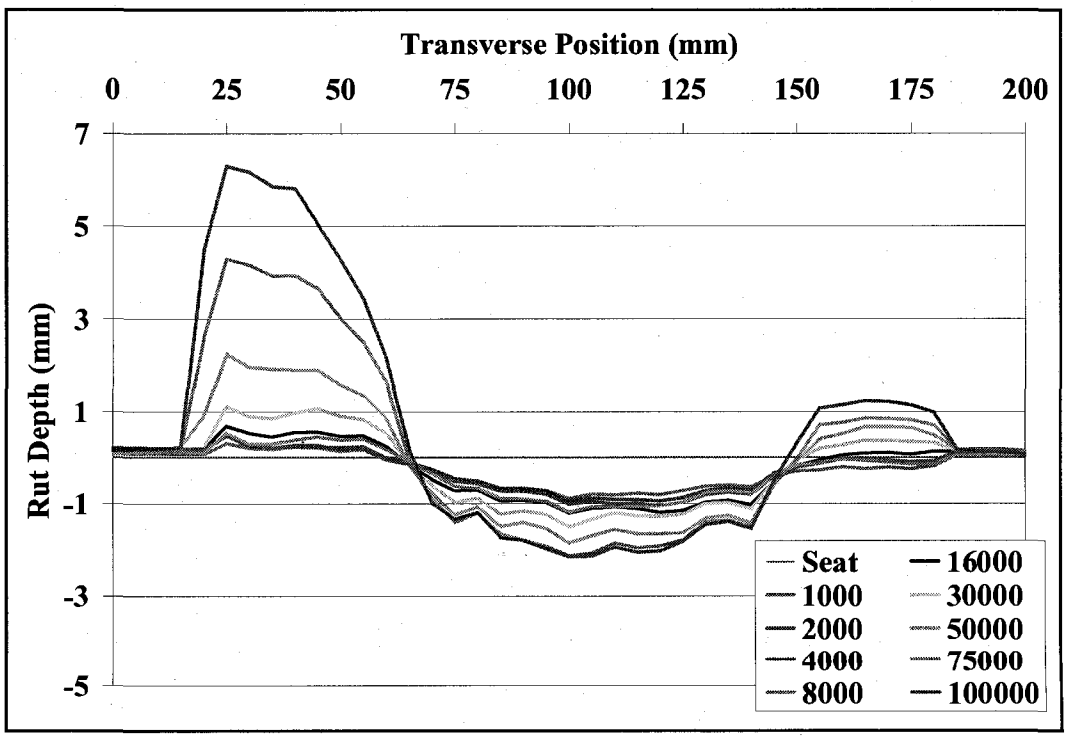

Figure A6.37: Cont 19 Brick 7 Transverse Profiles

Table A6.10: Cont 19 Avg Rut Depth from Base Line

Brick	Long Pos	Thousands of Loading Cycles								
		1	2	4	8	16	30	50	75	100
1	157.5	0.67	0.78	0.84	0.90	0.93	1.15	1.50	1.90	2.16
2	262.5	0.37	0.76	0.78	0.68	0.97	1.05	1.45	1.92	2.59
3	367.5	0.18	0.52	0.48	0.44	0.67	0.66	0.87	1.26	1.81
4	472.5	0.45	0.56	0.64	0.71	0.80	0.87	1.13	1.44	1.78
5	577.5	0.56	0.60	0.71	0.78	0.85	1.00	1.20	1.44	1.87
6	682.5	0.62	0.66	0.73	0.88	0.92	1.22	1.57	2.06	2.52
7	787.5	0.74	0.80	0.87	0.96	1.03	1.21	1.54	1.80	1.85
Avg		0.51	0.67	0.72	0.76	0.88	1.02	1.32	1.69	2.08

Table A6.11: Cont 19 Max Rut Depth from Base Line

Brick	Long Pos	Thousands of Loading Cycles								
		1	2	4	8	16	30	50	75	100
1	157.5	0.97	1.13	1.15	1.21	1.26	1.49	1.90	2.35	2.67
2	262.5	0.50	0.90	0.93	0.79	1.12	1.23	1.67	2.18	3.04
3	367.5	0.45	0.78	0.75	0.66	0.88	0.97	1.18	1.69	2.18
4	472.5	0.59	0.74	0.84	0.89	0.96	1.08	1.35	1.69	2.18
5	577.5	0.71	0.78	0.91	0.93	1.06	1.23	1.43	1.72	2.22
6	682.5	0.89	0.98	1.00	1.24	1.24	1.59	1.94	2.46	2.91
7	787.5	0.89	0.95	1.04	1.19	1.21	1.51	1.86	2.14	2.15
Avg		0.71	0.89	0.95	0.99	1.10	1.30	1.62	2.03	2.48

Table A6.12: Cont 19 Max Rut Depth from Max Heave

Brick	Long Pos	Thousands of Loading Cycles								
		1	2	4	8	16	30	50	75	100
1	157.5	1.58	1.67	1.74	1.87	2.00	2.60	4.00	5.50	6.25
2	262.5	1.72	1.95	2.19	2.36	2.82	4.17	7.46	9.35	13.50
3	367.5	1.32	1.49	1.67	1.78	2.12	3.61	5.56	9.06	11.96
4	472.5	1.17	1.41	1.53	1.64	2.00	3.13	4.77	8.21	10.52
5	577.5	1.04	1.18	1.32	1.35	1.55	1.94	2.92	4.01	4.82
6	682.5	1.56	1.72	1.81	2.04	2.53	3.61	5.66	10.14	13.22
7	787.5	1.20	1.42	1.51	1.72	1.89	2.62	4.09	6.44	8.44
Avg		1.37	1.55	1.68	1.82	2.13	3.10	4.92	7.53	9.82

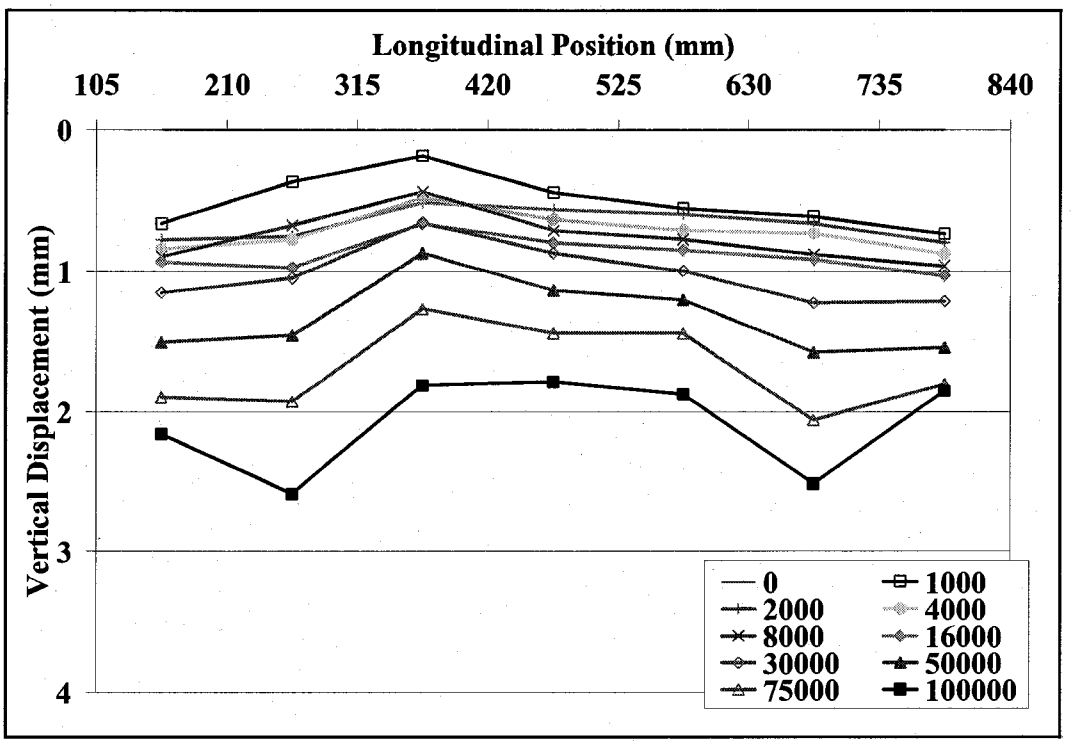

Figure A6.38: Cont 19 Avg Rut from Base Line Longitudinal Profiles

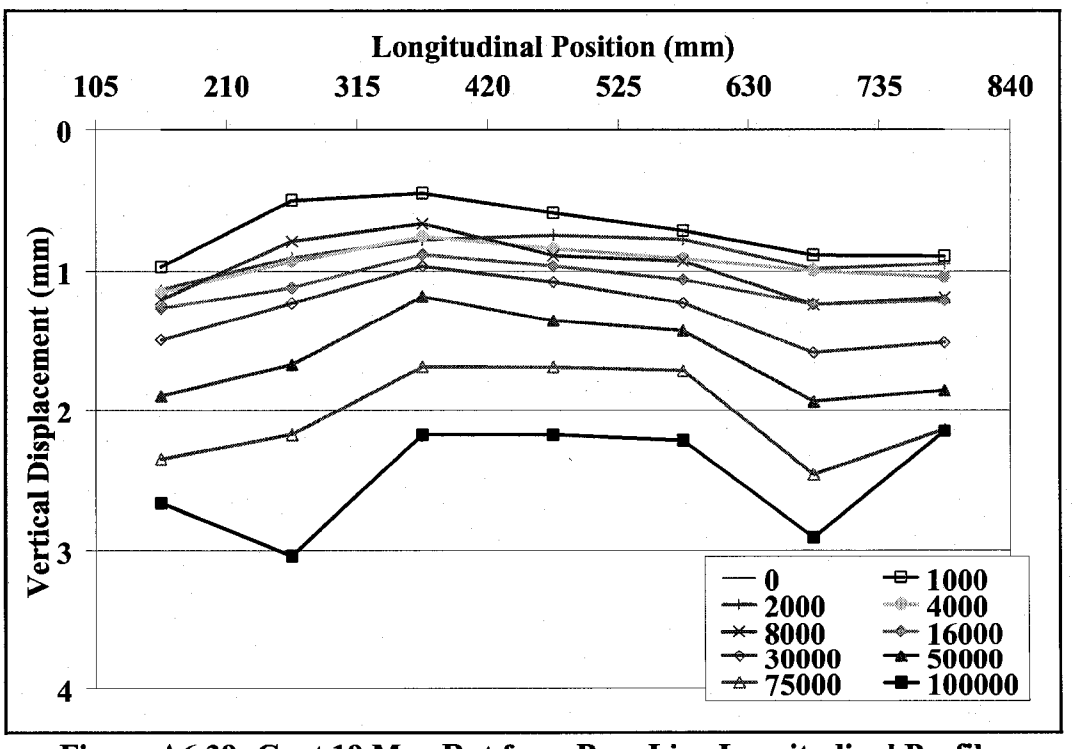

Figure A6.39: Cont 19 Max Rut from Base Line Longitudinal Profiles

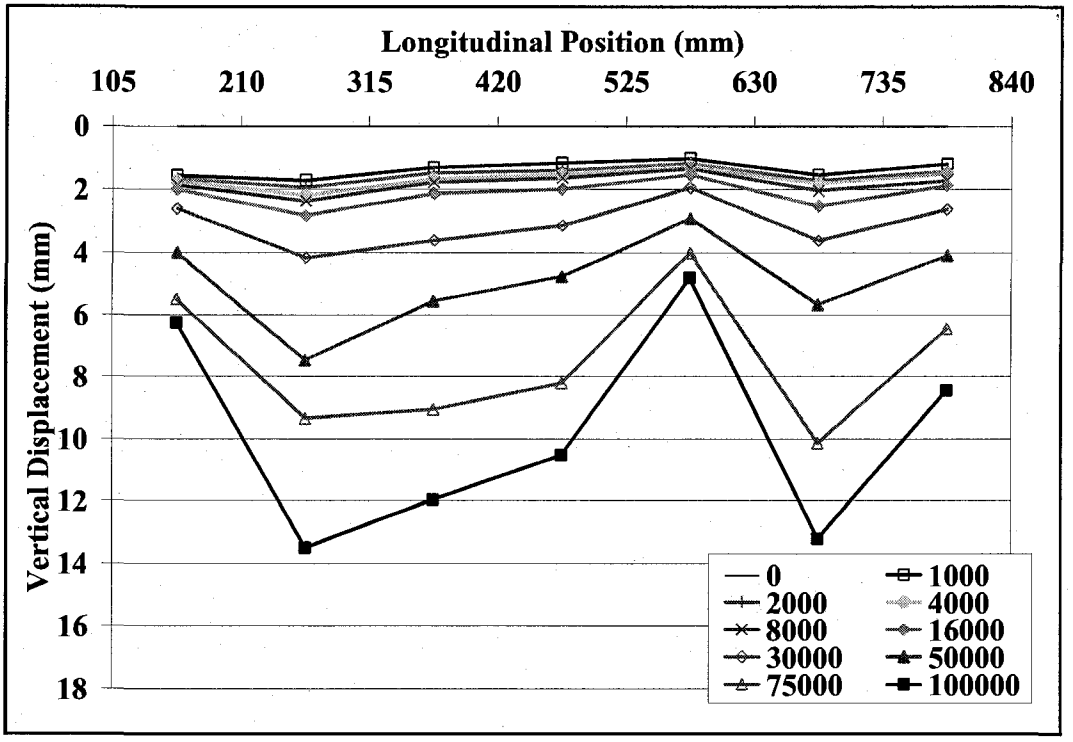

Figure A6.40: Cont 19 Max Rut from Max Heave Longitudinal Profiles

Farm

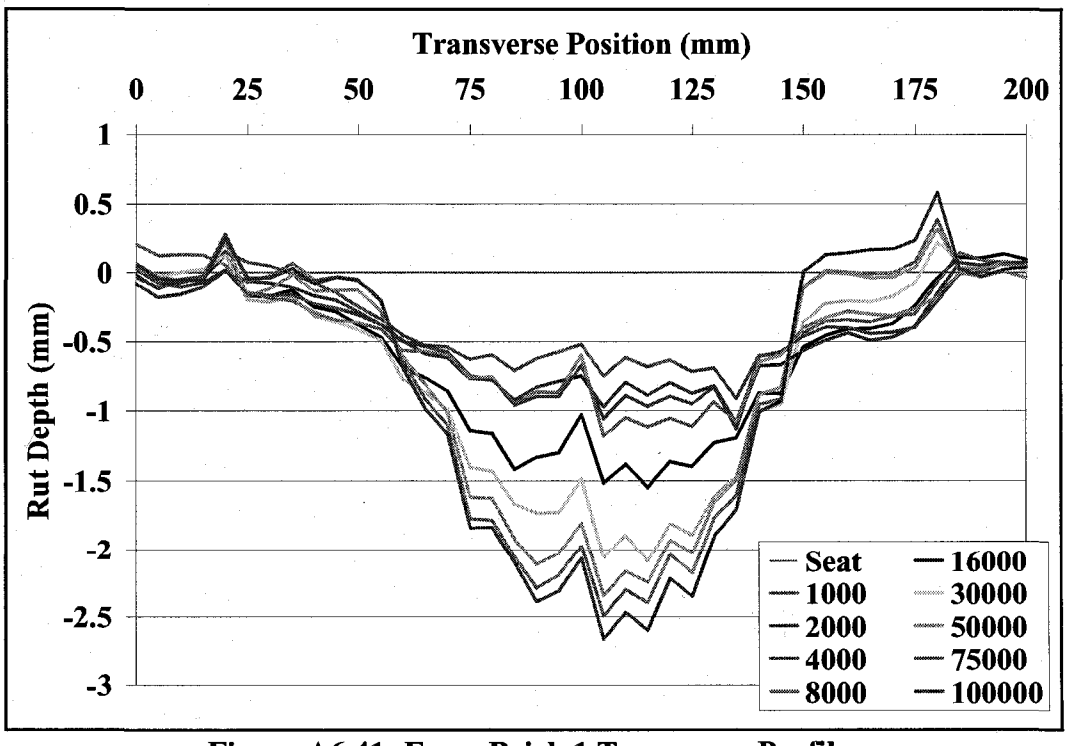

Figure A6.41: Farm Brick 1 Transverse Profiles

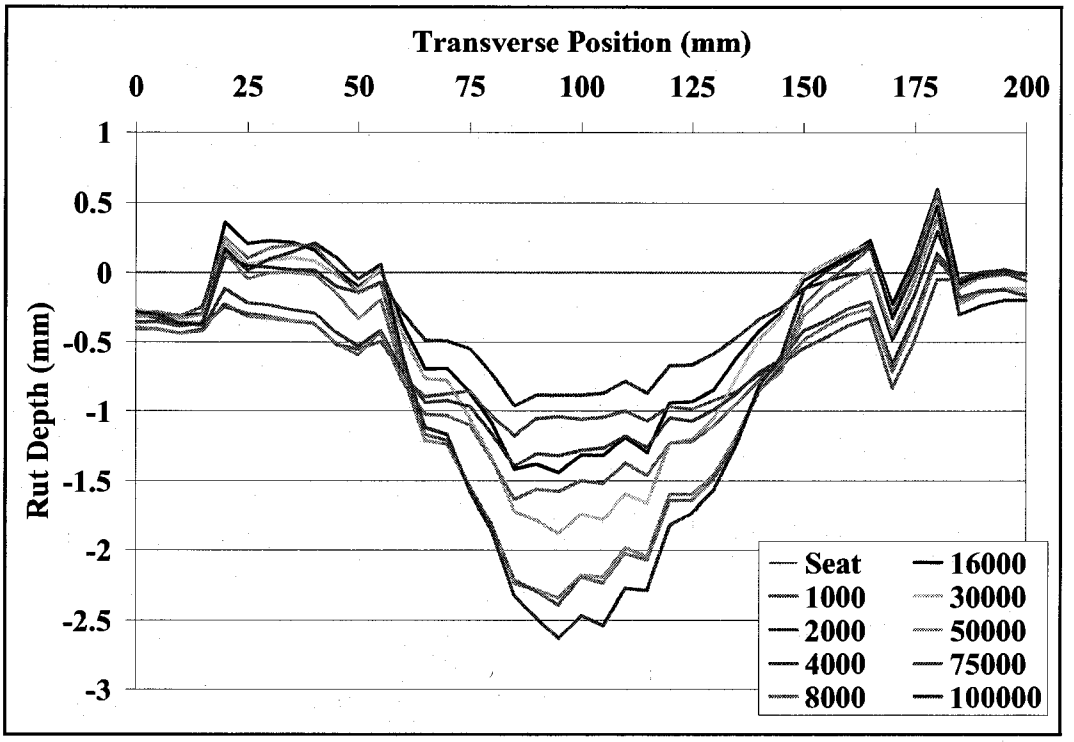

Figure A6.42: Farm Brick 2 Transverse Profiles

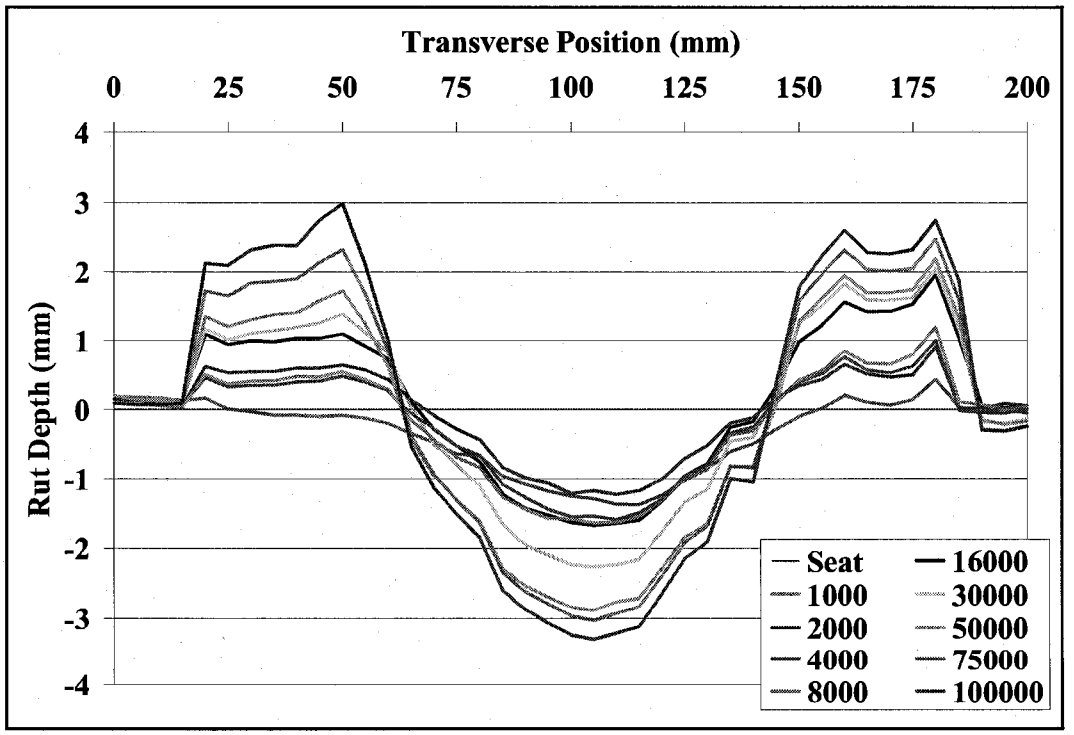

Figure A6.43: Farm Brick 3 Transverse Profiles

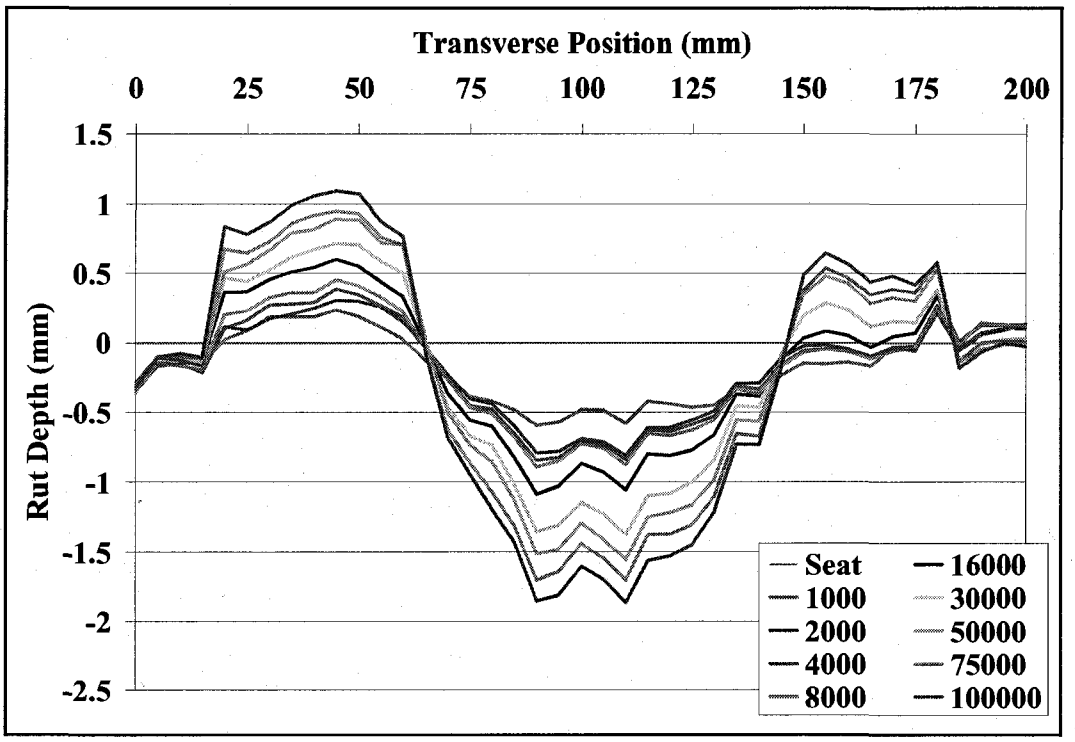

Figure A6.44: Farm Brick 4 Transverse Profiles

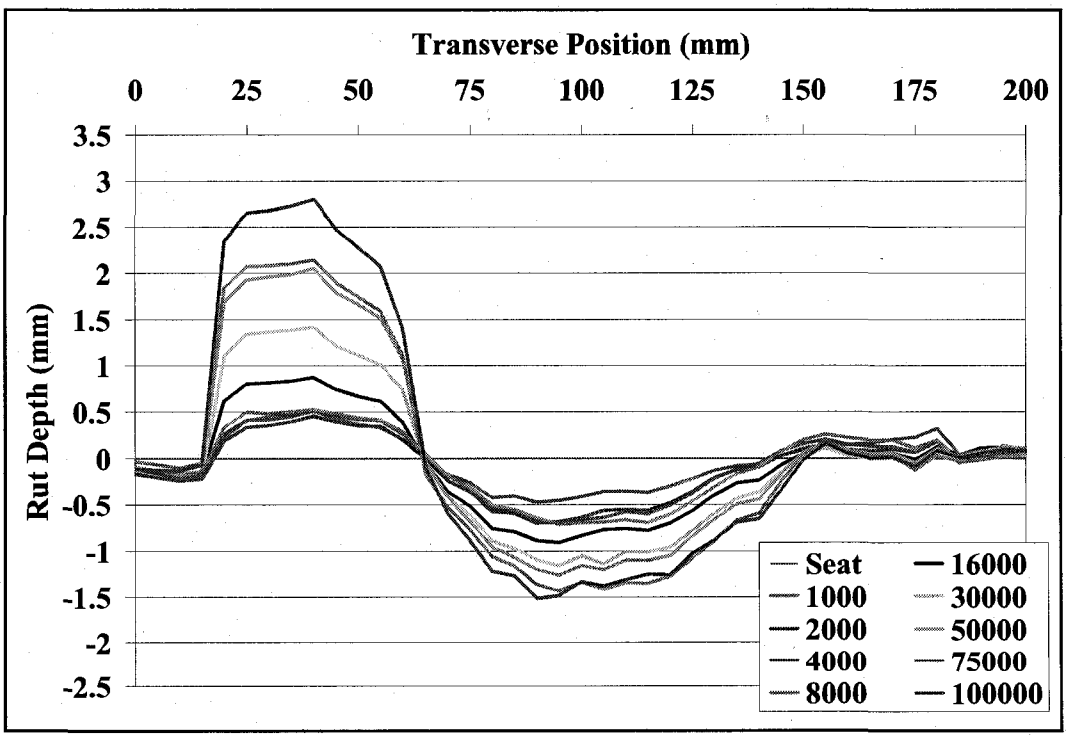

Figure A6.45: Farm Brick 5 Transverse Profiles

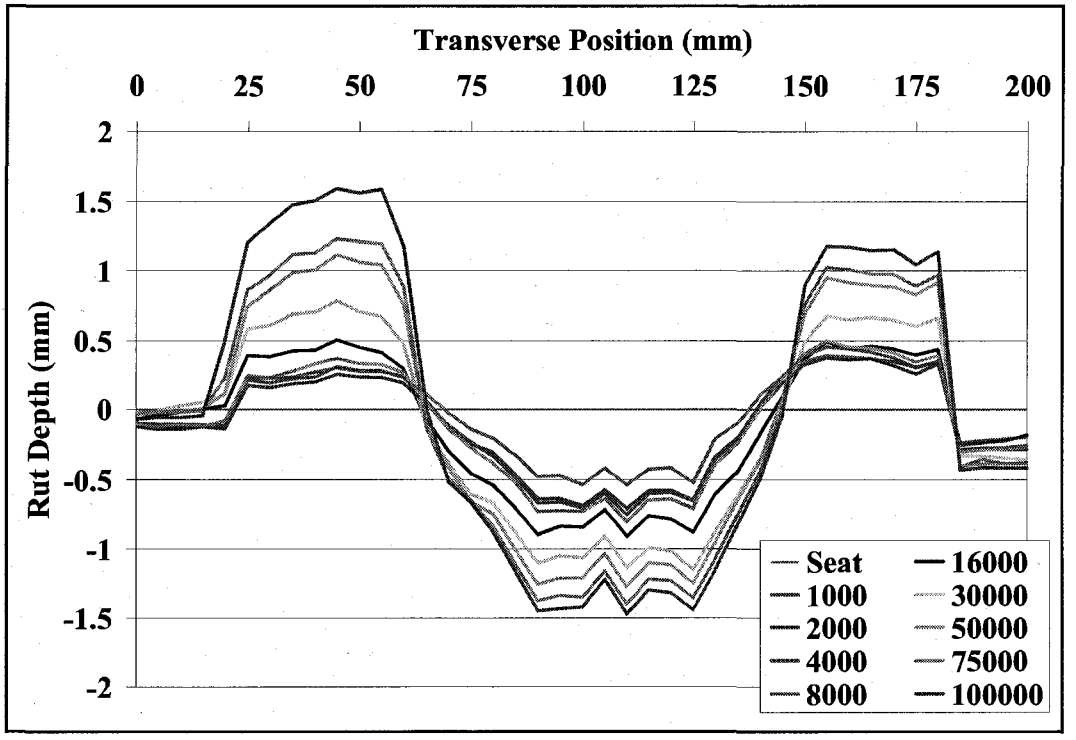

Figure A6.46: Farm Brick 6 Transverse Profiles

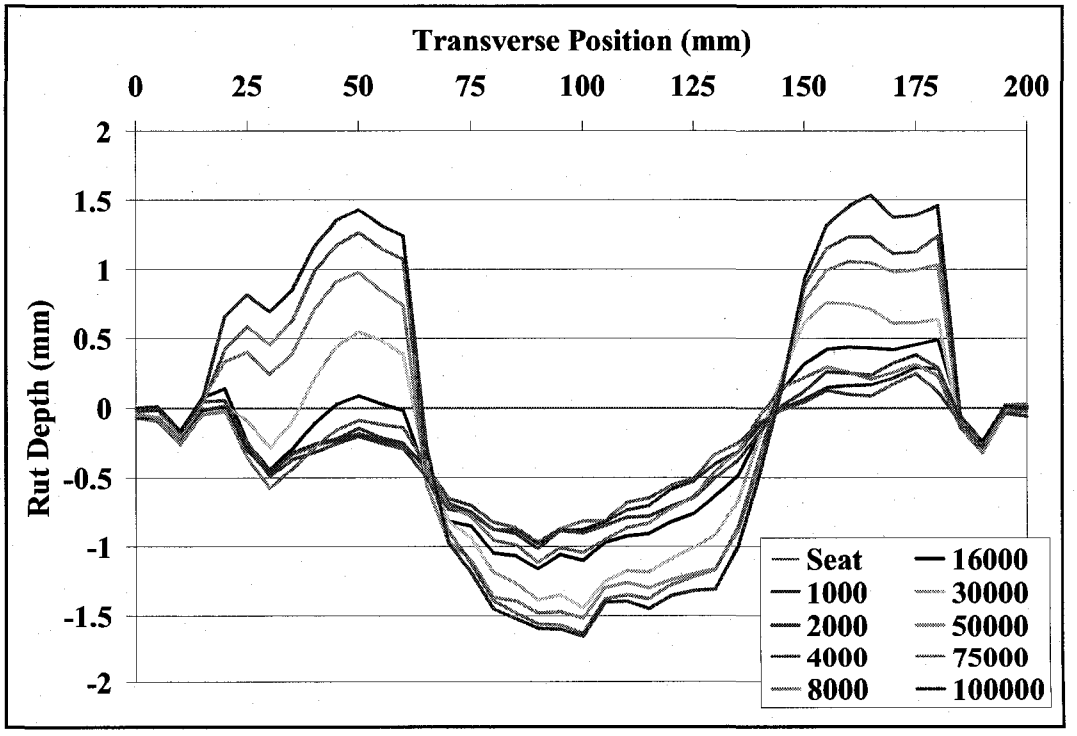

Figure A6.47: Farm Brick 7 Transverse Profiles

Table A6.13: Farm Avg Rut Depth from Base Line

Brick	Long Pos	Thousands of Loading Cycles								
		1	2	4	8	16	30	50	75	100
1	157.5	0.64	0.83	0.89	0.95	1.33	1.76	1.99	2.13	2.27
2	262.5	1.03	0.80	1.21	1.41	1.20	1.54	1.98	2.00	2.18
3	367.5	1.12	0.94	1.25	1.34	1.32	1.81	2.37	2.47	2.72
4	472.5	0.49	0.65	0.68	0.71	0.86	1.11	1.26	1.41	1.57
5	577.5	0.36	0.54	0.55	0.59	0.74	0.97	1.05	1.24	1.26
6	682.5	0.41	0.56	0.58	0.63	0.77	0.98	1.10	1.22	1.29
7	787.5	0.72	0.76	0.80	0.87	0.95	1.21	1.34	1.40	1.46
Avg		0.68	0.73	0.85	0.93	1.02	1.34	1.58	1.70	1.82

Table A6.14: Farm Max Rut Depth from Base Line

Brick	Long Pos	Thousands of Loading Cycles								
		1	2	4	8	16	30	50	75	100
1	157.5	0.91	1.09	1.13	1.18	1.55	2.09	2.35	2.50	2.67
2	262.5	1.18	0.96	1.40	1.63	1.44	1.88	2.34	2.39	2.63
3	367.5	1.38	1.23	1.60	1.64	1.68	2.26	2.88	3.03	3.31
4	472.5	0.60	0.81	0.85	0.90	1.09	1.37	1.56	1.70	1.87
5	577.5	0.48	0.70	0.70	0.71	0.90	1.15	1.26	1.43	1.52
6	682.5	0.54	0.71	0.75	0.80	0.91	1.15	1.27	1.40	1.47
7	787.5	0.97	1.02	0.98	1.11	1.16	1.45	1.52	1.63	1.65
Avg		0.86	0.93	1.06	1.14	1.25	1.62	1.88	2.01	2.16

Table A6.15: Farm Max Rut Depth from Max Heave

Brick	Long Pos	Thousands of Loading Cycles								
		1	2	4	8	16	30	50	75	100
1	157.5	1.06	1.17	1.21	1.39	1.68	2.31	2.67	2.88	3.25
2	262.5	1.18	1.26	1.54	1.74	2.03	2.43	2.74	2.97	3.10
3	367.5	1.81	2.14	2.59	2.83	3.63	4.31	5.07	5.50	6.30
4	472.5	0.85	1.12	1.23	1.35	1.69	2.09	2.45	2.65	2.96
5	577.5	0.98	1.15	1.21	1.23	1.78	2.57	3.31	3.57	4.32
6	682.5	0.93	1.08	1.20	1.30	1.41	1.93	2.38	2.63	3.06
7	787.5	1.22	1.30	1.36	1.43	1.65	2.21	2.58	2.90	3.19
Avg		1.15	1.32	1.48	1.61	1.98	2.55	3.03	3.30	3.74

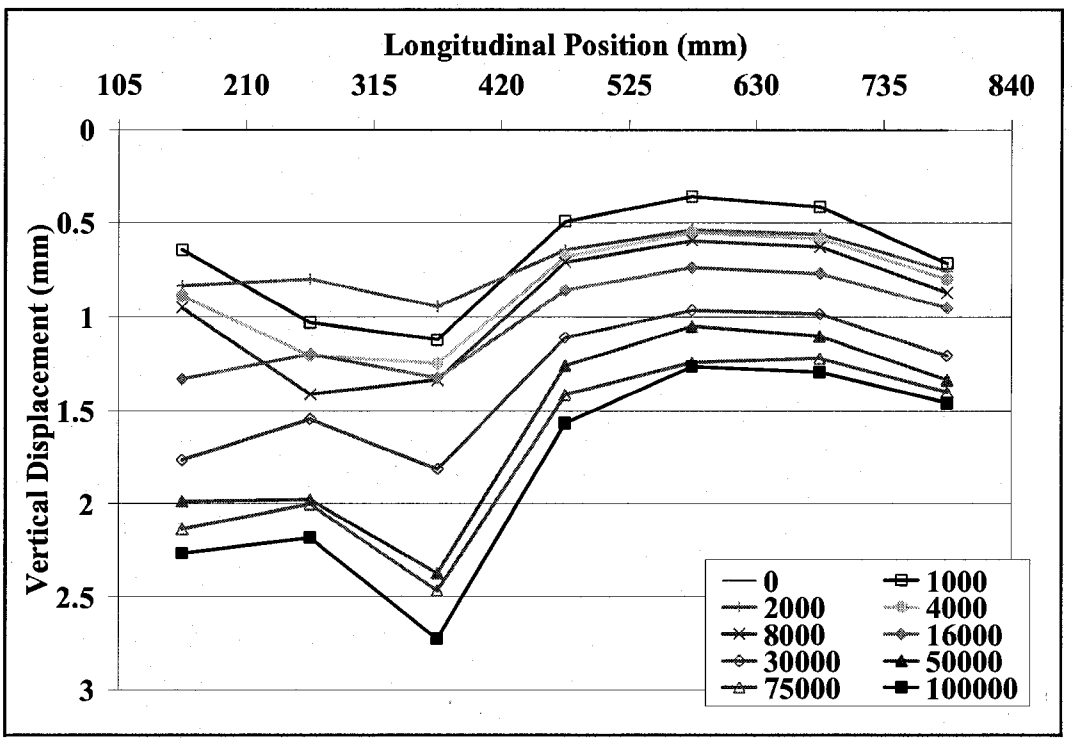

Figure A6.48: Farm Avg Rut from Base Line Longitudinal Profiles

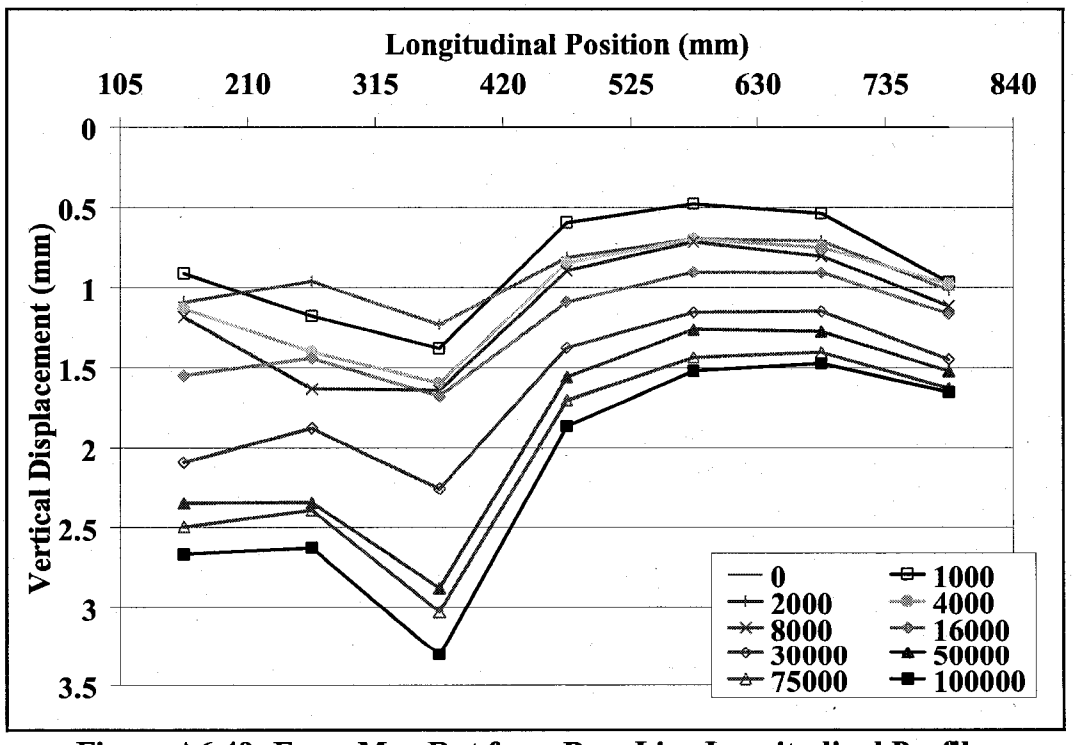

Figure A6.49: Farm Max Rut from Base Line Longitudinal Profiles

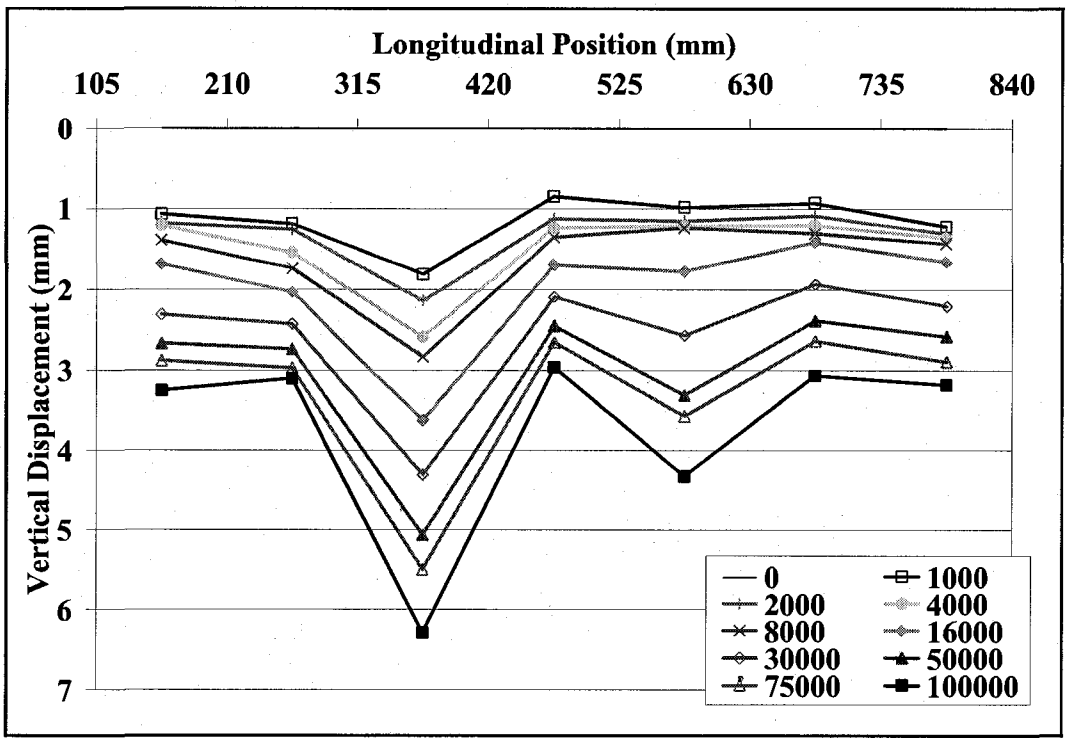

Figure A6.50: Farm Max Rut from Max Heave Longitudinal Profiles

Hook

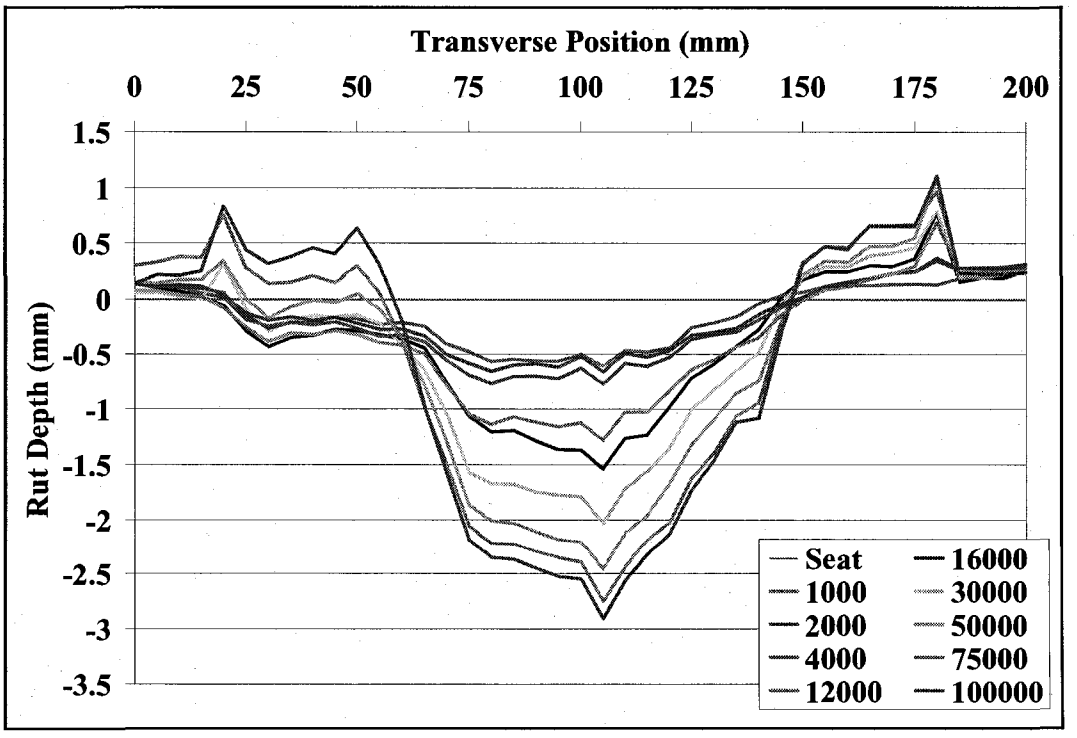

Figure A6.51: Hook Brick 1 Transverse Profiles

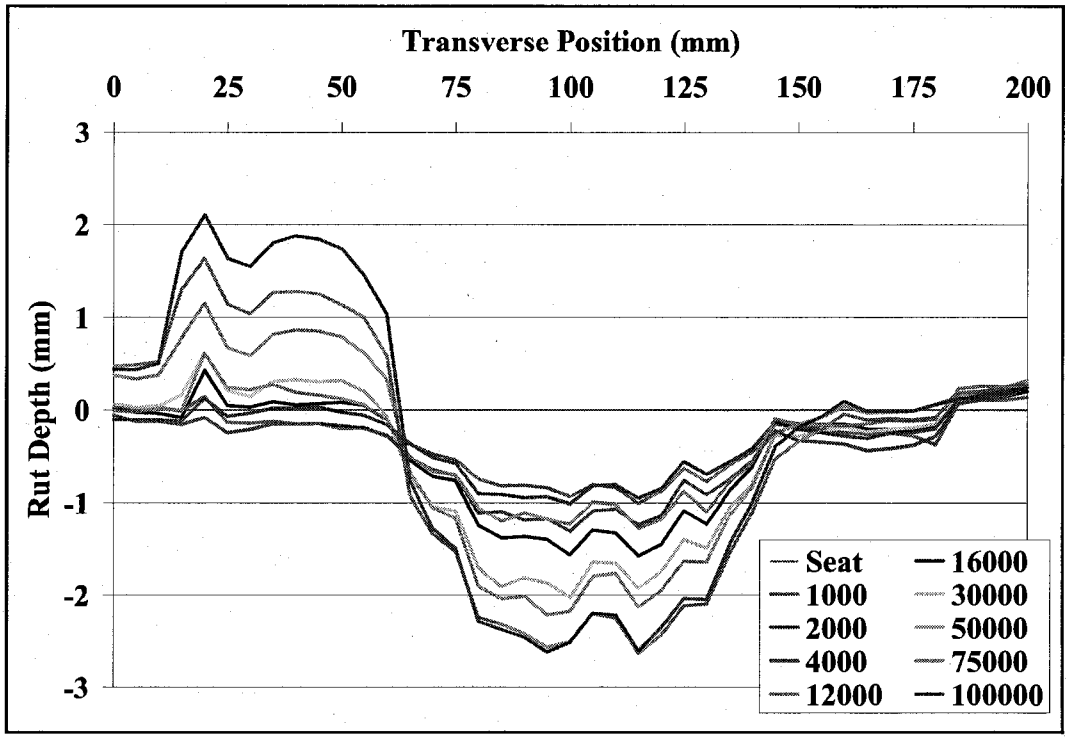

Figure A6.52: Hook Brick 2 Transverse Profiles

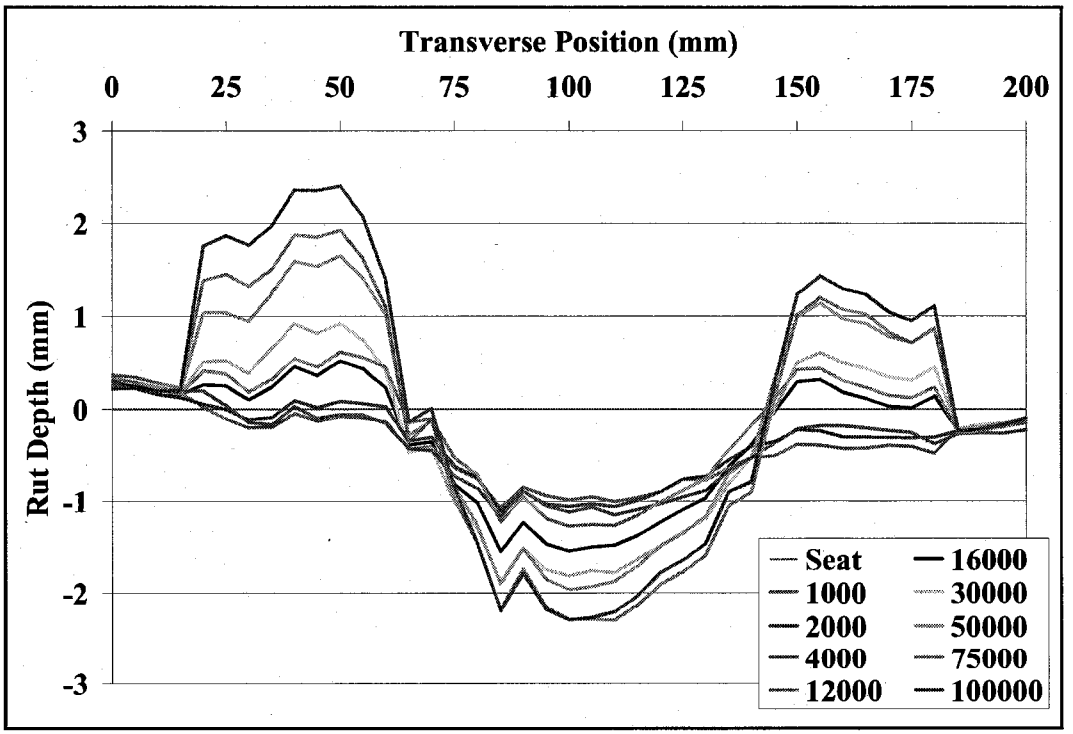

Figure A6.53: Hook Brick 3 Transverse Profiles

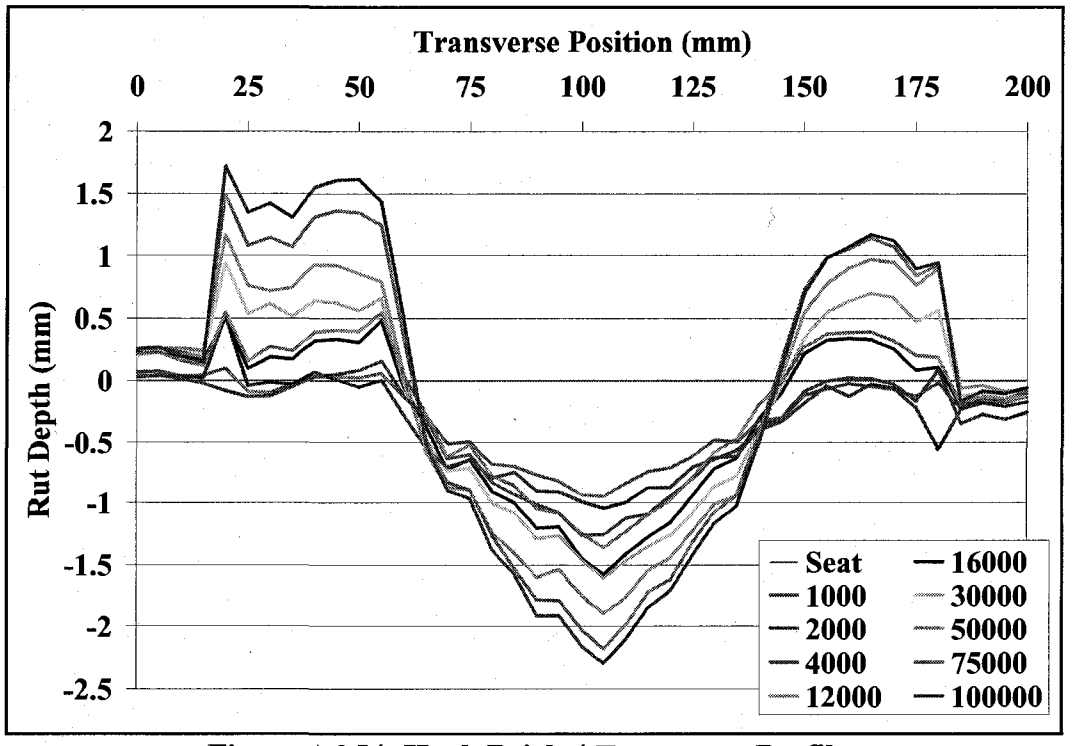

Figure A6.54: Hook Brick 4 Transverse Profiles

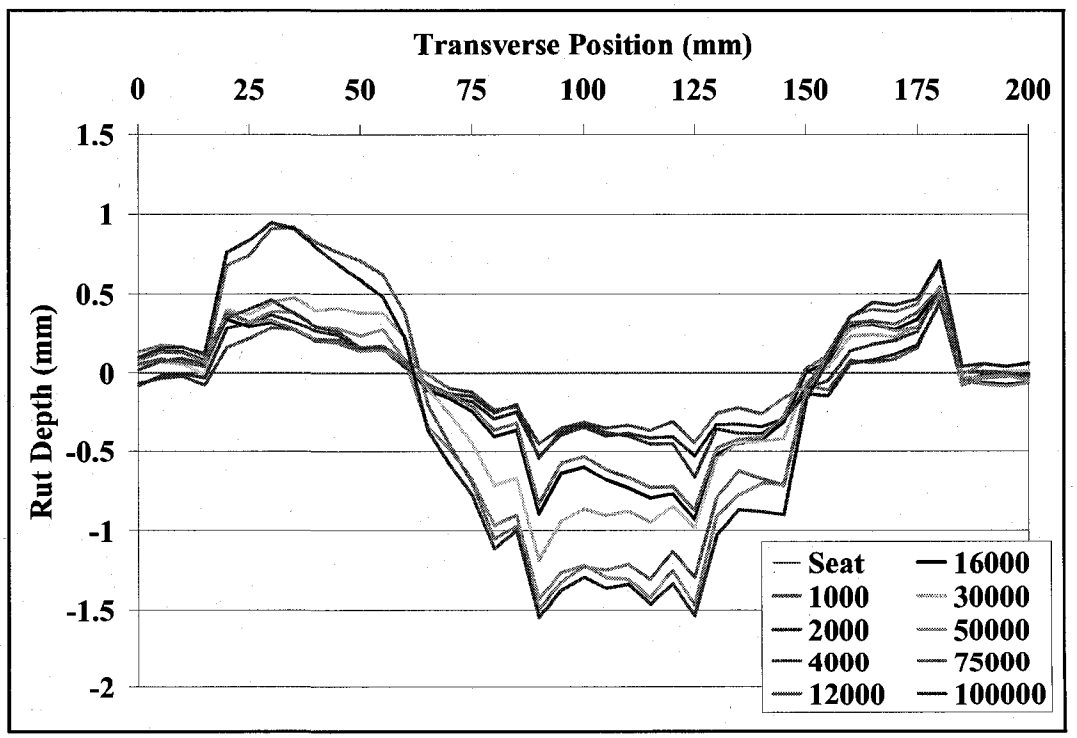

Figure A6.55: Hook Brick 5 Transverse Profiles

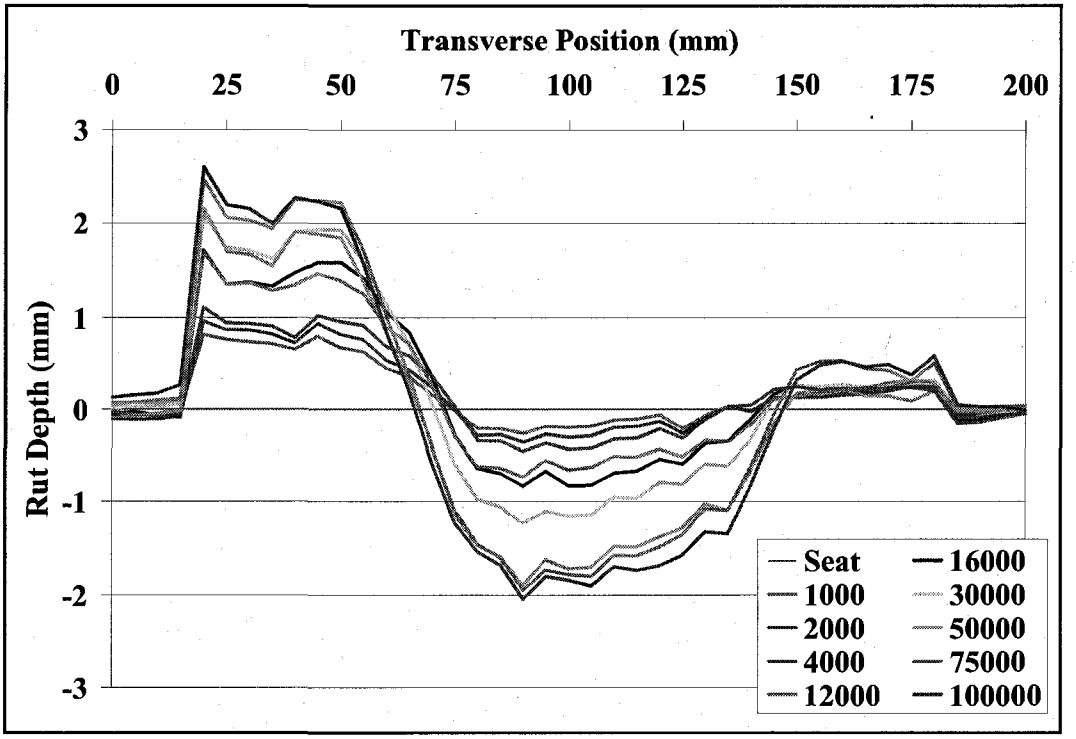

Figure A6.56: Hook Brick 6 Transverse Profiles

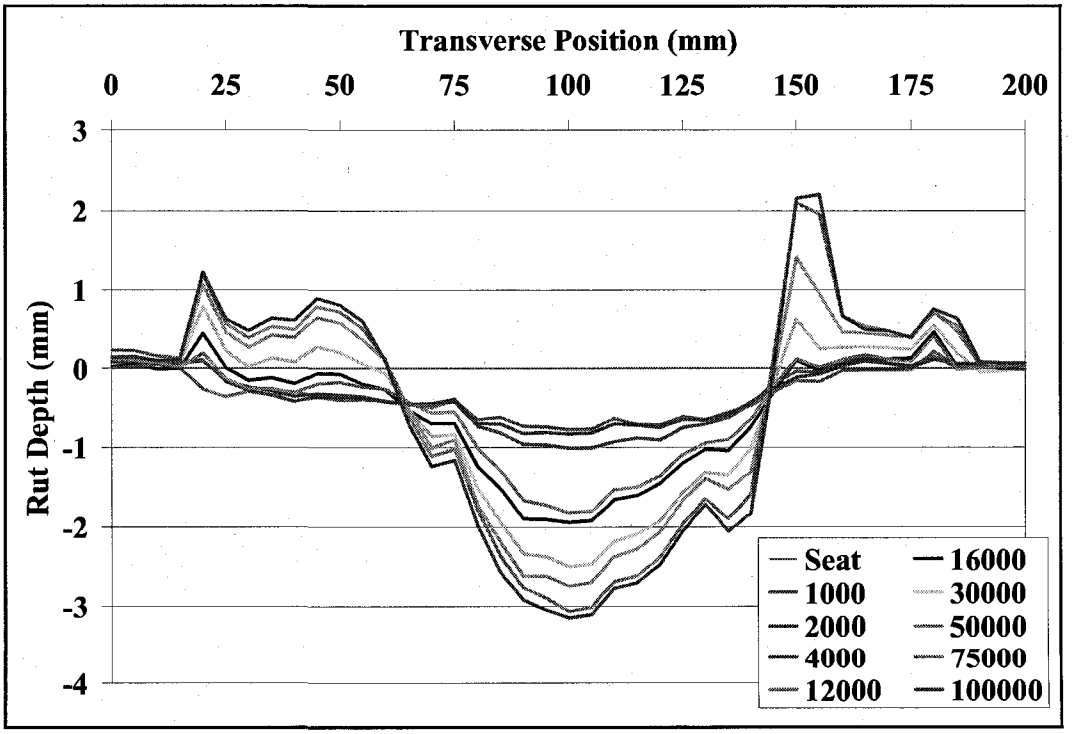

Figure A6.57: Hook Brick 7 Transverse Profiles

Table A6.16: Hook Avg Rut Depth from Base Line

Brick	Long Pos	Thousands of Loading Cycles								
		1	2	4	12	16	30	50	75	100
1	157.5	0.48	0.52	0.61	1.00	1.16	1.56	1.92	2.17	2.31
2	262.5	0.82	0.85	1.10	1.11	1.36	1.75	1.94	2.35	2.34
3	367.5	0.91	0.94	1.02	1.06	1.31	1.58	1.64	1.98	1.93
4	472.5	0.75	0.86	1.00	1.00	1.17	1.25	1.49	1.66	1.77
5	577.5	0.33	0.39	0.40	0.61	0.67	0.86	1.22	1.19	1.31
6	682.5	0.16	0.24	0.33	0.56	0.67	0.98	1.51	1.58	1.71
7	787.5	0.69	0.74	0.88	1.43	1.58	2.02	2.22	2.47	2.59
Avg		0.59	0.65	0.76	0.97	1.13	1.43	1.71	1.92	1.99

Table A6.17: Hook Max Rut Depth from Base Line

Brick	Long Pos	Thousands of Loading Cycles								
		1	2	4	12	16	30	50	75	100
1	157.5	0.61	0.66	0.77	1.28	1.54	2.03	2.47	2.75	2.91
2	262.5	1.00	1.01	1.31	1.28	1.58	2.03	2.21	2.63	2.62
3	367.5	1.07	1.11	1.17	1.27	1.55	1.89	1.96	2.29	2.28
4	472.5	0.95	1.04	1.26	1.36	1.58	1.61	1.89	2.18	2.30
5	577.5	0.45	0.54	0.66	0.87	0.93	1.19	1.47	1.50	1.55
6	682.5	0.26	0.35	0.46	0.73	0.83	1.23	1.90	1.95	2.04
7	787.5	0.78	0.83	1.01	1.82	1.94	2.50	2.74	3.07	3.15
Avg		0.73	0.79	0.95	1.23	1.42	1.78	2.09	2.34	2.41

Table A6.18: Hook Max Rut Depth from Max Heave

Brick	Long Pos	Thousands of Loading Cycles								
		1	2	4	12	16	30	50	75	100
1	157.5	0.87	1.03	1.12	1.97	2.31	2.82	3.55	3.72	4.02
2	262.5	1.15	1.26	1.56	1.90	2.01	2.65	3.36	4.27	4.73
3	367.5	1.31	1.33	1.43	1.88	2.07	2.80	3.61	4.21	4.69
4	472.5	1.04	1.56	1.42	1.91	2.07	2.55	3.06	3.67	4.01
5	577.5	0.91	0.98	1.21	1.41	1.46	1.68	1.97	2.41	2.49
6	682.5	1.08	1.32	1.57	2.43	2.55	3.33	4.06	4.41	4.64
7	787.5	0.99	0.94	1.16	2.22	2.40	3.30	4.15	5.16	5.35
Avg		1.05	1.20	1.35	1.96	2.12	2.73	3.39	3.98	4.27

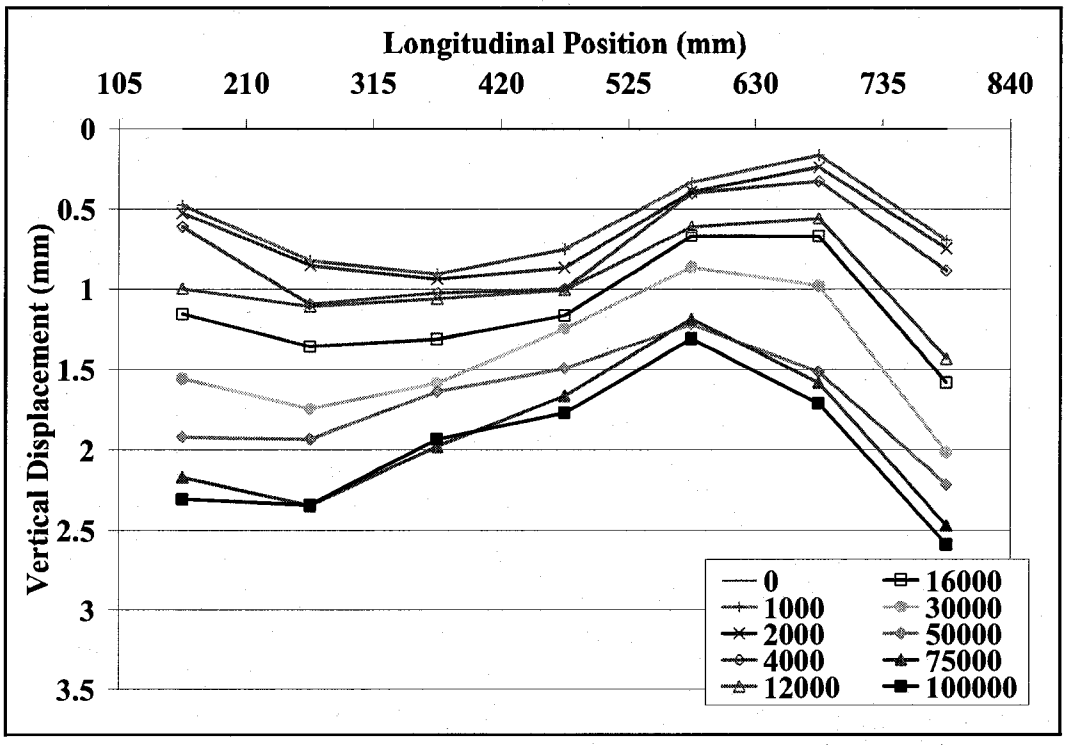

Figure A6.58: Hook Avg Rut from Base Line Longitudinal Profiles

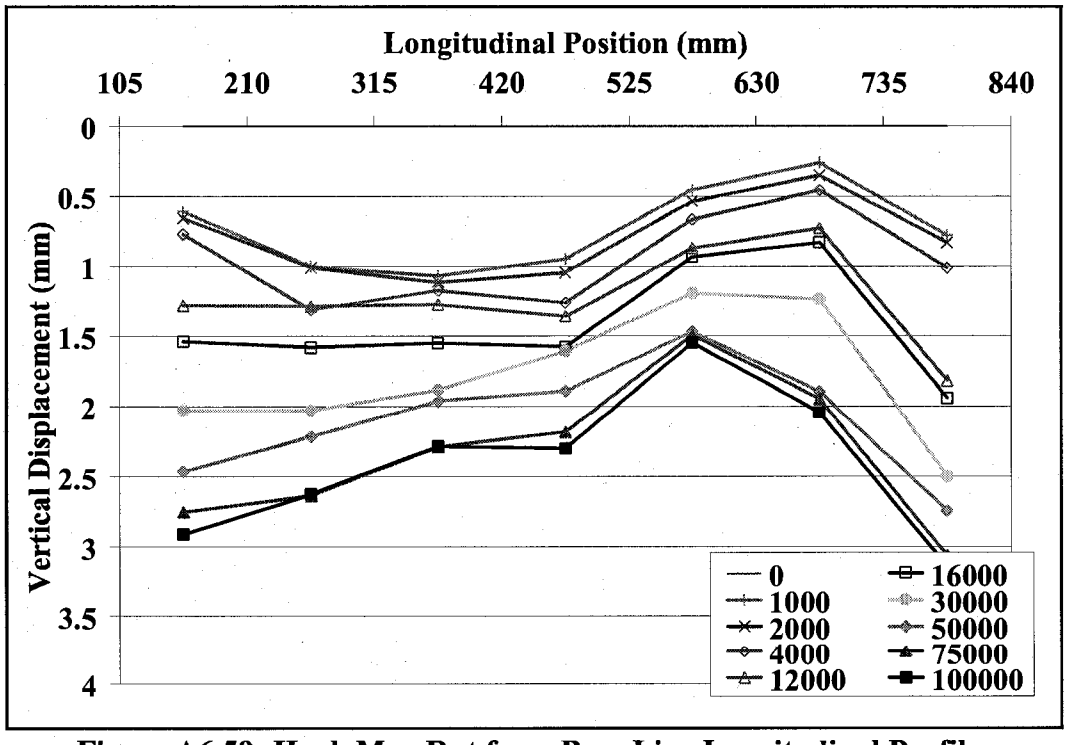

Figure A6.59: Hook Max Rut from Base Line Longitudinal Profiles

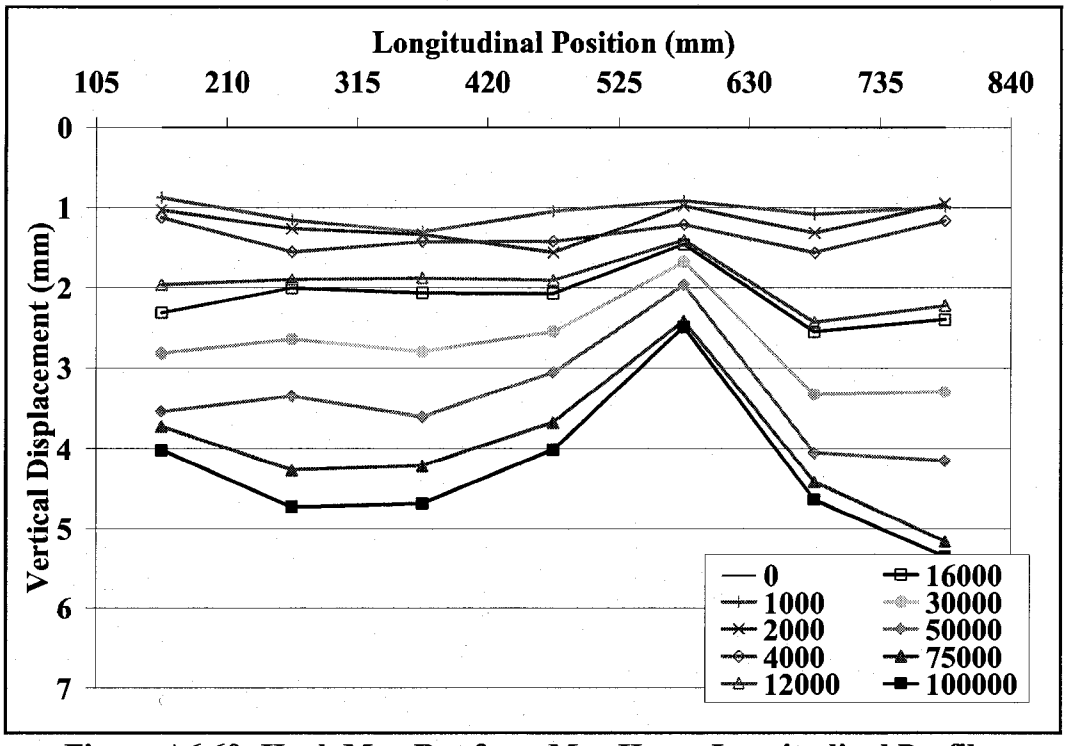

Figure A6.60: Hook Max Rut from Max Heave Longitudinal Profiles

Oss 12.5 Bailey

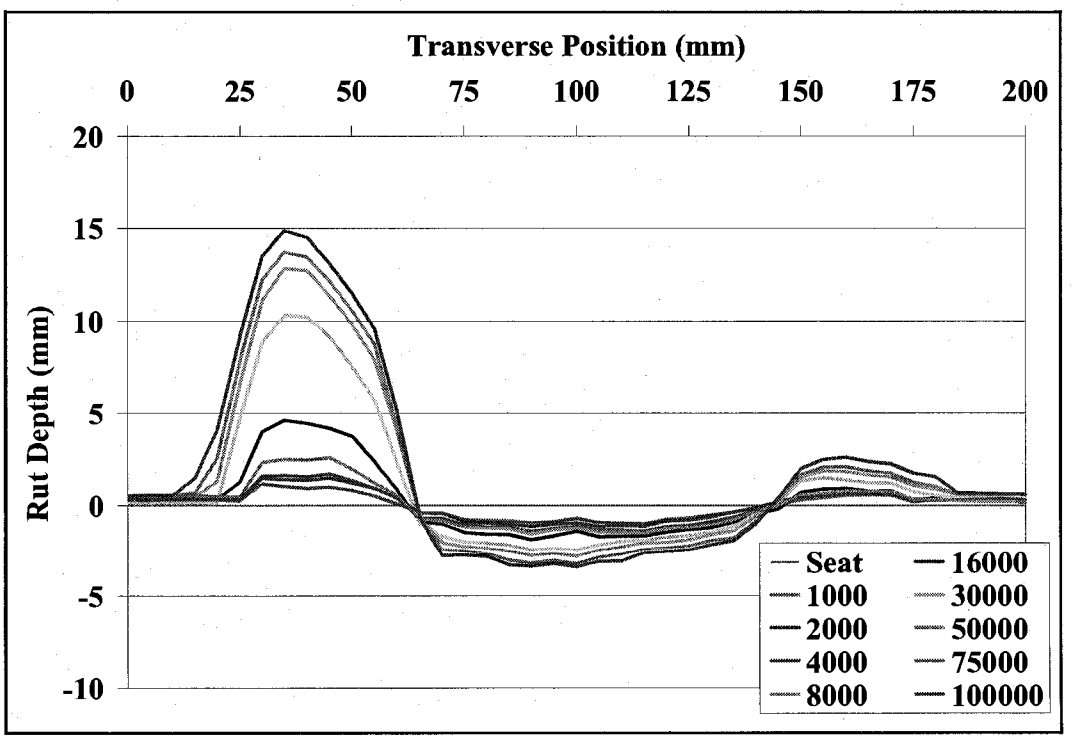

Figure A6.61: Oss 12.5 Bailey Brick 1 Transverse Profiles

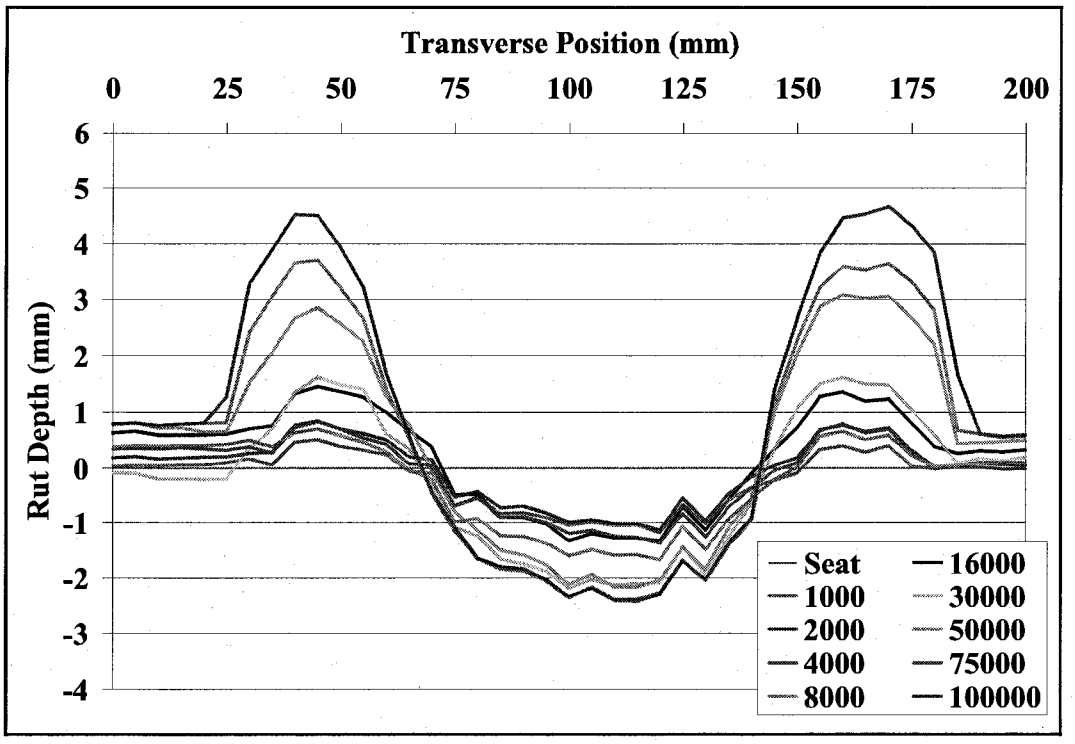

Figure A6.62: Oss 12.5 Bailey Brick 2 Transverse Profiles

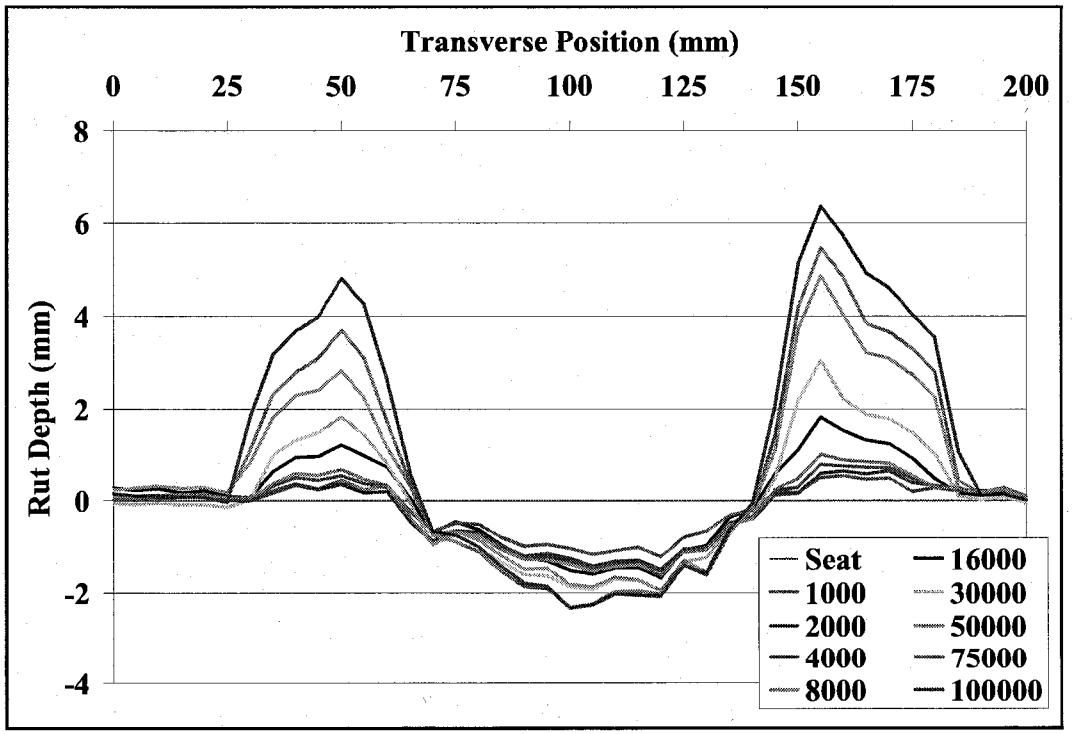

Figure A6.63: Oss 12.5 Bailey Brick 3 Transverse Profiles

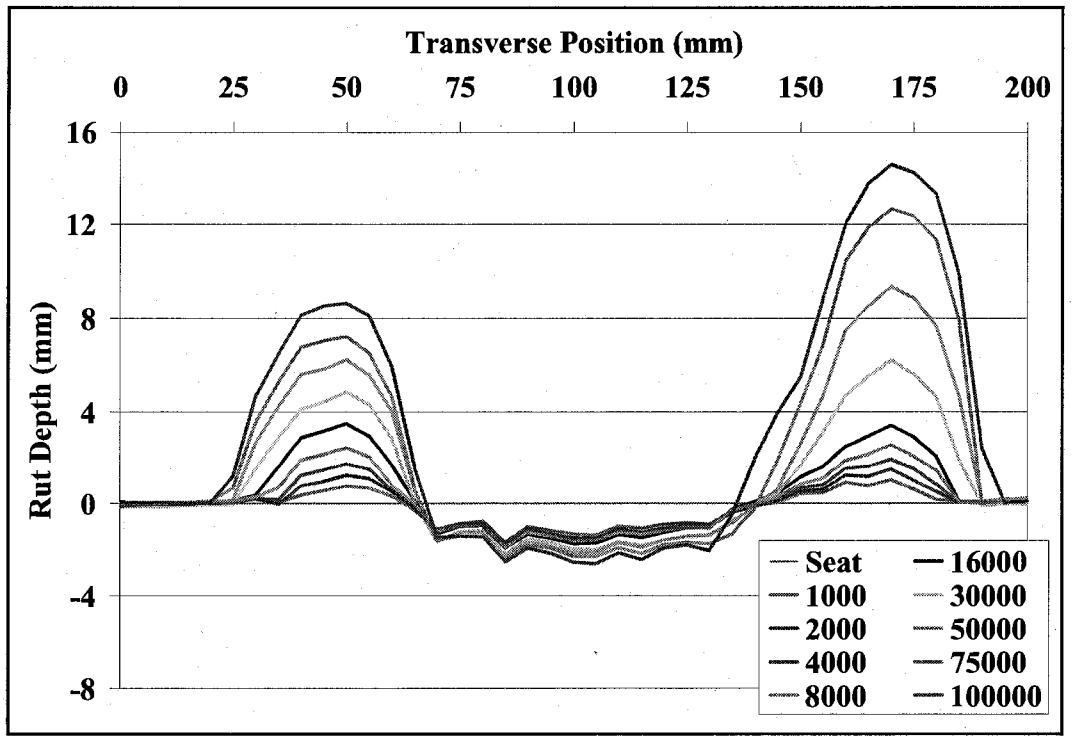

Figure A6.64: Oss 12.5 Bailey Brick 4 Transverse Profiles

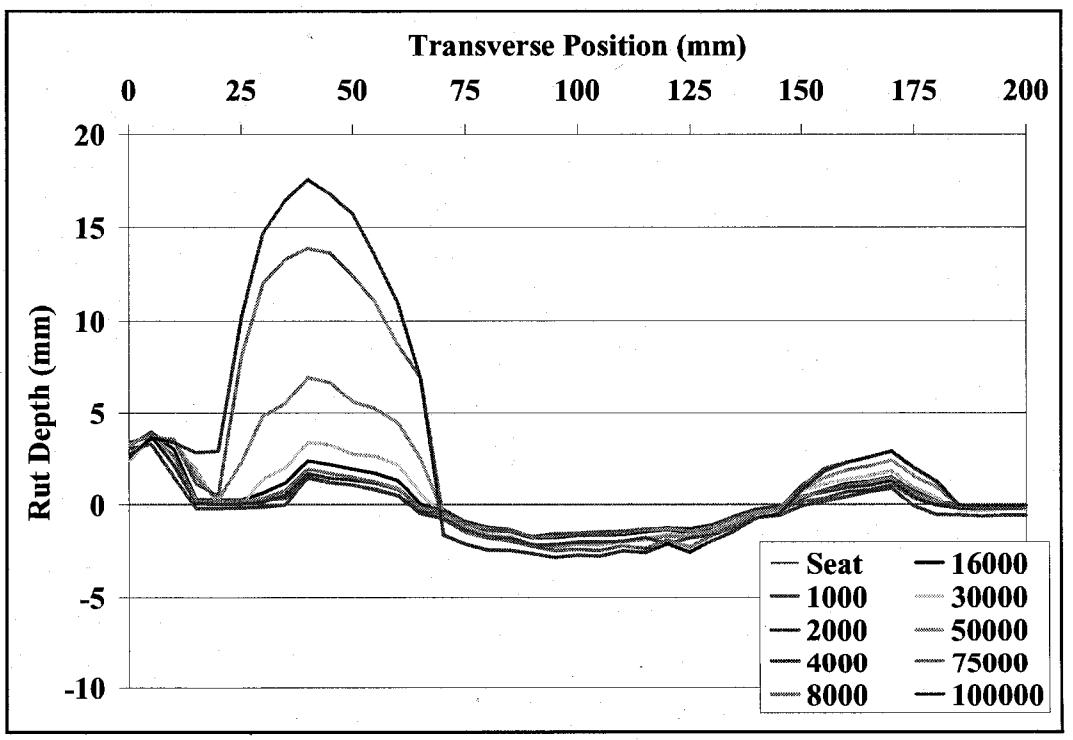

Figure A6.65: Oss 12.5 Bailey Brick 5 Transverse Profiles

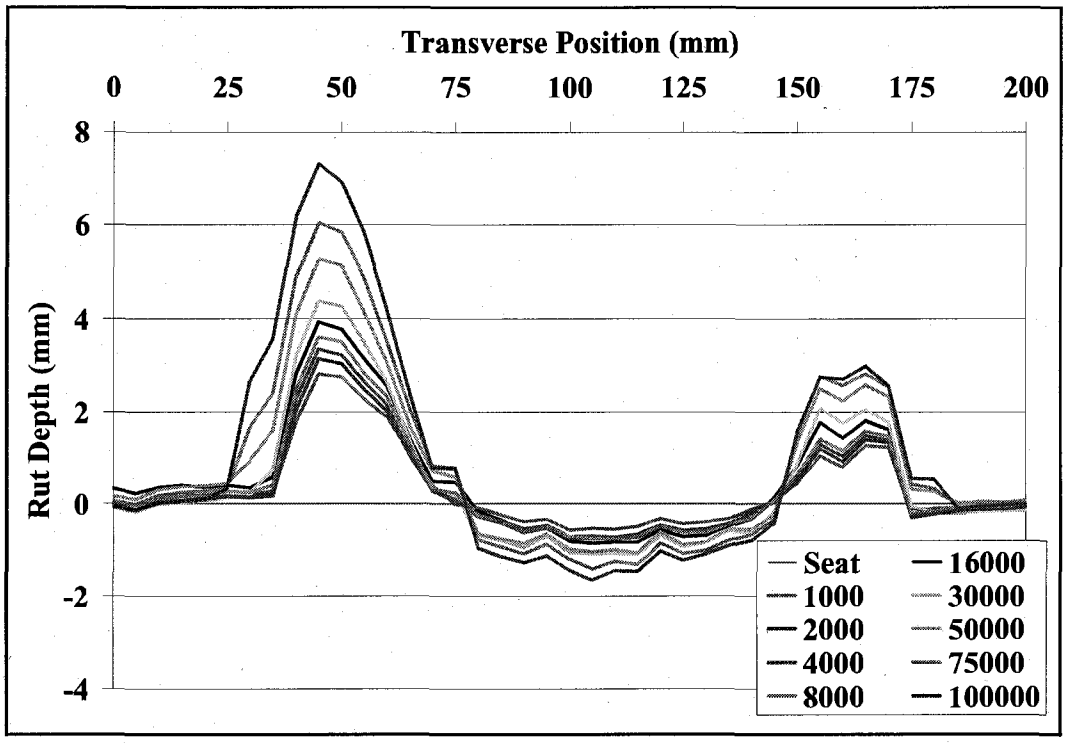

Figure A6.66: Oss 12.5 Bailey Brick 6 Transverse Profiles

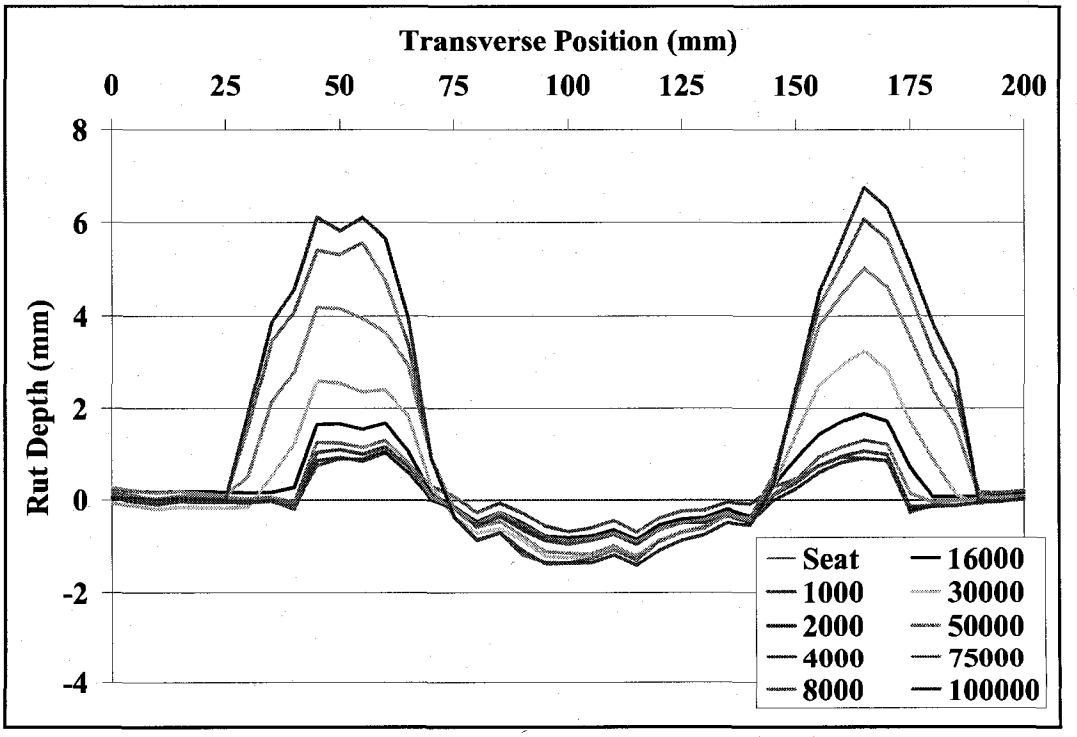

Figure A6.67: Oss 12.5 Bailey Brick 7 Transverse Profiles

Table A6.19: Oss 12.5 Bailey Avg Rut Depth from Base Line

Brick	Long Pos	Thousands of Loading Cycles								
		1	2	4	8	16	30	50	75	100
1	157.5	0.80	0.95	1.19	1.30	1.54	2.02	2.31	2.70	2.93
2	262.5	0.91	0.84	1.05	1.38	1.05	1.85	1.79	2.06	2.06
3	367.5	0.93	1.17	1.21	1.27	1.26	1.58	1.54	1.81	1.80
4	472.5	1.09	1.23	1.31	1.33	1.40	1.69	1.77	1.98	2.16
5	577.5	1.44	1.44	1.94	1.48	1.54	1.85	1.93	2.18	2.52
6	682.5	0.40	0.55	0.60	0.58	0.63	0.90	0.85	1.07	1.26
7	787.5	0.41	0.65	0.69	0.63	0.59	0.94	0.88	1.04	1.11
Avg		0.85	0.98	1.14	1.14	1.14	1.55	1.58	1.83	1.98

Table A6.20: Oss 12.5 Bailey Max Rut Depth from Base Line

Brick	Long Pos	Thousands of Loading Cycles								
		1	2	4	8	16	30	50	75	100
1	157.5	0.99	1.13	1.40	1.55	1.83	2.46	2.83	3.23	3.42
2	262.5	1.17	1.14	1.36	1.66	1.33	2.18	2.16	2.38	2.41
3	367.5	1.22	1.49	1.53	1.63	1.68	1.94	1.96	2.29	2.31
4	472.5	1.66	1.79	1.90	1.92	1.96	2.22	2.37	2.51	2.64
5	577.5	1.74	1.74	2.20	1.76	1.80	2.20	2.30	2.48	2.85
6	682.5	0.58	0.73	0.76	0.76	0.86	1.10	1.06	1.42	1.65
7	787.5	0.71	0.93	0.96	0.91	0.86	1.26	1.25	1.37	1.43
Avg		1.15	1.28	1.44	1.46	1.47	1.91	1.99	2.24	2.39

Table A6.21: Oss 12.5 Bailey Max Rut Depth from Max Heave

Brick	Long Pos	Thousands of Loading Cycles								
		1	2	4	8	16	30	50	75	100
1	157.5	2.17	2.64	3.12	4.12	6.43	12.78	15.66	16.94	18.30
2	262.5	1.68	1.99	2.19	2.36	2.79	3.81	5.24	6.09	7.09
3	367.5	1.77	2.14	2.31	2.64	3.50	5.00	6.84	7.75	8.67
4	472.5	2.70	3.27	3.83	4.48	5.45	8.46	11.74	15.19	17.24
5	577.5	5.61	5.46	5.46	5.61	5.73	5.72	9.21	16.35	20.42
6	682.5	3.40	3.88	4.13	4.37	4.79	5.47	6.34	7.46	8.97
7	787.5	1.78	1.96	2.12	2.21	2.73	4.49	6.28	7.44	8.18
Avg		2.73	3.05	3.31	3.68	4.49	6.53	8.76	11.03	12.69

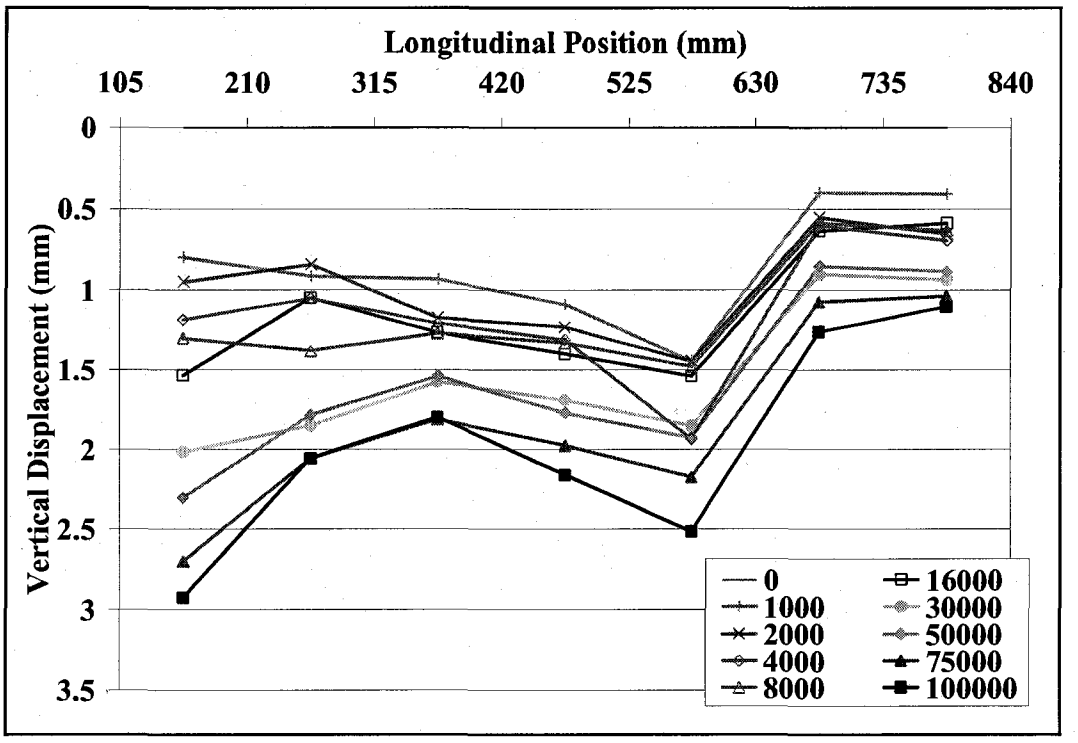

Figure A6.68: Oss 12.5 Bailey Avg Rut from Base Line Longitudinal Profiles

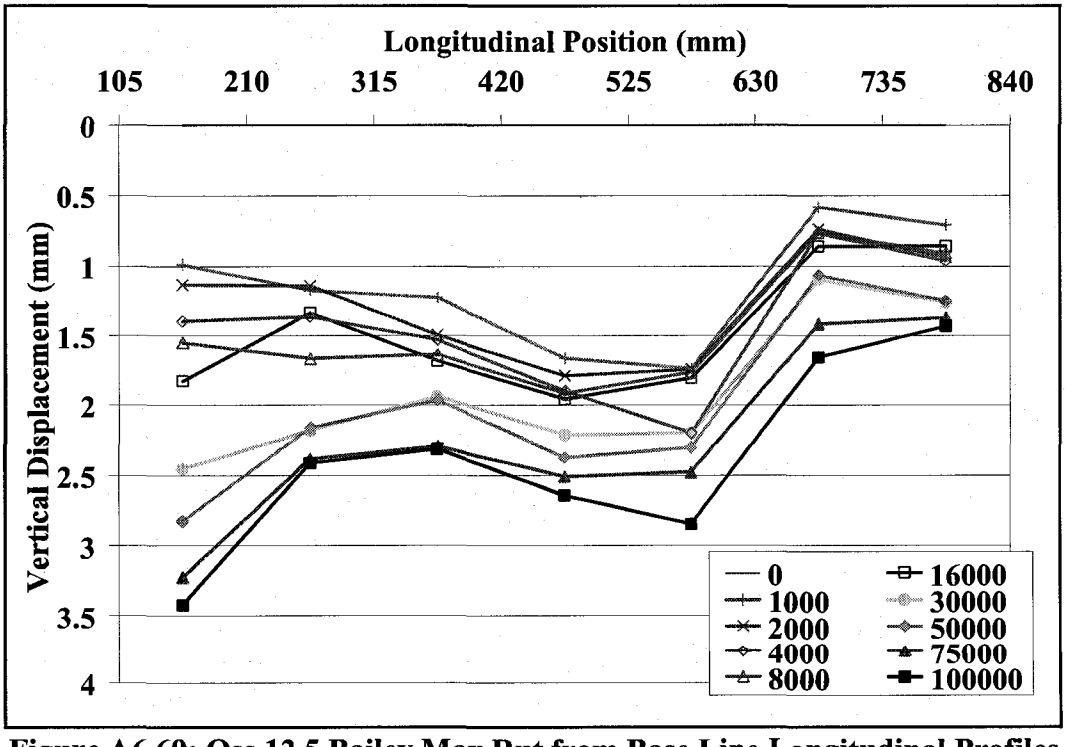

Figure A6.69: Oss 12.5 Bailey Max Rut from Base Line Longitudinal Profiles

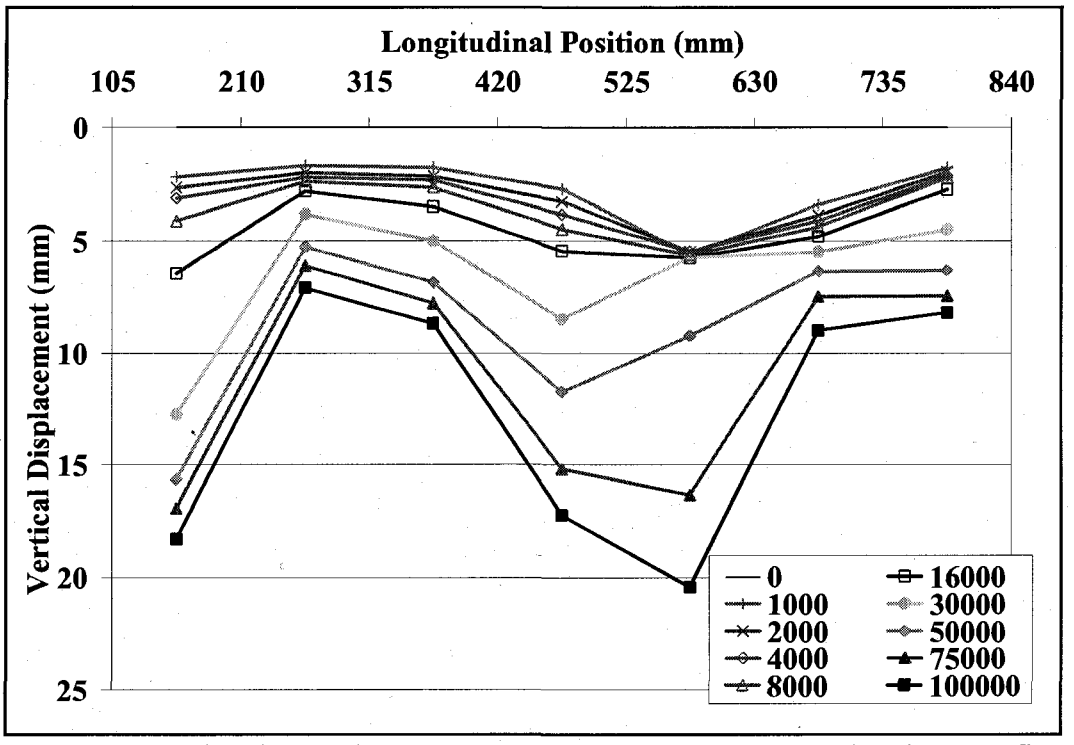

Figure A6.70: Oss 12.5 Bailey Max Rut from Max Heave Longitudinal Profiles

Cont 19 Bailey

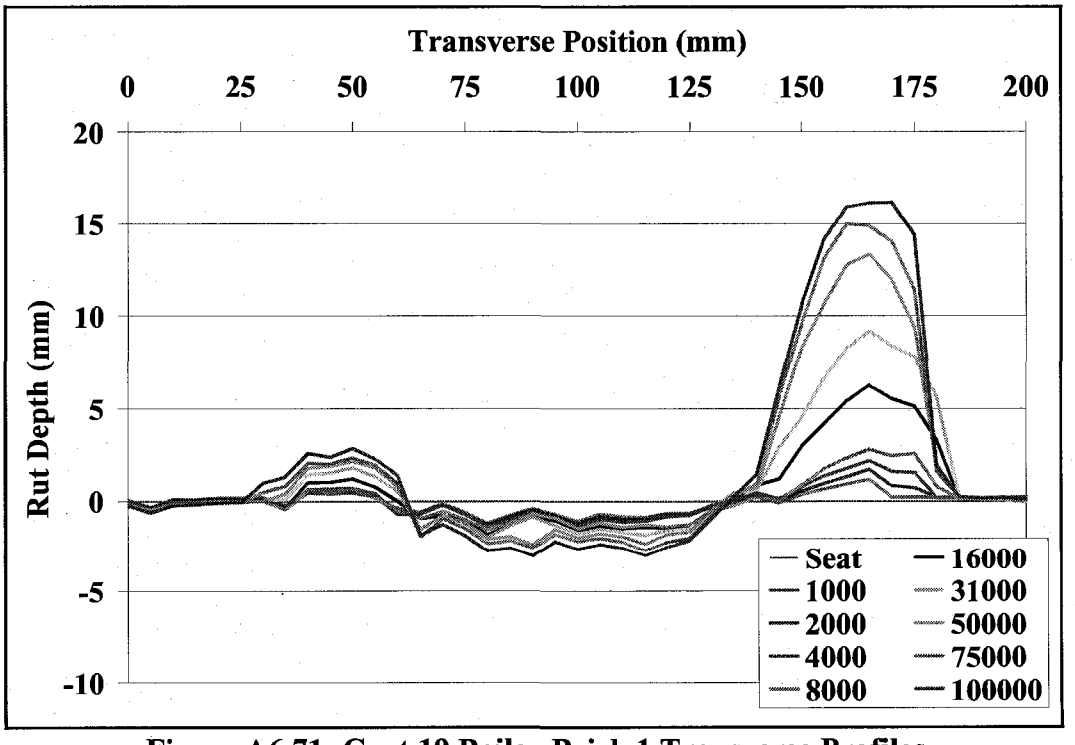

Figure A6.71: Cont 19 Bailey Brick 1 Transverse Profiles

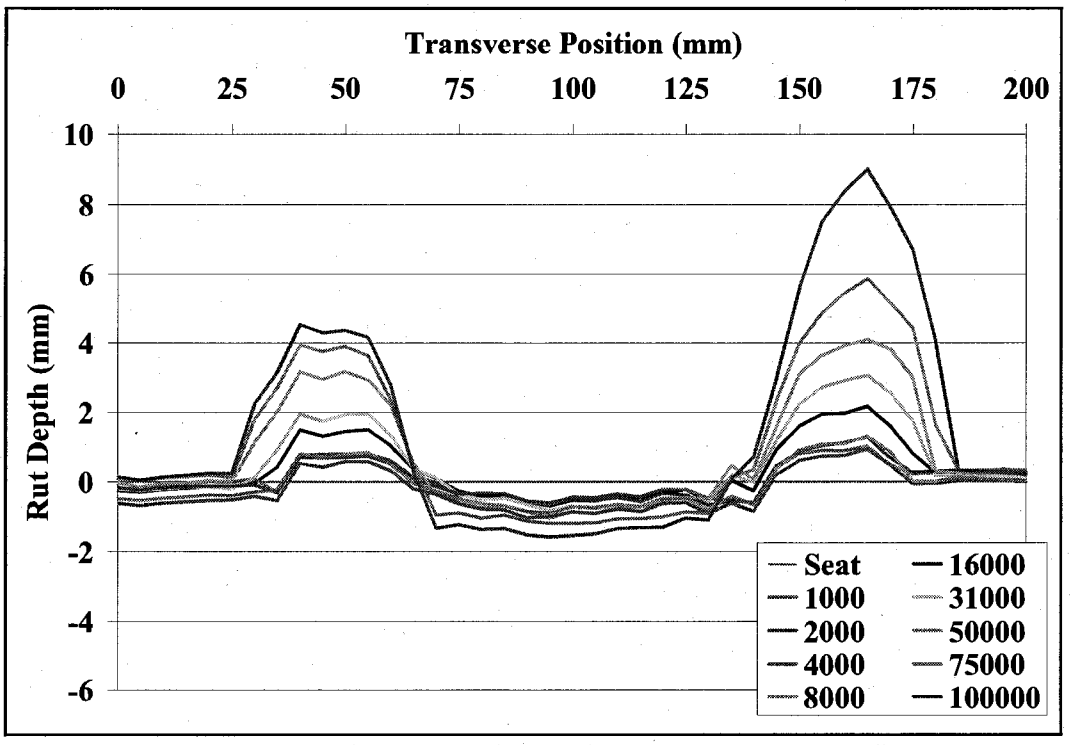

Figure A6.72: Cont 19 Bailey Brick 2 Transverse Profiles

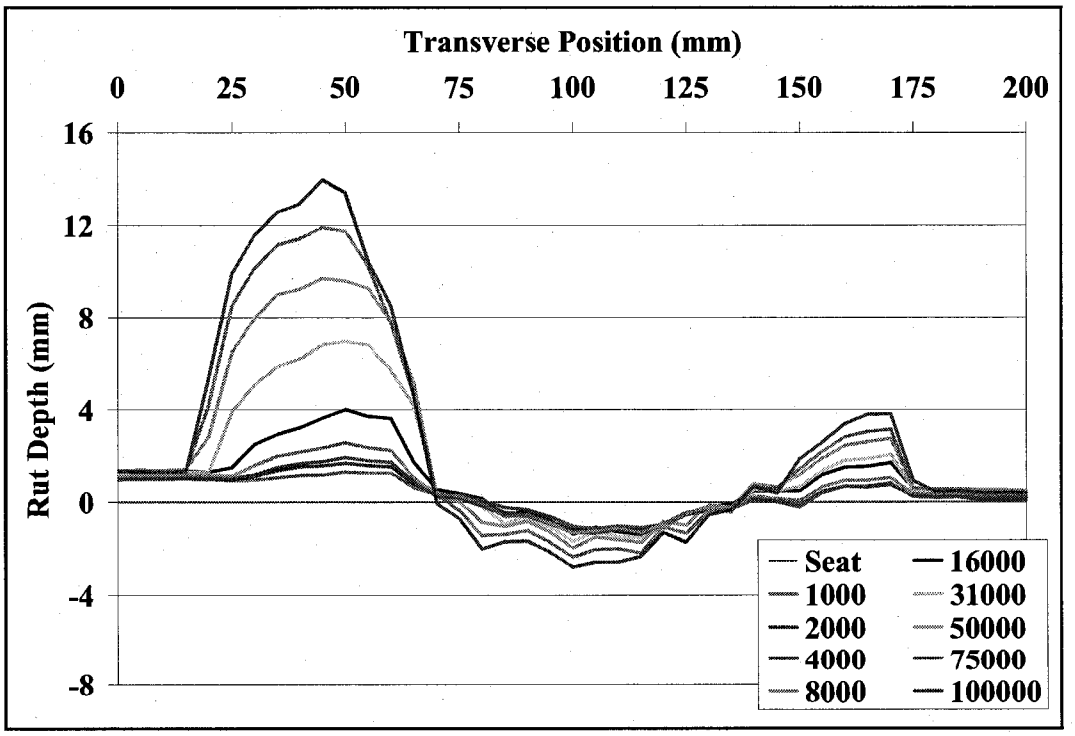

Figure A6.73: Cont 19 Bailey Brick 3 Transverse Profiles

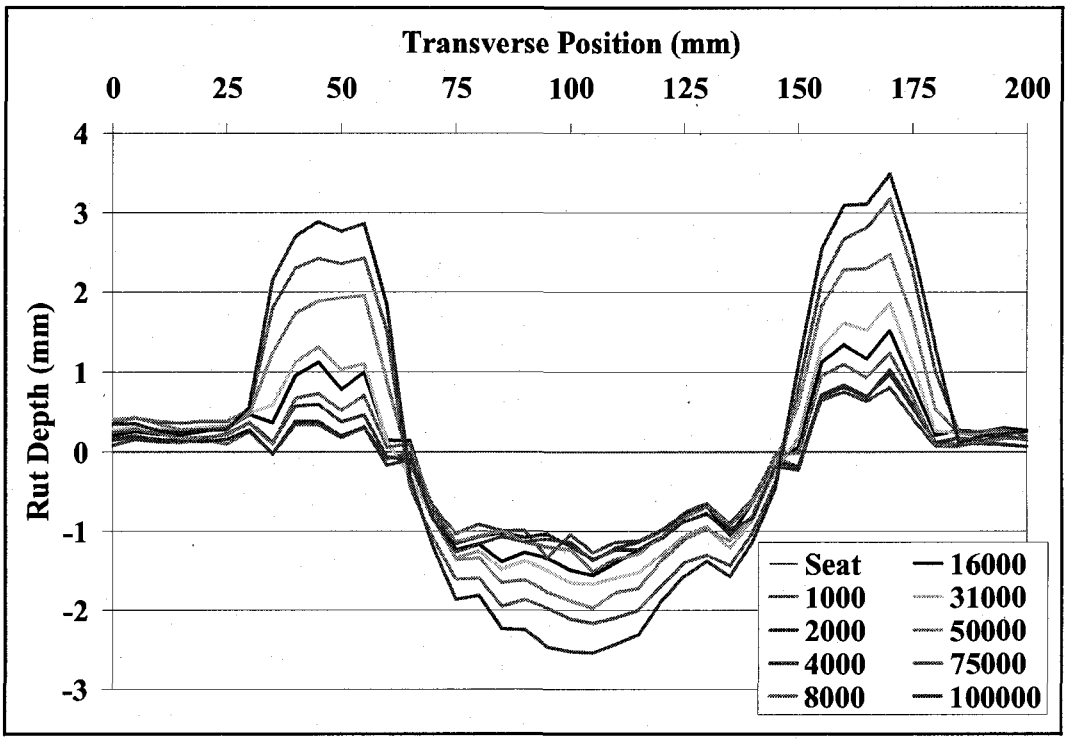

Figure A6.74: Cont 19 Bailey Brick 4 Transverse Profiles

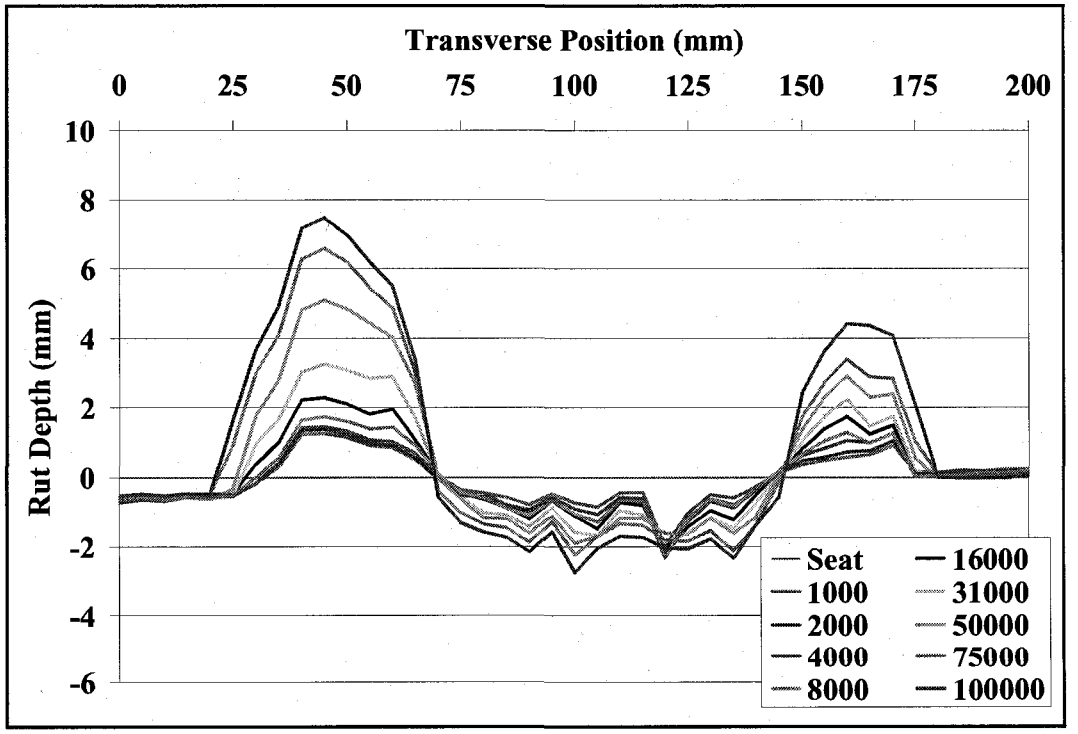

Figure A6.75: Cont 19 Bailey Brick 5 Transverse Profiles

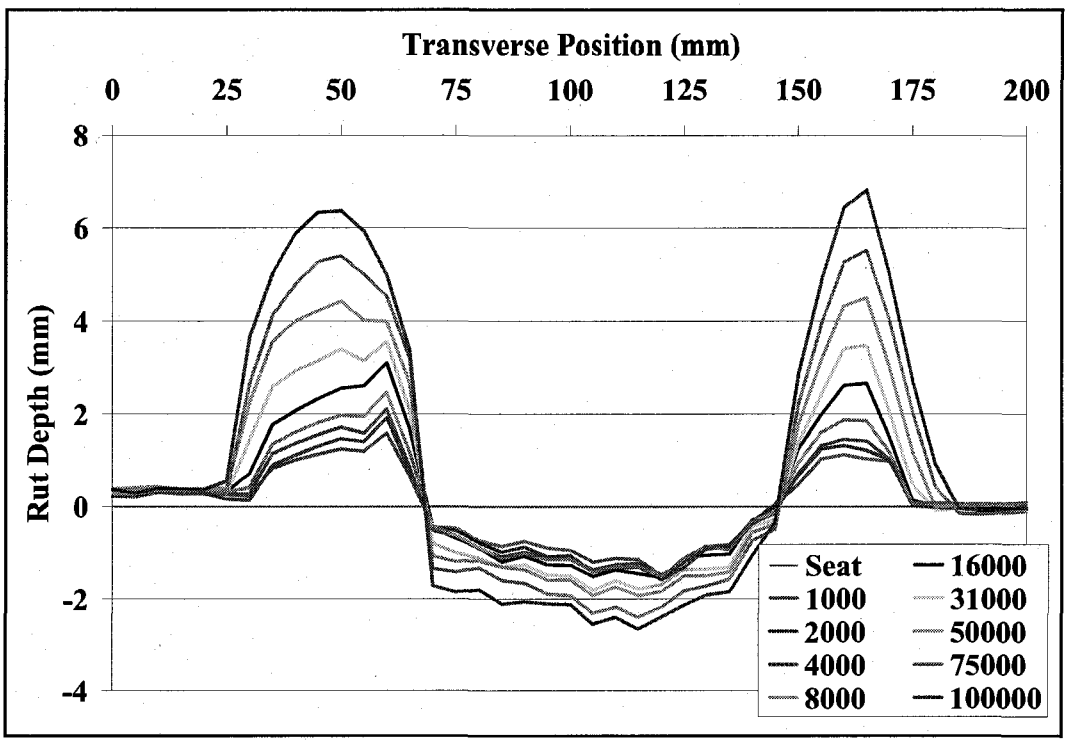

Figure A6.76: Cont 19 Bailey Brick 6 Transverse Profiles

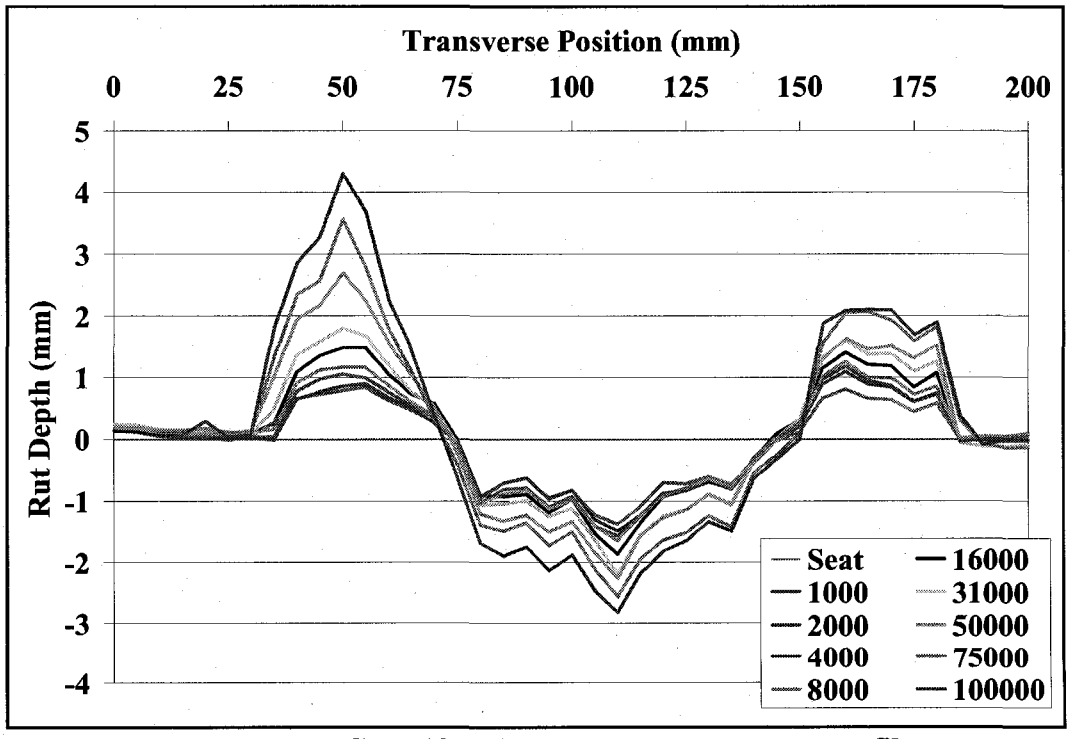

Figure A6.77: Cont 19 Bailey Brick 7 Transverse Profiles

Table A6.22: Cont 19 Bailey Avg Rut Depth from Base Line

Brick	Long Pos	Thousands of Loading Cycles								
		1	2	4	8	16	30	50	75	100
1	157.5	0.72	0.82	0.91	1.16	1.25	1.40	1.79	2.08	2.43
2	262.5	0.41	0.48	0.82	0.69	0.47	0.63	0.73	1.05	1.36
3	367.5	0.64	0.75	0.84	0.79	0.77	0.96	1.15	1.55	1.94
4	472.5	1.02	1.08	1.07	1.12	1.21	1.39	1.56	1.83	2.12
5	577.5	0.75	0.93	0.93	1.01	1.09	1.31	1.41	1.62	1.92
6	682.5	1.01	1.15	1.15	1.16	1.24	1.47	1.58	1.91	2.20
7	787.5	0.89	0.95	1.02	1.04	1.10	1.28	1.41	1.68	1.97
Avg		0.78	0.88	0.96	1.00	1.02	1.21	1.38	1.67	1.99

Table A6.23: Cont 19 Bailey Max Rut Depth from Base Line

Brick	Long Pos	Thousands of Loading Cycles								
		1	2	4	8	16	30	50	75	100
1	157.5	1.18	1.28	1.37	1.57	1.80	1.95	2.39	2.71	3.06
2	262.5	0.65	0.66	1.02	0.89	0.68	0.81	1.03	1.19	1.58
3	367.5	1.13	1.21	1.34	1.33	1.39	1.68	1.95	2.37	2.81
4	472.5	1.33	1.35	1.36	1.51	1.55	1.66	1.97	2.16	2.54
5	577.5	1.98	2.25	2.33	2.33	2.08	1.87	1.90	2.23	2.74
6	682.5	1.47	1.58	1.53	1.52	1.53	1.81	1.92	2.39	2.66
7	787.5	1.37	1.49	1.57	1.64	1.86	2.20	2.27	2.56	2.82
Avg		1.30	1.40	1.50	1.54	1.56	1.71	1.92	2.23	2.60

Table A6.24: Cont 19 Bailey Max Rut Depth from Max Heave

Brick	Long Pos	Thousands of Loading Cycles								
		1	2	4	8	16	30	50	75	100
1	157.5	2.37	3.00	3.57	4.39	8.06	11.08	15.71	17.68	19.20
2	262.5	1.67	1.96	1.96	2.20	2.85	3.87	5.12	7.06	10.57
3	367.5	2.42	2.90	3.26	3.90	5.39	8.63	11.65	14.30	16.77
4	472.5	2.14	2.33	2.39	2.75	3.07	3.53	4.45	5.33	6.03
5	577.5	3.24	3.60	3.76	4.06	4.37	5.12	7.00	8.82	10.22
6	682.5	3.07	3.51	3.63	3.98	4.63	5.36	6.43	7.92	9.47
7	787.5	2.21	2.58	2.74	2.90	3.34	3.99	4.95	6.13	7.13
Avg		2.45	2.84	3.04	3.45	4.53	5.94	7.90	9.60	11.34

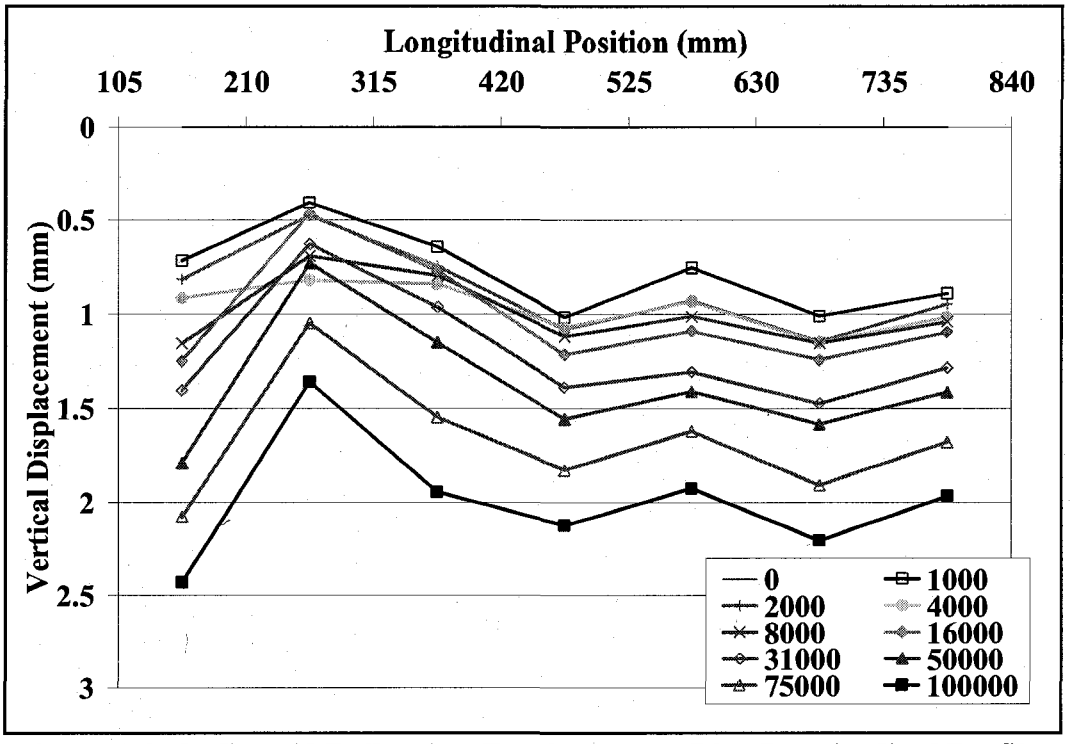

Figure A6.78: Cont 19 Bailey Avg Rut from Base Line Longitudinal Profiles

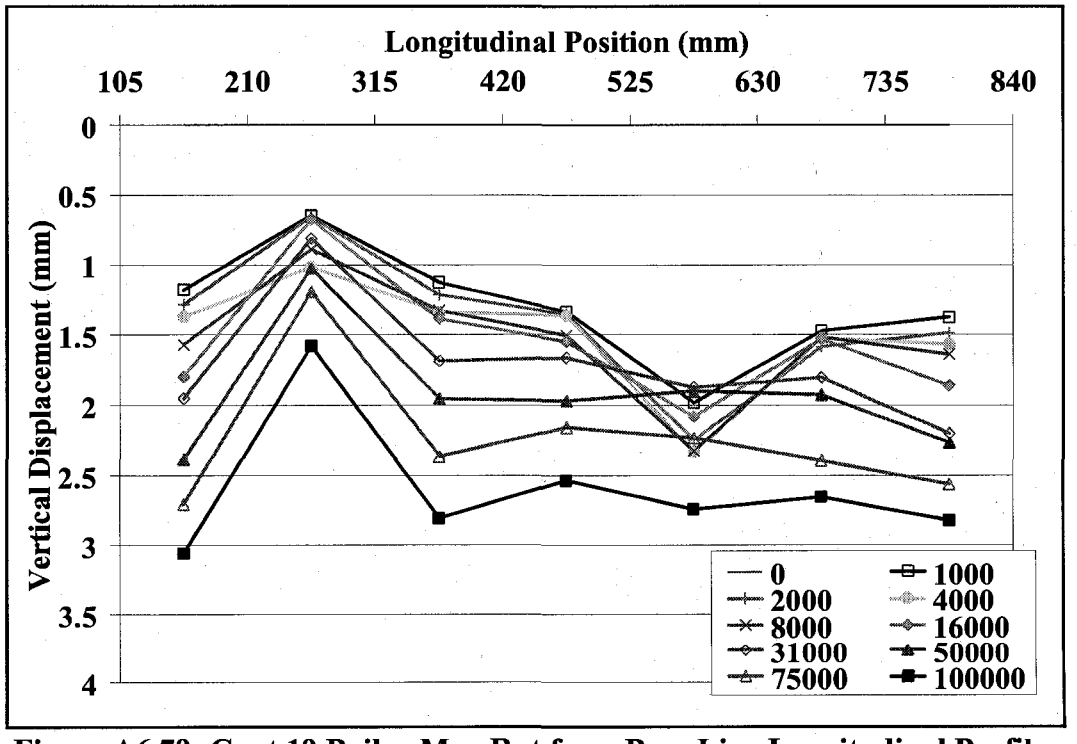

Figure A6.79: Cont 19 Bailey Max Rut from Base Line Longitudinal Profiles

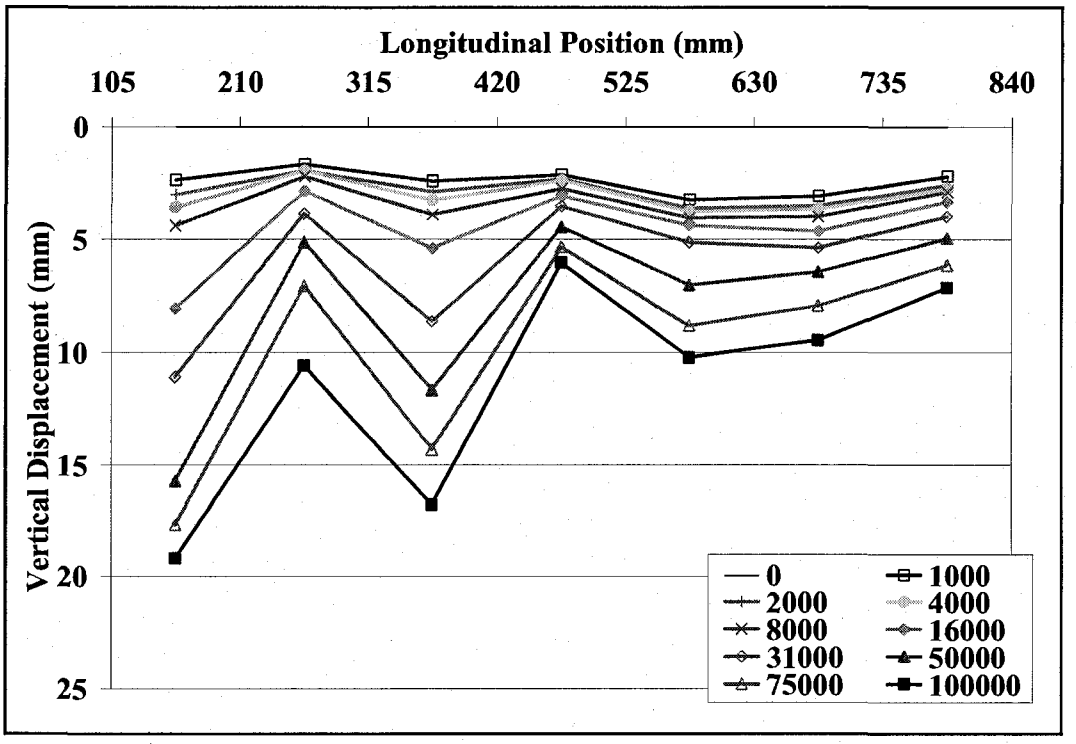

Figure A6.80: Cont 19 Bailey Max Rut from Max Heave Longitudinal Profiles

Oss 12.5 Field Cores

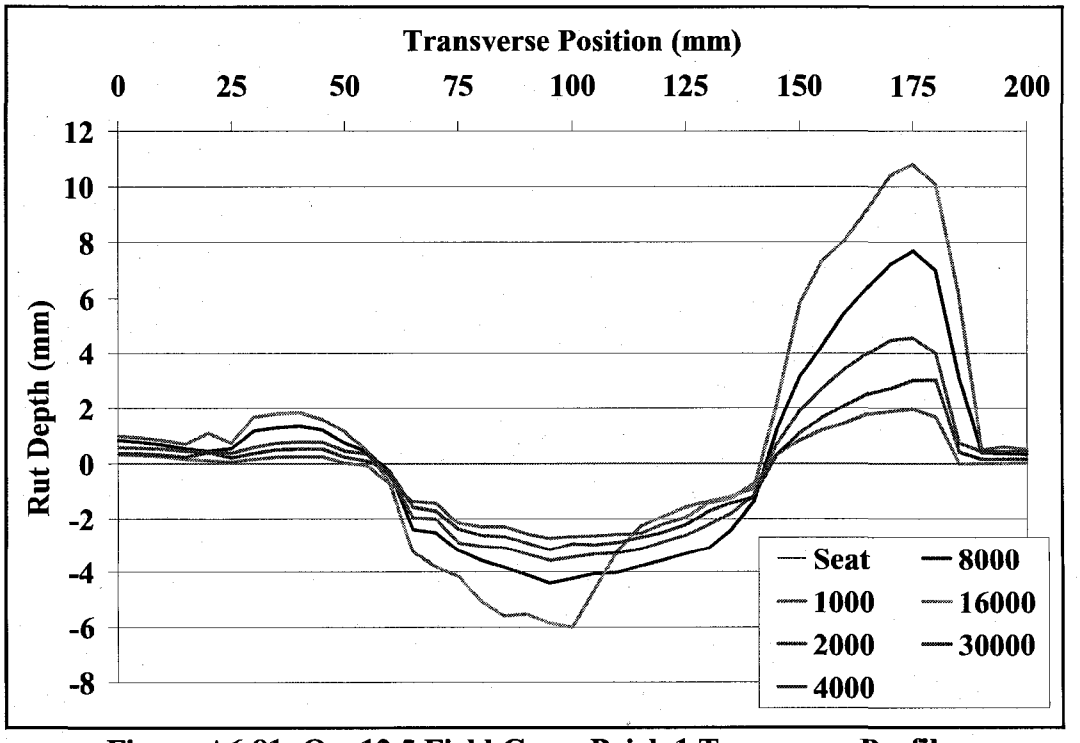

Figure A6.81: Oss 12.5 Field Cores Brick 1 Transverse Profiles

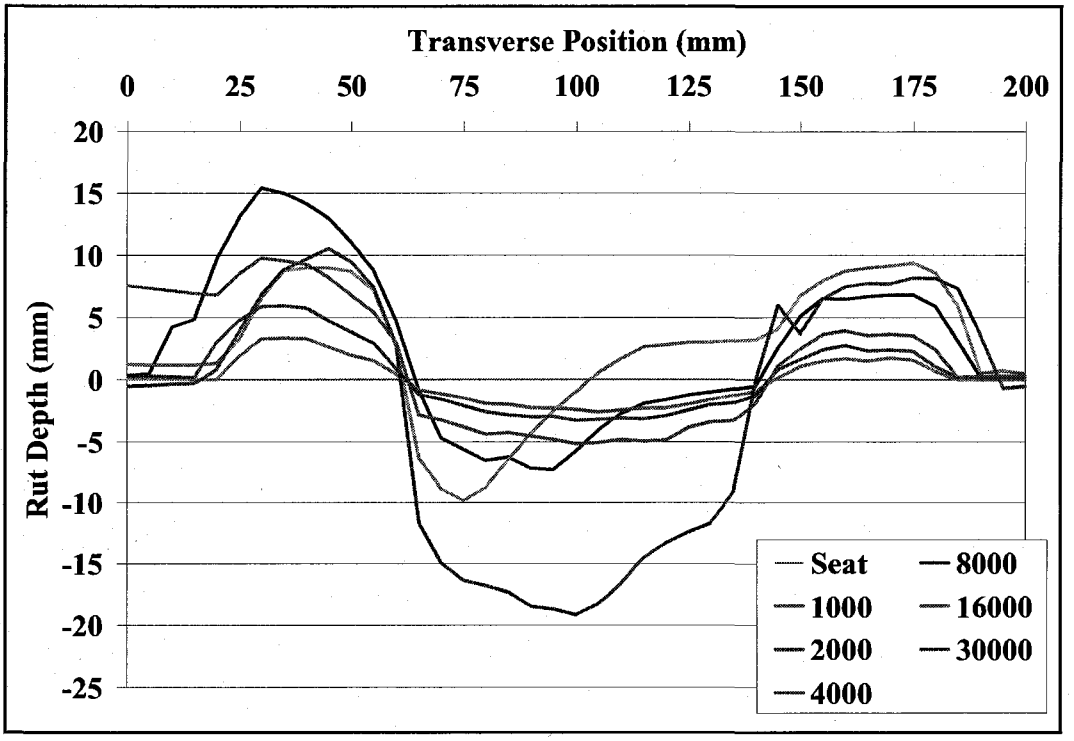

Figure A6.82: Oss 12.5 Field Cores Brick 2 Transverse Profiles

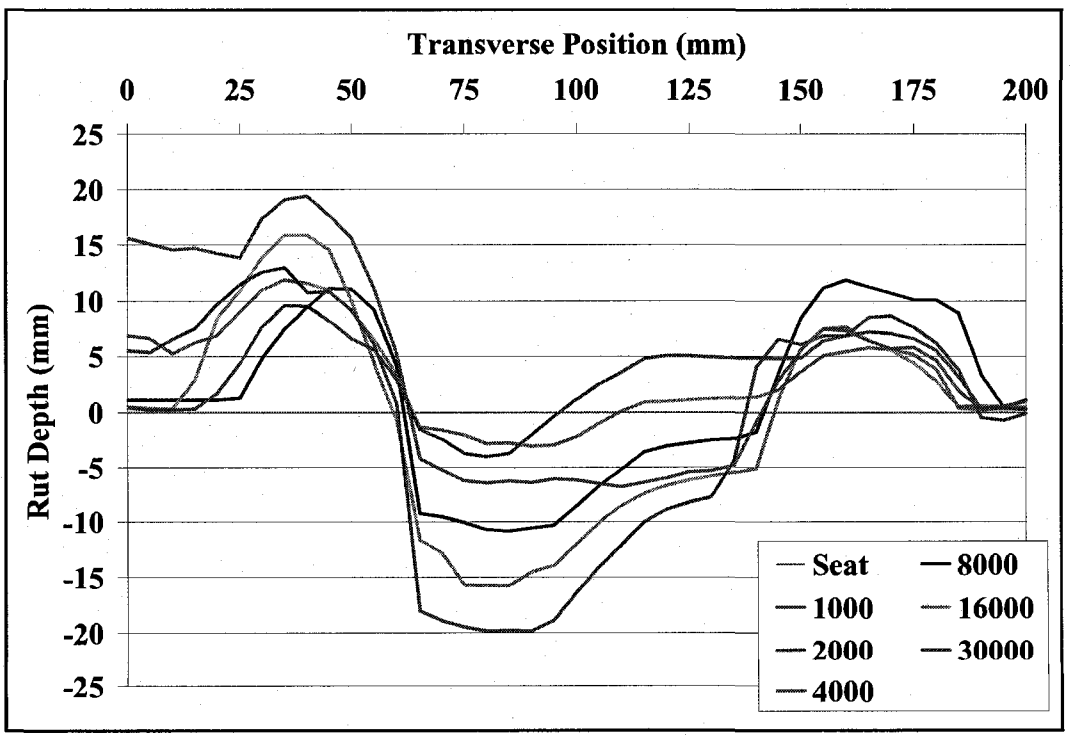

Figure A6.83: Oss 12.5 Field Cores Brick 3 Transverse Profiles

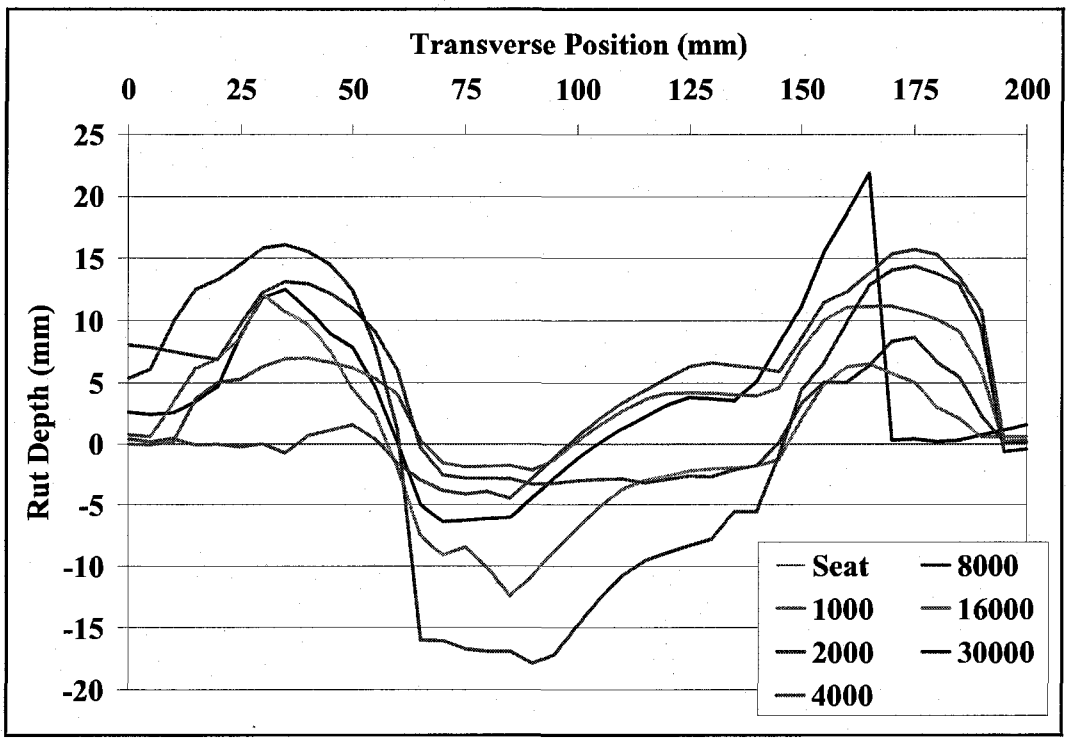

Figure A6.84: Oss 12.5 Field Cores Brick 4 Transverse Profiles

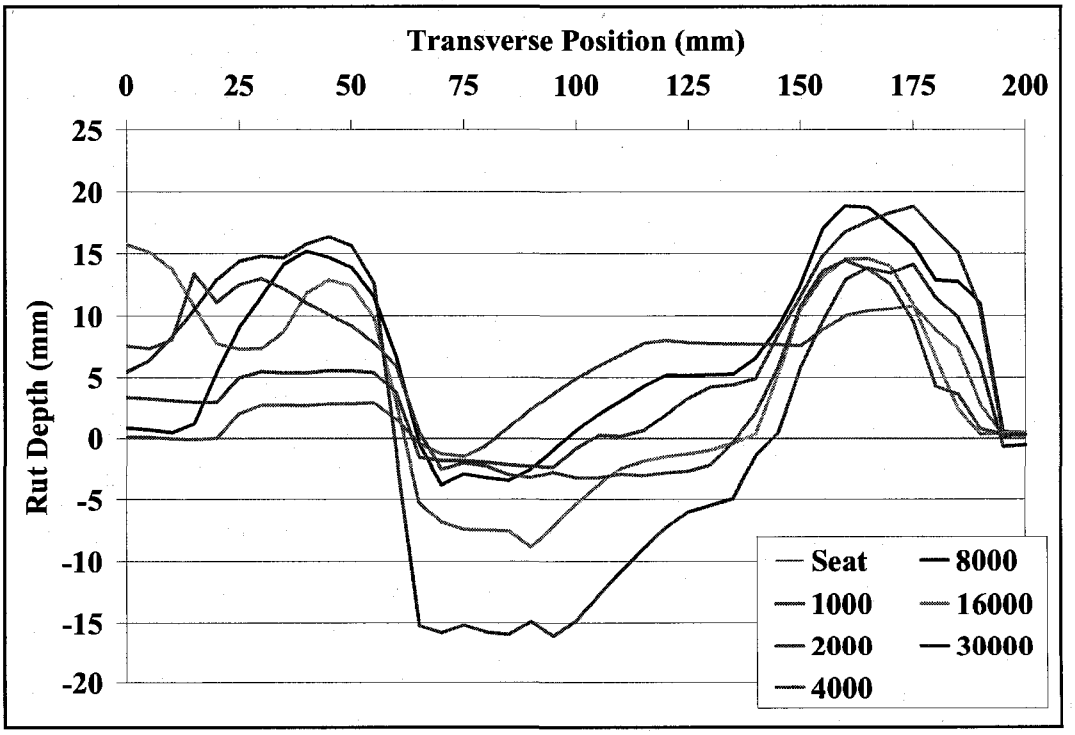

Figure A6.85: Oss 12.5 Field Cores Brick 5 Transverse Profiles

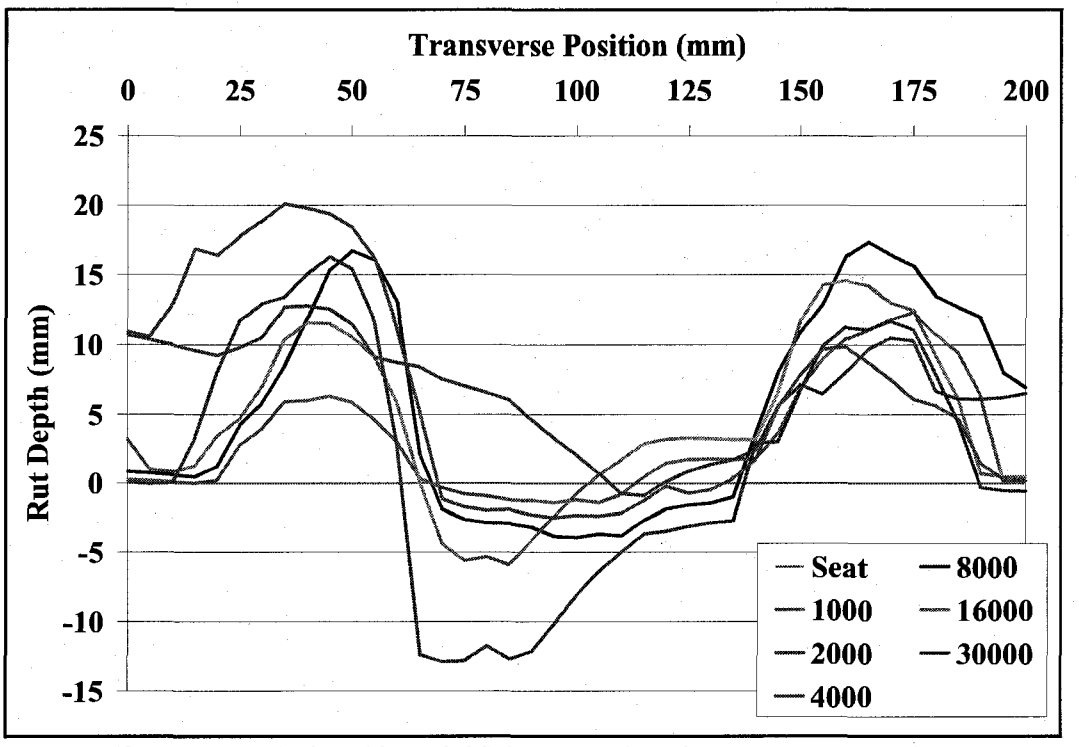

Figure A6.86: Oss 12.5 Field Cores Brick 6 Transverse Profiles

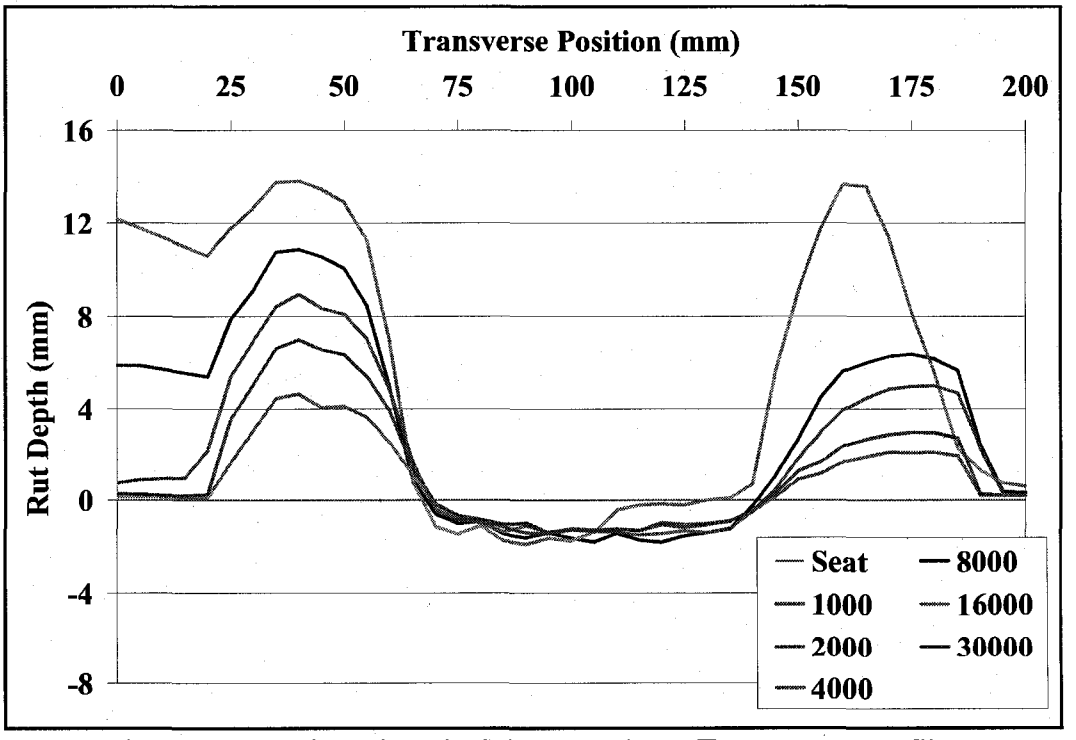

Figure A6.87: Oss 12.5 Field Cores Brick 7 Transverse Profiles

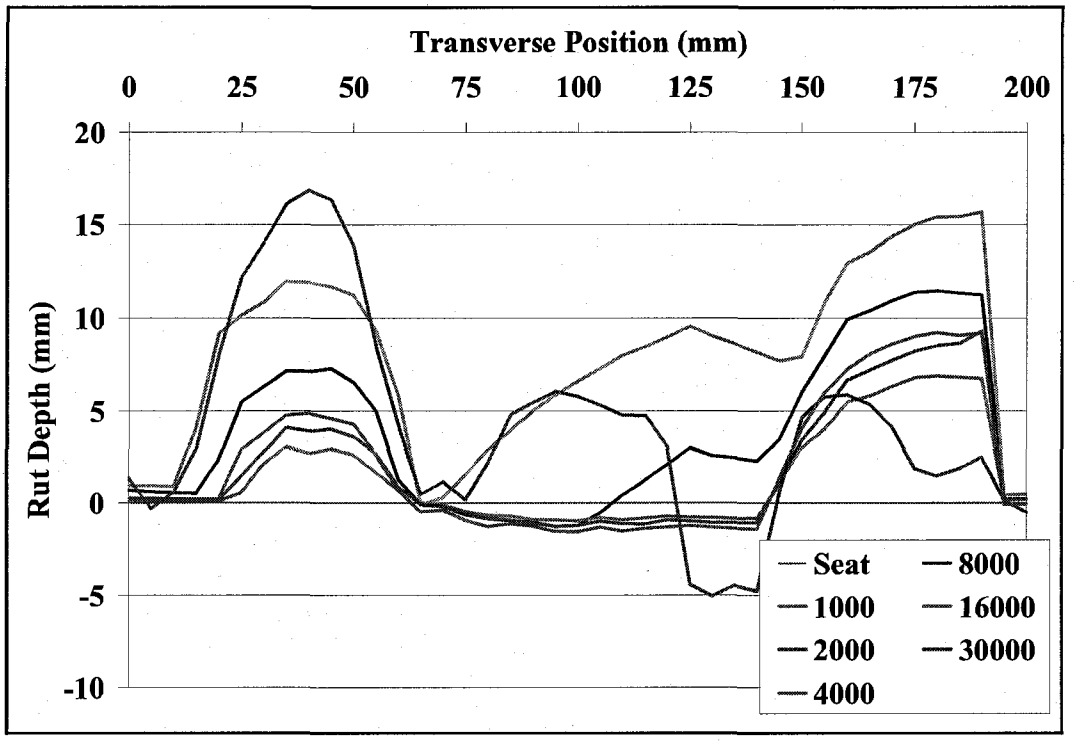

Figure A6.88: Oss 12.5 Field Cores Brick 8 Transverse Profiles

Table A6.25: Oss 12.5 Field Cores Avg Rut Depth from Base Line

Brick	Long Pos	Thousands of Loading Cycles					
		1	2	4	8	16	30
1	52.5	2.34	2.66	3.09	3.83	4.92	*
2	157.5	2.19	2.84	4.56	6.26	8.45	16.10
3	262.5	0.98	3.14	6.17	10.17	14.29	19.24
4	367.5	1.87	2.98	3.88	5.96	9.52	16.77
5	472.5	0.96	2.07	2.86	2.79	7.25	15.46
6	577.5	1.06	0.52	1.65	2.88	5.07	12.12
7	682.5	1.18	1.15	1.33	1.53	1.52	*
8	787.5	0.81	1.05	1.36	0.75	0.09	**
Avg		1.51	2.20	3.36	4.77	7.29	15.94

* No profile could be measured

** Bad data

All the highlighted values used a modified range for the average rut

Table A6.26: Oss 12.5 Field Cores Max Rut Depth from Base Line

Brick	Long Pos	Thousands of Loading Cycles					
		1	2	4	8	16	30
1	52.5	2.73	3.18	3.58	4.40	6.00	
2	157.5	2.60	3.27	5.16	7.30	9.84	19.11
3	262.5	3.13	4.09	6.80	10.84	15.76	19.82
4	367.5	2.21	3.36	4.51	6.38	12.41	17.86
5	472.5	1.46	2.32	3.27	3.81	8.88	16.05
6	577.5	1.39	0.90	2.45	3.91	5.90	12.87
7	682.5	1.39	1.43	1.50	1.83	1.90	
8	787.5	0.98	1.27	1.59	1.28	0.09	
Avg		2.13	2.65	3.90	5.49	8.67	17.14

Table A6.27: Oss 12.5 Field Cores Max Rut Depth from Max Heave

Brick	Long Pos	Thousands of Loading Cycles					
		1	2	4	8	16	30
1	52.5	4.69	6.22	8.13	12.09	16.79	
2	157.5	5.95	9.19	14.95	22.71	19.24	29.63
3	262.5	14.99	13.69	26.24	22.67	31.64	32.77
4	367.5	13.41	16.48	20.26	28.27	24.53	33.98
5	472.5	12.24	21.14	17.73	22.68	24.64	32.39
6	577.5	13.70	13.64	22.55	21.27	20.48	29.14
7	682.5	6.03	8.43	10.45	12.69	15.72	
8	787.5	7.88	10.58	10.79	12.73	15.78	
Avg		10.15	12.68	17.19	20.34	21.86	31.58

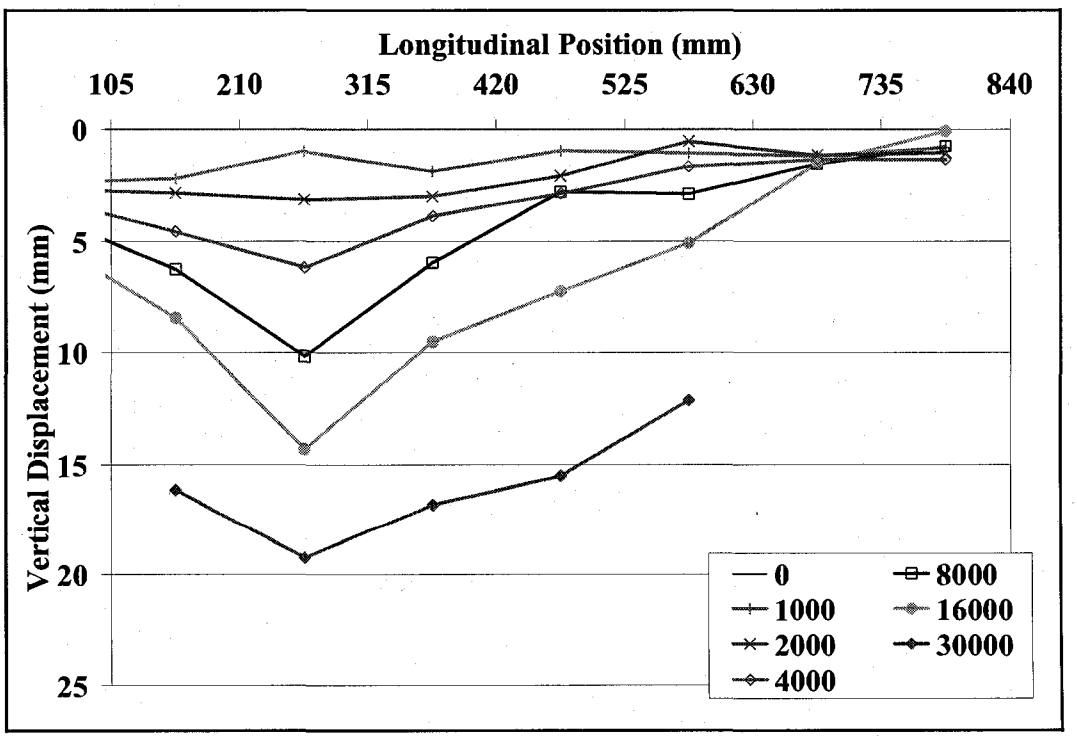

Figure A6.89: Oss 12.5 Field Cores Avg Rut from Base Line Longitudinal Profiles

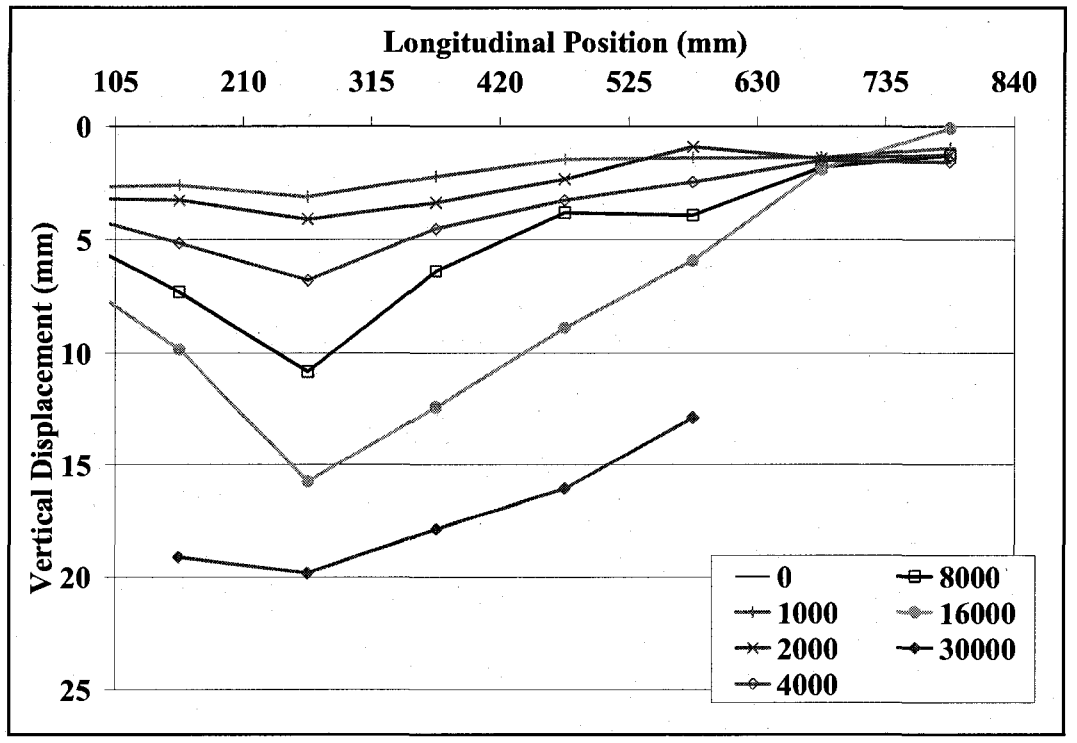

Figure A6.90: Oss 12.5 Field Cores Max Rut from Base Line Longitudinal Profiles

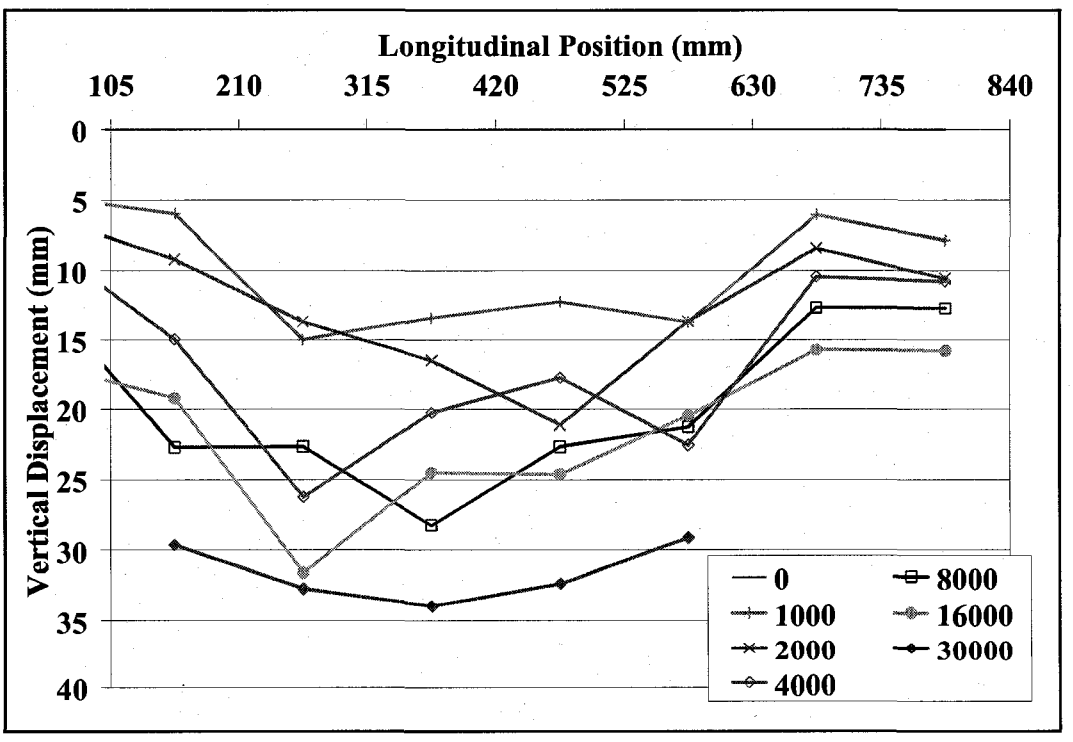

Figure A6.91: Oss 12.5 Field Cores Max Rut from Max Heave Longitudinal Profiles

Oss 19 Field Cores

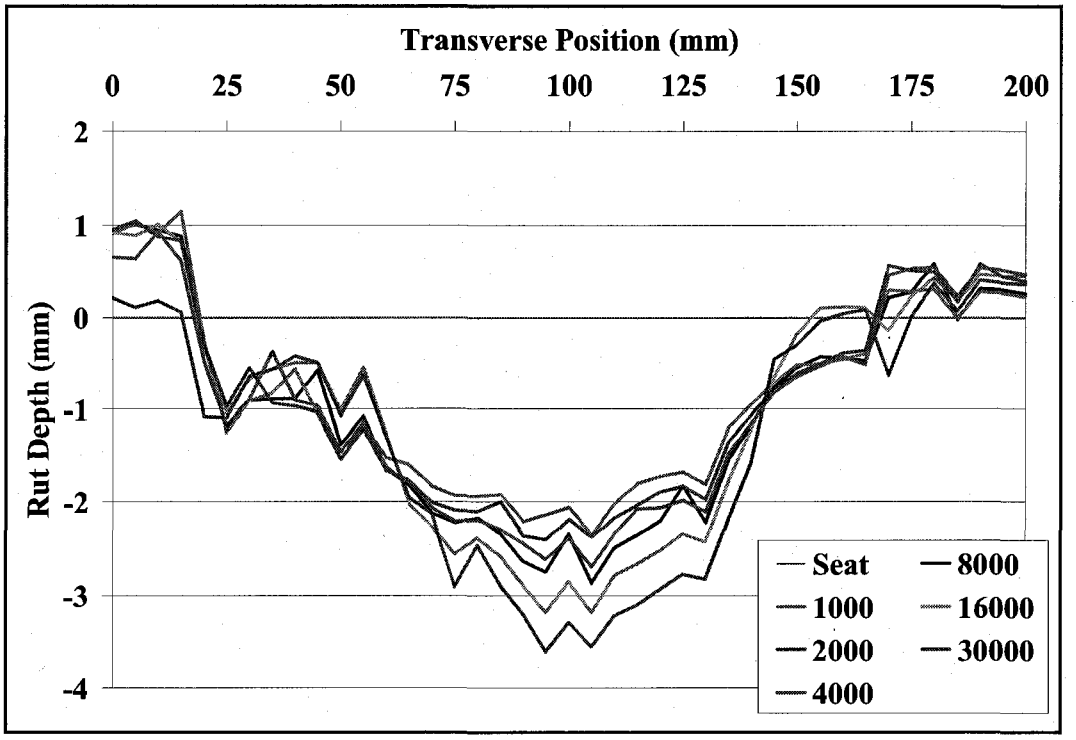

Figure A6.92: Oss 19 Field Cores Brick 1 Transverse Profiles

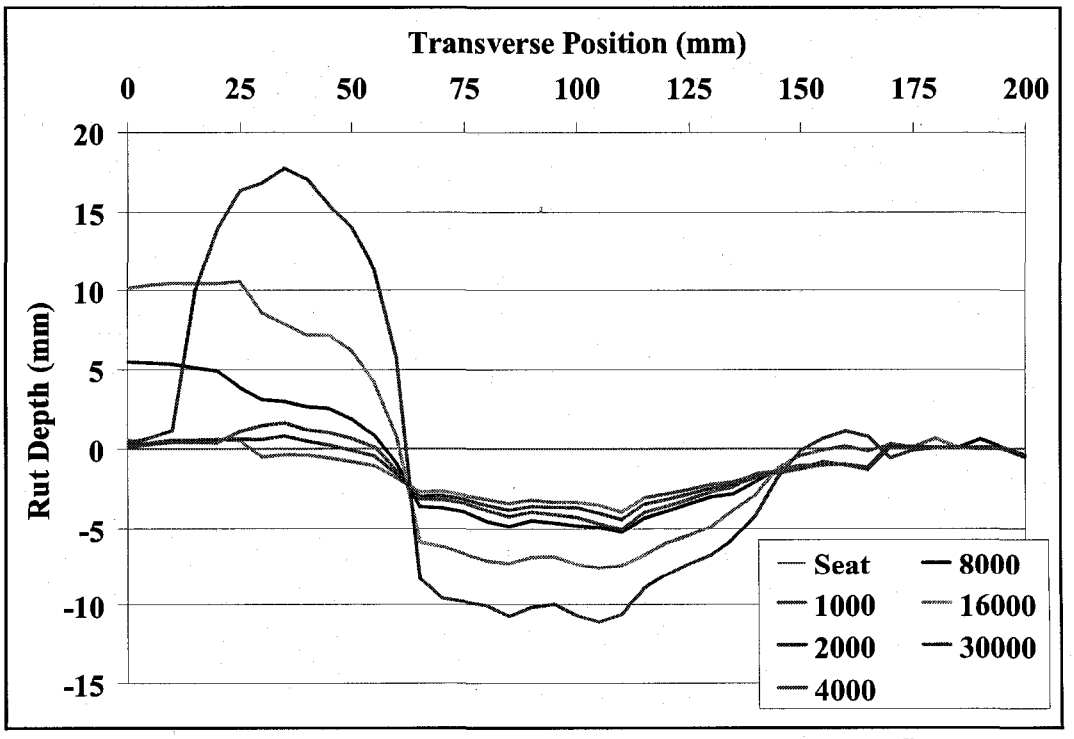

Figure A6.93: Oss 19 Field Cores Brick 2 Transverse Profiles

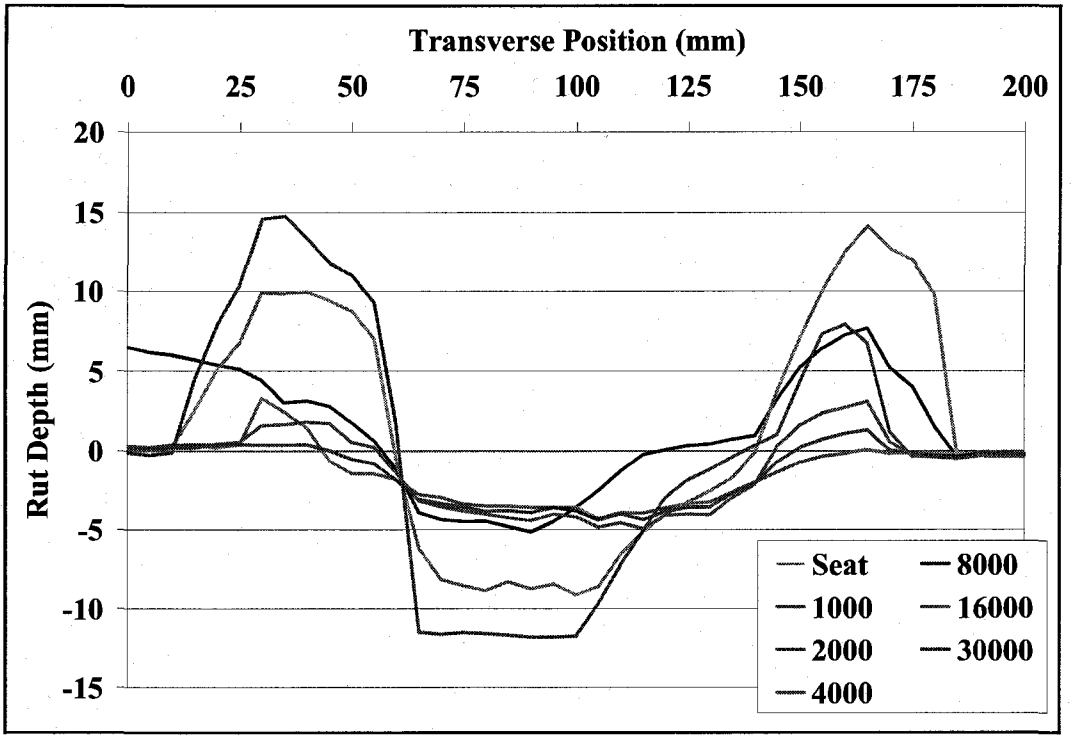

Figure A6.94: Oss 19 Field Cores Brick 3 Transverse Profiles

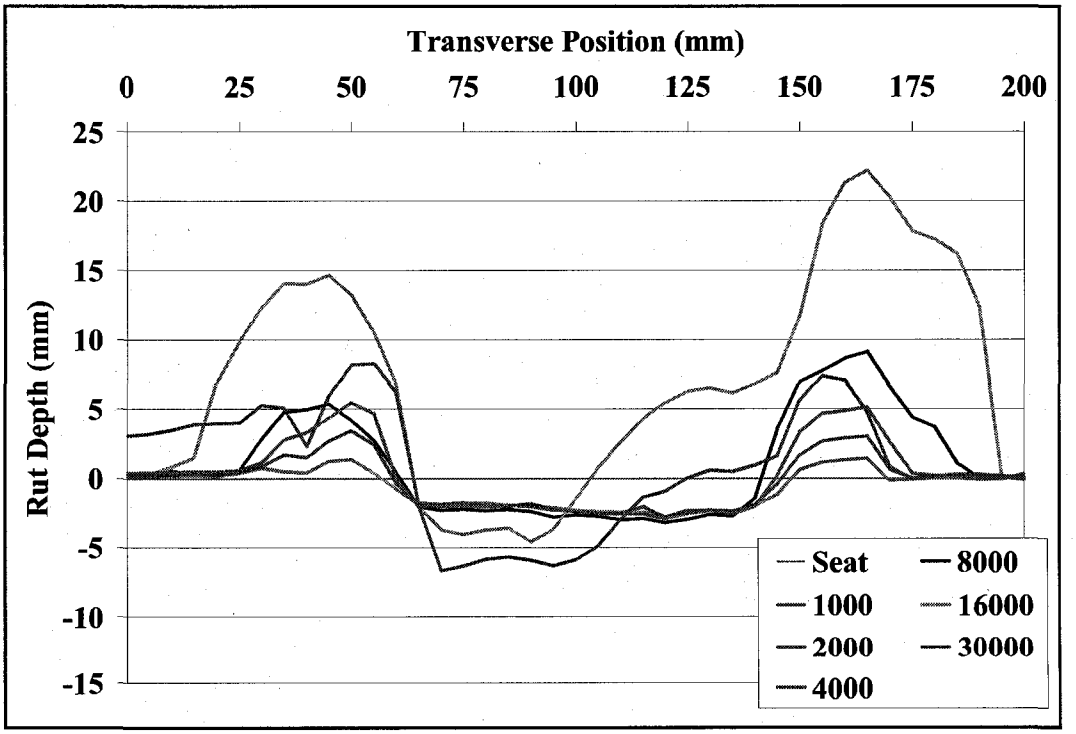

Figure A6.95: Oss 19 Field Cores Brick 4 Transverse Profiles

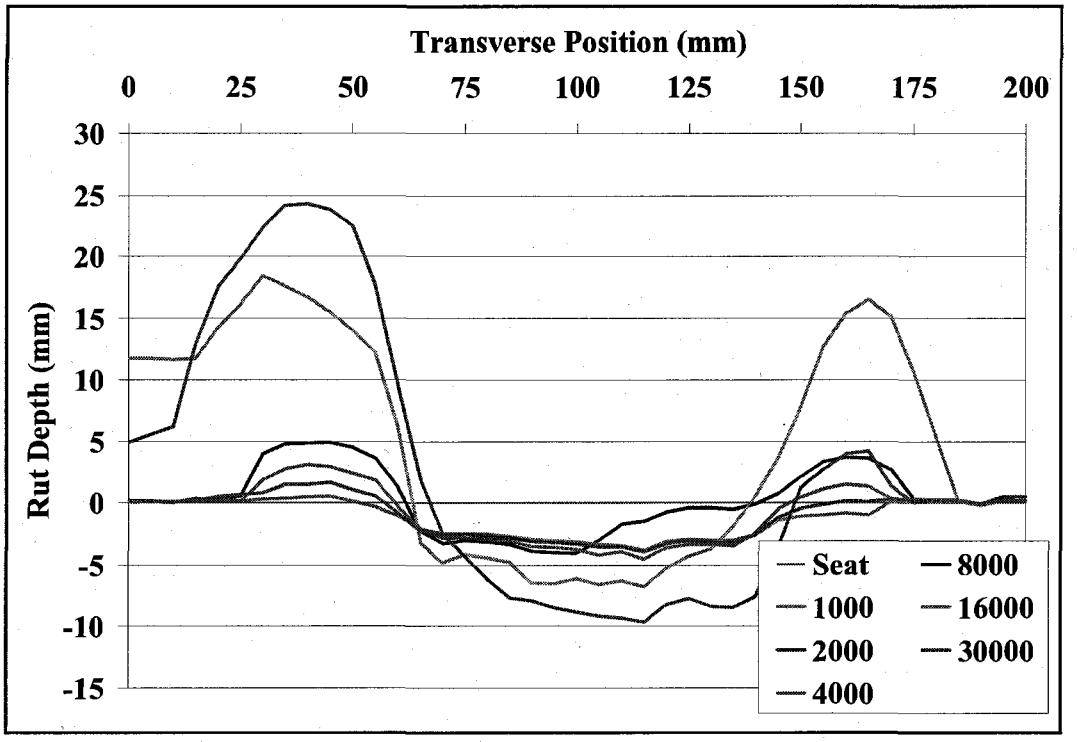

Figure A6.96: Oss 19 Field Cores Brick 5 Transverse Profiles

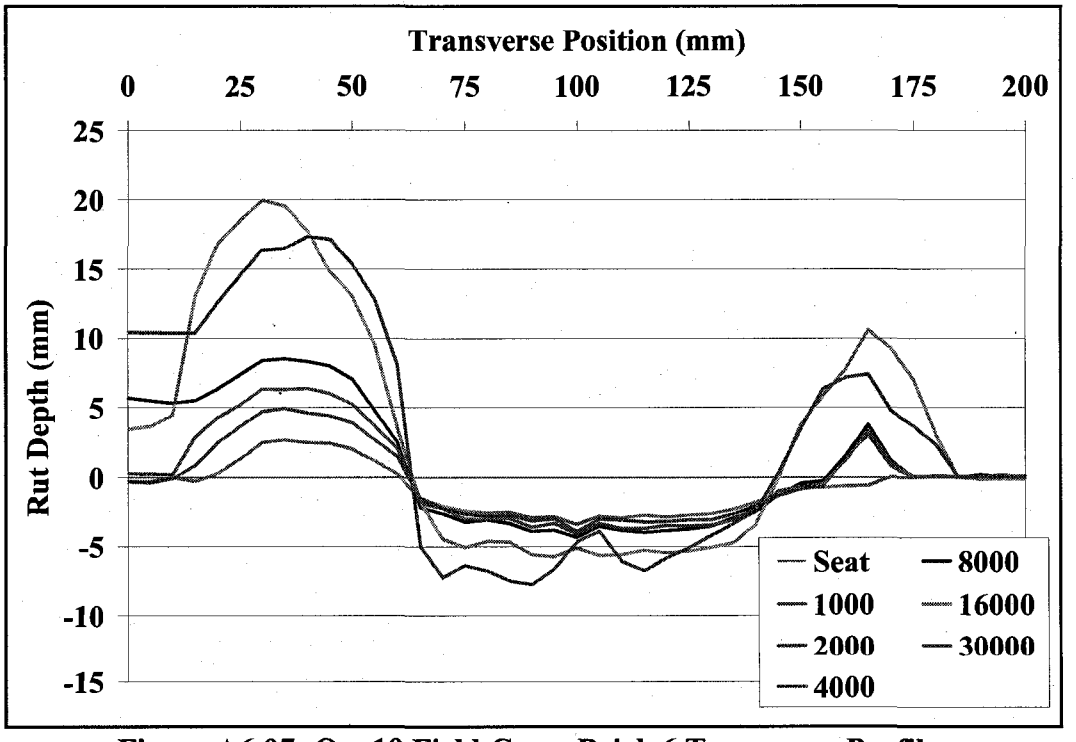

Figure A6.97: Oss 19 Field Cores Brick 6 Transverse Profiles

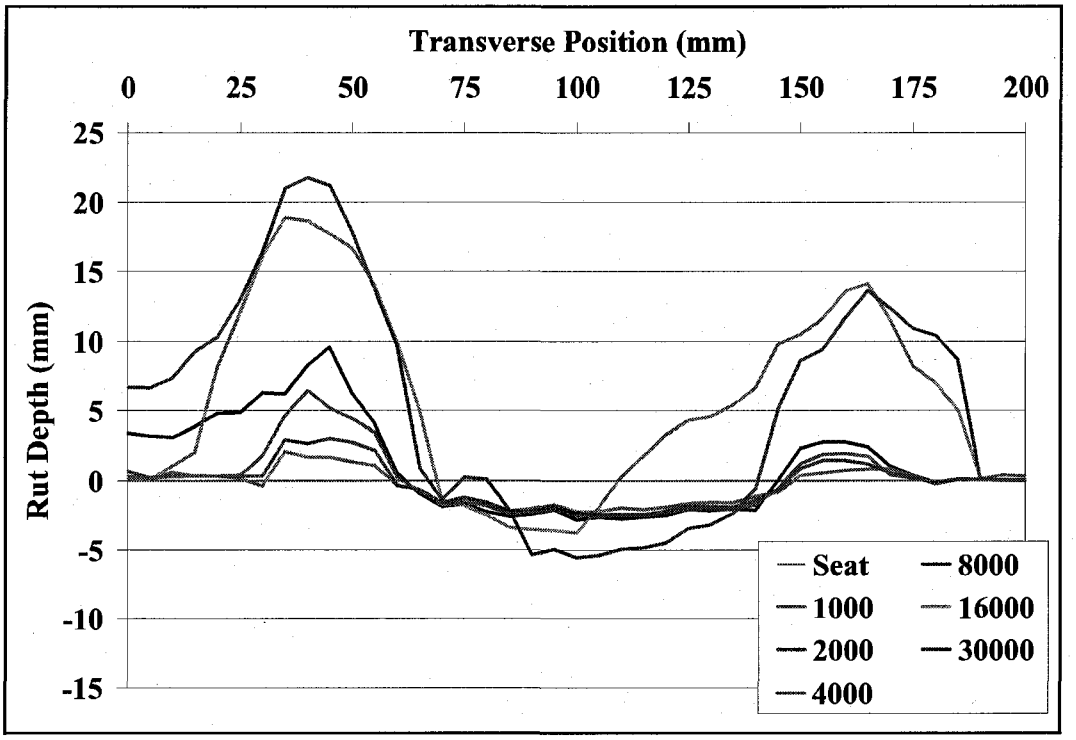

Figure A6.98: Oss 19 Field Cores Brick 7 Transverse Profiles

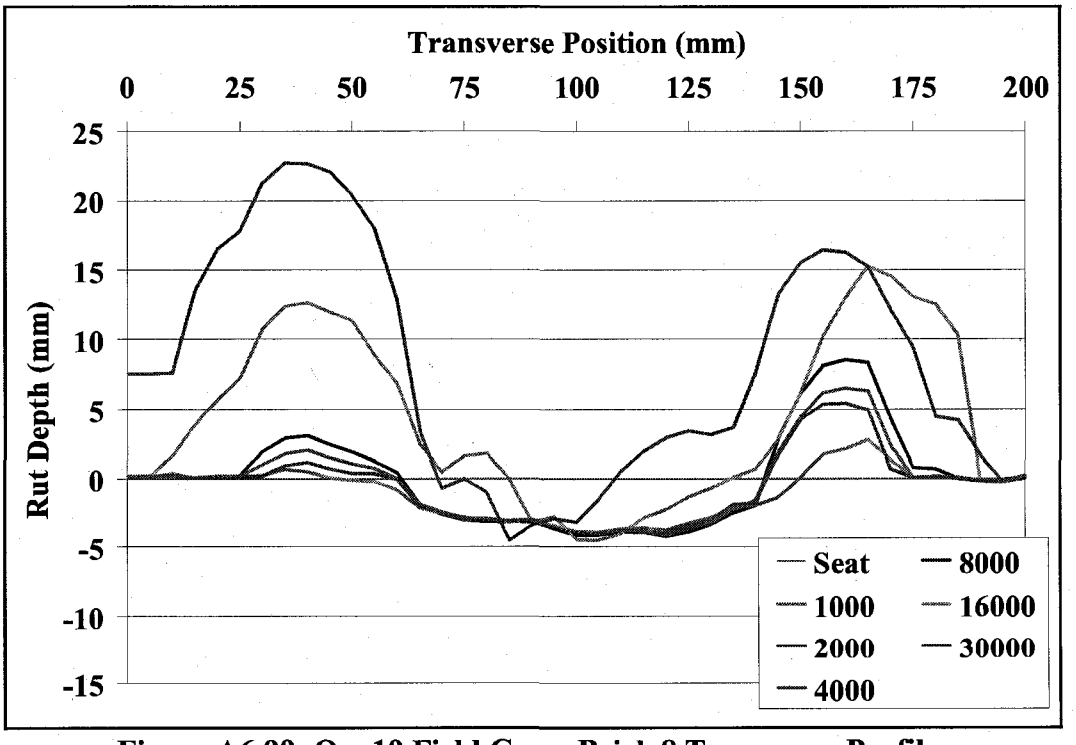

Figure A6.99: Oss 19 Field Cores Brick 8 Transverse Profiles

Table A6.28: Oss 19 Field Cores Avg Rut Depth from Base Line

Brick	Long Pos	Thousands of Loading Cycles					
		1	2	4	8	16	30
1	52.5	1.96	2.12	2.29	2.38	2.71	3.08
2	157.5	3.13	3.50	3.95	4.36	6.62	9.46
3	262.5	3.63	3.85	4.29	4.51	8.27	11.64
4	367.5	2.25	2.28	2.37	2.71	3.89	5.96
5	472.5	3.05	3.21	3.58	3.50	5.55	8.31
6	577.5	2.79	3.10	3.45	3.69	5.26	5.91
7	682.5	1.89	2.09	2.24	2.40	2.83	4.66
8	787.5	3.42	3.53	3.57	3.71	3.80	4.54
Avg		2.67	2.88	3.17	3.36	5.02	7.00

All the highlighted values used a modified range for the average rut

Table A6.29: Oss 19 Field Cores Max Rut Depth from Base Line

Brick	Long Pos	Thousands of Loading Cycles					
		1	2	4	8	16	30
1	52.5	2.35	2.39	2.69	2.86	3.19	3.61
2	157.5	3.95	4.41	5.01	5.22	7.51	11.11
3	262.5	4.27	4.38	4.92	5.11	9.11	11.79
4	367.5	2.78	2.82	2.92	3.20	4.59	6.70
5	472.5	3.77	3.92	4.50	4.02	6.76	9.65
6	577.5	3.36	3.87	4.08	4.33	5.72	7.73
7	682.5	2.16	2.41	2.53	2.79	3.75	5.54
8	787.5	3.94	4.03	4.17	4.24	4.50	4.54
Avg		3.24	3.46	3.81	3.93	5.81	8.02

Table A6.30: Oss 19 Field Cores Max Rut Depth from Max Heave

Brick	Long Pos	Thousands of Loading Cycles					
		1	2	4	8	16	30
1	52.5	3.50	3.44	3.62	3.87	4.19	4.02
2	157.5	4.62	5.23	6.67	10.67	18.09	28.88
3	262.5	7.58	5.70	8.00	12.78	23.27	26.56
4	367.5	4.20	6.23	8.38	12.27	26.78	14.98
5	472.5	4.31	5.55	7.60	8.92	25.19	33.99
6	577.5	6.02	8.80	10.43	12.87	25.69	25.04
7	682.5	4.27	5.40	8.96	12.36	22.65	27.29
8	787.5	6.74	9.43	10.68	12.74	19.75	27.27
Avg		4.93	5.76	7.67	10.53	20.84	22.97

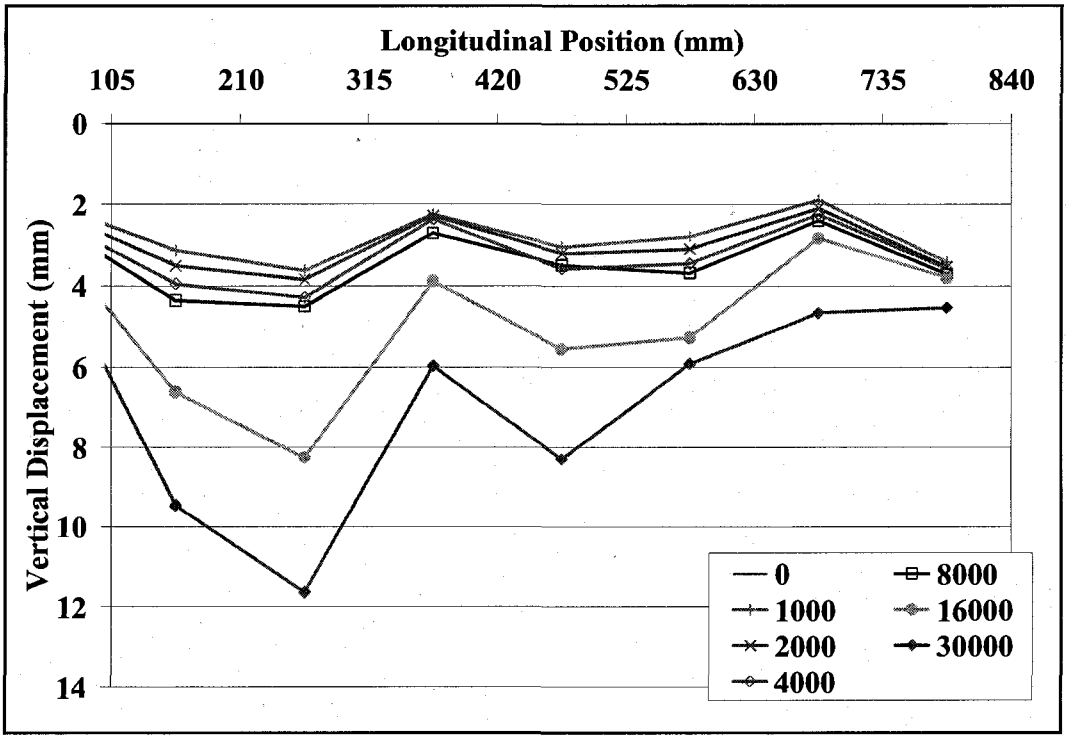

Figure A6.100: Oss 19 Field Cores Avg Rut from Base Line Longitudinal Profiles

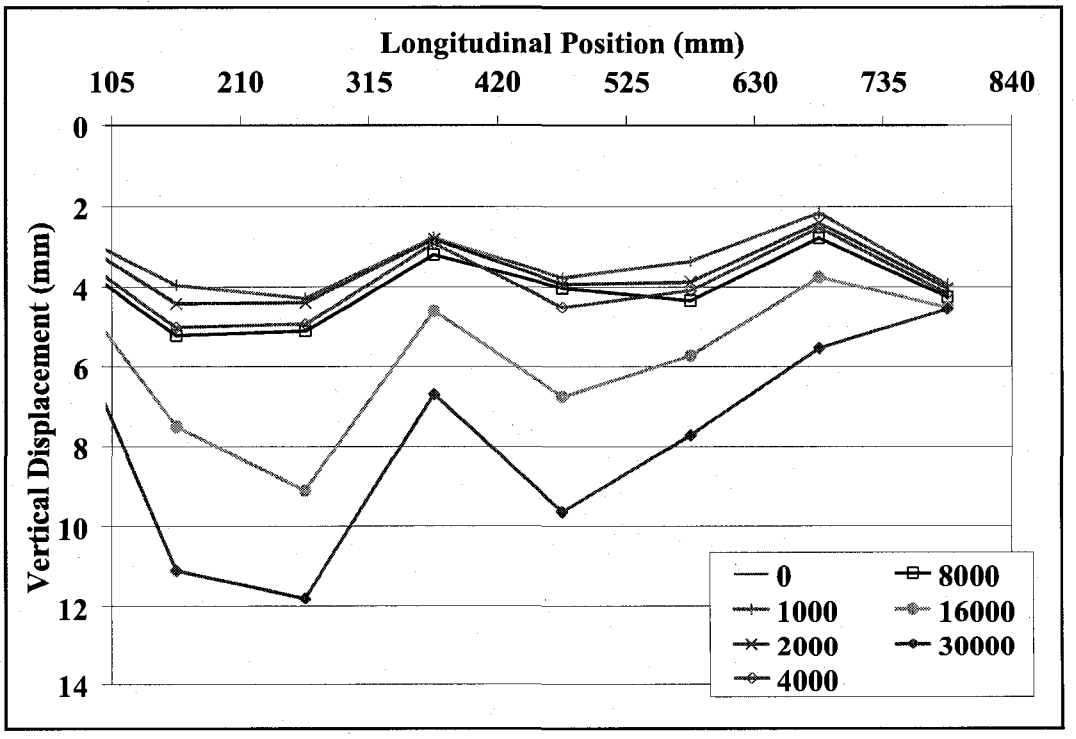

Figure A6.101: Oss 19 Field Cores Max Rut from Base Line Longitudinal Profiles

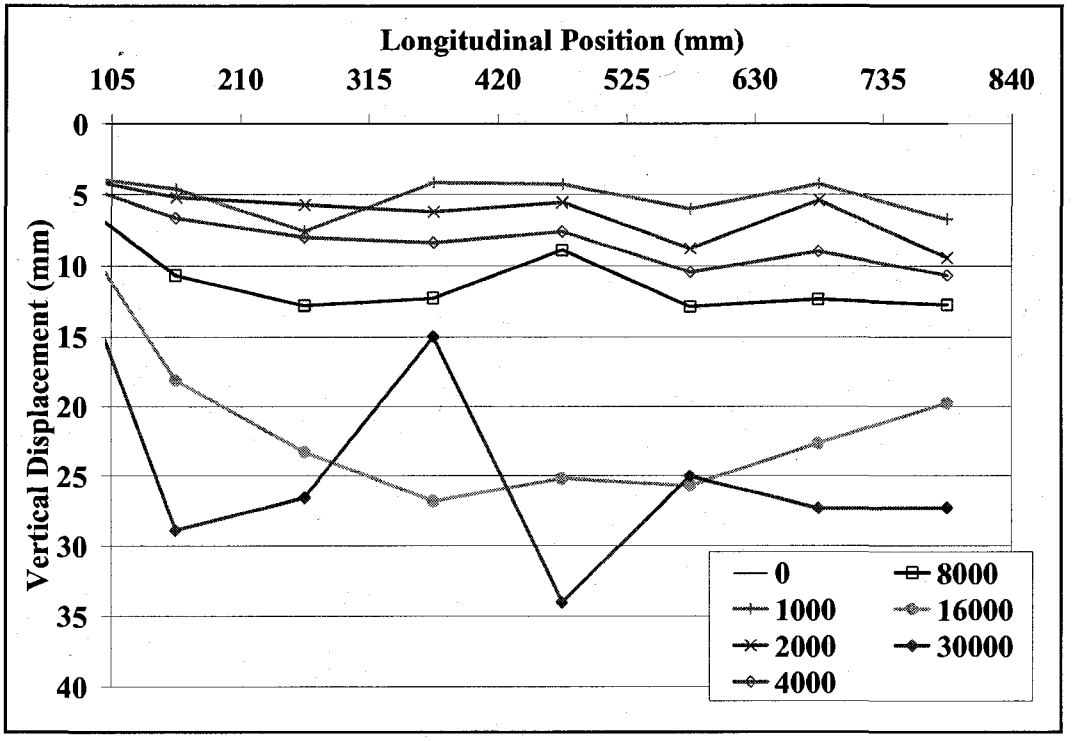

Figure A6.102: Oss 19 Field Cores Max Rut from Max Heave Longitudinal Profiles

Test Logs and Temperature Data

For all test logs, the Counter column shows the reading on the control box. Every time the control box was shut off and turned back on the counter increments by 1. The Relative column is the number of cycles run for that test only.

Oss 12.5

Table A6.31: Oss 12.5 MMLS3 Test Log

Action	Time	Date	Counter	Relative	Notes
Heat	1:44	1/12/2006	155482	0	
Profile	10:14		155482	0	
MMLS	10:42		155483	0	Seating load, no heat and vents off, approx 10 axles at 10 on the speed dial
Profile	10:42		155484	10	
Heat	11:10		155484	10	Heated to warm asphalt back up after first two profiles
MMLS	12:10		155485	10	
Profile	12:19		155585	1000	AIR thermocouple got caught under profilometer during #7 profile - screwed up profilometer for a bit
Demo	13:05		155586	1000	Demonstration, no heat and vents off
Heat	13:07		155600	1000	Search for Dr. Daniel
MMLS	13:30		155600	1000	
Profile	13:40		155700	2000	
Heat	14:05		155700	2000	Took a nap
MMLS	16:42		155700	2000	
Profile	17:00		155901	4000	
MMLS	17:28		155901	4000	
Profile	18:03		156300	8000	
MMLS	18:25		156300	8000	
Heat	19:34		157100	16000	Personal break
Profile	20:33		157100	16000	
MMLS	20:53		157100	16000	
Profile	22:54		158500	30000	
Heat	23:16		158500	30000	Personal break
MMLS	0:07	1/13/2006	158500	30000	
Profile	2:59		160500	50000	
MMLS	3:22		160500	50000	
Profile	7:00		163000	75000	
MMLS	7:27		163000	75000	
Profile	11:05		165500	100000	

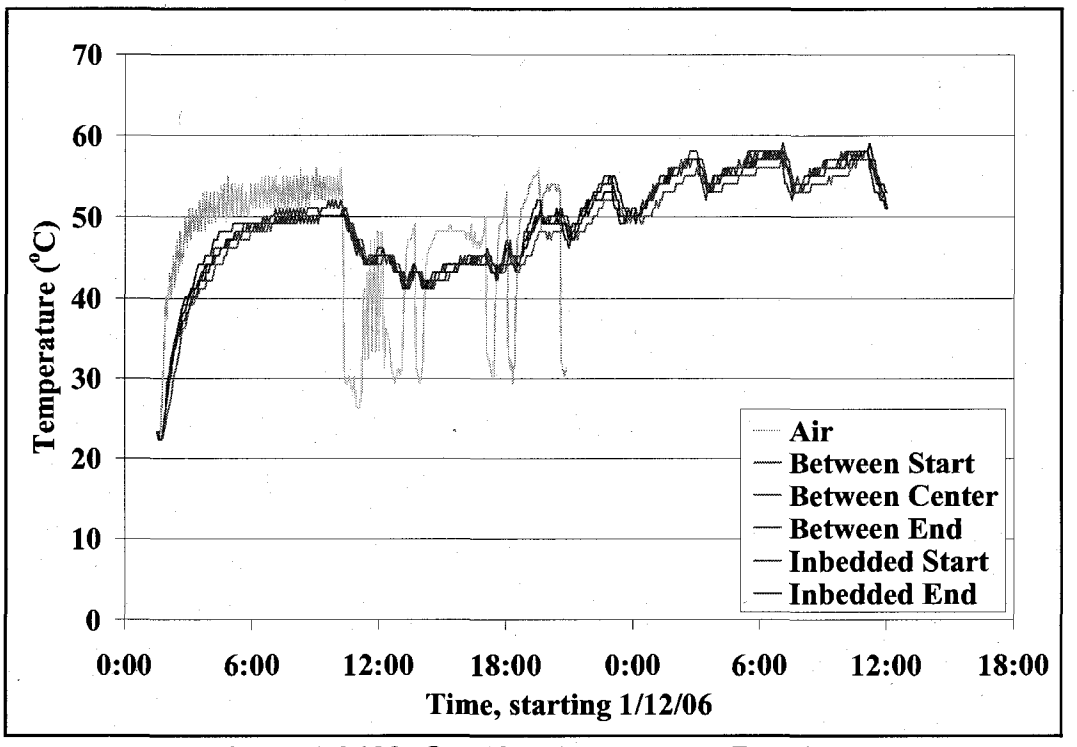

Figure A6.103: Oss 12.5 Temperature Readings

Oss 19

Table A6.32: Oss 19 MMLS3 Test Log

Action	Time	Date	Counter	Relative	Notes
Heat	00:25	10/30/05	144293	0	
Profile	15:43		144293	0	MMLS wouldn't start after the 0 load profile. I had to take off the envi. chamber and check connections and pull the track to make sure all small castor wheels were on the track. I tested it for a few cycles (~5 sec.) put envi. chamber back on and continued.
MMLS	16:34		144296	0	
Profile	16:42		144396	1000	
MMLS	17:07		144397	1000	
Profile	17:16		144497	2000	
MMLS	17:45		144498	2000	
Profile	18:02		144698	4000	
MMLS	18:27		144699	4000	
Profile	19:02		145099	8000	
MMLS	19:26		145100	8000	
Profile	20:36		145906	16000	I missed the turn-off time and stopped the MMLS at ~16060 cycles by mistake. I realized that during this last run I forgot to turn on the heater.

Table A6.32: Oss 19 MMLS3 Test Log (continued)

Action	Time	Date	Counter	Relative	Notes
					Also I forgot to tighten the jack screws on the End side. They did move by some unknown amount and there may have been heave on the End side due to this uneven loading.
Heat	21:00		145906	16000	
Off	22:42		145906	16000	Turned off heater to readjust jack screws on End side - no sure if they're perfect. I did it with a wheel resting on samples #6 and #7
Heat	22:56		145906	16000	
MMLS	00:48	10/31/05	145907	16000	I opened the end panels to lower jack screws with out turning heater off before starting the MMLS
Profile	02:49		147307	30000	
MMLS	03:15		147307	30000	
Profile	06:07		149307	50000	
Off	06:40		149307	50000	Everything was shut off because the room was needed by another class
Heat	18:35	11/01/05	149307	50000	Heat turned back on to finish the last 50k cycles of the test
MMLS	22:58		149308	50000	Again lowered jack screws without turning the heater off, before starting the MMLS.
Adjust	23:03		149361	50530	Noticed that there was a squeaking while the MMLS was running. I checked under the heater vent and found it was shaking due to uneven legs.
					I stopped the MMLS and raised the jack screws on the Start side until it was "OK".
MMLS	23:10		149361	50530	Squeaking persists - I will let it continue and will lubricate the machine after the test
Profile	02:34	11/02/06	151808	75000	
MMLS	02:57		151808	75000	
Off	08:15		155482	111740	I turned off the MMLS late. I left the machine raised to take the profile later on
Profile	17:45		155482	111740	for future reference: if you miss a stop point by a lot, let it run to a full 1000 cycle increment before stopping for convenience sake.

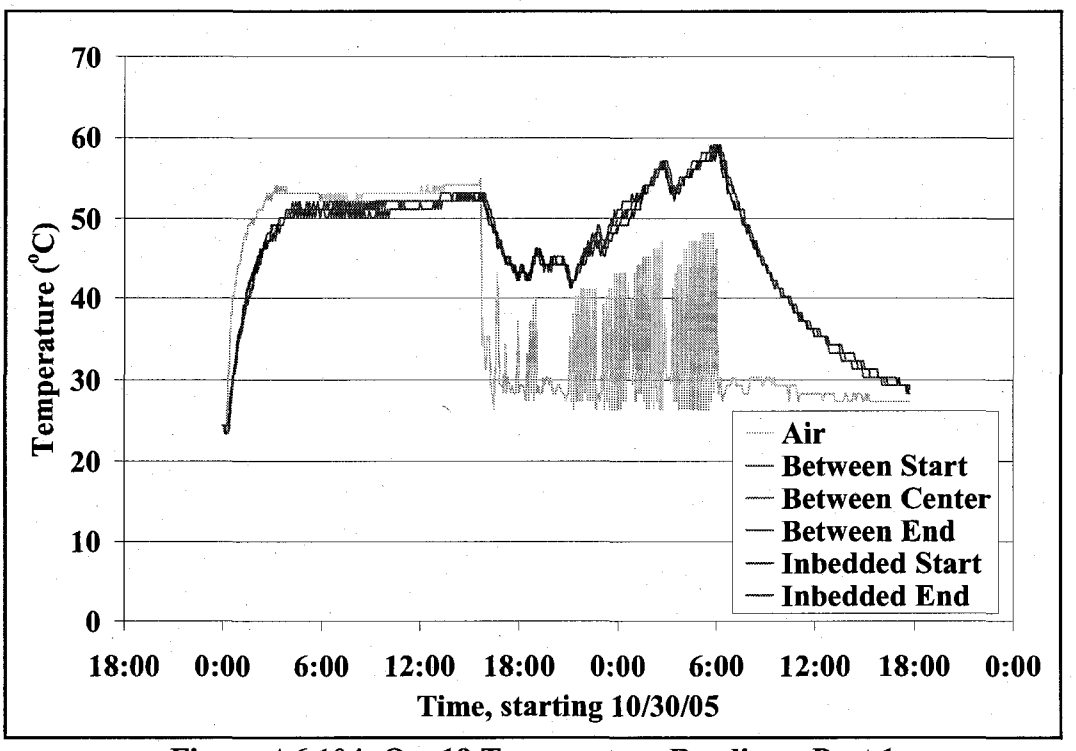

Figure A6.104: Oss 19 Temperature Readings, Part 1

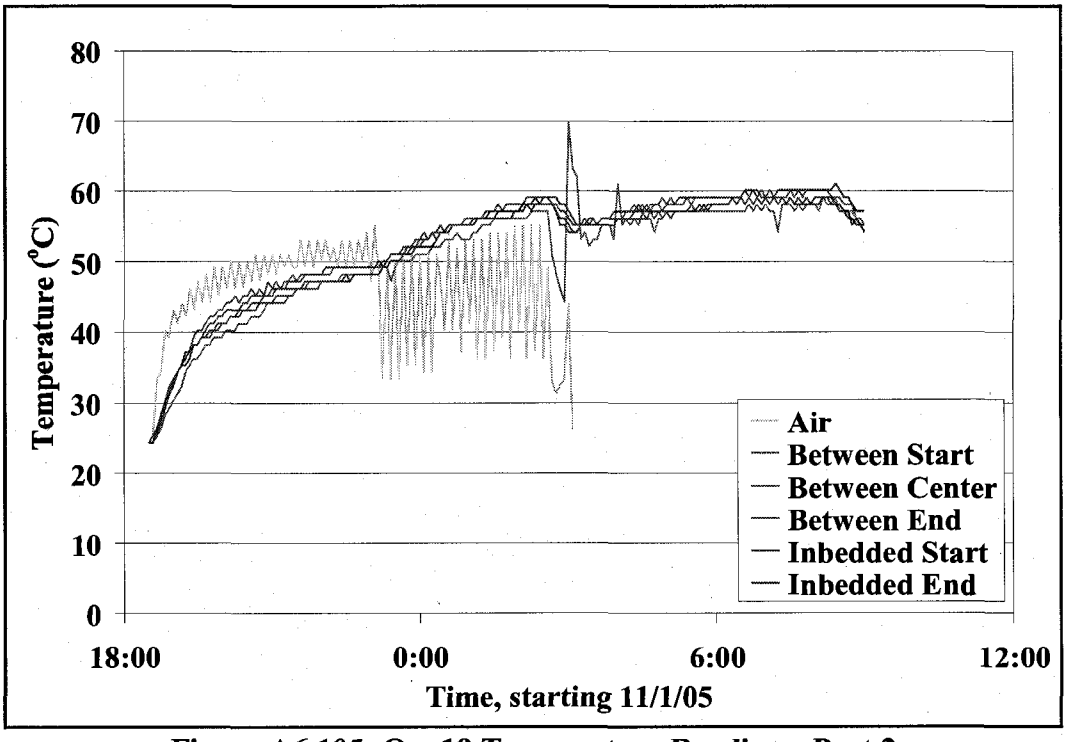

Figure A6.105: Oss 19 Temperature Readings, Part 2

Cont 12.5

Table A6.33: Cont 12.5 MMLS3 Test Log

Action	Time	Date	Counter	Relative	Notes
Profile	20:00	3/14/2006	165500	0	
MMLS	17:00	3/15/2006	165501	0	seating load, specimens cold, approx 10 axles at 10 on the speed dial
Profile	17:05		165503	20	
Heat	23:25		165503	20	beginning of heat, tried using the orange cover only instead of the white environmental chamber
Check	9:55	3/16/2006	165503	20	checked the heat, the heater read 44 C, the inb_strt thermocouple read ~43 C, set heater to 77.5 C
Stop	10:35		165504	20	the MMLS wouldn't start, so I stopped the heater to check things out
Heat	10:42		165505	20	MMLS display: oL3, would not go away even after pushing STOP and flipping off switches.
					I unplugged it, waited 10 sec. and replugged it and started it up and it worked; now heating specimens back up
MMLS	11:00		165505	20	
Profile	11:11		165603	1000	
Heat	12:00		165603	1000	using the orange vinyl cover was too difficult because the MMLS cannot be raised perfectly straight up and down with the crane and it is impractically difficult for one person to do the job, so I put the envi. chamber back on and will raise and lower the jack screws
MMLS	18:51		165603	1000	opened sides to lubricate jack screws before starting MMLS
Profile	18:59		165703	2000	
MMLS	19:22		165703	2000	
Profile	19:39		165903	4000	
MMLS	20:04		165903	4000	
Profile	20:39		166303	8000	
MMLS	21:09		166303	8000	
Heat	22:20		167103	16000	Personal break
Profile	23:45		167103	16000	
MMLS	0:07	3/17/2006	167103	16000	
Profile	2:11		168503	30000	
MMLS	2:44		168504	30000	
Profile	5:37		170504	50000	
MMLS	6:07		170504	50000	
Profile	9:43		173004	75000	
MMLS	10:10		173004	75000	

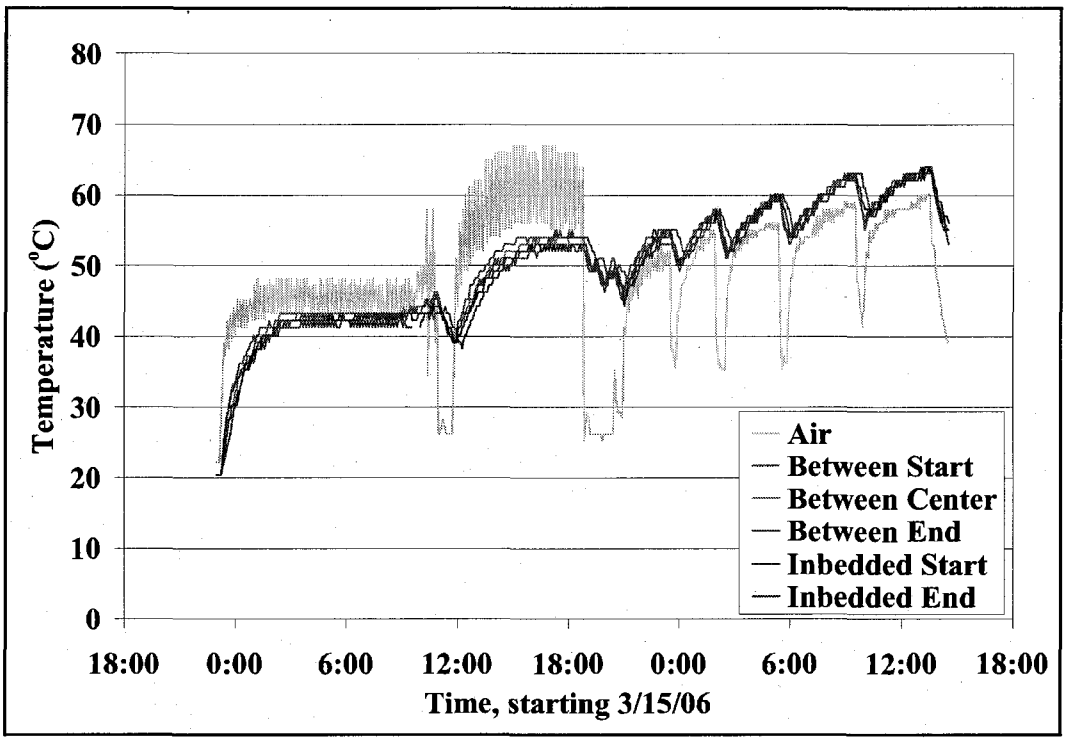

Figure A6.106: Cont 12.5 Temperature Readings

Cont 19

Table A6.34: Cont 19 MMLS3 Test Log

Action	Time	Date	Counter	Relative	Notes
Profile	2:45	3/25/2006	175504	0	
MMLS	3:08		175505	0	seating load, specimens cold, approx 10 axles at 18 on the speed dial
Profile	3:09		175506	10	not much change in profile, probably because I tightened the specimens in so much
Heat	3:52		175506	10	beginning of heat
MMLS	11:23		175506	10	
Profile	11:32		175606	1000	mistake on profile #3: the red line is bad (accidentally took #4 profile), overwrote file
MMLS	12:09		175606	1000	
Profile	12:18		175706	2000	
MMLS	12:46		175708	2000	
Profile	13:16		175908	4000	
MMLS	13:49		175908	4000	
Profile	14:39		176308	8000	
MMLS	15:06		176309	8000	
Profile	16:22		177115	16000	went a few extra axles on this one; should have stopped at 177109
MMLS	17:12		177116	16000	

Table A6.34: Cont 19 MMLS3 Test Log (continued)

Action	Time	Date	Counter	Relative	Notes
Profile	19:15		178510	32000	
Heat	19:43		178510	32000	took time to fix markings on profilometer bar
MMLS	20:07		178510	32000	
Profile	23:28		180587	50000	went a few extra axles on this one; should have stopped at 180510
MMLS	0:01	3/26/2006	180588	50000	
Profile	3:33		183011	75000	
MMLS	4:11		183012	75000	
Profile	7:55		185512	100000	

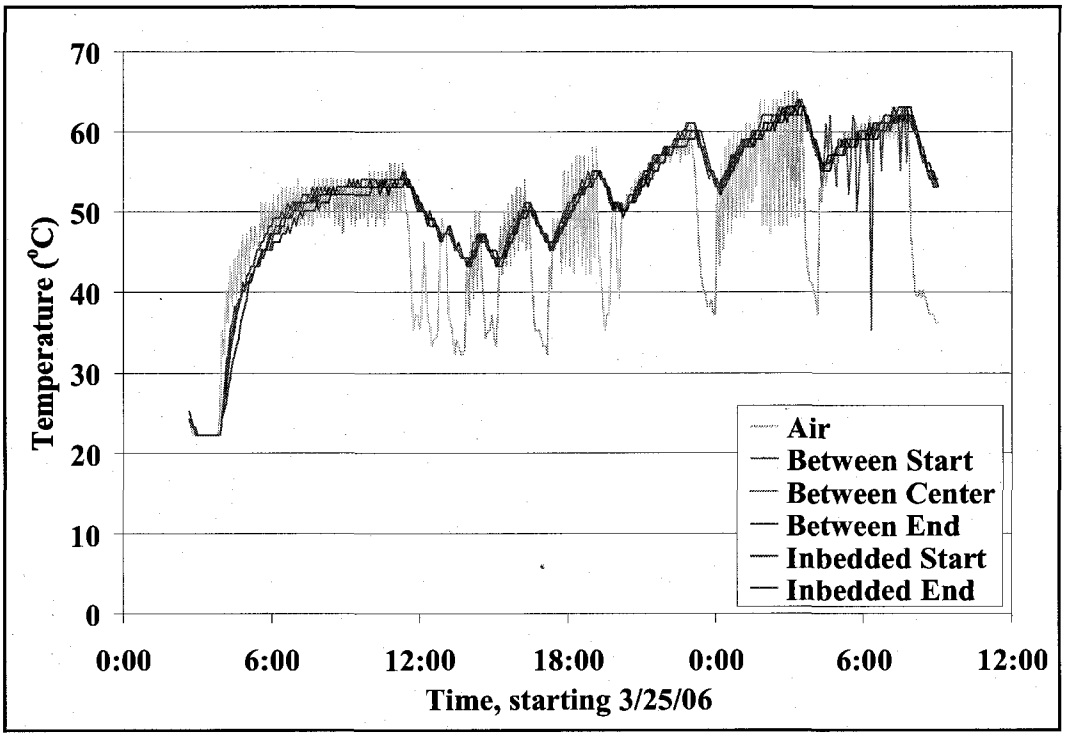

Figure A6.107: Cont 19 Temperature Readings

Farm

The original test log for the Farm MMLS3 test was lost. The log shown is extrapolated from the profile and temperature data files.

Table A6.35: Farm MMLS3 Test Log

Action	Time	Date	Counter	Relative	Notes
Heat	13:45	5/30/2006			
Profile	14:20			0	
MMLS	14:42				
Profile	14:45			10	
Heat	16:30				
MMLS	21:51				
Profile	22:00			1000	
Heat	22:45				
MMLS	23:32				
Profile	23:40			2000	
MMLS	0:13	5/31/2006			
Profile	0:30			4000	
MMLS	1:18				
Profile	1:50			8000	
MMLS	2:13				
Profile	3:20			16000	
MMLS	3:57				
Profile	6:00			30000	
MMLS	6:30				
Heat	9:17				
Profile	10:05			50000	
MMLS	10:45				
Profile	14:15			75000	
MMLS	14:55				
Stop	18:25				
Profile	19:20			100000	

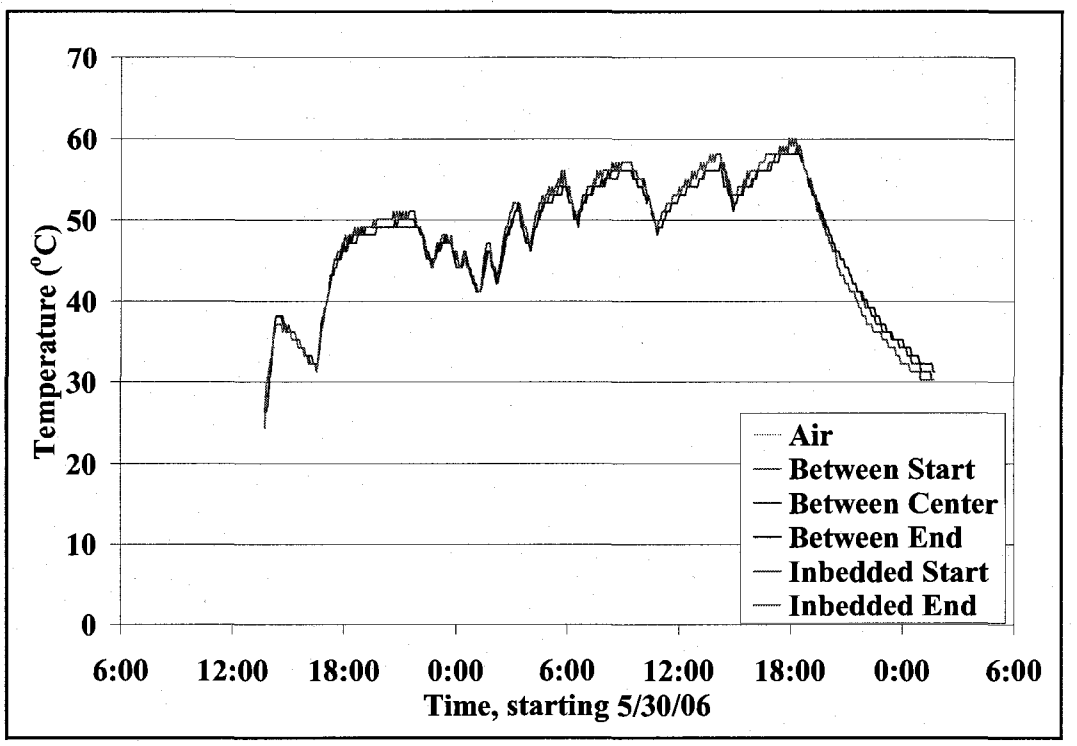

Figure A6.108: Farm Temperature Readings

Hook

Table A6.36: Hook MMLS3 Test Log

Action	Time	Date	Counter	Relative	Notes
Profile	11:35	6/13/2006	195519	0	
MMLS	11:40		195520	0	
Profile	11:45		195521	10	
Heat	12:14		195521	10	
MMLS	18:16		195522	10	
Profile	18:29		195623	1000	
MMLS	18:55		195624	1000	
Profile	19:04		195724	2000	
MMLS	19:27		195725	2000	
Profile	19:44		195925	4000	
MMLS	20:03		195926	4000	
Profile	21:12		196726	12000	
MMLS	21:56		196727	12000	
Profile	21:33		197127	16000	
MMLS	23:10		197128	16000	
Profile	1:12	6/14/2006	198528	30000	
MMLS	1:38		198529	30000	
Profile	4:32		200529	50000	
MMLS	4:56		200529	50000	
Profile	8:34		203029	75000	
MMLS	9:12		203030	75000	
Profile	12:50		205530	100000	

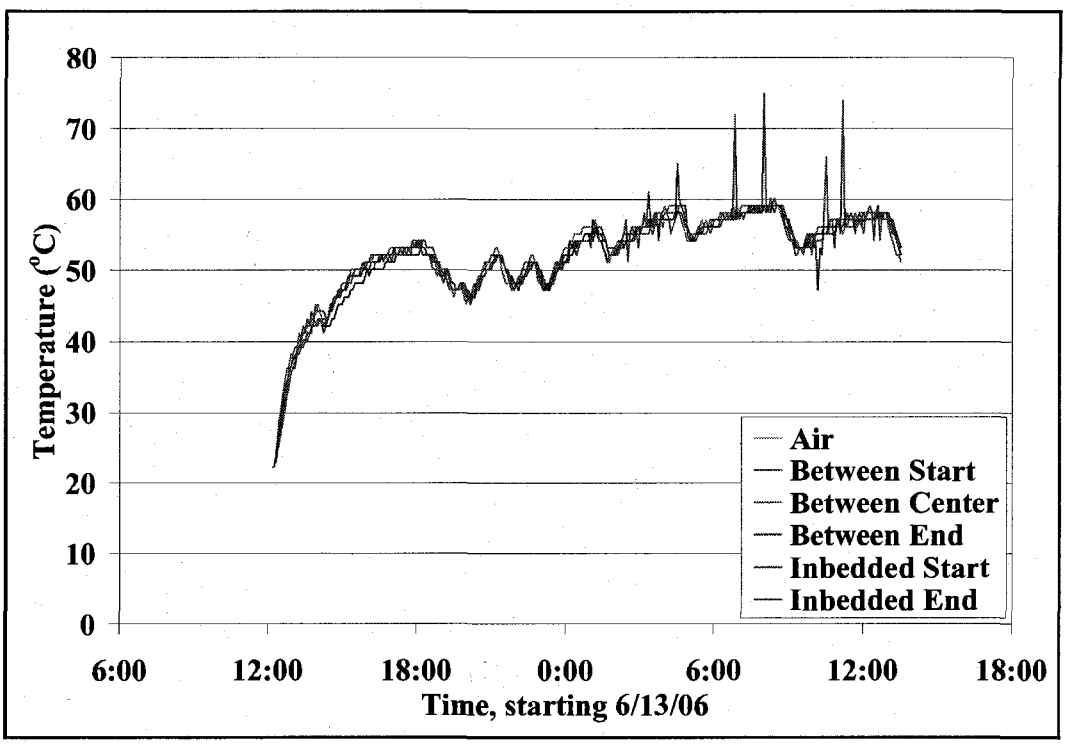

Figure A6.109: Hook Temperature Readings

Oss 12.5 Bailey

Table A6.37: Oss 12.5 Bailey MMLS3 Test Log

Action	Time	Date	Counter	Relative	Notes
Profile	18:00	05/19/08	475260	0	
MMLS	18:27		475261		
Profile	18:30		475263	20	
Heat	19:15		475263		
MMLS	23:31		475263		
Profile	23:39		475363	1000	
MMLS	00:00	05/20/08	475363		
Profile	00:08		475463	2000	
MMLS	00:29		475463		
Profile	00:46		475663	4000	
MMLS	01:10		475663		
Profile	01:43		476063	8000	
MMLS	02:05		476063		
Profile	03:12		476863	16000	
MMLS	03:37		476863		
Stop	05:30		478213	29500	tire #4 blew, will replace and restart test this evening
Profile	20:00		478213		
Heat	20:21		478213		
MMLS	01:00	05/21/08	478213		
Profile	03:50		480263	50000	

Table A6.37: Oss 12.5 Bailey MMLS3 Test Log (continued)

Action	Time	Date	Counter	Relative	Notes
MMLS	04:14		480263		
Profile	07:42		482771	75000	
MMLS	08:05		482771		
Stop	11:32		485263		Heather stopped and raised MMLS at 11:32am, she left heater going
Heat	11:32		485263		
Profile	20:44		485263	100000	

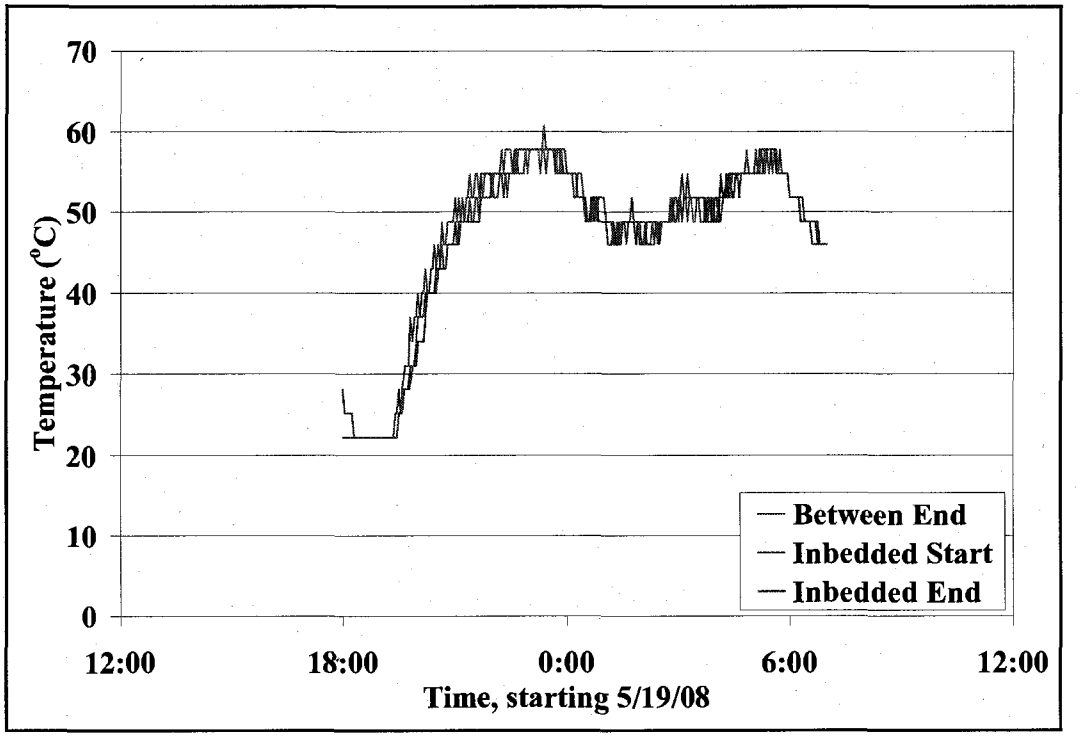

Figure A6.110: Oss 12.5 Bailey Temperature Readings, Part 1

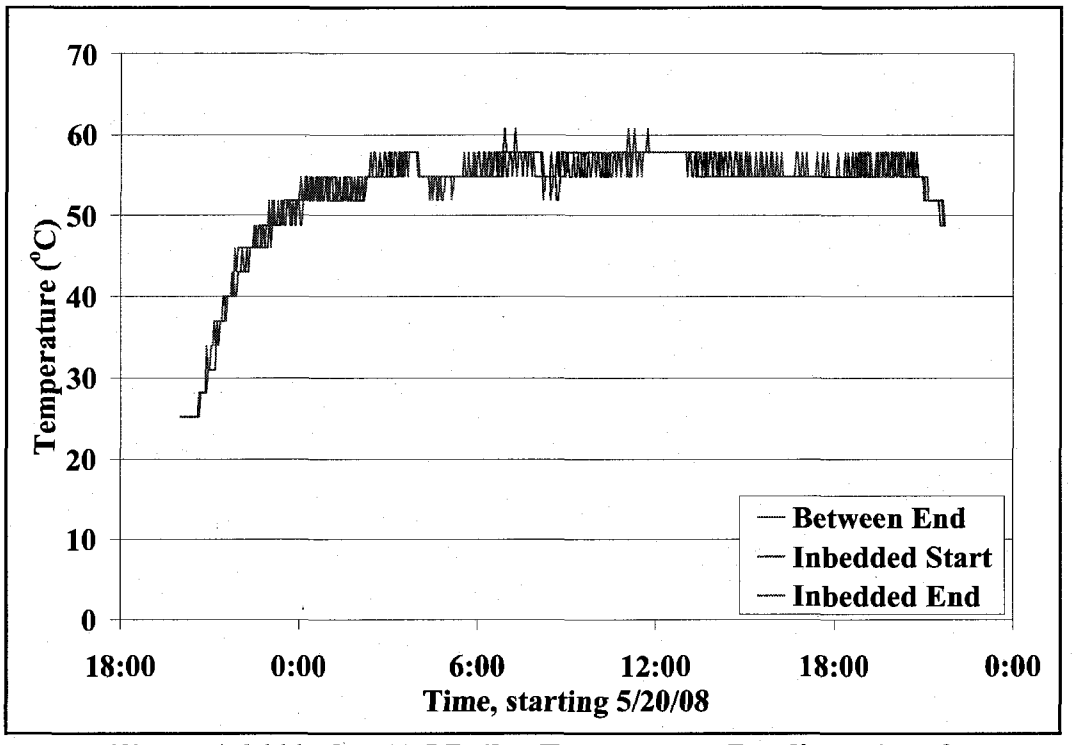

Figure A6.111: Oss 12.5 Bailey Temperature Readings, Part 2

Cont 19 Bailey

Table A6.38: Cont 19 Bailey MMLS3 Test Log

Action	Time	Date	Counter	Relative	Notes
Profile	18:20	06/19/08	505268	0	
MMLS	19:05		505269		
Profile	19:06		505271	20	
Heat	19:52		505271		
MMLS	01:01	06/20/08	505271		
Profile	01:09		505371	1000	
MMLS	01:33		505371		
Profile	01:41		505471	2000	
MMLS	02:02		505471		
Profile	02:18		505671	4000	
MMLS	02:38		505671		
Profile	03:10		506071	8000	
MMLS	03:30		506071		
Profile	04:35		506871	16000	
MMLS	04:56		506871		
Profile	06:59		508371	31000	Over slept a little
MMLS	07:28		508371		
Profile	10:04		510272	50000	
MMLS	10:25		510272		
Profile	13:51		512771	75000	
MMLS	14:13		512771		
Profile	17:39		515271	100000	

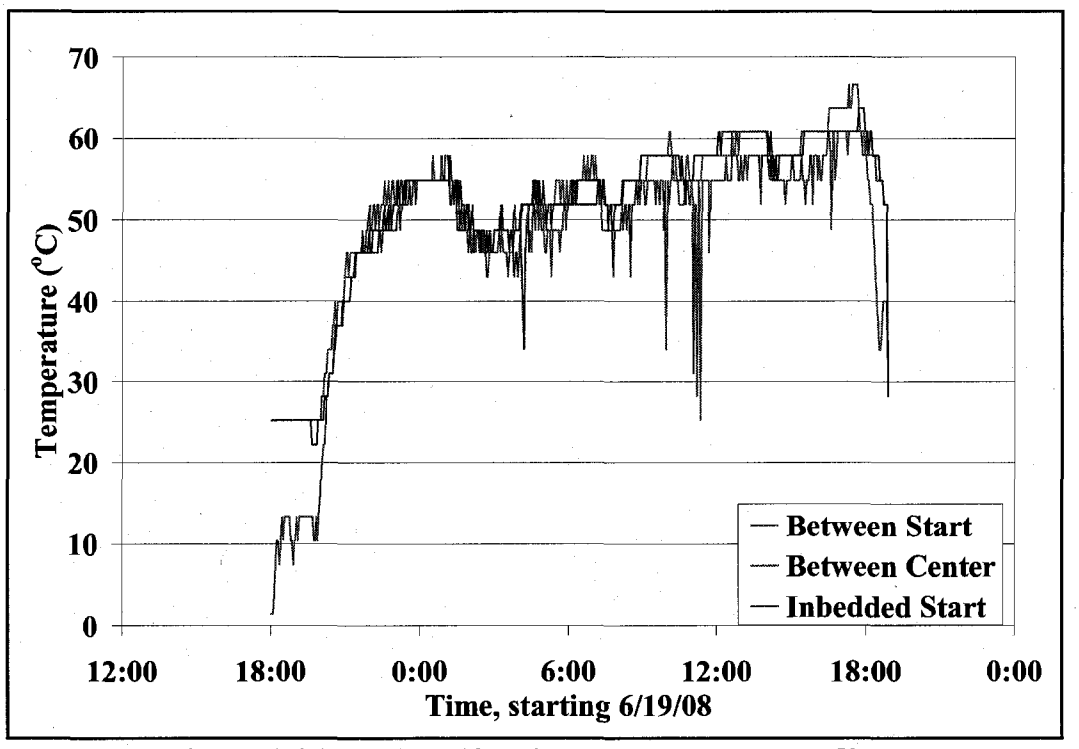

Figure A6.112: Cont 19 Bailey Temperature Readings

Oss 12.5 Field Cores

Table A6.39: Oss 12.5 Field Core MMLS3 Test Log

Action	Time	Date	Counter	Relative	Notes
Start	5:00	9/11/05			Started data collectors, some were not plugged in right away. Inbed Center was put off to the side
Heat	5:30				Started heater
Heat	22:25				Checked Air and Inbed End, readings were approx 50 to 55 C, increased heater setting to 70 C and decided to give it more time to heat up
Profile	2:25	9/12/2005			Checked Inbed End and found it to be 55 C, decided to begin testing with taking profile No. 1 at 0 cycles

The rest of the log file was lost.

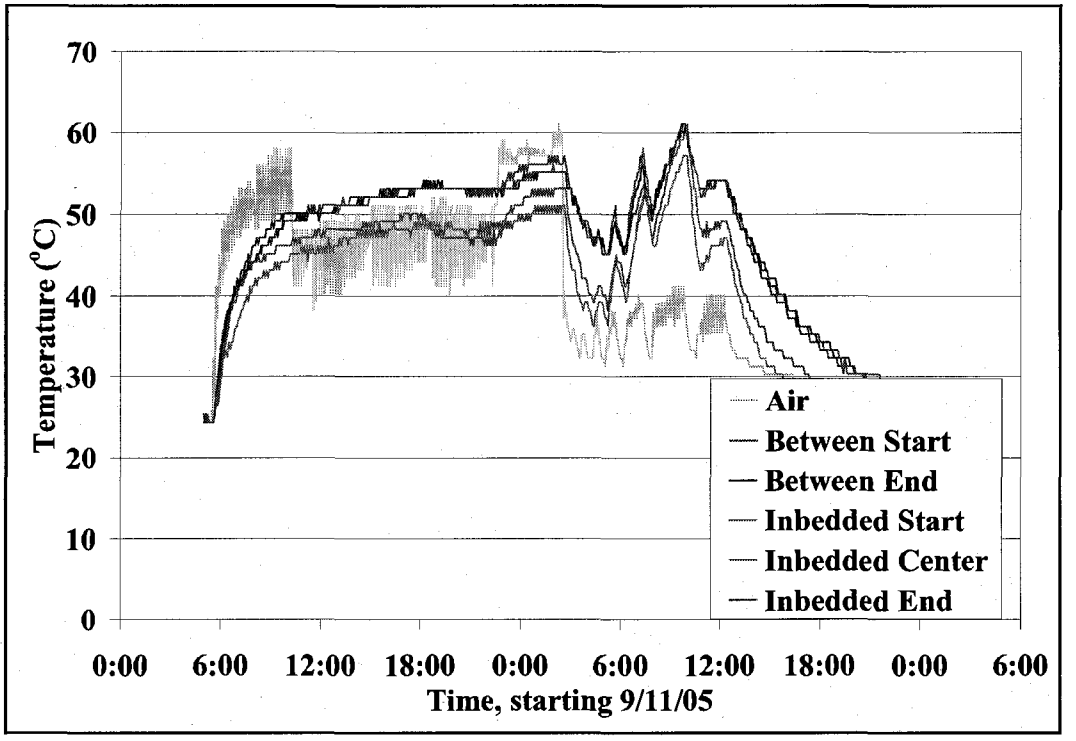

Figure A6.113: Oss 12.5 Field Core Temperature Readings

Oss 19 Field Cores

Table A6.40: Oss 19 Field Core MMLS3 Test Log

Action	Time	Date	Counter	Relative	Notes
Profile	16:00	9/18/05	141290	0	
Heat	19:20		141290	0	started heater
Off	2:20	9/19/2005	141290	0	turned off heater - will start test tomorrow
Heat	15:40		141290	0	Heater turned on - set to 70 C
Heat	21:55			0	checked temperature - was 55 C, increased heater to 75 C
MMLS	1:57	9/20/2005	141291	0	cranked down the MMLS 10 cranks, checked gap and found to be < 10 mm, cranked 2 more and gap was > 10 mm on a 14 1/2 wheel, started run.
					Noticed that when I turn on orange power box, counter increases by 1
Profile	2:05		141391	1000	After initial lowering of machine, I forgot to lock the jack screws, they were out of place after 1000 cycles. I put they back - gap seems OK - not sure they are in the right spots/ heights
MMLS	2:33		141391	1000	

Table A6.40: Oss 19 Field Core MMLS3 Test Log (continued)

Action	Time	Date	Counter	Relative	Notes
Profile	2:42		141491	2000	During 0840 profile, a piece of asphalt seemed to interfere w/ profile. Looked like large heave.
					Upon inspection I found a broken piece - I removed it and retook the profile
					NOTE: Lift profilometer to move, do not slide or drag
MMLS	3:08		141491	2000	
Profile	3:26		141691	4000	Personal break
MMLS	4:07		141691	4000	
Profile	4:42		142091	8000	Personal break
Heat	5:08		142091	8000	turned heater back on, left MMLS raised
MMLS	6:59		142092	8000	
Profile	8:08		142892	16000	retook the #7 profile because it looked horrible – was the same.
					the #5 profile topped out due to debris
					C-01 16000 cycles -> didn't work
					raised profilometer 10 mm
Heat	10:14		142892	16000	Heat back on
MMLS	12:01		142893	16000	lowered MMLS 1 crank to give 10 mm gap; gap was just at 10mm
Profile	14:02		144293	30000	

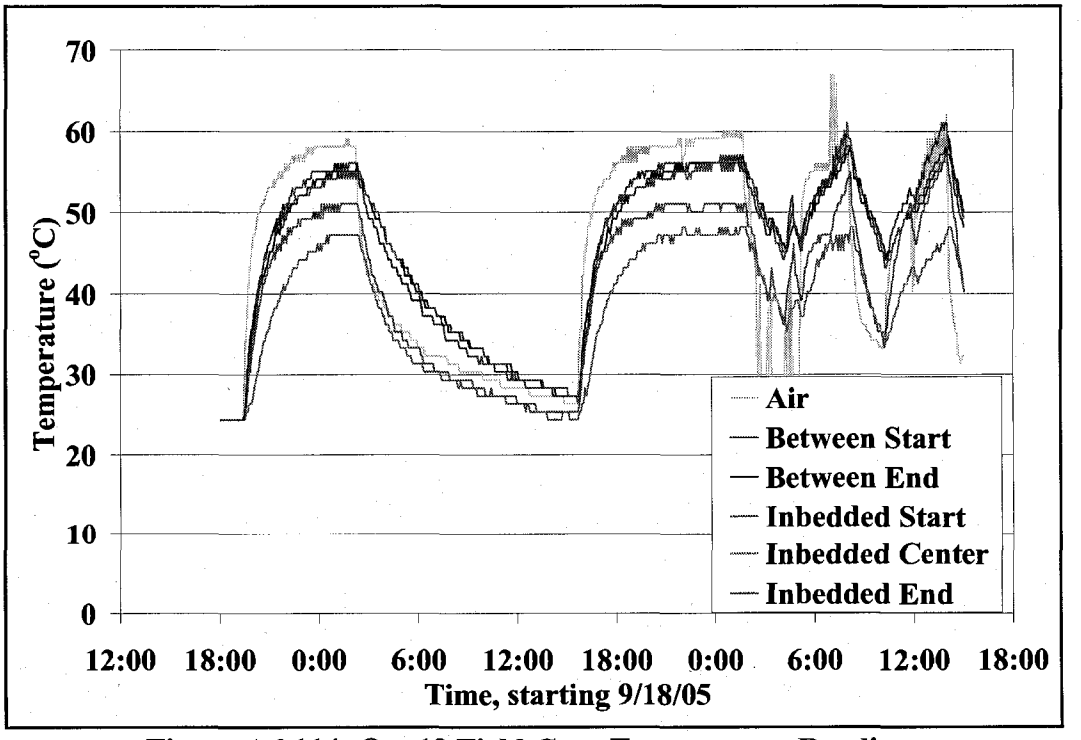

Figure A6.114: Oss 19 Field Core Temperature Readings

APPENDIX 7

STATISTICAL COMPARISONS

The statistical test used for this project was the Mann-Whitney/Wilcoxon Rank Sum Test. The average rut depths for the Oss 12.5-Original and the Oss 12.5-Bailey MMLS3 tests will be used to explain how the test works. Tables A7.1 and A7.2 show the average rut depth measurements for these tests.

Table A7.1: Oss 12.5-Original Avg Rut Depth

Brick	Long Pos	Thousands of Loading Cycles								
		1	2	4	8	16	30	50	75	100
1	157.5	1.20	1.24	2.06	2.15	3.14	4.22	5.17	5.77	6.18
2	262.5	0.27	0.82	1.47	1.46	2.31	2.63	3.39	4.41	4.38
3	367.5	0.05	0.26	0.65	0.61	1.06	1.10	1.56	2.45	2.61
4	472.5	0.78	0.84	0.99	1.14	1.32	1.65	1.92	2.18	2.38
5	577.5	0.63	1.03	0.55	1.22	1.06	1.58	2.02	2.27	2.84
6	682.5	0.62	1.15	0.99	1.29	1.66	2.35	3.09	3.37	3.60
7	787.5	0.55	0.65	1.12	1.56	2.12	2.48	2.88	3.11	3.22

Table A7.2: Oss 12.5-Bailey Avg Rut Depth

Brick	Long Pos	Thousands of Loading Cycles								
		1	2	4	8	16	30	50	75	100
1	157.5	0.80	0.95	1.19	1.30	1.54	2.02	2.31	2.70	2.93
2	262.5	0.91	0.84	1.05	1.38	1.05	1.85	1.79	2.06	2.06
3	367.5	0.93	1.17	1.21	1.27	1.26	1.58	1.54	1.81	1.80
4	472.5	1.09	1.23	1.31	1.33	1.40	1.69	1.77	1.98	2.16
5	577.5	1.44	1.44	1.94	1.48	1.54	1.85	1.93	2.18	2.52
6	682.5	0.40	0.55	0.60	0.58	0.63	0.90	0.85	1.07	1.26
7	787.5	0.41	0.65	0.69	0.63	0.59	0.94	0.88	1.04	1.11

A separate statistical comparison was done at each measuring point in the tests. Therefore, a total of nine separate comparisons are calculated for these two data sets. For a single comparison, the first step is to combine the values from both data sets into a single list. This list is then arranged in order from highest to lowest while keeping a tab on which data set each value originally came from. Once the values are in order, each is assigned a rank; the highest is rank 1 and the lowest is rank 14. An example using the rut depths at 4,000 loading cycles is shown in Table A7.3.

Table A7.3: Combined Rut Values at 4,000 Loading Cycles

Data Set	Rut Value	Rank
Original	2.06	1
Bailey	1.94	2
Original	1.47	3
Bailey	1.31	4
Bailey	1.21	5
Bailey	1.19	6
Original	1.12	7
Bailey	1.05	8
Original	0.99	9
Original	0.99	10
Bailey	0.69	11
Original	0.65	12
Bailey	0.60	13
Original	0.55	14

At this point, the values with their assigned rank are split up into their respective data sets again. Then, ranks in each data set are totaled. The sums of the ranks from each data set are the test statistics for the comparison. Table A7.4 shows the two data sets with their sums of ranks.

Table A7.4: Sum of Ranks

Brick	Oss 12.5 Original		Oss 12.5 Bailey	
	Rut Value	Rank	Rut Value	Rank
1	2.055	1	1.186	6
2	1.468	3	1.053	8
3	0.654	12	1.208	5
4	0.989	10	1.312	4
5	0.554	14	1.937	2
6	0.994	9	0.602	13
7	1.122	7	0.693	11
Sum		56		49

In this example, the sums, 56 and 49, differ by 7. The p-value for these two test statistics is 0.7104. This means that there is approximately a 71% chance that one would get two sums of ranks at least 7 apart if the ranks were randomly assigned to each data set. For a p-value this high, the null hypothesis is not rejected. In this case the null hypothesis says that the two data sets are not significantly different. For the rut values measured 46,000 cycles later, the two rank sums are 70 and 35. The probability that one would get two sums 35 apart by random chance with only ranks 1 through 14 to work with is about 3%. The limit for the p-value is 0.05, which is 5%. Therefore, at 50,000 loading cycles the null hypothesis is rejected, meaning that the two data sets are significantly different.

Sometimes, two or more values tie for the same rank in the combined list. In such a case, an average rank is assigned to all of the values. However, if this happens too much, the results can be skewed. This is especially true when working with a low number of data points. When there were too many ties in the data, the statistical analysis used for this project employed an assumed normal distribution, which yielding a single value for the test statistic that could be positive or negative. The larger the absolute value of this test statistic, the smaller the p-value.

For each pair of mix designs, two sets of comparisons were calculated. The first used the average rut depth measured from the base line and the second used the maximum rut depth measured from the base line. Tables A7.5 through A7.13 show the results from the statistical comparisons. The first column is the number of thousands of loading cycles applied up to the set of profiles that were statistically compared. The test statistics labeled W are sums of ranks. The test statistics labeled Z are the normal distribution approximations. If the null hypothesis, H_0, is rejected, then the two data sets are significantly different at the corresponding number of loading cycles.

Table A7.5: Oss 12.5 verses Oss 19

	Avg Rut Depth			Max Rut Depth		
Cycles	Test Statistics	P-Value	Reject H_0?	Test Statistics	P-Value	Reject H_0?
1	W = 28, 77	0.0006	Yes	W = 28, 77	0.0006	Yes
2	W = 28, 77	0.0006	Yes	W = 28, 77	0.0006	Yes
4	W = 31, 74	0.0041	Yes	W = 31, 74	0.0041	Yes
8	W = 31, 74	0.0041	Yes	W = 32, 73	0.007	Yes
16	W = 42, 63	0.2086	No	W = 64, 41	0.1649	No
30	W = 68, 37	0.053	No	W = 42, 63	0.2086	No
50	W = 42, 63	0.2086	No	W = 60, 45	0.3829	No
75	W = 60, 45	0.3829	No	W = 59, 46	0.4557	No
100	Z = -0.9594	0.3374	No	W = 59, 46	0.4557	No

Table A7.6: Oss 12.5 verses Cont 12.5

	Avg Rut Depth			Max Rut Depth		
Cycles	Test Statistics	P-Value	Reject H_0?	Test Statistics	P-Value	Reject H_0?
1	W = 56, 49	0.7104	No	W = 52, 53	1	No
2	W = 56, 49	0.7104	No	W = 50, 55	0.8048	No
4	W = 58, 47	0.535	No	W = 58, 47	0.535	No
8	W = 48, 57	0.62	No	W = 56, 49	0.7104	No
16	W = 48, 57	0.62	No	W = 48, 57	0.62	No
30	W = 59, 46	0.4557	No	W = 58, 47	0.535	No
50	Z = -0.7035	0.4817	No	W = 59, 46	0.4557	No
75	W = 60, 45	0.3829	No	W = 61, 44	0.3176	No
100	W = 60, 45	0.3829	No	W = 58, 47	0.535	No

Table A7.7: Oss 12.5 verses Farm

	Avg Rut Depth			Max Rut Depth		
Cycles	Test Statistics	P-Value	Reject H_0?	Test Statistics	P-Value	Reject H_0?
1	W = 49, 56	0.7104	No	W = 58, 47	0.535	No
2	W = 63, 42	0.2086	No	W = 60, 45	0.3829	No
4	W = 60, 45	0.3829	No	W = 62, 43	0.2593	No
8	W = 65, 40	0.1282	No	W = 66, 39	0.0973	No
16	W = 69, 36	0.0379	Yes	W = 70, 35	0.0262	Yes
30	W = 68, 37	0.053	No	W = 70, 35	0.0262	Yes
50	W = 70, 35	0.0262	Yes	W = 70, 35	0.0262	Yes
75	W = 31, 74	0.0041	Yes	W = 31, 74	0.0041	Yes
100	W = 75, 30	0.0023	Yes	W = 31, 74	0.0041	Yes

Table A7.8: Oss 19 verses Cont 19

	Avg Rut Depth			Max Rut Depth		
Cycles	Test Statistics	P-Value	Reject H_0?	Test Statistics	P-Value	Reject H_0?
1	W = 28, 77	0.0006	Yes	W = 28, 77	0.0006	Yes
2	W = 28, 77	0.0006	Yes	W = 28, 77	0.0006	Yes
4	W = 28, 77	0.0006	Yes	W = 28, 77	0.0006	Yes
8	W = 28, 77	0.0006	Yes	W = 28, 77	0.0006	Yes
16	W = 28, 77	0.0006	Yes	W = 28, 77	0.0006	Yes
30	W = 28, 77	0.0006	Yes	W = 28, 77	0.0006	Yes
50	W = 28, 77	0.0006	Yes	W = 28, 77	0.0006	Yes
75	Z = -3.07	0.0021	Yes	W = 28, 77	0.0006	Yes
100	W = 28, 77	0.0006	Yes	Z = -3.07	0.0021	Yes

Table A7.9: Cont 12.5 verses Cont 19

	Avg Rut Depth			Max Rut Depth		
Cycles	Test Statistics	P-Value	Reject H_0?	Test Statistics	P-Value	Reject H_0?
1	W = 59, 46	0.4557	No	W = 56, 49	0.7104	No
2	W = 35, 70	0.0262	Yes	W = 38, 67	0.0728	No
4	W = 70, 35	0.0262	Yes	W = 70, 35	0.0262	Yes
8	W = 70, 35	0.0262	Yes	W = 70, 35	0.0262	Yes
16	W = 70, 35	0.0262	Yes	W = 70, 35	0.0262	Yes
30	W = 71, 34	0.0175	Yes	W = 72, 33	0.0111	Yes
50	W = 72, 33	0.0111	Yes	W = 32, 73	0.007	Yes
75	Z = 2.3025	0.0213	Yes	W = 32, 73	0.007	Yes
100	W = 38, 67	0.0728	No	Z = 2.3025	0.0213	Yes

Table A7.10: Cont 12.5 verses Hook

	Avg Rut Depth			Max Rut Depth		
Cycles	Test Statistics	P-Value	Reject H_0?	Test Statistics	P-Value	Reject H_0?
1	W = 52, 53	1	No	W = 56, 49	0.7104	No
2	W = 65, 40	0.1282	No	W = 66, 39	0.0973	No
4	W = 69, 36	0.0379	Yes	W = 70, 35	0.0262	Yes
8	W = 64, 41	0.1649	No	W = 65, 40	0.1282	No
16	W = 65, 40	0.1282	No	W = 62, 43	0.2593	No
30	W = 62, 43	0.2593	No	W = 61, 44	0.3176	No
50	Z = 1.3431	0.1792	No	W = 42, 63	0.2086	No
75	W = 66, 39	0.0973	No	Z = 1.471	0.1413	No
100	W = 66, 39	0.0973	No	W = 68, 37	0.053	No

Table A7.11: Farm verses Hook

	Avg Rut Depth			Max Rut Depth		
Cycles	Test Statistics	P-Value	Reject H_0?	Test Statistics	P-Value	Reject H_0?
1	W = 56, 49	0.7104	No	W = 48, 57	0.62	No
2	W = 56, 49	0.7104	No	W = 59, 46	0.4557	No
4	W = 56, 49	0.7104	No	W = 56, 49	0.7104	No
8	W = 56, 49	0.7104	No	W = 58, 47	0.535	No
16	W = 50, 55	0.8048	No	W = 60, 45	0.3829	No
30	W = 50, 55	0.8048	No	W = 58, 47	0.535	No
50	W = 56, 49	0.7104	No	W = 58, 47	0.535	No
75	W = 46, 59	0.4557	No	W = 61, 44	0.3176	No
100	W = 60, 45	0.3829	No	W = 58, 47	0.535	No

Table A7.12: Oss 12.5 Original verses Oss 12.5 Bailey

	Avg Rut Depth			Max Rut Depth		
Cycles	Test Statistics	P-Value	Reject H_0?	Test Statistics	P-Value	Reject H_0?
1	W = 42, 63	0.2086	No	W = 65, 40	0.1282	No
2	W = 48, 57	0.62	No	W = 59, 46	0.4557	No
4	W = 49, 56	0.7104	No	W = 50, 55	0.8048	No
8	W = 49, 56	0.7104	No	W = 50, 55	0.8048	No
16	W = 66, 39	0.0973	No	W = 65, 40	0.1282	No
30	W = 64, 41	0.1649	No	W = 64, 41	0.1649	No
50	W = 70, 35	0.0262	Yes	W = 36, 69	0.0379	Yes
75	W = 31, 74	0.0041	Yes	W = 31, 74	0.0041	Yes
100	W = 32, 73	0.007	Yes	W = 32, 73	0.007	Yes

Table A7.13: Cont 19 Original verses Cont 19 Bailey

	Avg Rut Depth			Max Rut Depth		
Cycles	Test Statistics	P-Value	Reject H_0?	Test Statistics	P-Value	Reject H_0?
1	W = 36, 69	0.0379	Yes	W = 32, 73	0.007	Yes
2	W = 38, 67	0.0728	No	W = 70, 35	0.0262	Yes
4	W = 32, 73	0.007	Yes	W = 75, 30	0.0023	Yes
8	W = 36, 69	0.0379	Yes	W = 32, 73	0.007	Yes
16	W = 41, 64	0.1649	No	W = 70, 35	0.0262	Yes
30	W = 65, 40	0.1282	No	W = 70, 35	0.0262	Yes
50	W = 49, 56	0.7104	No	W = 68, 37	0.053	No
75	Z = 0	1	No	W = 42, 63	0.2086	No
100	W = 51, 54	0.9015	No	Z = -0.6396	0.5224	No